

**An XPS Investigation into the Chemical Composition of Metal
Surfaces modified by the Individual Cure Components of Anaerobic
Adhesives and Functionalised Thiols**

by

Clodagh Michele Stewart



Ollscoil Chathair Bhaile Átha Cliath

A thesis submitted for the Degree of
Doctor of Philosophy

Research Supervisors: Dr. G. Hughes, Prof. M.R. Smyth and Dr. R.
Leonard.

School of Chemical/Physical Sciences

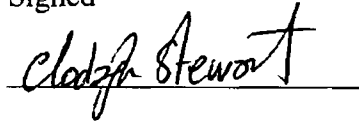
Dublin City University

November 2002

Declaration

I hereby certify that this material, which I now submit for assessment on the programme of study leading to the award of Doctor of Philosophy (PhD) is entirely my own work and has not been taken from the work of others save and to the extent that such work has been cited and acknowledged within the text of my work

Signed

A handwritten signature in black ink, appearing to read 'Clodagh Stewart', is written over a horizontal line.

Clodagh Stewart

November 2002

ID No 98970798

Acknowledgements

My sincerest thanks to the following people without their support I may have followed a very different path

My supervisors, Dr Greg Hughes and Prof Malcolm Smyth, for the opportunities they have given me over the past four years

Dr Ray Leonard from Loctite Ltd, for all his help and input throughout the years, also Dr Martin Brennan and Dr Killian Quigley for their patients while teaching me ICP and IR

Prof Z Meikalif, Prof J Dehalle, Fabrice Laffineaur and all at the LISE, Namur, Belgium

For all in the surface science research group, Jason, Darren, Philippe and Tony, “coffee breaks” will never be the same again

My family, Michael, Breege, Siobhan, Niamh, Ciara, John B, John O Sullivan and “litle” Aoife, for supporting (financially and emotionally) the eternal student lifestyle and for their belief in me

For MRS research group, Kathleen, Emily, Aoife, Maire, Niamh, Blainid, John, Emeir, Tony and Dave, weekends away and nights out were very therapeutic

*Marco and Edna, when getting away from it all was just what was needed, and
the many counselling 'sessions' over the years*

*For all in the Chemistry and Physics departments at DCU without their help this
would not have been possible*

*For Dr Caroline Whelan who has been inspirational throughout my time in
DCU, Namur and today*

*The friendship and support I received from everybody is greatly appreciated
What more can I say!*

Table of Contents

| | PAGE NUMBER |
|-------------------|-------------|
| TITLE PAGE | I |
| DECLARATION | II |
| ACKNOWLEDGEMENTS | III |
| TABLE OF CONTENTS | V |
| ABSTRACT | XI |

Chapter 1

| | |
|--|---|
| <i>General introduction outlining thesis</i> | 1 |
|--|---|

Chapter 2

| | |
|--|----|
| <i>Cure chemistry of anaerobic adhesives</i> | 4 |
| 2 1 Introduction to adhesives | 5 |
| 2 2 Anaerobic adhesives | 6 |
| 2 2 1 Background of anaerobic adhesives | 6 |
| 2 2 2 Components of anaerobic adhesives | 6 |
| 2 2 3 Chemistry of anaerobic adhesives | 11 |
| 2 3 Analysis of anaerobic adhesives | 13 |
| 2 4 Conclusions | 31 |
| 2 5 References | 33 |

Chapter 3

An X-ray Photoelectron Spectroscopy study into different cleaning procedures performed on mild steel substrates

| | | |
|-------|---|----|
| 3 1 | Introduction | 35 |
| 3 2 | X-Ray Photoelectron Spectroscopy | |
| 3 2 1 | Instrument - VG-Microtech ESCA | 39 |
| 3 2 2 | Introduction to XPS | 39 |
| 3 2 3 | Vacuum system | 42 |
| 3 2 4 | X-ray source | 43 |
| 3 2 5 | Analysers | 43 |
| 3 2 6 | Treatment of results | 46 |
| 3 3 | Experimental | |
| 3 3 1 | Materials | 48 |
| 3 3 2 | Sample preparation | 48 |
| 3 3 3 | Procedures | 49 |
| 3 4 | Results and discussion | |
| 3 4 1 | Surface composition of untreated lapshear | 50 |
| 3 4 2 | Cleaning procedures / lapshear surface | 54 |
| 3 4 3 | Cleaning procedures / polished lapshears | 61 |
| 3 4 4 | Pin/collar assemblies | 67 |
| 3 5 | Conclusions | 68 |
| 3 6 | References | 69 |

Chapter 4

An XPS study into the effect individual cure components of anaerobic adhesives produce on a copper substrate surface

| | | |
|-------|--------------------|----|
| 4 1 | Introduction | 71 |
| 4 1 1 | The cure chemistry | 74 |

| | | |
|-------|---|-----|
| 4 2 | X-Ray Photoelectron Spectroscopy | |
| 4 2 1 | Instrumentation | 78 |
| 4 2 2 | Quantification | 79 |
| 4 2 3 | Binding energy scale referencing | 80 |
| 4 2 4 | Background considerations | 81 |
| 4 2 5 | Auger parameters | 82 |
| 4 3 | Experimental | |
| 4 3 1 | Reagents and apparatus | 84 |
| 4 3 2 | Sample preparation | 85 |
| 4 4 | Results and discussion | |
| 4 4 1 | Organic acids – saccharin and maleic acid | 89 |
| 4 4 2 | Substituted aromatic amines | 99 |
| 4 4 3 | Saccharin and substituted aromatic amines | 103 |
| 4 4 4 | Maleic acid and substituted aromatic amines | 112 |
| 4 4 5 | Model formulations | 118 |
| 4 4 6 | Reduced copper substrate | 127 |
| 4 5 | Conclusions | 130 |
| 4 6 | References | 132 |

Chapter 5

An XPS Study into the effect individual cure components of anaerobic adhesives produce on an iron containing substrate surface

| | | |
|-------|---|-----|
| 5 1 | Introduction | 135 |
| 5 1 1 | The cure chemistry | 136 |
| 5 2 | Experimental | |
| 5 2 1 | Instrument | 139 |
| 5 2 2 | Reagents and sample | 139 |
| 5 3 | Results and Discussion | |
| 5 3 1 | Organic acids – saccharin and maleic acid | 140 |
| 5 3 2 | Substituted aromatic amines | 148 |

| | | |
|-------|---|-----|
| 5 3 3 | Saccharin and substituted aromatic amines | 151 |
| 5 3 4 | Maleic acid and substituted aromatic amines | 157 |
| 5 3 5 | Organic acids and cumene hydroperoxide | 162 |
| 5 3 6 | Model formulations | 166 |
| 5 4 | Conclusions | 169 |
| 5 5 | References | 171 |

Chapter 6

A FT-IR, ICP-AES and XPS study of the individual cure components of anaerobic adhesives on a copper substrate

| | | |
|-------|---|-----|
| 6 1 | Introduction | 174 |
| 6 2 | Experimental | |
| 6 2 1 | Fourier transform infrared spectroscopy | 176 |
| 6 2 2 | Inductively coupled plasma – atomic emission spectroscopy | 178 |
| 6 2 3 | Reagents and instruments | 180 |
| 6 2 4 | Sample preparation | 180 |
| 6 3 | Results and Discussion | |
| 6 3 1 | FT-IR | 182 |
| 6 3 2 | ICP-AES | 192 |
| 6 3 3 | XPS | 195 |
| 6 4 | Conclusions | 200 |
| 6 5 | References | 201 |

Chapter 7

Surface characterisation of alkane-thiol adsorption on polycrystalline copper surface and Au single crystal surfaces

| | | |
|-------|--|-----|
| 7 1 | Introduction | 203 |
| 7 2 | SAM formation | 204 |
| 7 2 1 | The self-assembly process | 204 |
| 7 3 | SAMs on Au (111) | 209 |
| 7 4 | SAMs on copper | 210 |
| 7 5 | SAMs protect copper against corrosion / oxidation | 213 |
| 7 6 | Effect of solvents and concentration on the SA process | 226 |
| 7 7 | Multi-component and mixed SAMs | 229 |
| 7 8 | Adsorption on SAMs | 229 |
| 7 9 | Discussion | 230 |
| 7 10 | Conclusions | 232 |
| 7 11 | References | 233 |

Chapter 8

A combined XPS (X-ray Photoelectron Spectroscopy) and electrochemical study into alcohol and carboxylic terminated thiols on reduced copper

| | | |
|-------|---------------------------------|-----|
| 8 1 | Introduction | 237 |
| 8 2 | Purpose and aims of research | 238 |
| 8 3 | Experimental | |
| 8 3 1 | Materials | 239 |
| 8 3 2 | Sample preparation | 241 |
| 8 4 | Instrumentation | |
| 8 4 1 | XPS | 244 |
| 8 4 2 | Contact angle measurements | 245 |
| 8 4 3 | Cyclic voltammetry | 246 |
| 8 4 4 | Polarisation curves | 247 |
| 8 5 | Results and discussion | |
| 8 5 1 | Contact angle measurements | 249 |
| 8 5 2 | Cyclic voltammetry measurements | 252 |
| 8 5 3 | Polarisation curves | 256 |

| | | | |
|-----|-------|-------------|-----|
| | 8 5 4 | XPS results | 262 |
| 8 6 | | Conclusions | 277 |
| 8 7 | | References | 278 |

Chapter 9

Overall conclusions and future work

| | | | |
|-----|--|-------------------------------------|-----|
| 9 1 | | Overview | 281 |
| 9 2 | | General conclusions and future work | 282 |

Abstract

This thesis investigates the application of surface sensitive techniques to analyse the chemical composition of metal surfaces modified by a variety of surface treatments. The first part of this thesis involves an XPS investigation of the surface chemical composition of mild steel which has been subjected to two different cleaning procedures, an organic cleaning procedure employed by the adhesive industry, and an aqueous-based formula. The switch from an organic-based formulation to an aqueous based-formula has been driven by environmental concerns. These studies conclude that the aqueous-based procedure offers superior surface cleaning properties to those of the organic clean.

The crucial role played by transition metals in the cure chemistry of anaerobic adhesives was then studied. Polished copper and iron-containing mild steel substrates have been systematically modified with the individual cure components of anaerobic adhesives. XPS was then utilised to study the interaction of a variety of anaerobic adhesives molecules with these substrates. The organic acids used readily form complexes with these substrates, with saccharin having a better affinity for the copper substrate and maleic acid producing a better result on the iron containing substrate. The complexes formed between the organic acids and the tertiary amines depend on the position of the substituted group, with only the para-substituted amine forming a salt at the metal interface.

The copper substrate was further modified with functionalised thiols and analysed, with respect to the effect these thiols produce on the corrosion resistance of the underlying substrate. XPS combined with electrochemistry was used to study polycrystalline copper modified with functionalised thiols, $\text{HS}-(\text{CH}_2)_n\text{-X}$, where $\text{X} = \text{COOH}$ and OH . The influence that chain length and immersion time had on monolayer formation was investigated, concluding that the longer chain carboxylic functionalised thiols lead to significantly better corrosion resistance for the time limits investigated.

Chapter 1

| |
|--------------|
| Introduction |
|--------------|

X-Ray Photoelectron Spectroscopy (XPS) has become one of the most important spectroscopic techniques available for surface analysis in the past twenty years. Throughout this thesis XPS is the main experimental technique used to analyse and quantify copper and mild steel surfaces modified with different components.

The initial part of the thesis is devoted to the study of the cure chemistry of anaerobic adhesives. XPS was the surface technique employed, to gain further insight into the complex cure chemistry involving anaerobic adhesives. Throughout this investigation the objective was to advance the knowledge of the underlying chemical mechanisms which form the basis for the cure of advanced engineering adhesives, and gain an understanding of the chemical interactions that occur between the adhesive and the material surface.

In chapter two, a review is given into the cure chemistry of industrial anaerobic adhesives and sealants. Particular emphasis was placed on the cure system employed in these anaerobic adhesives, the cure system consisting of an aromatic amine, combined with an organic acid and a hydroperoxide initiator. The crucial role played by the transition metals in this cure chemistry are highlighted.

Chapter three focuses on the cleaning procedures employed on the metal surface prior to adhesive bonding. As with most adhesives, anaerobic adhesives require decontamination of the materials to be bonded and a surface treatment, which can sometimes modify some characteristics of polymerisation. Two different cleaning procedures were investigated, that of an organic vapour degreasing clean and an aqueous-based clean. These studies revealed that the aqueous cleaning procedure results in improved surface cleaning as indicated by the chemical composition of the substrate surfaces.

Chapter four and five deal with the effect that each of the individual cure components in the adhesive and combinations of these components have on the transition metal surface, where the metals of interest are copper and iron respectively. These two transition metals are studied as they make up the vast

majority of metals encountered in anaerobic adhesives applications. The effect that organic acids individually and combined with substituted aromatic amines produce on the substrate surface, and the ability of this combination to reduce the underlying metal substrate to its active valence state was investigated.

Chapter six investigates copper substrates modified with the organic acids such as saccharin and maleic acid, and substituted tertiary aromatic amines and hydrazines. Additional analytical techniques employed in this chapter to elucidate the chemical interactions were, FT-IR (Fourier Transform Infrared Spectroscopy) and ICP-AES (inductively coupled plasma – atomic emission spectroscopy). FTIR assisted in identifying residual chemical components on the surface following treatment with the cure components, while ICP-AES provided information on the amount of metal dissolved by the cure component.

In chapter seven, a review into the surface characterisation and the self-assembly process of alkane-thiol adsorption on polycrystalline copper and gold (111) is presented. This leads on to an XPS and electrochemical study of polycrystalline copper modified with functionalised thiols, $\text{HS}-(\text{CH}_2)_n\text{-X}$, where $\text{X} = \text{COOH}$ and OH . The influence chain length and immersion time had on monolayer formation was also investigated, concluding that the longer chain carboxylic functionalised thiols leads to significantly better corrosion resistance for the time limits investigated.

Chapter 2

Cure chemistry of anaerobic adhesives

2.1 Introduction to Adhesives

Adhesives, also known as glues or pastes, are defined as “substances which are capable of holding materials together by surface attachment” Almost 4,000 years ago, the Egyptians were using hide glue for their furniture adhesive Hairs found in the Pharaohs’ tombs and stone carvings depicting the process of gluing different woods prove this Hide glue is still in use today for wood gluing, and over the years much has been written about the manufacture and use of hide glue for hundreds of other adhesive applications With the evolution of synthetic (ready to use) adhesives, hide glue has taken a lesser role, and these days the range of applications for adhesives is extensive, from printed circuit boards to industrial processes using adhesives in assembly lines, to woodwork, footwear, packaging, and general home use

The many advantages associated with adhesives, as the method of choice for joining materials together, has resulted in the rapid growth of the adhesive industry The adhesives favoured by industry for technological applications can be separated into the following categories (1) Anaerobic sealants (methacrylate ester-based), (2) acrylic ‘toughened’ adhesives, (3) alkyl-cyanoacrylate ester-based ‘instant’ adhesives, (4) acrylate/methacrylate ester-based radiation-curable adhesives, and (5) epoxy adhesives

Most of the literature that was available regarding anaerobic adhesives until the end of the 1980s consisted of patents where the adhesive components such as the monomer and/or the accelerator were improved [1,2] It is only since the 1990s, that anaerobic adhesives have become an important field for fundamental investigation

2.2 Anaerobic Adhesives

2.2.1 Background

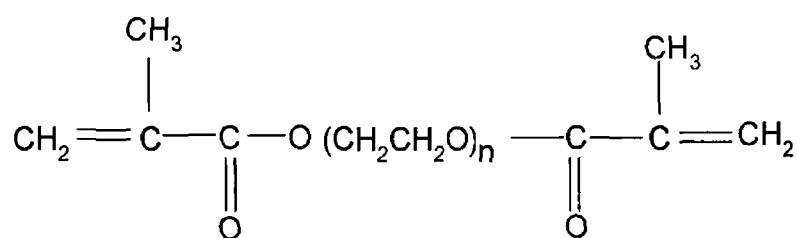
Anaerobic adhesives take their name from the characteristic of requiring a relatively oxygen-free environment for a proper cure and are single component acrylic adhesives which cure rapidly and at room temperature. These anaerobic sealants remain in liquid form in the presence of air, but when air is excluded the monomeric constituents in the liquid polymerise (i.e. cure rapidly) resulting in a tough heat and solvent resistant solid material [3].

Anaerobic adhesives originated in the United States in the 1950s when Burnett and Nordlander [4] produced a product called 'Permafil' which was an anaerobic monomer based on polyethyleneglycol dimethacrylates. When this monomer was heated in the presence of oxygen, between 60°-80°C, and cooled, it remained as a liquid while aeration was maintained. Once aeration was discontinued, rapid cross-linking occurred which resulted in a solid polymeric material. Krieble [5,6] developed the first anaerobic sealant in 1953 which was composed of methacrylate monomers and containing a small amount of cumene hydroperoxide. This grouping of polyethyleneglycol dimethacrylate and organic hydroperoxide forms the basis of many U.S. adhesive patents issued since then. The cure rate and the shelf-life of these products have improved over the years with other components being added to the formulations.

2.2.2 Components of Anaerobic Adhesives

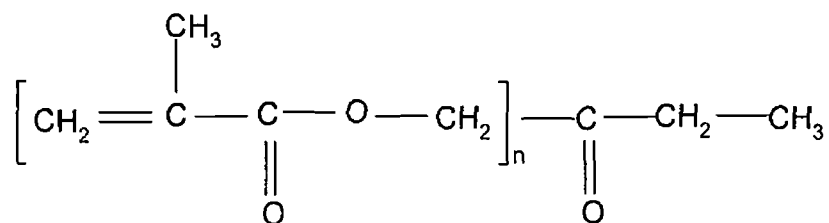
Anaerobic adhesives contain the following five basic components: monomers, initiators, catalysts (accelerators), stabilizers/inhibitors and modifiers. These components are combined to provide formulations of various strengths and adhesives.

Monomers (Figure 2 1) are typically low molecular mass compounds, which are involved in the polymerisation process, earlier monomer studies led to the use of methacrylates of polyalkoxy polyols [7] In later studies, many other monomers have proven useful in the preparation of anaerobic adhesives, with methacrylates remaining the most commonly used monomers due to their performance, cure speed, ease of synthesis and lower sensitivity to oxygen than simple acrylates



where $n > 2$

Polyethylene glycol di-(methacrylate)

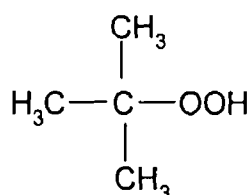


where $n = 3$

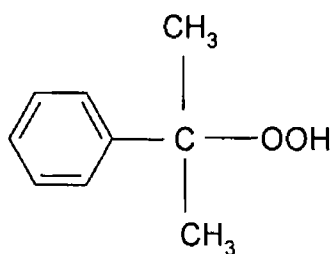
Trimethylolpropane trimethacrylate

Figure 2 1 Examples of monomers used in anaerobic adhesives

Initiators, as their name suggests, begin the curing process and tend to be free radical in nature with hydroperoxides being one of the most important groups of initiators (Figure 2 2) [8]



Tertiary butylhydroperoxide



Cumene Hydroperoxide

Figure 2 2 Examples of initiators used in anaerobic adhesives

Accelerators or cure promoters comprise a wide range of compounds, which include organic acids, organic reducing agents and organic peroxides (Figure 2 3) These compounds, when combined together, result in the desired performance from the adhesive The percentage of polymer polymerised and also the rate of curing is increased when using these additives

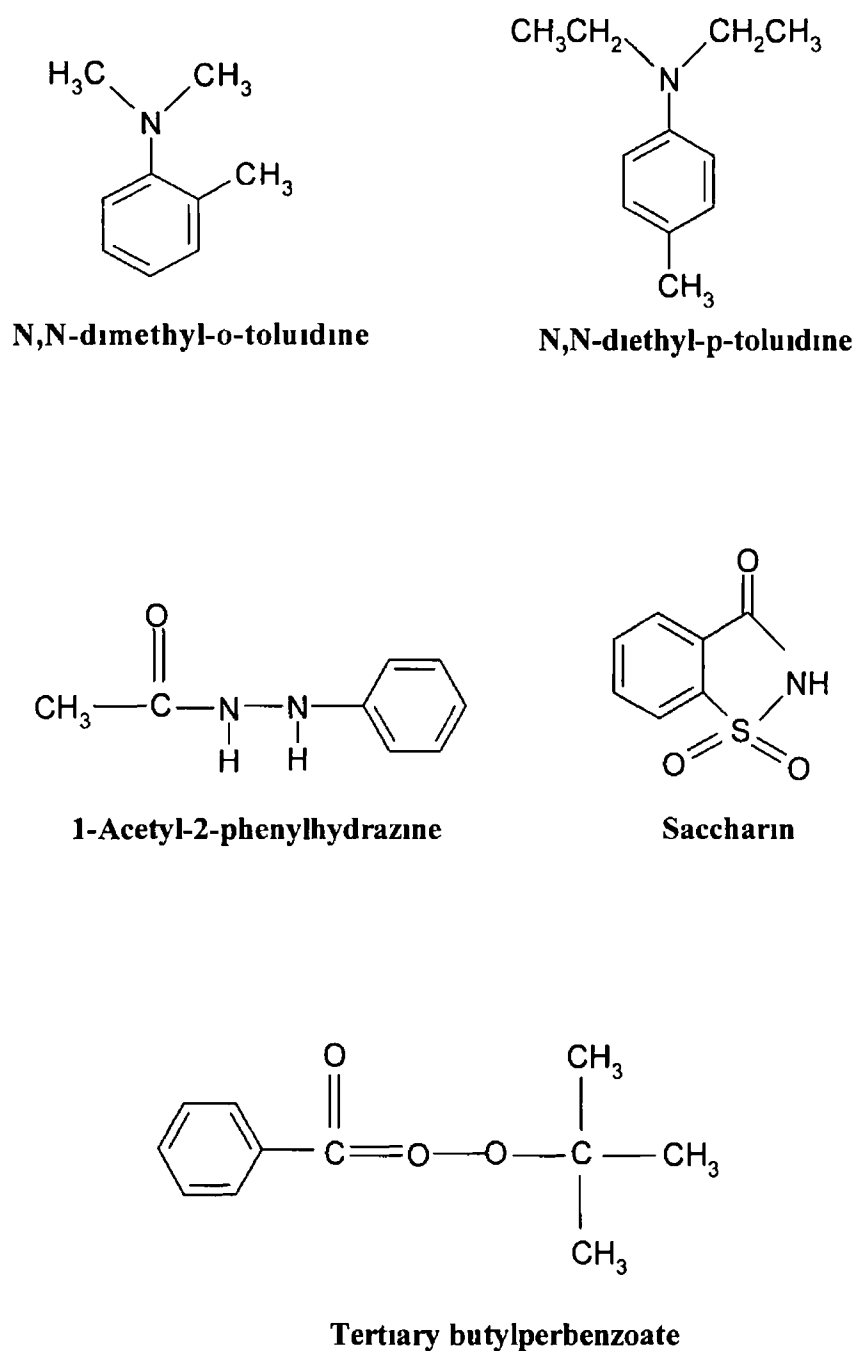


Figure 2 3 Examples of accelerators used in anaerobic adhesives

Anaerobic adhesives are packaged in low-density polyethylene containers, as they require oxygen during storage. The dissolved oxygen content is unable to provide all the needed stabilization, therefore stabilizers or inhibitors are used in anaerobic formulations to extend the product shelf-life. There is a difference between stabilizers and inhibitors. A stabilizer, such as certain chelating agents, is an additive that reacts with a chemical species that can lead to initiation. These can then coordinate with traces of transition metals present in many monomers, preventing premature peroxide decomposition and polymerisation. Inhibitors are additives which are used to stop polymerisation once it has begun, like oxygen (Figure 2.4)

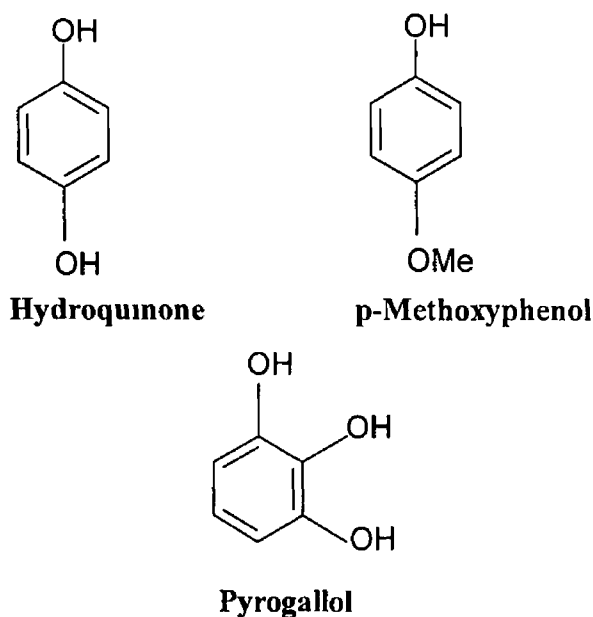


Figure 2.4 Examples of inhibitors used in anaerobic adhesives

There are several types of modifiers which can be added to the adhesive formulations to alter characteristics such as temperature performance - without altering the cure chemistry of the adhesive. Modifiers are used for thickening,

toughening, changing the viscosity and altering the high-temperature performance of the adhesive. These are also incorporated into the adhesive formulations in order to get the desired physical form and appearance. Calcium carbonate is used as a filler, while polystyrene is an example of a thickener.

2.2.3 Chemistry of Anaerobic Adhesives

Anaerobic adhesives cure or polymerise by a metal catalysed redox-based system [9]

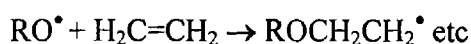
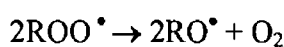
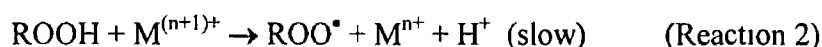
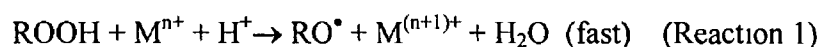


Figure 2.5 Reaction scheme of the redox-based cure chemistry of anaerobic adhesives

When the adhesive is placed between two closely fitted metal parts (e.g. nut and bolt), and air is excluded, the decomposition of the peroxide component to form free radicals is catalysed by the active metal surface. Hydroperoxides react with transition metals in two ways, one fast (reaction 1) and one slow (reaction 2). The slow reaction (reaction 2) produces ROO^\bullet radicals that are much less efficient than the RO^\bullet but are essential to regenerate the metal cations at the lower oxidation state (M^{n+} in the above reaction sequence), in order to maintain the initiation rate. These free radicals go on to initiate the polymerisation process. This is known as a

chain propagation sequence, which occurs by the reaction of these free radicals with one of the terminal bonds of a monomer molecule. This process will continue until termination occurs, usually by disproportionation (Figure 2.6). A three-dimensional cross-linked thermoset resin that is solvent resistant and heat stable can be produced if the linear polymer chain undergoes further reaction with more free radicals. If oxygen were present, the radicals would react with the molecular oxygen forming an inactive peroxyradical, which is unable to initiate polymerisation. The initiation process is the main characteristic of anaerobic polymerisation that sets it apart from other acrylic polymerisations.

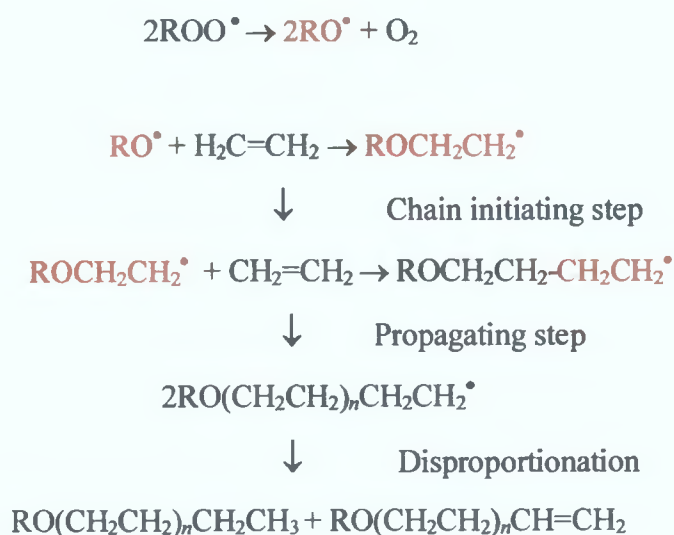


Figure 2.6 Sequence of events involved in free radical chain propagation polymerisation.

2.3 Analysis of Anaerobic Adhesives

In 1990 a study was carried out by Okamoto *et al* [10] on the cure mechanism of anaerobic adhesives, utilising methyl methacrylate (MMA) in combination with N,N- dimethyl-p-toluidine (DMpT), saccharin (BS) and cumene hydroperoxide (CHP). MMA was used as the model monomer. The effect that temperature had on the polymerisation rate was examined, as well as a kinetic study of the MMA polymerisation activated by the DMpT-BS-CHP system and a structure-cure speed study. From these results a polymerisation mechanism was devised, and found most likely to cure via redox radical polymerisation. The reducing agent of this redox system was assumed to be a charge-transfer complex (Figure 2.7) that was formed between BS and DMpT, while the oxidising agent was thought to be traces of oxygen in the system or residual oxygen in the monomer, as this redox polymerisation took place in the absence of the CHP.

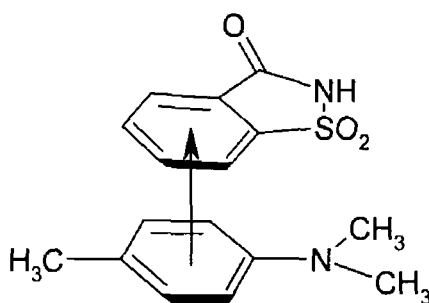


Figure 2.7 Proposed structure of charge-transfer complex formed between saccharin and the DMpT

The low activation energy recorded by Okamoto implies that the polymerisation proceeds via a redox-radical polymerisation

$$R_p = k[BS]^{0.36} [DMpT]^{0.34} [CHP]^0$$

$$E_a = 43.5 \text{ kJ mol}^{-1}$$

where R_p is the rate of polymerisation, k is the rate constant and E_a is the activation energy

Also in 1990, Hudak *et al* [11] carried out XPS analysis on the interface between anaerobic adhesive and metal substrates. The role that the metal substrate played in the cure mechanism of a model anaerobic adhesive system was investigated. The fracture surfaces of adhesive joints prepared on different metals such as copper, iron, aluminium and zinc were analysed. The spectra obtained of the adhesive sides of the samples were similar to the spectra obtained from the bulk-fractured adhesive. The spectra obtained from the metal sides of these fractured samples showed that the intensity of the sulphur, nitrogen and the metal substrate were more intense, indicating that the debonding occurred close to the adhesive/substrate, possibly within the metal oxide. Hudak *et al* [11] also reported that the BS and the APH accumulate at the interface. This was deduced from the relative intensities of the nitrogen and sulphur peaks in the XPS spectra of the metal side. The expected N/S ratio for the presence of saccharin would be 1/1. A larger nitrogen signal was detected indicating that APH has also accumulated at the metal surface.

In order to investigate the oxidation state of the metal during complex formation, Hudak *et al* [11] used modified Auger parameters (α'), which were calculated from the following equation

$$\alpha' = BE_p + (h\nu - BE_a) \quad \text{Equation 2.1}$$

where BE_p is the binding energy of the photoelectron line, BE_a is the apparent binding energy of the Auger line and $h\nu$ is the x-ray energy. From this Hudak *et al* surmised that initially a Cu(I) complex is formed between the saccharin and the copper, but after a period of time (110 hr) only the Cu(II) complex is formed. Hudak *et al* also reported that prolonged exposure of the Cu(II) species to x-rays resulted in its reduction to a Cu(I) species. Sesselmann and Chuang observed this effect on their work involving the interactions of chlorine with copper [12].

More recently in 1994, Wellmann *et al* [13] concentrated on the chemical interactions that occur between cumene hydroperoxide, saccharin and N,N – dimethyl-p-toluidine. As radical polymerisation was the mechanism assumed in previous literature, their studies focused on anaerobic as well as aerobic conditions. Throughout their investigations the model reactions were performed at room temperature in dichloromethane and the concentrations of each of the components were equal, with a reaction time of 12 hours. For anaerobic conditions, the solutions were degassed with argon, whereas the aerobic reactions had air bubbled through the solution for 1 hr. NMR (nuclear magnetic resonance) and MS (mass spectrometry) were the techniques used by Wellmann to characterise the model reactions.

Under anaerobic condition, using equimolar concentrations of cumene hydroperoxide and N,N – dimethyl-p-toluidine, N,N – dimethyl-p-toluidine-tert-N-oxide was found to be the end product along with cumene alcohol (Figure 2.8).

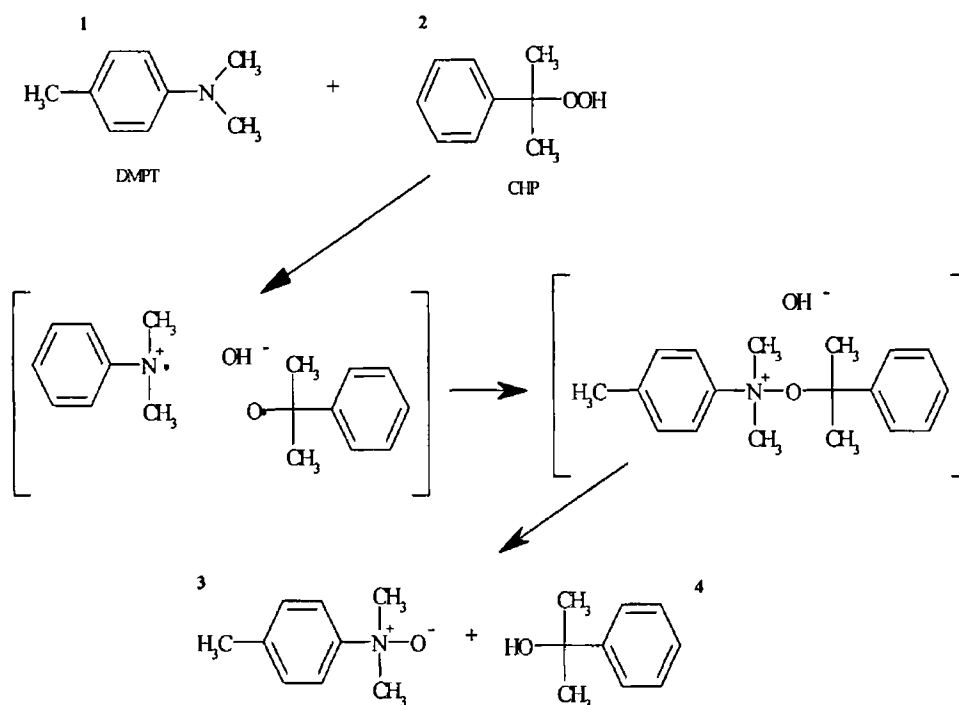


Figure 2 8 Reaction of DMpT (1) with CHP (2) yielding N,N-dimethyl-p-tert-N-oxide(3) and cumene alcohol (4)

Under anaerobic conditions the CHP oxidises the DMpT to its equivalent N-oxide and cumene alcohol. This reaction was quenched in the presence of air, which is an indication of its radical nature. This N-oxide (3) can be formed aerobically by the reaction of DMpT with air. A equimolar solution of this N-oxide was reacted with saccharin and a small amount of copper(I)chloride for a catalytic effect. Using anaerobic conditions, a new compound was created which is now known as aminal, or 2,3-dihydro-2-(n-methyl-N-p-tolyl)-aminomethyl-3-one-benzisothiazole-1,1-dioxide (Figure 2.9)

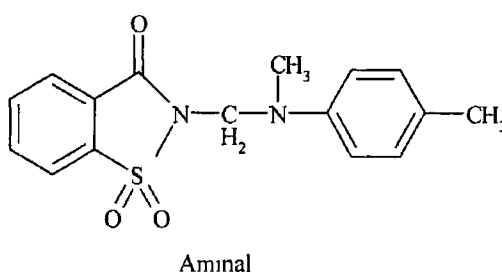


Figure 2.9 Structure of Aminal (2,3-dihydro-2-(n-methyl-N-p-tolyl)-aminomethyl-3-one-benzisothiazole-1,1-dioxide)

Therefore, this compound, aminal, could be accountable as a further compound of the curing system. On carrying out reactivity investigations, Wellmann *et al* concluded that in the absence of aminal no curing took place, with the shortest curing time being recorded when all these four ingredients were present, i.e. aminal, CHP, DMpT and saccharin. Based on their study the curing mechanism displayed in Figure 2.10 for anaerobic adhesives was proposed by Wellmann *et al*. In air, DMpT and saccharin react to form aminal which, in turn, can form metal chelates and can act as a reducing agent for metal ions. Therefore the saccharin provides metal ions from the substrate surface and these ions are reduced to a lower oxidation state by the aminal. These metal ions then create active radicals from the hydroperoxide and back to reactions 1 and 2 and the cycle. Figure 2.11 depicts how aminal reduces Cu(II) to Cu(I).

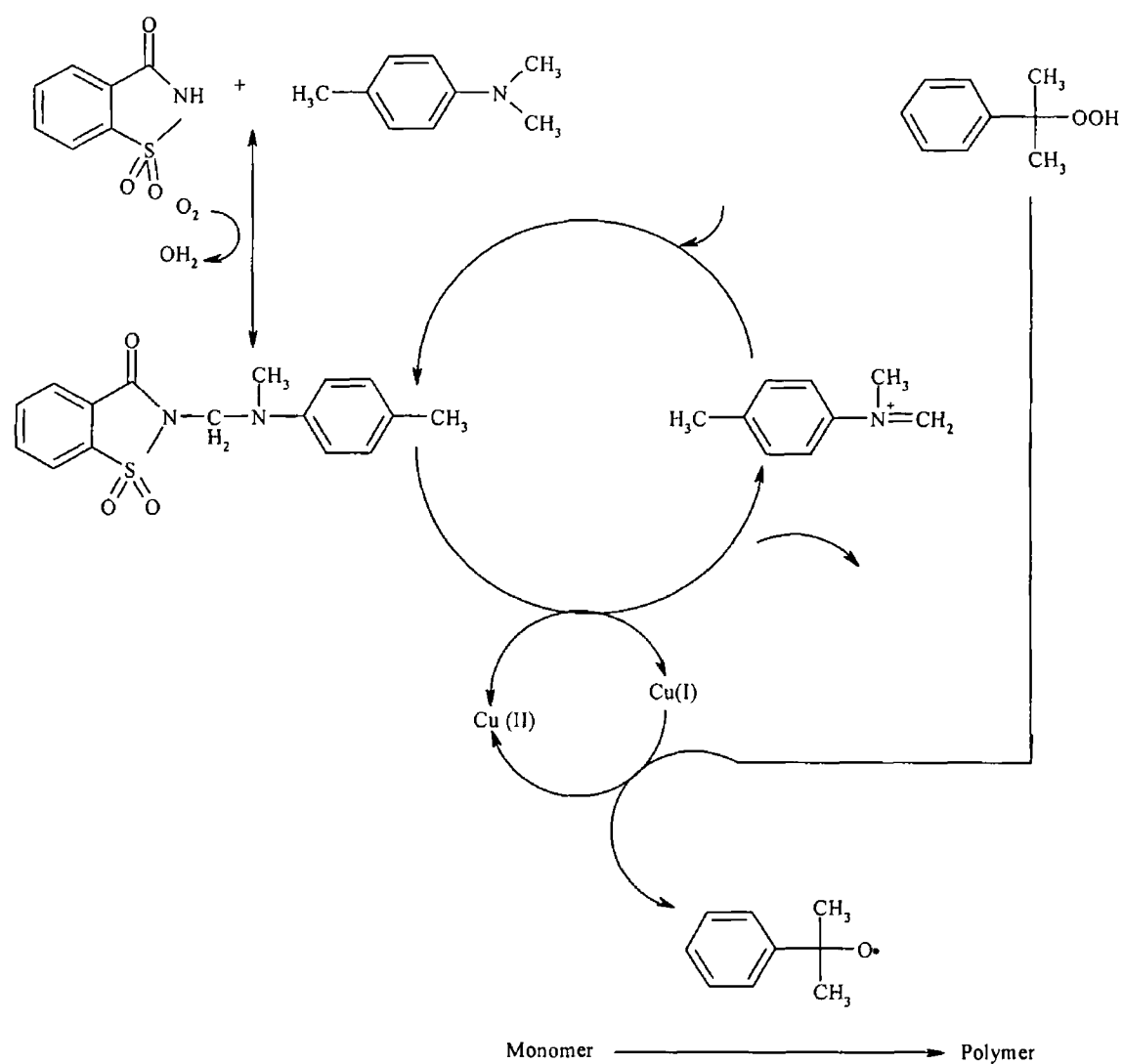


Figure 2 10 Anaerobic adhesive cure mechanism as proposed by Wellmann *et al* [13]

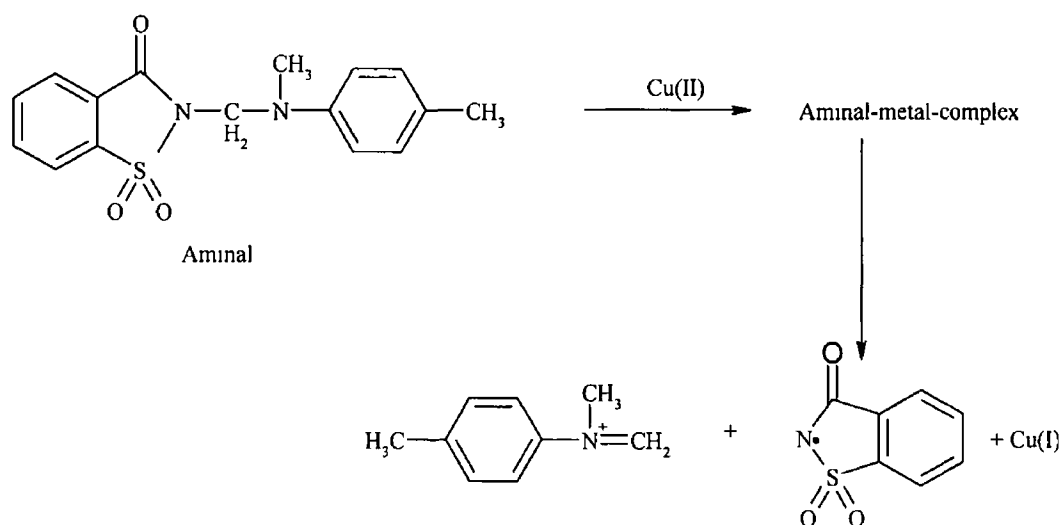


Figure 2 11 Reduction of Cu(II) to Cu(I) by aminal

In 1994, a kinetic study carried out by Beaunez and co-workers [14] investigated the role of DMpT in combination with saccharin, to see what effect these complexes had on the catalytic cycle. Copper(II) saccharinate was the copper salt used to initiate the polymerisation of the MMA monomer. The influence of the tertiary amine, DMpT, was also investigated. It was assumed that DMpT had an accelerating effect on the polymerisation of the monomer, two suppositions were put forward and investigated.

The first of these hypotheses was that DMpT reduces Cu(II) to Cu(I). Electronic absorption spectroscopy experiments carried out showed that this was untrue and that DMpT was unable to reduce Cu(II) to Cu(I) ions. The second supposition was that the metal ions were activated by complexation due to the nucleophilicity of the tertiary amine. It was also proven unlikely that DMpT could complex copper(II) saccharinate, due to the steric effects of the two-methyl groups linked to the nitrogen atom. The most probable mechanism was that DMpT complexes the Cu(I) ions and increases their reducing power towards the

hydroperoxide Saccharin, which is an acid, was found to protonate the hydroperoxide and thereby lowers the energy required to cleave the O — O bond The contribution of this protonated hydroperoxide to the initiation process was some 13000 times greater than that of an unprotonated species

Beaunez *et al* [15] continued their work regarding the role of DMpT and saccharin in the radical polymerisation of an anaerobic system, substituting copper with iron They wanted to know if the accelerator DMpT was a reductant for the Fe(III) or a ligand for the Fe(II) cations, which in turn activated the redox decomposition of the hydroperoxide The results indicated that CHP was unable to reduce the Fe(III) ions, and that DMpT was the reductant with respect to these iron ions They also showed that DMpT was able to act as a ligand for the Fe(II) ions, and the kinetics of polymerisation showed that Fe(II) complexed with 2 molecules of DMpT and that the reactivity of this complex was much greater in the decomposition of the CHP than uncomplexed Fe(II) ions Saccharin makes the decomposition of the CHP easier, but not to the extent in the case of monovalent Cu(I) This difference was assumed to be due to the effect of electrostatic repulsion, which takes place during the bimolecular reaction of protonated CHP, and the metal cation, which is larger in the case of Fe(II) (two positive charges and a small ionic radius of 0.76 Å as opposed to one charge and an ionic radius of 0.96 Å for the Cu) So saccharin has a catalytic effect on the decomposition of CHP only in the presence of the DMpT

In 1996 Raftery *et al* [16] began an investigation into the reactions of APH, 1-acetyl-2-phenylhydrazine, in the presence of Fe(III) and Cu(II) ions, identifying the major reaction products and proposing a cure mechanism No reaction was found to have taken place in the absence of the metal ions, but when Cu(II) ions were placed in solutions of the APH, CHP and an organic acid, it was found that the hydrazine was cleaved homolytically They also reported that reaction products of the homolytic cleavage depended on whether the acid used was saccharin or maleic acid as shown in Figure 2.12

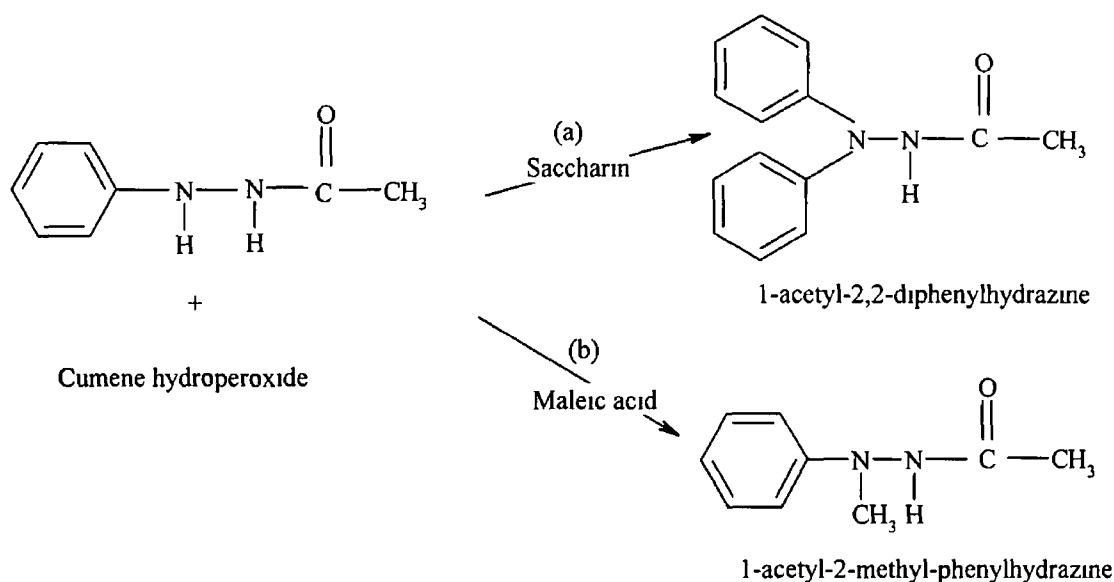


Figure 2 12 Reaction of APH/CHP in a copper based system in the presence of (a) saccharin and (b) maleic acid

When Fe(III) was substituted in place of Cu(II), the only reaction observed was the decomposition of the hydroperoxide, resulting in cumyl alcohol and methyl cumyl ether

The initial oxidation product of APH was identified as the azo compound APD (1-acetyl-2-phenyldiazene), this in turn was reacted with the Cu(II) and Fe(III) salts resulting in the formation of very different reaction products. The major reaction product when using the Cu(II) salt was identified as 1-acetyl-2,2-diphenylhydrazine by GC-MS (gas chromatography-mass spectrometry)

measurements, while azobenzene and biphenyl were the main reaction products from reaction with the Fe(III). The overall conclusion drawn was that reactions of APH are influenced by both the nature of the organic acid used and of the transition metal present.

Raftery *et al* [17] also used polarography to investigate the reactions of elemental copper and iron in the presence of APH and APD accelerators. It was found that higher levels of Cu(II) were generated when a APH/maleic acid cure system was in contact with elemental copper, whereas when the cure system examined was APH/saccharin higher levels of Cu(I) were recorded. This was regarded to be similar for the Fe(III) and Fe(II) ions also. Trace levels of metal ions were only detected in solutions containing the amine and the metal, indicating that the acid releases or liberates metal ions from the metal particles in solution. The explanation proposed by Raftery *et al* for the differences in the behaviour of the two organic acids was that maleic acid is a stronger acid than saccharin, therefore it has a stronger tendency to protonate the APH which in turn could lead to it interfering with its reducing ability.

When CHP was added to these solutions it was found that in the case of APH/saccharin cure system, higher levels of Fe(II) were generated compared to the maleic acid solutions, but overall there was a decline in the levels of both Fe(III) and Fe(II). Staying with the iron catalysed system, and using the APD/maleic acid solution, high levels of Fe(III) were generated when compared with the APD/saccharin solutions. The differences in the Fe(II) content recorded were small, but when CHP was added to the APD/saccharin system, the relative levels of the Fe(II) and Fe(III) increased. When maleic acid was substituted for saccharin in this APD/saccharin/CHP system, an increase in the Fe(II) was noted. The implication of this is that maleic acid could be the better organic acid to use in the cure system when working with iron, but only in the presence of CHP.

For the copper-based systems, addition of CHP to the APH/maleic acid results in a decrease in the Cu(II) levels, whereas the levels of Cu(I) reported remain unchanged when CHP is added to this system. Taking the APH/saccharin with CHP, the Cu(II) remains the same, with an increase in the Cu(I) levels. The overall conclusion was that both the concentration and the oxidation state of the metal ions depend on the acid used.

Raftery and co-workers [18] went on to investigate the role played by the cumene hydroperoxide in the cure chemistry of anaerobic adhesives. They used polarography to monitor the changes in the concentration of the CHP in the presence of various cure components. They found that after a very short time period, i.e. 2 minutes, the Fe(II) decomposed 98% of the CHP, and after 40 minutes 90% of the CHP had been decomposed by the Fe(III) ions. These results are contradictory to those proposed by Beaunez *et al.* who suggested that uncomplexed Fe(II) is ineffective at decomposing CHP [15].

The result recorded for the cupric ions showed only 10% decomposition of the CHP after 1 hr and 10 minutes, where the cuprous ions were inactive. Raftery then added organic acids to the reactions involving copper with no detectable increase in reaction rates. Tertiary amines, namely DMpT and APH were added to these CHP/Cu(I) solutions in a 1:1 ratio to Cu(I), producing no effect on the reaction. When the ratio of the amine was increased to 2:1 a dramatic increase in activity was recorded. When the tertiary amine DEpT (N,N-diethyl-p-toluidine) was added to the Cu(I)/CHP complex a reaction was observed between the Cu(I) and the CHP. The decomposition rate of the CHP was hindered when the concentration of the DEpT was increased to a level of 2:1 in relation to Cu(I). The addition of organic acids such as saccharin and maleic to the solutions did not affect the decomposition rate of the CHP, in fact they inhibited the decomposition to different degrees depending on the tertiary amine used. The only time that an increase in the decomposition rate of the CHP was recorded was with maleic acid and APH, when the ratio of maleic acid:CHP equalled 2:1. The conclusion drawn

from this was that as acids affect the reducing ability of the accelerators, they could also affect the ability of the accelerators to form complexes with the Cu(I). This study showed that the tertiary amines or anaerobic accelerators, especially APH and DMpT, not only act as reducing agents, but they can also act as complexing agents for copper (I), in order to catalyse the decomposition of cumene hydroperoxide.

FT-IR (Fourier Transform Infra Red) microscopy was used by George *et al* in 1997 to investigate the adhesive/substrate interface [19]. Their work focused on the usefulness of absorption spectroscopy for probing the surface metallic ions. The kinetics of the cure-reactions was studied by monitoring the decrease in the carbon-carbon double bond adsorption peaks for the substrate under investigation, i.e. saccharin. Copper had been found by Yang *et al* to be the most active surface in initiating the polymerisation process [20, 21]. George *et al* [19] noted that even though anaerobic adhesives cure rapidly on the copper surface, this fast curing reaction could lead to poor maximal strain, whereas a surface that has a lower reactivity could provide a better mechanical performance.

In 1998, George *et al* used differential scanning calorimetry (DSC) to investigate the influence that a) the atmosphere (oxygen or inert gas) b) temperature and c) metallic catalyst (copper, iron and aluminium), exert on the cure reaction of anaerobic adhesives [22]. It was surmised that the most important factor to have an influence on the rate of polymerisation was the metallic catalysts, and that the reaction was accelerated in anaerobic conditions and/or at high temperatures. Copper was found to be the most reactive surface, however it was reported that the adhesive curing at moderate to high temperature and in the absence of air led to the adhesive becoming brittle. Therefore in order to optimise the performance of the material adhesive the reactivity of the anaerobic adhesive must be carefully controlled.

George *et al* [23] continued on this line of investigation, and by studying copper in a 10^{-2} M saccharin solution in air, observed after a time span of 5 hrs that

small yellowish crystals had grown on the surface of the copper substrate. These crystals were put through elemental analysis and the results found the copper salt to be that of a cuprous saccharinate, $C_7H_4NO_3S Cu^+$, abbreviated BSCu(I) (Figure 2 13)

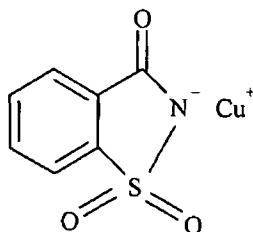


Figure 2 13 Structure of cuprous saccharinate or BSCu(I)

When this saccharin solution was deaerated for 5hr in an argon environment, no salt was formed. After 8hr in this degassed solution, bright blue crystals were observed on the copper plates which were found to be copper (II) saccharinate, i.e. BSCu(II)

George *et al* then went on to explain the formation mechanism of the BSCu(I) in the presence of air from an electrochemical viewpoint involving Cu/O₂/BS interactions. Saccharin, which is a weak acid, is in equilibrium with its dissociated form, so in the half equation for the reduction of oxygen, hydronium ions are produced, which requires electrons to be extracted from metallic copper. The sequence proposed is highlighted in Figure 2 14. For the anaerobic system that consists of Cu/Ar/BS, and the formation of BSCu(II) still had to be elucidated.

From reactions 1 and 2 in Figure 2 5, it can be seen that both of the oxidation states of the copper can decompose the hydroperoxide, but the Cu(II) is not necessarily needed to generate the Cu(I) ions. The Cu(I) oxidation state can be produced in the reaction between the saccharin and the copper in the presence of air, in turn generating the efficient radicals RO[•], which initiate the propagation and

termination reactions. In contrast to this, on the copper surface a small amount of the Cu(II) salt is formed, in the absence of air, leading to the decomposition of the hydroperoxide, which reduces the cupric to cuprous providing the RO^\bullet radicals

The same type of redox process used to explain the formation of $BSCu(I)$ was proposed to explain the formation of the $BSFe(II)$ complex (Figure 2.15) [23]. However, reaction times were much longer (3 week period) for the crystals to be formed and collected. George *et al.* did not investigate if the formation of $BSFe(III)$ could occur in the absence of air, but referred back to the work of Beaunez *et al.* in assuming that the oxidation of $Fe(II)$ to $Fe(III)$ was impossible [15].

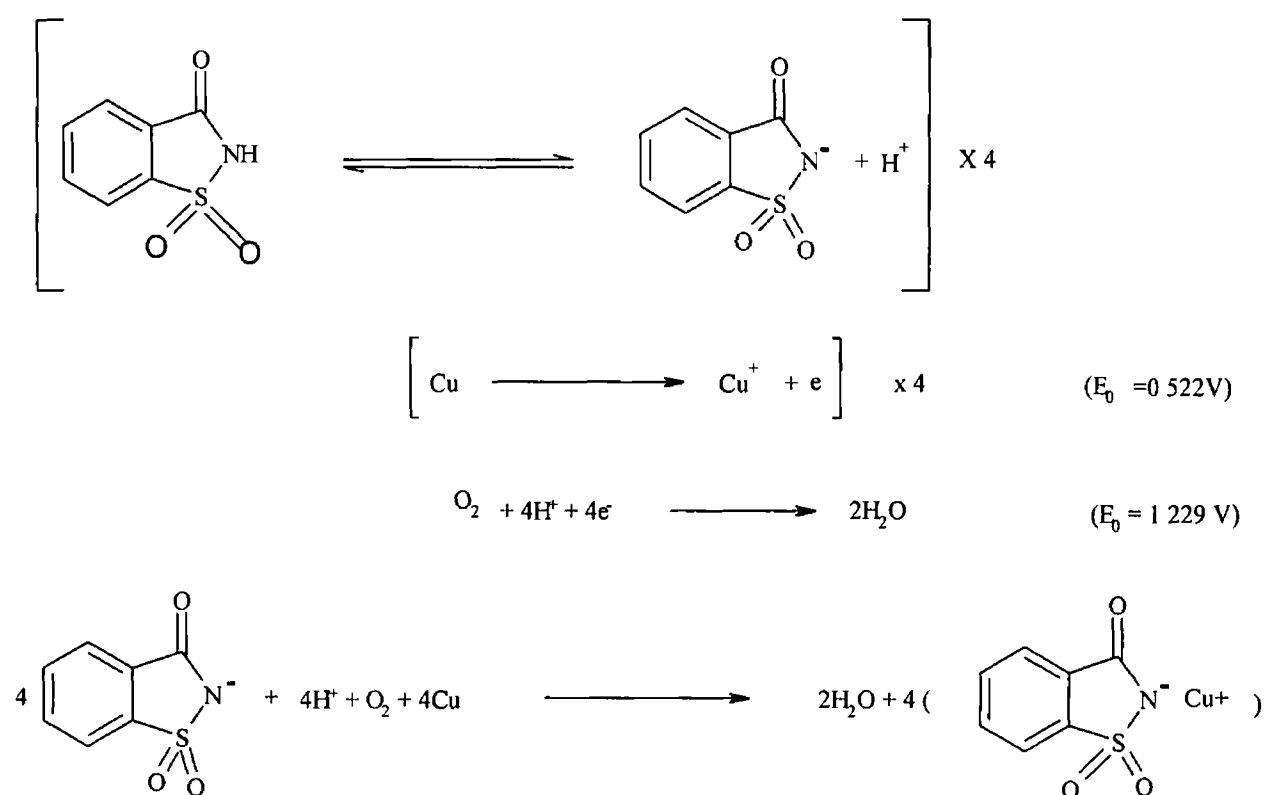


Figure 2 14 Reaction scheme for the formation of BSCu(I) under aerobic conditions [23]

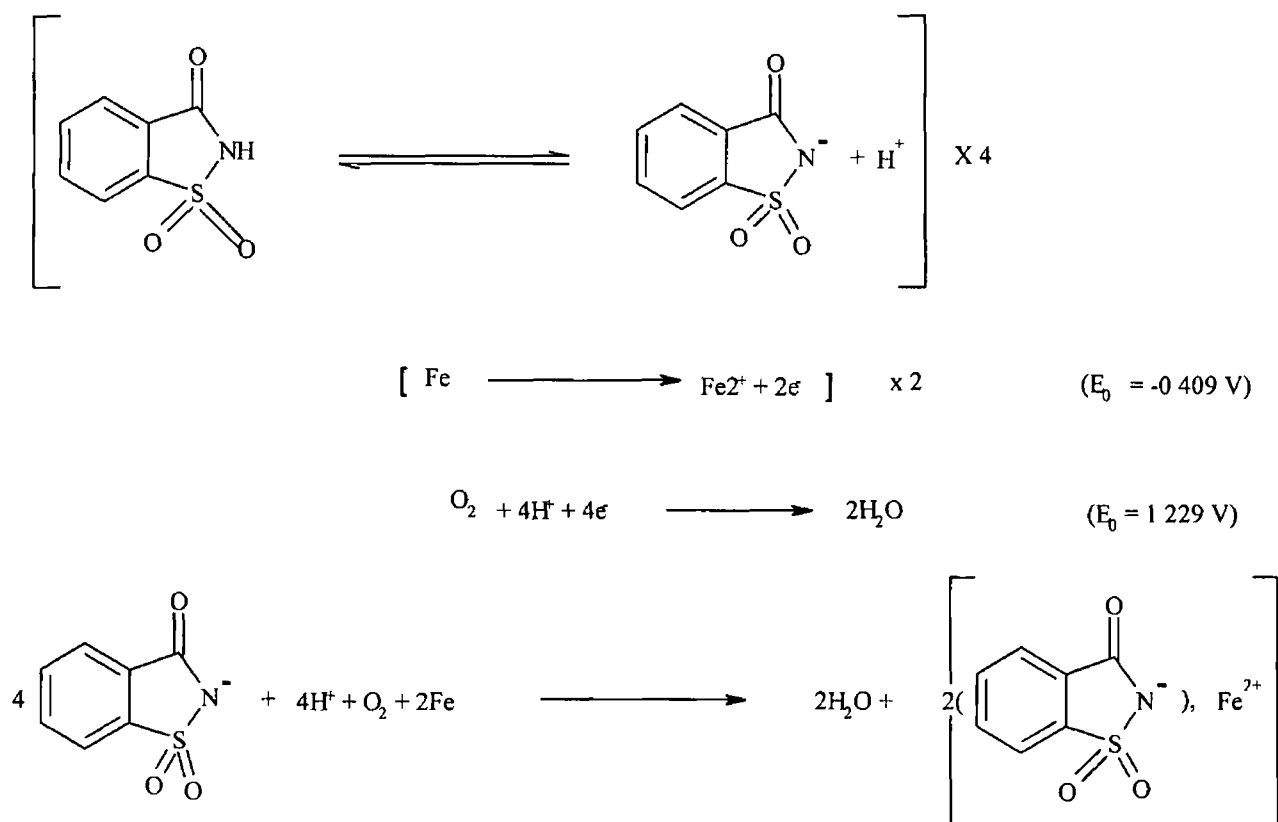


Figure 2 15 Reaction scheme for the formation of BSFe(II) under aerobic conditions [23]

From this study it would seem that air, and metallic catalysis, play an important role in the reaction of anaerobic adhesives, with the formation of copper (I) possible in the presence of air and copper (II) in deaerated media. These copper complexes determine the type of free radicals that are generated during the initiation steps of curing for anaerobic adhesives. For the case of iron, iron (II) would appear to be the only saccharinate salt generated, and this is unlikely to happen in anaerobic conditions [23].

A recent paper published on anaerobic adhesives in 2000 by George and co-workers [24], investigated the rheological behaviour as a function of time of model adhesives formulations in contact with metallic copper. Using model formulations, George *et al* found that in a tertiary system, which involved the components saccharin/DMpT/CHP, monomer gelation occurred within 10 minutes. Gelation in this case is the polymerisation of the adhesive and the formation of a 3-D network. No gelation took place in formulations that contained only the monomer and any of these components individually. When the formulations omitted CHP, the gelation period was 45 min. On the omission of the DMpT, the gel time was even longer, leading to the overall conclusion that saccharin plays a dominant role in the formulation of anaerobic adhesives. When BSCu(I) replaced the saccharin in the formulation and CHP was removed, no gelation occurred. However, polymerisation occurred with or without DMpT, leading to the conclusion that the amine complexes the Cu(I) salts, as suggested by Beaunez [14]. With all of these three components present in the system, a gelation time of 1 minute was recorded.

George *et al* then carried out these experiments in the presence of aminal, which was the complex thought to be formed by Wellmann *et al* [13]. He believed that the assumption regarding a redox mechanism involving a charge-transfer complex between the accelerating agents [10] is more probable than the scheme postulated by Wellmann *et al* involving the aminal compound. The reason being that if the initiator is present, then the complex can be involved in the reduction of Cu(II) via its delocalized electrons.

Throughout this study [24] it had been shown that the copper (I) salts which are formed by the acid oxidation of the metal due to saccharin, are vital in the initiation reaction of anaerobic adhesives and that two processes that of metallic catalysis and also complexation can occur simultaneously

2.4 Conclusions

Throughout this chapter various types of investigations carried out on anaerobic adhesives have been discussed, with the main points summarised as follows. Okamoto *et al* [10] suggested that the anaerobic adhesives cure system cures via redox radical polymerisation, the reducing agent being the charge-transfer complex that is formed between the BS and the DMpT, and the oxidising agent is traces of oxygen in the system or residual oxygen in the monomer, CHP was not essential for this redox polymerisation to occur. Hudak *et al* [11] reported that the BS and the APH accumulated at the surface, with a Cu(I) complex being formed between the copper and the saccharin initially and a Cu(II) complex after a time period of 110 hours. Wellmann *et al* [13] discovered a novel compound called “aminal” which was produced by the reaction of the CHP oxidising DMpT in the absence of air, and on addition of saccharin. In aerobic conditions “aminal” was created without CHP being present in the system. So the BS produces metal ions and the aminal forms metal chelates with these metal ions therefore acting as the reducing agent for metal ions.

Beaunez *et al* [14] proposed that the CHP reduces the cupric ions to cuprous ions, where a small fraction of Cu(I) is complexed by DMpT in a 1:2 complex, and these complexed ions act as reducing agent with respect to CHP, whereas uncomplexed Cu(I) is inactive. The saccharin catalyses the decomposition of the CHP as the saccharin lowers the energy required to cleave the O – O bond. In the second study based on iron, Beaunez *et al* [15] reported that the iron (II) was complexed by two DMpT molecules and was much more reactive than the uncomplexed iron (II), with regard to the decomposition of CHP, which again is activated by saccharin. In studies carried out by Raftery *et al* [16] it was concluded that both the nature of the organic acid, as well as the transition metal present, had an influence on the reactions of APH within the cure system. Higher levels of Cu(II) were generated with a APH/maleic acid system, with the levels of Cu(I) recorded higher when the system used was APH/saccharin [17]. This was found to

be similar to the Fe(III) and Fe(II) scenario also, overall stating that both the concentration and oxidation state of the metal ions depend on the acid used. In investigating the role of CHP, Raftery *et al* [18] showed that the tertiary amines, APH and DMpT, can act as reducing agents but also act as complexing agents for Cu(I) in order to catalyse the decomposition of CHP.

George *et al* [23] investigated copper in a saccharin solution and deduced that after 5 hrs a copper salt is formed which is cuprous saccharinate, BSCu(I), they also stated that the BSCu(II) salt could not be formed in aerobic conditions under the time limits investigated. Using model formulations George *et al* [24] found that the fastest curing time occurred when BSCu(I)/CHP/DMpT were all present in the system, and that the copper (I) salts are vital in the initiation reaction of anaerobic adhesives, also metal catalysis and complexation can also occur simultaneously.

From the above literature it can be seen that what occurs at the interface between the metal substrate and the adhesive component needs to be elucidated. So throughout the following study, the chemical interactions that occur between the individual components of the anaerobic adhesive and the substrate surfaces, such as copper and iron, were investigated using XPS. Questions such as which component of the anaerobic adhesive most strongly interacts with the metal surface and in what manner will be addressed in the following chapters, and model formulations and their interactions with polished copper surfaces will be clarified.

2.5 References

- [1] Emmons, W D , US patent 4,234,711, (1980)
- [2] Rich, R D , British patent 1,546,468, (1979)
- [3] Rooney, J M and Malofsky, B M , in “Handbook of Adhesives”, I Skeist (Ed), Reinhold, NewYork, (1977) 451
- [4] General Electric Company, U S Patent 2628178, (1953)
- [5] Krieble, V K , U S Patent, 2,895,950, (1959)
- [6] Krieble, V K , U S Patent 3,041,322, (1962)
- [7] Boeder, C W , in “Structural Adhesives”, Hartshorn S R , (Ed), Plenum Press, New York, (1986) 217
- [8] Toback, A S , U S Patent, 3616040, (1971)
- [9] Leonard, R G in “Chemical Analysis in Complex Matrices”, M R Smyth (Ed), Ellis Horwood, Chichester, (1992) 149
- [10] Okamoto, Y , J Adhesion, 32 (1990) 227
- [11] Hudak, S J , Boerio, F J , Okamoto, Y and Clark P J , Surface Interface Anal , 15 (1990) 167
- [12] Sesselmann, W and Chuang, T J , Surf Sci , 176 (1986) 32
- [13] Wellmann, St and Brockmann, H , Int J Adhesion and Adhesives, 14 (1994) 47
- [14] Beaunez, P , Helary, G and Sauvet, G , J of Polymer Science, 32 (1994) 1459
- [15] Beaunez, P , Helary, G and Sauvet, G , J of Polymer Science, 32 (1994) 1471

- [16] Raftery, D , Smyth, M R , Leonard, R and Heatley, D , Int J Adhesion and Adhesives, 17 (1997) 151
- [17] Raftery, D , Smyth M R , Leonard, R and Brennan, M , Int J Adhesion and Adhesives, 17 (1997) 9
- [18] Raftery, D , Smyth, M R , and Leonard, R , Intl J Adhesion and Adhesives, 17 (1997) 349
- [19] George, B , Grohens, Y , Touyeras, F , and Verbrel, J , Int J Adhesion and Adhesives, 17 (1997) 121
- [20] Yang, D B , J Adhesion, 43 (1993) 273
- [21] Yang D B, Wolf, D , Wakamatsu, T and Holmes, M , J Adhesion Sci Technol , 9 (1995) 1369
- [22] George, B , Grohens, Y , Touyeras, F and Verbrel, J , Eur Polym J , 34 (1998) 399
- [23] George, B , Grohens, Y , Touyeras, F and Verbrel J , J Adhesion Sci Technol , 12 (1998) 1281
- [24] George, B , Grohens, Y , Touyeras, F and Verbrel, J , Int J Adhesion and Adhesives 20 (2000) 245

Chapter 3

An X-ray photoelectron spectroscopy study into different cleaning
procedures performed on mild steel substrates

3.1 Introduction

Anaerobic acrylic adhesives are monocomponent systems that are able to cure via a redox radical mechanism at room temperature and in the absence of air. Anaerobic adhesives are mainly used in industry in the automotive, aeronautics and electronics fields because of the advantages associated with these anaerobic adhesives, primarily because mixing is not required, the handling time is 15 minutes, an ultimate strength is obtained after 24 hours, and they are eminently suited to the rhythms imposed by assembly lines. However, the surfaces of metals that are used in practical adhesion situations are not always clean, unless they are noble metals such as that of gold or platinum. Most will have a surface layer associated with them, which reflects the interaction of the metal with the atmosphere, such as that of a simple oxide. Thus, as with most adhesives, anaerobic adhesives require a decontamination of materials to be bonded and a surface treatment which can sometimes modify some characteristic of polymerisation.

The ability of adhesives to bond to a particular surface can critically depend on the chemical composition of that surface. In many instances, the surface chemical composition of a surface depends as much on the surface treatment history as on the chemical composition of the bulk material. ESCA (electron spectroscopy for chemical analysis) / XPS analysis has the capability of quantifying the surface chemical composition of a material, as well as providing information on the oxidation states of the elemental species present. XPS also has the sampling depth of the order of 5-10 nm, which is the region of the material surface directly involved in the adhesive process.

Many metal surfaces arrive from their original destination with a relatively thick layer of grease on the surface. This can be the result of a mechanical foaming process, which relies on a lubricant, and can be described by the generic term 'grease', or can be applied to protect the surface temporarily against corrosion. Prior to adhesion these surfaces must have these grease residues removed or 'degreased' to an acceptable level. Cleaning processes fall

into the following categories organic solvents, alkaline solutions or an emulsion of organic and aqueous solutions

Organic solvents, in the vapour and liquid phase, are very effective degreasing agents. The basic design of these degreasing tanks is as follows: an organic solvent is heated to provide a vapour blanket above the liquid. In this vapour phase the surface to be cleaned is placed for a short time, prior to total immersion into the liquid. Chlorinated hydrocarbons, such as trichloroethane, trichloroethylene and perchloroethylene, were widely used as degreasing solvents for metals. For health and safety reasons today, in situations where chlorinated solvents are used, the system is closed rather than fumes being vented directly into the atmosphere.

Alkaline cleaners offer an appealing alternative to organic solvent cleaners, with the principle of the alkaline cleaner being the saponification of the grease layer by the alkali to produce carboxylate salts. The reaction products are then removed from the surface by emulsification, peptization and dissolution. Other chemicals such as trisodium phosphate can be added to the alkali itself to aid wetting and emulsification, and this alkali cleaning procedure can be carried out as a dip process or a spray process, with agitation also playing an important role. In the metal finishing industry, these alkaline cleaners can sometimes be used in combination with an electric potential, referred to as electrolytic degreasing. This involves the metal being made the anode, therefore resulting in the build up of oxygen which can help to loosen the grease. The disadvantage of this process is that the metal itself may be dissolved slightly, depending on the potential applied. As with the anodic version, a cathodic type of this process can be used to provide electrochemical reduction of the surface oxide, which can be very effective. The disadvantage associated with this is the hydrogen produced at the cathode which can cause problems of embrittlement in some steels.

Emulsion cleaners are another type of degreasing product that can be applied directly to the soiled article. These emulsion cleaners are made up by a mixture of aqueous and organic phases and can be rinsed with water as an

emulsion of grease, solvent and water. These solutions are less effective on greasy surfaces compared to the alkaline and organic degreasing [1]

So, environmental issues have been the driving force behind many recent technological changes in industries today. Loctite Ltd. have evaluated a number of aqueous-based cleaning procedures in the hope that they can diverge away from the volatile organic compounds (VOC) used at present. In addition to reducing VOC emissions, these water-based formulations are not subject to the same waste disposal problems as their organic counterpart.

3.2 X-RAY Photoelectron Spectroscopy

3.2.1 Instrument

The instrument used in the following analysis was a VG-Microtech ESCA instrument (Figure 3.1).

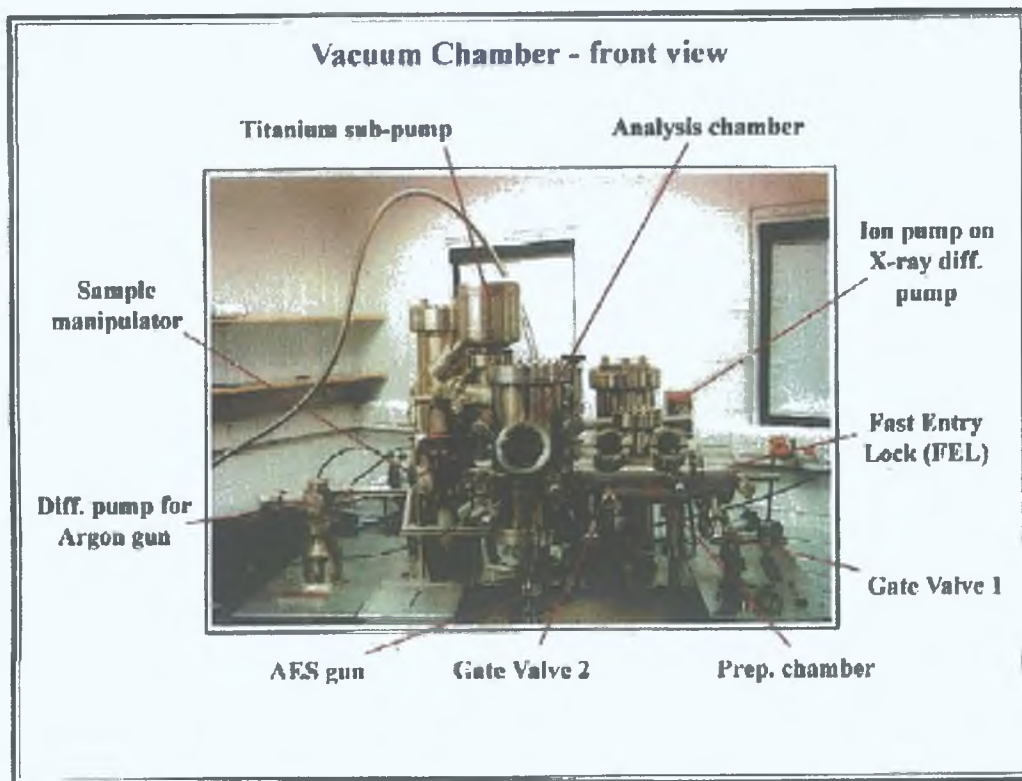


Figure 3.1: VG-Microtech ESCA

3.2.2 Introduction

Surface analysis by XPS involves irradiating a sample in vacuum with monoenergetic soft x-rays and energy analysing emitted core level electrons resulting from photoionisation [2,3]. The photoelectrons, which are emitted, are energy analysed producing a spectrum. Since the inelastic scattering length or 'mean free path' of low-energy electrons in solids is very small, the detected electrons originate from the top few atomic layers, making XPS a surface sensitive technique.

The basis of electron spectroscopy lies in the explanation that merited Einstein being awarded a Nobel Prize in 1921. The photoelectric effect in which Einstein stated that photons can cause the emission of electrons from a solid providing that the energy of the photon ($h\nu$) is greater than the workfunction (ϕ) of the solid. In 1914, Robinson and Rawlinson performed a study in which the photoemission from x-ray irradiated gold produced a distinguishable gold photoelectron spectrum. This was followed in 1951, when Steinhardt and Serfass used photoemission as an analytical tool. Throughout the period of 1950-1970, Kai Siegbahn and his research group developed the theory and instrumentation of ESCA, providing us with the method we use today. For his work in 1981, Kai Siegbahn was awarded the Nobel Prize in Physics [3]. In 1972, Brundle and Roberts performed UHV (ultra-high Vacuum) work, and XPS truly became a surface technique.

The principle behind XPS is as follows. The surface to be analysed is placed in a vacuum environment and irradiated with a monochromatic source of x-rays. The material emits electrons (photoelectrons) after direct transfer of energy from the x-ray photon to the core level electron (Fig. 3.2). These emitted electrons are subsequently separated according to their kinetic energy, in an electron energy analyser, and counted (detected). These photoelectrons have a kinetic energy (E_k), which is related to the X-ray energy ($h\nu$) and the binding energy (E_b) by the Einstein equation as seen in Equation 3.1.

$$E_b = h\nu - E_k - \phi \quad \text{Equation 3.1}$$

where E_k = kinetic energy of the emitted electrons (measured), $h\nu$ = energy of the x-ray source (known), E_b = binding energy of the electrons in the atom and ϕ = the work function, which is specific to spectrometer and sample.

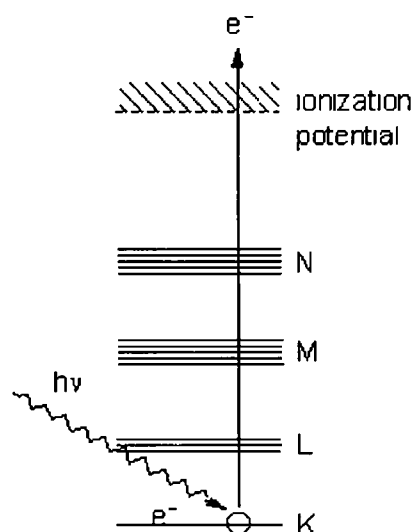


Figure 3 2 Energy level diagram for ejected electron

The binding energy of the emitted photoelectrons can be measured and is related to specific energy levels of atoms in the material. The spectrum obtained, which is unique for each element, is a plot of number of detected photoelectrons versus their kinetic energy (or binding energy). There are three types of peaks that are superimposed on a secondary background, core level peaks which are due to the photoelectrons that are emitted from the atomic (core) levels of the atom present, such as that of O1s which is the electron emitted from the 1s level of oxygen.

Auger peaks, which are broader peaks and are caused by Auger electrons which arise from the relaxation of an excited atom or ion following the photoemission of a core level electron. Figure 3 3 gives a schematic representation of what is involved in the generation of a $KL_1L_{2,3}$ Auger electron. Initially an electron must be ejected from a surface atom in the ground state (a K electron). This process leaves a 'hole' or vacancy which can be filled by an electron dropping down from a higher level, L_1 . This in turn releases considerable energy $E_K - E_{L1}$, part of which is absorbed by an electron in a higher orbital $L_{2,3}$ which is ejected with a kinetic energy representing the excess of $E_K - E_{L1}$ over $E_{L_{2,3}}$, this is known as a $KL_1L_{2,3}$ Auger electron. As energy must be conserved, the energy released by the electron dropping down must be

equal to the energy taken up by the ejection electron with kinetic energy E_{Auger} . Therefore one can write Equation 3.2

$$E_{\text{Auger}} = E_K - E_{L1} - E_{L2,3} \quad \text{Equation 3.2}$$

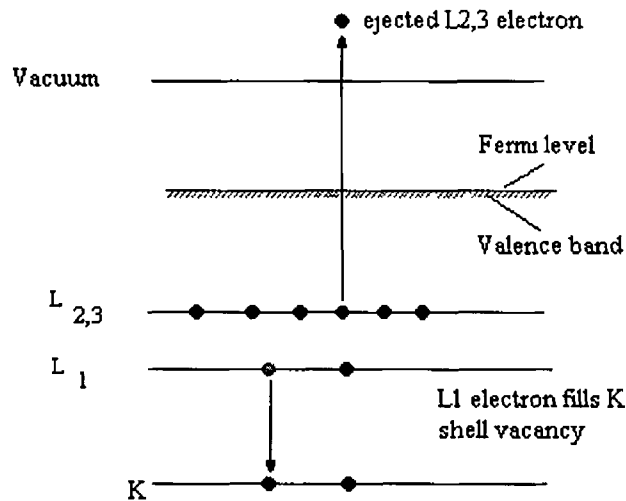


Figure 3.3 Energy level diagram for a KL₁L_{2,3} Auger electron emission

The third type of peak that can be superimposed on a secondary level background are valence band peaks. These are electrons that are emitted from the valence band or bonding orbitals which have a very low binding energy. These peaks are very weak and are of limited analytical value.

The basic components of any XPS instrument are

- (a) the vacuum system,
- (b) the x-ray source,
- (c) the electron energy analyser,
- (d) the data system,

3.2.3 Vacuum system

ESCA experiments must be performed under ultra-high vacuum for the following reasons

- 1 The photoelectrons must be able to travel from the sample through the analyser to the detector without colliding with gas phase particles
- 2 Components such as the x-ray source need vacuum conditions to operate
- 3 The surface composition of the sample must not change while being investigated

3.2.4 X-ray Source

Two factors must be taken into account when choosing the type of material for the X-ray source the characteristic X-ray energy must be high enough so that the core electrons which are ejected fall within this energy range, and secondly the line width must not limit the energy resolution needed for this technique. For analytical work involving XPS the best resolution is of the order of 1.0 eV.

Most spectrometers use only one or two anodes with Al (aluminum) – energy 1486.6 eV, line width 0.85 eV, and Mg (magnesium) – 1253.6 eV line width 0.7 eV, being the most common. Other anodes are Si (silicon) – 1739.5 eV line width 1.0 eV, Ti (titanium) – 4510 eV line width 2.0 eV and Cr (chromium) – 5417 eV line width 2.1 eV.

3.2.5 Analysers

The collection lens, the energy analyser and the detector are the three components that make up the analyser system. The most common type of energy analyser used in ESCA experiments is the electrostatic hemispherical analyser (Figure 3.4).

An electrostatic hemispherical analyser consists of two hemispheres of radius R_1 and R_2 . A potential of ΔV is placed across the hemispheres, such that there is an electric field between the two hemispheres, hence the outer hemisphere is negative and the inner hemisphere is positive with respect to the

centerline, $R_0 = (R_1 + R_2)/2$ The centre line potential is known as the pass energy. Most ESCA experiments are performed with constant pass energy. Once the electrons have passed through the energy analyser they are counted. As the electrons that arrive at the analyser exit have a range of different energies, the most efficient means of detection is to use a multichannel array to count the number of electrons leaving the analyser at each energy. Using a channel plate to magnify the electron current and a resistive strip anode to monitor the position and therefore energy of the electrons can achieve this. Another way would be to place a slit at the analyser exit so that only those electrons in a narrow energy range strike the detector. For this method a device called a channeltron is used to measure the number of electrons.

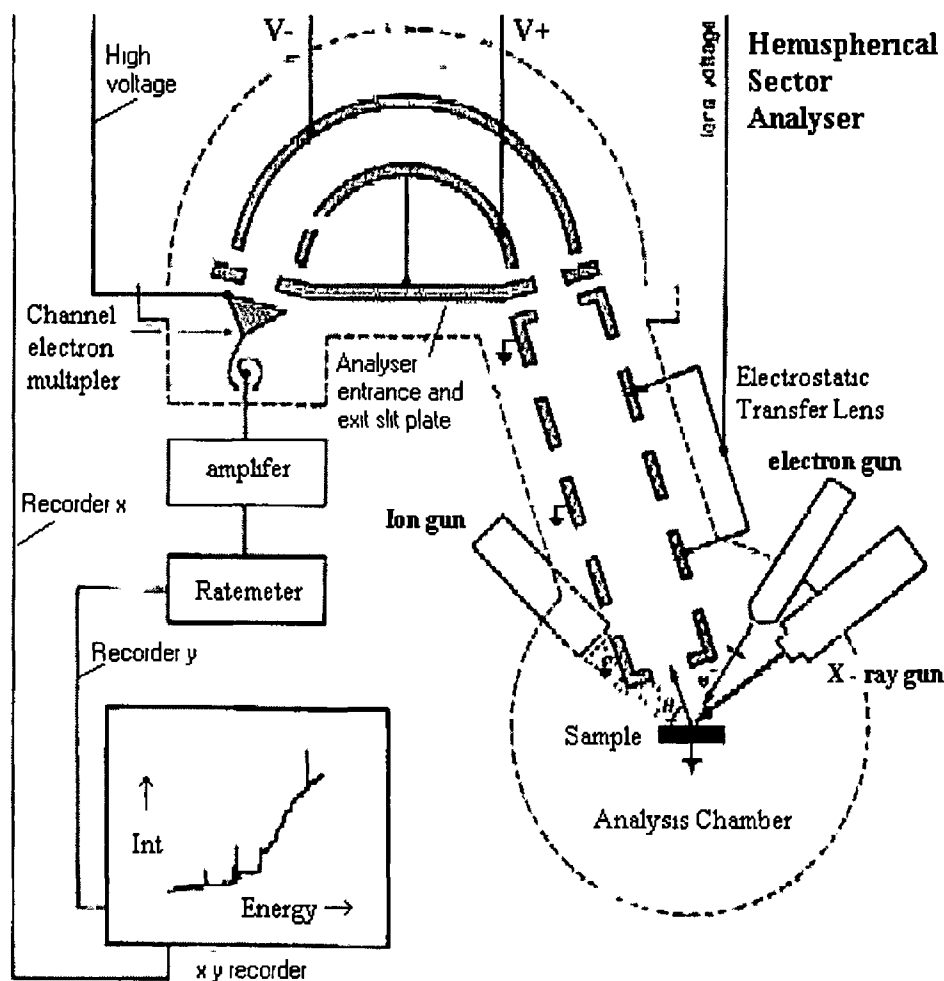


Figure 3 4 Schematic of electrostatic hemispherical analyser

XPS provides compositional information on approximately the top 10 nm of a sample surface from the elements lithium to uranium. From the binding energy one can learn some important facts about the sample under investigation:

- 1 Elements from which the sample is composed
- 2 The relative quantity of each element
- 3 Compositional depth profiling information
- 4 The chemical states of the elements present

Quantitative surface elemental composition can be extracted from peak areas or intensities, directly related to the quantity of that particular element at the sample surface, and most elements can be detected at $\geq 0.2\%$ atomic abundance.

Also, sampling depth in XPS is a function of the angle of emission of the photoelectrons. If one varies the 'take-off' angle or angle of emission of the photoelectrons towards grazing, the surface sensitivity is enhanced, as more surface atoms are probed with respect to bulk [4]. Angular resolved XPS provides a non-destructive depth profile to determine overlayer thickness, and distinguishes between substrate properties and surface phenomena, and allows one to reach conclusions on the orientation or depth distribution of different components on the surface.

Identification of chemical states comes from measurements of peak positions (based on Einstein's photoelectric equation), and changes in the binding energies of core electrons as a function of the chemical environment in terms of a 'chemical shift' in binding energy. Therefore, in addition to providing identification of atoms, XPS provides information on the charges associated with the bonding between atoms through subtle shifts in the exact binding energy values from $0.1 \rightarrow 10$ eV or more [5].

Chemical bonding has an effect on both the initial state energy of the atom and the final state energy of the ion that is created by emission of the

photoelectron. The changes that are brought about in the initial state energy by bond formation are basically due to the redistribution of electrons as the component atoms of a molecule or crystal come together in the solid state, and depend mainly on the electronegativities of the atoms involved. The creation of the ion by photoemission causes a further redistribution of the electrons that surround the target atom, and therefore have an impact on the final state energy. This process is known as electronic relaxation, and has an inter-atomic and an extra-atomic part, and is dominated by the polarizabilities of the atoms involved. Hence the presence of chemical bonding will cause binding energy shifts which are used to gain information of a chemical nature from the sample surface, i.e. oxidation states.

The popularity of XPS as an analytical technique for determining the chemical composition of surfaces is also attributed to its flexibility in analysing a wide variety of compounds, its high information content, and the valence state the elements present on the surface can be identified from the binding energy of the photoemission peak.

3.2.6 Treatment of results

Throughout this investigation the quantification was determined by using the atomic sensitivity factors from Briggs and Seah [2]. Methods have been developed using peak area and peak height sensitivity factors. For a sample that is homogeneous in the analysis volume, the number of photoelectrons per second in a specific spectra peak is given by equation 3.3

$$I = n f \sigma \theta \lambda y A T \quad \text{Equation 3.3}$$

where, n = number of atoms of the element per cm^3 of the sample, f = x-ray flux, photons/ $\text{cm}^2\text{-sec}$, σ = Photoelectric cross-section for the atomic orbital of interest, cm^2 , θ = Angular efficiency factor for instrumental arrangement based on the angle between the photon path and the deflected electron, λ = mean free path of the photoelectrons in the sample, y = efficiency in the photoelectric

process for formation of photoelectrons of the normal photoelectron energy, A = area of sample from which photoelectrons are detected and T = detection efficiency for e⁻s emitted from the sample Rearranging equation 3 3

$$n = I / f \sigma \theta \lambda y A T$$

Equation 3 4

The denominator in equation 3 4 can be defined as the atomic sensitivity factor, S

Figure 3 5 outlines an example how practical quantitative measurements were calculated using the atomic sensitivity factor, S [2]

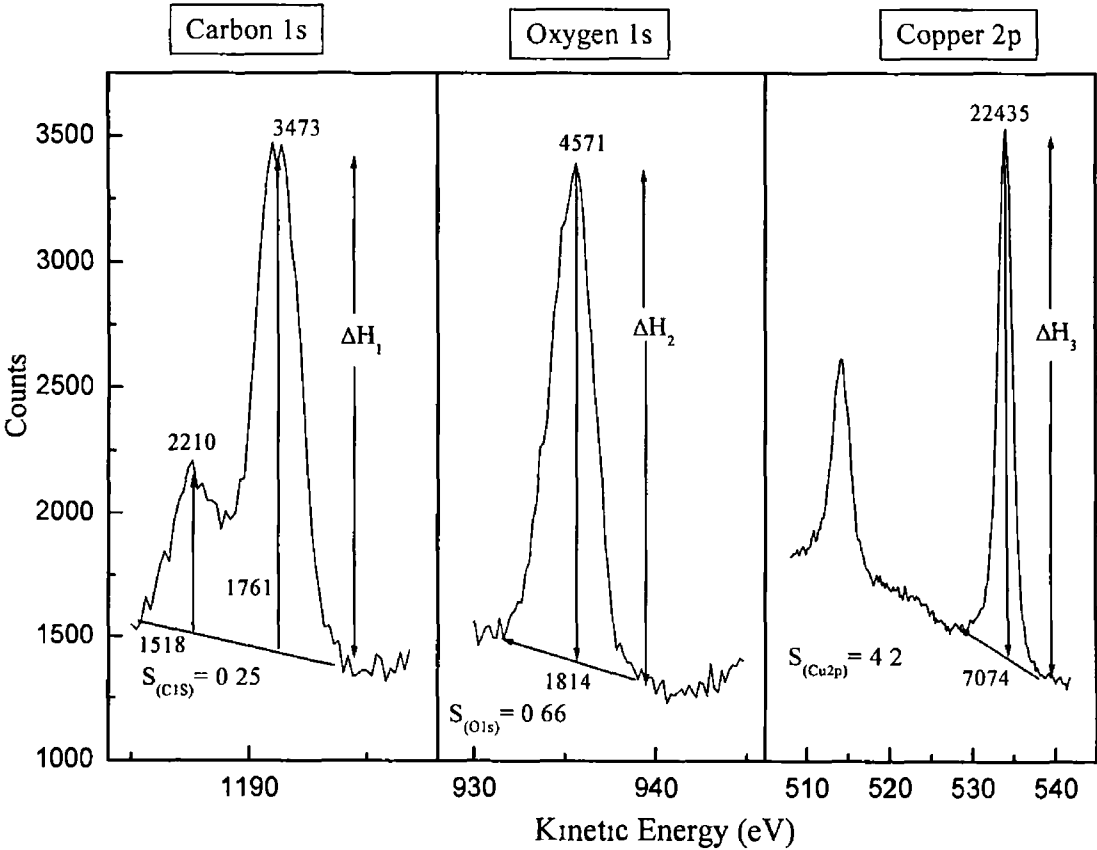


Figure 3 5 Example quantitative calculation for evaluation of the composition of the surface in atomic percentage, where $\Delta H_1/S_{(C1s)}$, $\Delta H_2/S_{(O1s)}$ and $\Delta H_3/S_{(Cu2p3/2)}$ are evaluated and the relative composition in atomic % calculated

3.3 Experimental

3 3 1 Materials

All work reported here was performed on mild steel lapshears and pin/collar assemblies which were supplied by Loctite. The cleaning procedures carried out on the test pieces were performed at Loctite and then returned for analysis.

3 3 2 Sample preparation

Lap shears and pin/collar assemblies

The lapshears and pin/collar assemblies were cut to the appropriate size, as they proved to be too large for analysis. The lapshears were cut down to 1cm x 1cm using a hacksaw, whereas the pin/collar assemblies were cut down to 1cm x 1cm utilizing a milling machine. Surface analyses studied were carried out on the exterior surface of the pins and the interior surface of the collars, as these are the two surfaces involved in bonding. All samples were then placed on a sample holder and held in place using silver epoxy glue. In order to realize a working pressure within a reasonable time scale the silver epoxy was allowed 24 hrs to dry, therefore minimizing outgassing during pumpdown.

For the study into the cleaning procedures, the lap-shears were sent to the National Physical Laboratory, in Teddington, Middlesex to be polished to a mirror finish using 1-micron diamond paste. They were then subjected to the aqueous and organic cleaning procedures in Loctite before being analysed.

3 3 3 Procedures

XPS of mild steel lap-shears

The optimum scanning parameters for the analysis of the mild steel lap shears and pin/collar assemblies were as follows,

| | |
|--------------------------|-----------|
| X-ray line Al K α | 1486.6 eV |
| Step increment | 1 eV |
| Dwell time | 0.5 s |
| Analyser pass energy | 50 eV |
| Number of scans | 10 |

Quantitative measurements were calculated using the atomic sensitivity factor, S and outlined in Figure 3.5

The photoelectrons were excited using Al K α radiation –photon energy 1486.6 eV, the source was operated at 15 KV and 20 mA, during data acquisition the chamber pressure was kept below 5×10^{-8} mbar

3.4 Results and Discussion

3.4.1 Study to determine the surface composition of untreated lapshears

The initial experiment was designed to establish the surface chemical composition of the mild steel lapshears supplied by Loctite. These lapshears had no pre-treatment performed on the surfaces, i.e. as received. The lapshears were analysed using XPS and the composition in atomic percentage was calculated. Figure 3.6 shows a spectrum, which was obtained for an untreated lapshear, indicating the peaks of interest. The results recorded were averaged over 4 spectra for each sample, Table 3.1, and a plot of the uncertainty in the surface composition resulting from this analysis is presented in Figure 3.7(a), (b), with the overall % error in the figures calculated outlined in Table 3.2.

| Chlorine | Carbon | Calcium | Oxygen | Manganese | Iron |
|----------|--------|---------|--------|-----------|------|
| 1.5 | 42.3 | 1.7 | 38.6 | 0.6 | 15.3 |
| 1.4 | 44.2 | 1.5 | 37.7 | 0.4 | 14.8 |
| 1.6 | 41.9 | 1.4 | 40.8 | 0.5 | 13.8 |
| 1.4 | 41.9 | 1.6 | 39.8 | 0.4 | 14.9 |

Table 3.1 Experimental values calculated (atomic %) for the elements found present on the surface of the untreated lapshears after XPS analysis

From the above results it can be seen that carbon and oxygen make up most of the surface of the untreated lapshear, i.e. C $42.6 \pm 2.3\%$ and O $39.3 \pm 3.1\%$ respectively, while iron was the main metal detected on the surface at $14.7 \pm 1.5\%$. A small percentage of chlorine, calcium and manganese were also detected on the surface in the following quantities, Cl $1.5 \pm 0.2\%$, Ca $1.6 \pm 0.3\%$ and Mn $0.5 \pm 0.2\%$. As already stated, the surfaces of metals used in adhesion are far removed from a clean metal surface. The surfaces of metals will have a layer which reflects the interaction of the metal with the atmosphere and water vapour. On exposure of the metal surface to the atmosphere/environment, the presence of many adventitious materials such as salts, sulphides, polar and non-

polar organics and adsorbed water also metal oxides and hydroxides, result from the reaction between substrate and the environment [6] The oxide layer may take the form of a simple oxide but in the case of mild steel it is most likely to be an oxyhydroxide phase This inorganic layer can be covered with a more labile mixture of adsorbed water and organic contaminants deposited during subsequent air exposure This would explain the high concentrations of carbon and oxygen found on the surface of the lapshear

These initial experiments gave an indication of what elements are present on the surface of the lap shears supplied by Loctite, so a comparison can be made between these untreated samples and samples that have being subjected to the cleaning procedures, prior to analysis

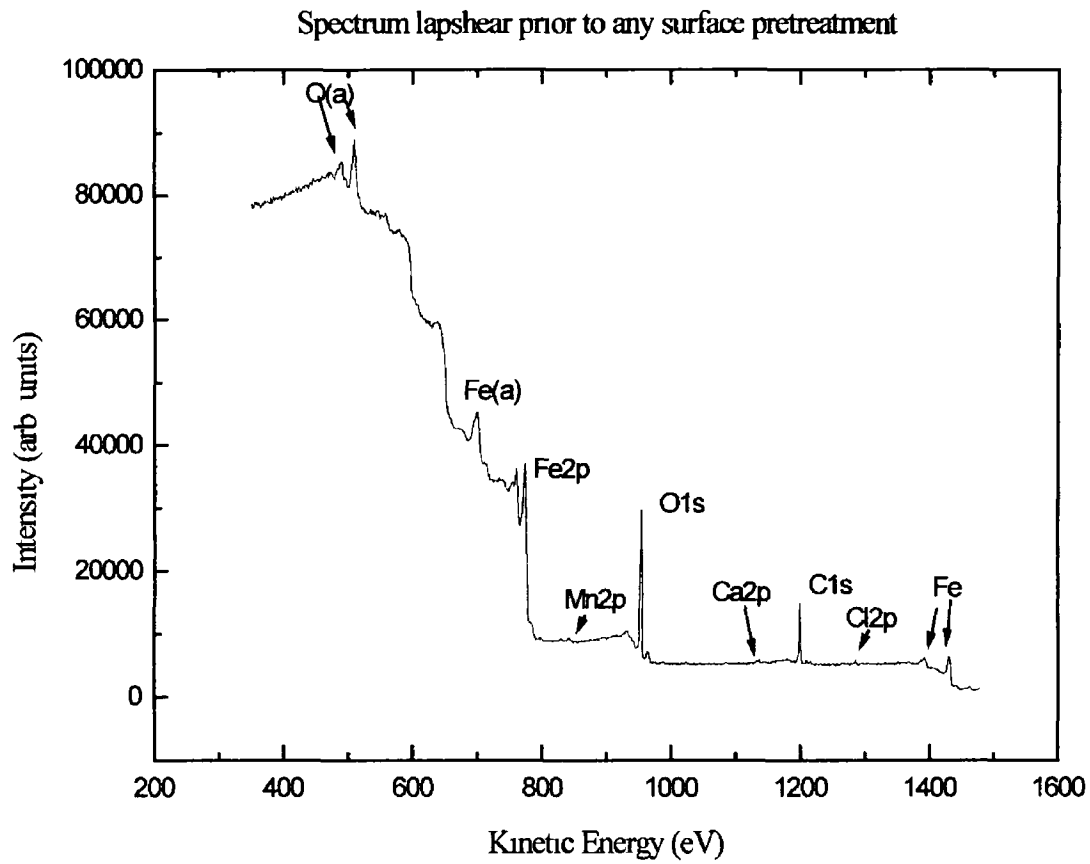


Figure 3 6 Spectrum obtained for untreated lapshear, indicating peaks of interest

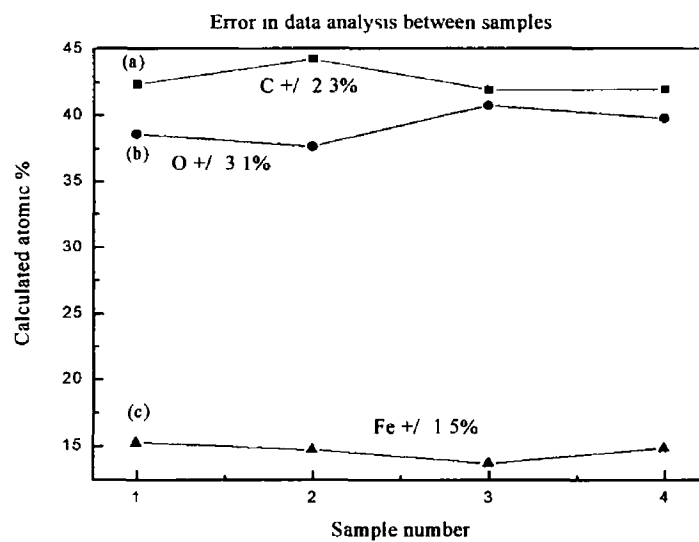


Figure 3.7(a) Error in calculated data between four samples a) \blacksquare C \pm 2.3%, b) \bullet O \pm 3.1% and c) \blacktriangle Fe \pm 1.5%

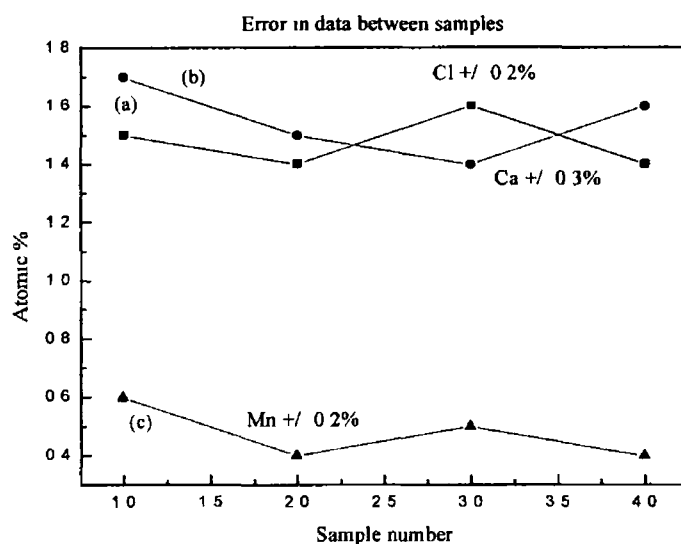


Figure 3 7(b) Error in calculated data between four samples a) \blacksquare Cl $\pm 0.2\%$,
b) \bullet Ca $\pm 0.3\%$ and c) \blacktriangle Mn $\pm 0.2\%$

| Element | Carbon | Oxygen | Iron | Chlorine | Calcium | Manganese |
|---------|-------------|-------------|-------------|-------------|-------------|--------------|
| % Error | $\pm 2.6\%$ | $\pm 3.5\%$ | $\pm 4.3\%$ | $\pm 6.5\%$ | $\pm 8.3\%$ | $\pm 20.1\%$ |

Table 3 2 Calculated percentage error between different samples

3 4 2 Study into the effect cleaning procedures have on the surface composition of lap shears

Two different types of cleaning procedures were carried out on the lapshears
These two cleaning procedures were

1 Degreased by organic vapour phase

This technique involves the heating of organic solvents which in turn provides a vapour blanket above the liquid and the substrate to be cleaned is positioned for a short time interval in this vapour phase, before being immersed into the liquid. The organic solvent used was trichloroethylene (TCE)

2 An aqueous cleaning procedure This procedure is as follows

The substrate to be cleaned is placed in a degreasing basket, the basket is suspended in the centre of the cleaning tank containing a 5% solution (by volume) of Henkel P3-neutrapon 5088 in deionised water with ultrasonication for 5 minutes at 58 → 61°C (136 → 142°F). The basket was removed from the cleaning tank and the excess cleaning solution allowed to drain off for 10 seconds. The basket was then placed in the first rinse tank containing deionised water at ambient temperature without ultrasonication for 30 seconds. The basket was then removed from this first rinse tank with the excess rinse water being allowed to drain for 10 seconds. The basket was then placed in a second rinse tank at ambient temperatures without ultrasonication for 20 seconds and then removed and the excess rinse water allowed to drain off for a further 10 seconds. The basket was then placed in a high temperature forced-air drier at 96.1 → 98.9°C (205 → 210°F) for seven minutes. The specimens were allowed to cool to room temperature in an atmosphere of < 60% R.H., if specimens were not used within 1 hour they are stored in a desiccator till needed [8]

Sample preparation and experimental conditions remained the same throughout this experiment. The results for four samples are reported in Table 3 3 and 3 4, with the spectra recorded shown in Figure 3 8, and 3 9 for the lapshear that was subjected to the degreased organic vapour clean and the aqueous cleaning procedure respectively

| Carbon | Calcium | Nitrogen | Oxygen | Manganese | Iron | Sodium | Silicon |
|--------|---------|----------|--------|-----------|------|--------|---------|
| 58 40 | 0 4 | 3 8 | 27 3 | 0 9 | 6 2 | 0 8 | 2 2 |
| 59 10 | 0 6 | 3 9 | 25 3 | 0 5 | 7 1 | 0 9 | 2 6 |
| 60 60 | 0 5 | 3 2 | 24 6 | 0 7 | 6 4 | 1 3 | 2 7 |
| 57 80 | 0 5 | 3 6 | 25 2 | 1 1 | 7 9 | 1 1 | 2 8 |

Table 3 3 Experimental values calculated (atomic %) for the elements found present on the lapshear surface after degreasing by organic vapour phase

| Carbon | Calcium | Nitrogen | Oxygen | Iron | Sodium | Silicon |
|--------|---------|----------|--------|------|--------|---------|
| 53 60 | 1 4 | 1 7 | 31 0 | 7 4 | 0 8 | 4 1 |
| 53 70 | 1 3 | 1 6 | 29 7 | 8 6 | 0 9 | 4 2 |
| 51 50 | 1 4 | 1 5 | 31 3 | 9 2 | 1 2 | 3 9 |
| 50 90 | 1 7 | 1 4 | 32 6 | 9 0 | 0 8 | 3 6 |

Table 3 4 Experimental values calculated (atomic %) for the elements found present on the lapshear surface after an aqueous cleaning procedure

XPS analysis and quantification of the metal surface of the lapshears produced the atomic percentage calculations for each element and a corresponding uncertainty in these calculations are given in Table 3 5

| Sample | C | Ca | N | O | Mn | Fe | Na | Cl | Si |
|-----------|----------|----------|----------|-----------|---------|----------|---------|---------|----------|
| Untreated | 42.6±2.3 | 1.6±0.3 | 0 | 39.3±3.1 | 0.5±0.2 | 14.7±1.5 | 0 | 1.5±0.2 | 0 |
| Organic | 58.9±2.8 | 0.5±0.2 | 3.6±0.7 | 25.6±2.7 | 0.8±0.6 | 6.9±1.7 | 1±0.5 | 0 | 2.6±0.6 |
| Aqueous | 52.4±2.8 | 1.45±0.4 | 1.55±0.3 | 31.15±2.9 | 0 | 8.55±1.8 | 0.9±0.4 | 0 | 3.95±0.6 |

Table 3 5 Averages and errors calculated from the compositions in atomic % of the lapshear surfaces following different cleaning procedures

Carbon was present on all of the lapshears, and comprises a large portion of the surface chemical composition. For the untreated lapshear the % carbon found on the surface was $42.6\% \pm 2.3$, which was increased by 10% to $52.4 \pm 2.8\%$ for the aqueous treatment and was even higher again at $58.9 \pm 2.8\%$ for the organic vapour degreased lapshear. Through the cleaning process it would seem that some of the cleaning material remained attached to the metal surface. It would seem logical that these two cleans would produce surfaces high in carbon and its associated chemisorbed water, especially with the organic wash.

The oxygen content of these modified surfaces varies considerably from one surface to another, oxygen making up the second largest percentage of elements found on these surfaces. For the untreated surface the % oxygen present on the sample was calculated at $39.3 \pm 3.1\%$, and calculated at $25.6 \pm 2.7\%$ and $31.15 \pm 2.9\%$ for the organic and aqueous-treated surface respectively. Although surfaces in ambient conditions will have an oxide layer associated with them, both of these cleaning processes decrease the amount of oxygen found present on the surface, with the organic wash being more effective in the removal of surface oxides.

Iron, which is one of the main components of mild steel, is present on all surfaces, which would be expected. The highest content of iron found on these surfaces was on the untreated surface which contained $14.7 \pm 1.5\%$, with a decrease in the iron content for the subsequent cleans of $6.9 \pm 1.7\%$ and $8.55 \pm 1.8\%$ for the organic and aqueous cleans respectively. This was not the expected result, as one would have expected a rise in the metal content after

cleaning, and from the above results the untreated surface contained a higher percentage of iron. An explanation, which could be put forward to explain the above results is that when dealing with percentages, a decrease in one element's percentage must subsequently lead to an increase in another element percentage. For the untreated sample the % of carbon detected on the surface was $\approx 43\%$, combining this with the oxygen content a total value of $\approx 83\%$ was calculated for these two elements. So for the organically treated and aqueous treated surfaces the combination of oxygen and carbon was $\approx 83\%$ also, so the distribution of the other elements that present themselves on the substrate surface must be split between the 17% left.

Chlorine was found in a small quantity on the untreated lapshear $1.5 \pm 0.2\%$. Chlorine was not present on either of the cleaned surfaces; it was however expected to be present on the surface that was degreased by the organic solvent, as the solvent used was that of trichloroethylene. Calcium was present on all of the surfaces, with the calcium content nearly similar for the untreated and aqueous surfaces, at $1.6 \pm 0.3 \%$ and $1.45 \pm 0.4 \%$ respectively, and a decrease in the calcium concentration to $0.5 \pm 0.2\%$ for the organic wash. These elements could be due to contamination, due to sample handling, as prior to analysis they were placed in a dessicator that contained CaCl_2 , which could have chemically reacted with the specimen. If this was the case, the organic wash appears to protect the underlying substrate more efficiently from environmental contamination, as there was no chlorine detected and a decreased amount of calcium found on this particular surface.

Manganese was detected on the untreated lap shear and also on the lap shears that had being subjected to the organic vapour phase cleaning, but was absent from the samples that had the aqueous cleaning procedure performed on them.

The principal difference observed between the untreated lap shears and the lap shears that were treated with a cleaning procedures, was the presence of silicon, nitrogen and sodium found on the cleaned surfaces. It was surmised that

washing with either the aqueous or the organic clean introduces sodium, nitrogen and silicon onto the surface. The reason that these signals are introduced by cleaning and not revealed by the clean is that the iron signal, which was definitely from the substrate, decreases following the cleaning procedure. Generally the effect that the cleaning procedures had on the lap shear surfaces was to increase the carbon signal, this in turn led to a decrease in the oxygen signal, which also may represent the removal of surface oxides.

Following on from the above experiment it was decided to polish the lapshears to a mirror finish, prior to any surface pre-treatment, and then subject them to the cleaning regimes of degreasing by organic vapour phase and the aqueous cleaning practice. The reason for using polished samples is that they offer a more controlled surface composition from that of the unpolished lapshears that have been previously used.

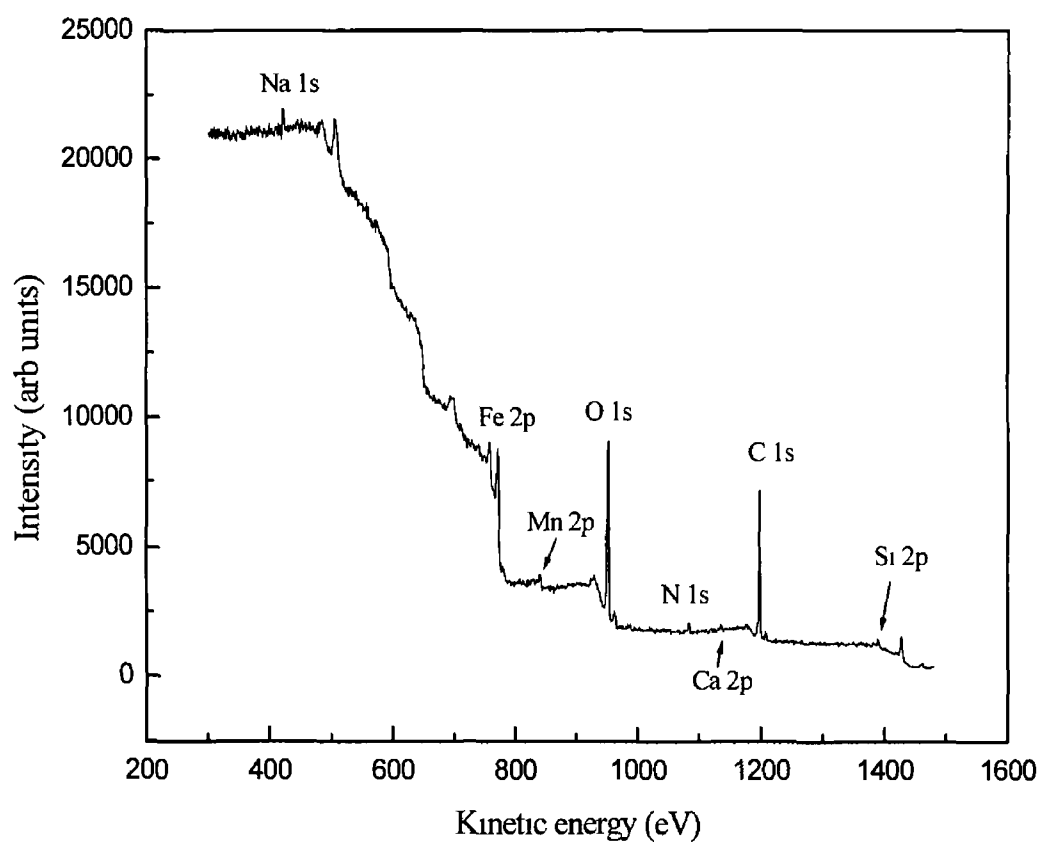


Figure 3 8 Spectrum obtained for lapshear after treatment with an organic vapour degrease cleaning procedure

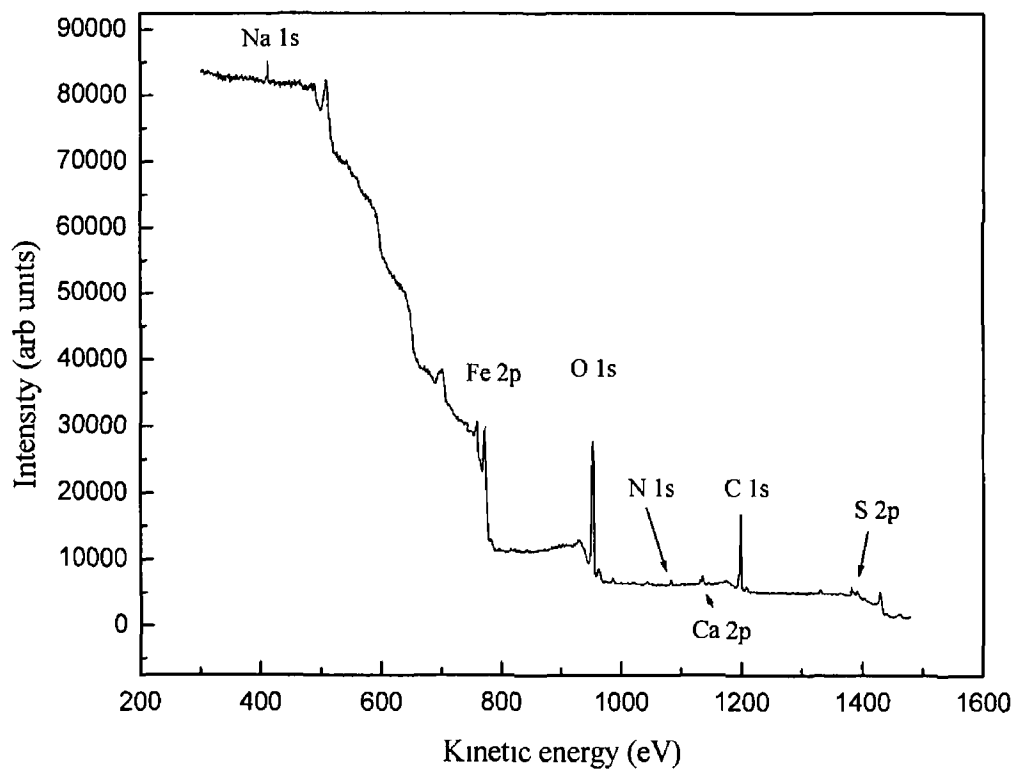


Figure 3 9 Spectrum obtained for lapshear after treatment with an aqueous cleaning procedure

3 4 3 Study into the effect of cleaning procedures on polished lap shears

In an attempt to make the surface analysis measurements more meaningful, polished lapshears were used in subsequent experiments. These lapshears had much reduced surface roughness and were therefore more 2-dimensional than the as received lapshears studied in the previous section.

As already mentioned the lap shears were cut to size, and then sent to the National Physical Laboratory, in Teddington, Middlesex, to be polished to a mirror finish using 1-micron diamond, and a synthetic felt/velvet cloth supplied by Buehlers. The polished pieces were then returned to Loctite, and subjected to both cleaning procedures, as described in the previous section (3 3 2). The results obtained were averaged over three samples and are presented in Tables 3 6-3 8. Spectra recorded can be seen in Figure 3 10-3 12.

| Lapshear | Silicon | Carbon | Calcium | Nitrogen | Oxygen | Iron |
|----------|---------|----------|---------|----------|----------|---------|
| 1 | 3 9 | 52 2 | 3 5 | 1 2 | 36 9 | 2 3 |
| 2 | 3 6 | 51 1 | 3 1 | 1 5 | 38 2 | 2 5 |
| 3 | 4 | 52 2 | 3 6 | 1 5 | 36 5 | 2 2 |
| % Error | 3 8±0 4 | 51 8±1 1 | 3 4±0 5 | 1 4±0 3 | 37 2±1 7 | 2 3±0 3 |

Table 3 6 Composition in atomic % for the polished lapshears

| Sample | Silicon | Carbon | Calcium | Nitrogen | Oxygen | Iron | Chlorine |
|---------|---------|----------|---------|----------|----------|---------|----------|
| 1 | 4 5 | 55 3 | 1 8 | 1 7 | 33 5 | 2 2 | 1 0 |
| 2 | 4 8 | 53 6 | 1 9 | 1 9 | 34 2 | 2 4 | 1 2 |
| 3 | 4 9 | 55 1 | 1 7 | 2 1 | 32 4 | 2 7 | 1 1 |
| % Error | 4 7±0 4 | 54 7±1 7 | 1 8±0 2 | 1 9±0 4 | 33 4±1 8 | 2 4±0 5 | 1 1±0 2 |

Table 3 7 Composition in atomic % for the polished lapshears after degreasing by organic vapour phase

| Lapshear | Carbon | Nitrogen | Oxygen | Iron |
|----------|----------------|---------------|----------------|---------------|
| 1 | 65.2 | 3.4 | 28.0 | 3.1 |
| 2 | 65.4 | 3.3 | 28.2 | 3.2 |
| 3 | 64.8 | 4.2 | 27.5 | 3.5 |
| % Error | 65.1 \pm 0.6 | 3.6 \pm 0.9 | 27.9 \pm 0.7 | 3.3 \pm 0.4 |

Table 3.8 Composition in atomic % for the polished lapshears after cleaning by an aqueous clean

The XPS results obtained for the polished lapshears show that carbon at $\approx 52\%$ and oxygen at $\approx 37\%$ are still the main components present on the lap shear surface, prior to any clean. In comparison to the unpolished and as received lapshear, the polishing produces an increase in the carbon content of approximately 10% with the oxygen content only varying by about 2% between the two samples. Silicon and calcium are present on the polished sample in the following percentages $3.8 \pm 0.4\%$ and $3.4 \pm 0.5\%$ respectively. Although calcium was present on the unpolished lapshear, the percentage recorded was only 1.6%, and there was no silicon present on the untreated sample. This would indicate that its presence was due to the polishing process. The percentage of nitrogen and iron detected was small at $1.4 \pm 0.3\%$ and $2.3 \pm 0.3\%$ respectively. The iron content had decreased from 14.7% with the unpolished sample to approximately 2.3% for the polished sample.

The reason for the high oxygen and carbon content found on all the analysed surface is attributed to the fact that metal surfaces which have been exposed to the atmosphere have an oxide layer on them [7]. The thickness of this oxide layer depends on the nature of the metal and the environment. Some metals form thin adhering oxides that can passivate the surface and prevent continued oxidation, e.g. aluminium. Iron forms oxides that continue to grow particularly in humid conditions, the various types of oxides for iron are as follows: Fe_2O_3 , Fe_3O_4 and FeO . The formation of a metal oxide initially

involves chemisorption of oxygen on the surface, followed by a chemical reaction to form the oxide

These metal oxides, in ambient conditions are covered with organic surface contamination and water adsorbed from the atmosphere, hence the high carbon content. Other sources of contamination can be as a result of oils or lubricants. Surface contamination can also occur from the bulk of the metal [7]. For example, iron that contains only 10 parts per million of carbon has been shown to form a carbon-rich structure on its surface upon heating or straining. Other species, apart from carbon, have been shown to diffuse from the interior of metals to their surfaces, these elements include sulphur, nitrogen, boron and oxygen.

From the composition in atomic % of the polished lapshears, very little difference was detected between the untreated and the trichloroethylene treated surface. The iron content calculated varied from $2.3 \pm 0.3\%$ for the polished lapshear, to $2.4 \pm 0.5\%$ for the organically washed lapshear. The main difference between these lapshears is that chlorine was present on the surface of the organically washed lapshear, attributed to the chlorine in trichloroethylene which was the solvent used in the degreasing process. In general, therefore, the organic wash had no effect on the surface composition except for the introduction of chlorine, which is not part of the substrate but a by-product of the wash.

Comparing the results obtained for the untreated polished lapshear and the aqueous washed polished lapshear, it would seem that this "wash" eliminated silicon and calcium from the substrate surface, leaving carbon, oxygen, nitrogen and iron present on the surface only. These elements are present on all surfaces analysed indicating that they are the constituent components of the substrate, and therefore enhanced by the aqueous wash. This result would also indicate that there is no residue left over from the aqueous wash in comparison to the organic clean, which left chlorine detectable on the surface.

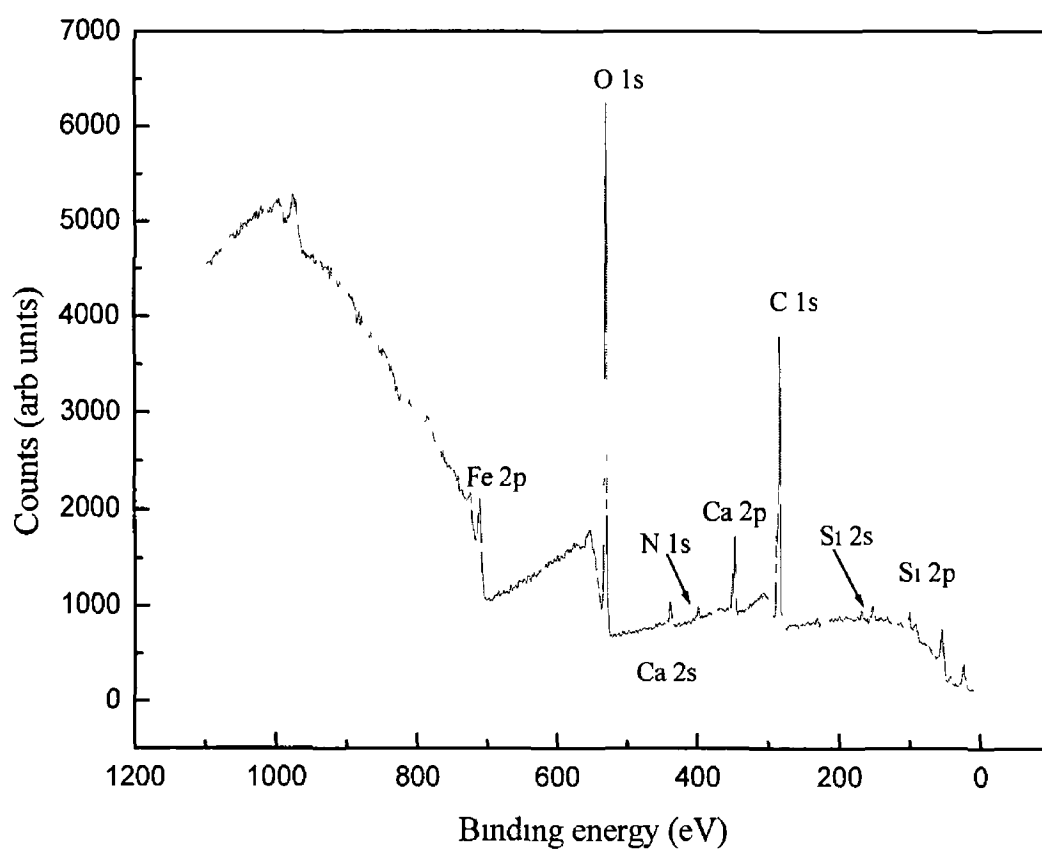


Figure 3 10 Spectrum obtained for lapshear after polishing and prior to any cleaning procedures

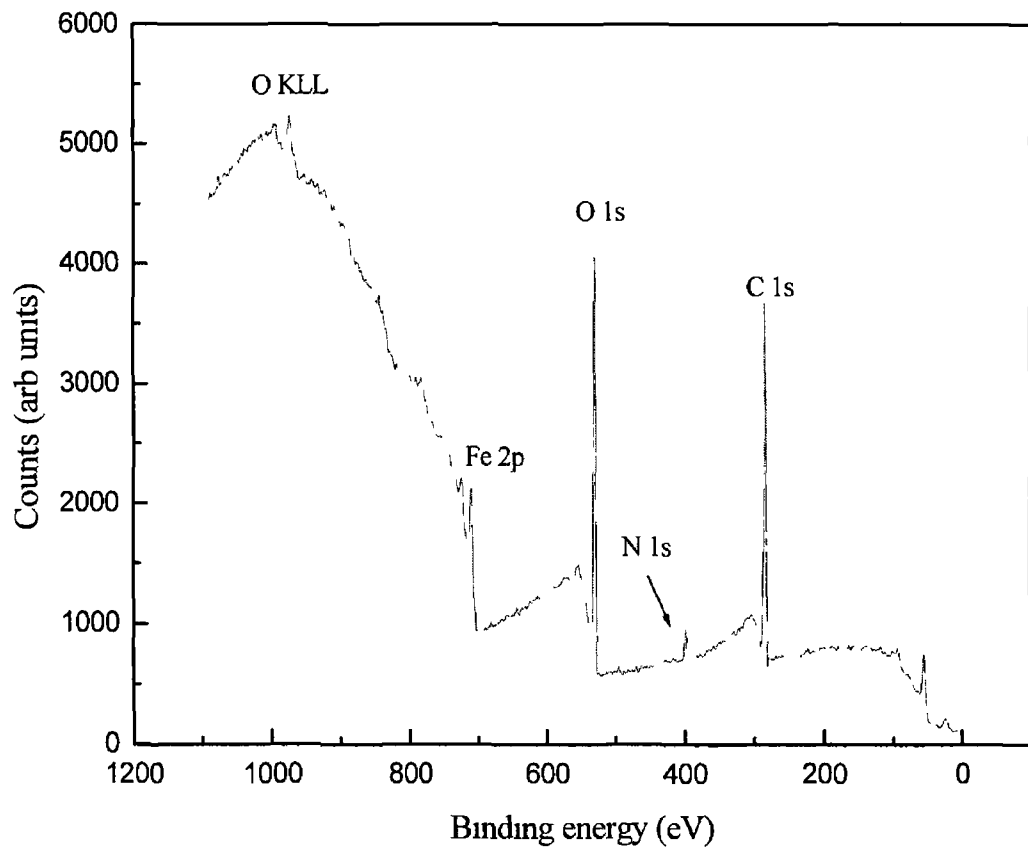


Figure 3 11 Spectrum obtained for lapshear after polishing and an aqueous clean procedure

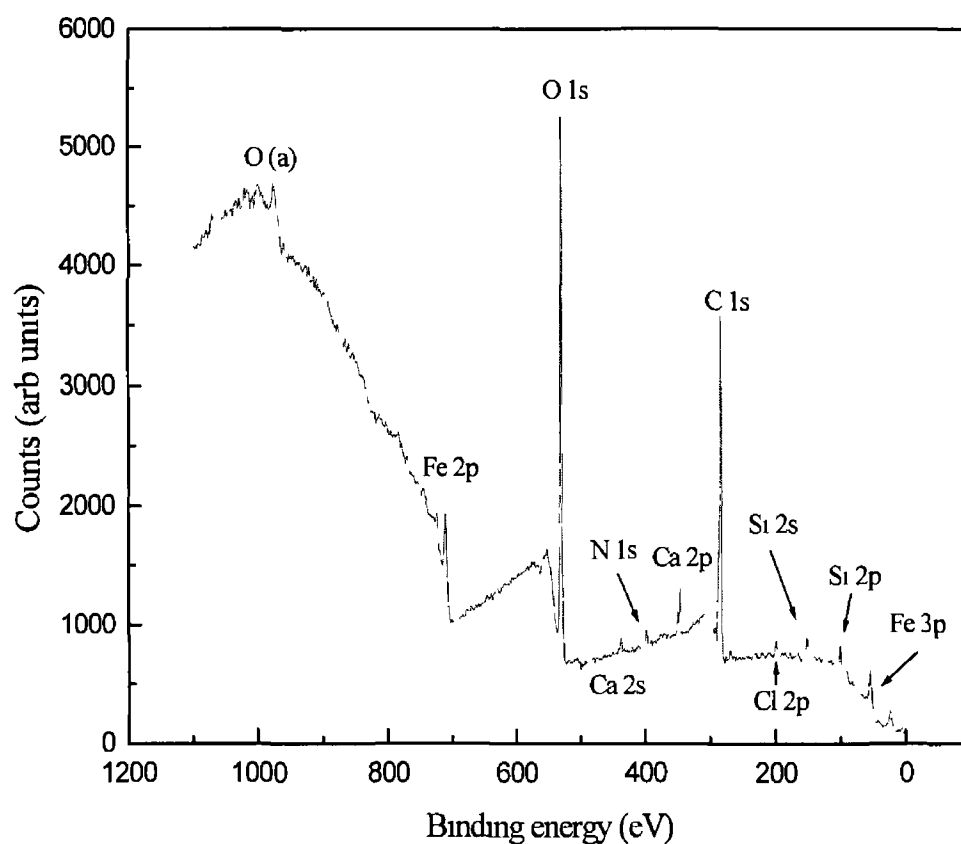


Figure 3 12 Spectrum obtained for lapshear after polishing and an organic vapour degrease

3 4 4 Pin/collar assemblies

The above experiments were carried out on pin/collar assemblies, with XPS analysis performed on the exterior surfaces of the pins and the interior surfaces of the collars, as these were the two surfaces involved in bonding. The sample preparation and analysis conditions were as for the lapshears (see section 3 4 2). The results recorded are summarised as follows

For both the pins and the collars analysed prior to any polishing regime the carbon signal was consistently twice as large as that recorded for the lapshears at $\approx 80\%$ of the surface. For the cleaning techniques, that of the organic vapour degrease offered a decrease in the carbon signal by $\approx 3\%$ and for the aqueous clean, the carbon composition of the surface was significantly altered by $\approx 20\%$. For this aqueous clean, the reduction in the surface carbon signal resulted in the surface oxygen signal increasing by a factor of 2-3, which was accompanied by a noticeable surface discolouration indicating the possible formation of iron oxides, suggesting that the surface carbon layer present on the surface prior to the aqueous cleaning procedure essentially protects the surface from significant ambient oxidation.

After polishing was performed on the pin/collar surfaces, the XPS results recorded were more representative of the mild steel surface, and more in agreement with those calculated for the lapshears. For these pin/collar assemblies following polishing and subjected to the aqueous clean, only the following four elements were determined to be present on the surface, that of carbon at $\approx 61\%$, oxygen at $\approx 32\%$ with nitrogen at $\approx 4\%$ and iron present at $\approx 3\%$. From these results it was concluded that the aqueous rinse, performed on a polished substrate, produced the best results with respect to the clean and also to the true nature of the surface of the substrate which was composed of carbon, oxygen, nitrogen and iron.

3.5 Conclusions

Throughout this chapter mild steel surfaces were analysed using XPS and their surface composition calculated. These surfaces were put through different cleaning procedures and XPS was utilised to determine which cleaning procedure produced a result that was more indicative of the actual composition of the underlying substrate.

The polished lap shear that was subjected to the aqueous rinse produced results that appeared to be more representative of the real surface. This polished surface was composed of the following elements: carbon, oxygen, iron and nitrogen, and as previously stated these elements appear to be present in all samples analysed, indicating that they are part of the substrate. These results were interpreted in terms of the aqueous clean removing other surface contaminants and indicating that no residue is left over from this aqueous wash.

This aqueous cleaning procedure also deals with environmental pressures that are placed on industry today and offers a more efficient alternative to organic solvents and methods previously used within the industry. Loctite now employs this aqueous cleaning procedure at present, as a consequence of the above study.

3.6 References

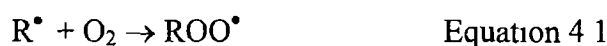
- [1] Watts, J F, "Handbook of Adhesion" Packham, D E (Ed), Longman Scientific and Technical, New York (1992) 109
- [2] Briggs, D , Seah, M P "Practical Surface Analysis by Auger and X-ray Photoelectron Spectroscopy", Wiley, New York (1994)
- [3] Vickerman, J C , "Surface Analysis-The Principal Techniques", Wiley, Chichester (1997)
- [4] Fadley, C S , Prog Surf Sci , 16 (1984) 275
- [5] Moulder, J F , Stickle, W F , Sobol, P E and Bomben, K D , "Handbook of Photoelectron Spectroscopy", Perkin-Elmer Corporation, Physical Electronics Division Eden Prairie, (1992)
- [6] Bolger, J C and Micheals, A S in "Interface conversion for Polymer Coatings", Weiss P, and Cheever G D (Eds), Elsevier, New York (1968) 3
- [7] Buckley, D H , in "Surface Effects in Adhesion, Friction, Wear and Lubrication", Elsevier, New York, (1981)
- [8] Leonard R G , Loctite (Irl) Ltd , *private communication*

Chapter 4

An X-Ray Photoelectron Spectroscopy Study into the effect
individual cure components of anaerobic adhesives produce on a
copper substrate surface

4.1 Introduction

Anaerobic adhesives and sealants are based on acrylic functionalised monomers and cure by a redox-initiated free radical polymerisation process. These adhesives derive their name due to their trait of requiring a relatively oxygen-free surrounding for proper cure, as oxygen inhibits free radical polymerisation by the mechanism shown in Equation 4.1, [1] thus making them ideal adhesives for the bonding and sealing of close-fitted metal components.



The formulations of anaerobic adhesives depend upon the properties that are sought in the cure and uncured compositions, but typically anaerobic adhesives contain the following five basic components: monomers (typically methacrylate monomers), initiators/accelerators of redox-initiated free radical polymerisation, stabilisers/inhibitors and modifiers [2]. The aspect of anaerobic polymerisation which sets it apart from other acrylic polymerisations is its initiation process. A balance must be obtained between the initiator/accelerator systems (Figure 4.1), and the inhibitors that are present to prevent premature polymerisation of the adhesive either during the manufacturing process or during subsequent storage prior to use in a bonding or sealing application.

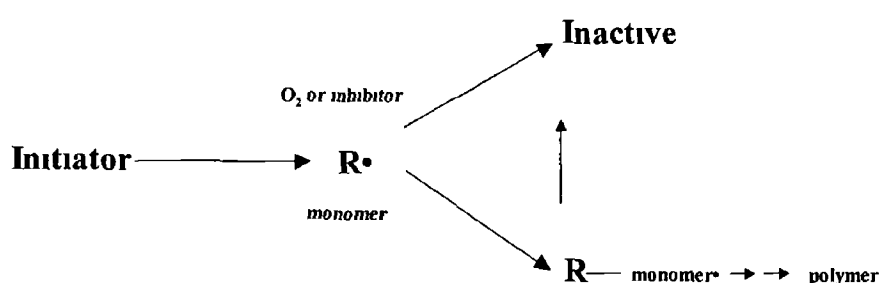


Figure 4.1 Simplified mechanism of polymerisation with side reactions such as chain transfer

An active metal surface encourages the redox decomposition of the initiator, in turn leading to the polymerisation. The amount of oxygen is

restricted, due to the confinement and can be rapidly used up by reaction with initiating or propagating radicals. Therefore the two key components of anaerobic adhesives are

- 1 They are initiated by surface chemistry (most particularly those embodying middle-row transition metals)
- 2 They require confinement between nonporous surfaces to limit the availability of oxygen

The metal substrate essentially functions as an intrinsic component of the cure system, which typically incorporates an organic peroxide, an organic reducing agent, e.g. usually an aromatic amine, and an organic acid. Therefore a rather basic schematic of the redox-based cure chemistry of anaerobic sealants is highlighted in Figure 4.2 below

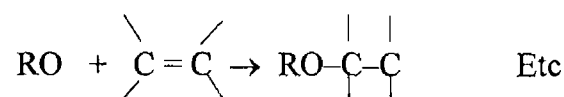
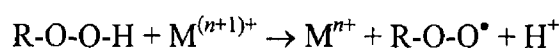
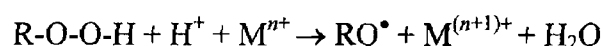


Figure 4.2 Reaction scheme of the redox based cure chemistry of anaerobic adhesives

Although anaerobic adhesives have been used to a large extent in industry for the past 25 years, the scientific literature related to the cure chemistry, and the role-played by each of the various cure components remains to be clarified.

One aspect of anaerobic adhesive technology that is only poorly understood is the interaction between the adhesive and the material surface

Questions such as which component of the adhesive most strongly interacts with the surface and in what manner will be addressed in the following pages, by investigating the interaction of model formulations and the interaction of the individual components of the curing system with polished copper and iron containing surfaces

4.1.1 The Cure Chemistry

The majority of investigations carried out to date into the cure chemistry of anaerobic adhesive are based on what happens within the reaction mixture. In the mid 80s, Okamoto *et al* performed the first published study using methyl methacrylate (MMA) polymerisation and various amine salts of saccharin. The amines that were examined were N,N-dimethyl-p-toluidine (DMpT), N,N'-dimethylaniline, mdoline and others and it was deduced that the highest rate of polymer conversion was obtained from the DMpT salts of saccharin. The rate of conversion depended on the square root of the amine salt concentration and the activation energy was determined to be 79 kJ/mol¹. Based on these results, polymerisation was thought to proceed via a radical polymerisation process.

In the 1990s, this study was extended and Okamoto *et al* investigated the kinetics of model adhesives and their mechanism further [3]. They began investigating systems which contained an organic acid (saccharin) and a tertiary amine (N,N-dimethyl-p-toluidine, DMpT) with the addition of an initiator (cumene hydroperoxide), and concluded that the kinetics of the reaction were independent of the concentration of the initiator and that a charge-transfer complex was formed between the tertiary amine and the organic acid which could act as a reducing agent and the oxidizing agent was the residual oxygen. The activation energy for this polymerisation system was determined to be 43 kJ/mol¹, and polymerisation took place with or without the cumene hydroperoxide (CHP), but was 20-50% faster when CHP was present.

A structure-cure speed relationship study was conducted by Okamoto using DMpT, saccharin otherwise known as o-benzoic sulphimide (BS) and their derivatives, and it was found that the cure speed was increased by an electron-donating methyl group on the para-position of the DMpT, but was decreased by the same group on the ortho-position (DMoT). Saccharin produced the fastest cure speed, but this was decreased by the addition of an electron-donating group in saccharin and by any substituents on the nitrogen atom in saccharin.

Okamoto extended his studies on the cure mechanism of anaerobic adhesives further again [4] by including copper(II) into his system, and it was found that the copper(II) acted like a catalyst, reducing the induction period from 5 hrs to 10-15 minutes. The following initiation reaction outlined in Figure 4.3 was put forward by Okamoto to explain the APH/CHP/saccharin metal-catalysed redox radical polymerisation.

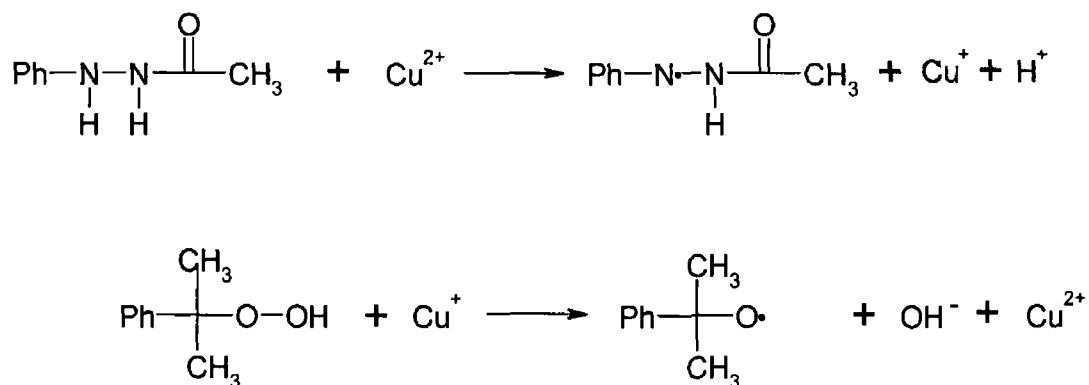


Figure 4.3 Reaction scheme postulated by Okamoto, APH/CHP/saccharin metal catalysed redox radical polymerisation

The cumyloxy radical initiates the MMA polymerisation, with the APH reducing the Copper (II) and the CHP acting as the oxidizing agent.

Investigations carried out by Hudak *et al* using XPS [5] concluded that saccharin (BS), which is a co-accelerator, and APH accumulated at the adhesive-metal interface. Complexes were formed between the saccharin and the copper, i.e. a Cu(I) complex initially but after time this was changed to a Cu(II) complex.

Kinetic studies carried out by Beaunez *et al* [6] into the role that DMpT and saccharin play in the radical polymerisation of MMA, showed that the CHP reduces the cupric ions to cuprous ions, a complex forms between the DMpT and a small fraction of Cu(I) in a 2:1 complex, and these complexed ions act as reducing agent with respect to CHP, whereas uncomplexed Cu(I) is inactive.

The organic acid, saccharin, catalyses the decomposition of the CHP as the saccharin lowers the energy required to cleave the O – O bond

The results of the second study carried out by Beaunez *et al* [7] reported that the DMpT reduces the Fe(III) to Fe(II) then the iron(II) is complexed by two DMpT molecules which are much more reactive than the uncomplexed iron (II), with regard to the decomposition of CHP, which again is activated by saccharin. Here again the uncomplexed iron(II) is unable to decompose the CHP no matter what concentration of saccharin is present. The two kinetic studies carried out by Beaunez, indicated similar reaction mechanisms for both copper saccharinate and iron saccharinate, where the key feature involves the metal-catalysed decomposition of CHP in order to produce free radical, and accelerators encourage this reaction.

Wellmann and Brockmann [8] concentrated on the chemical interactions that occurred between CHP-DMpT-saccharin, isolating a new compound called aminal (Figure 4 4) which is formed by the interaction of saccharin and DMpT.

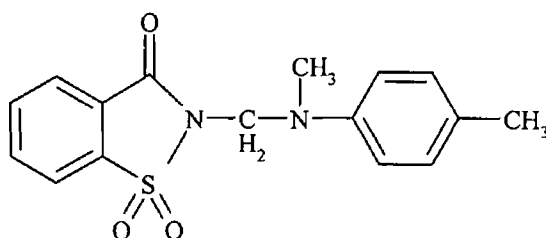


Figure 4 4 Structure of aminal

Aminal was capable of reducing metal ions from the higher to the lower oxidation state, and forming metal complexes, both of these characteristics necessary for cure chemistry, i.e. the metal ions which are in the higher oxidation state such as Cu(II) and Fe(III) produce the inactive free radical ROO[•] from the decomposition of the CHP, and by the formation of metal complexes metal ions are released from the substrate surface.

The formation of a charge-transfer complex suggested by Okamoto [4] was rejected by Wellmann *et al* who concluded that in the presence of air the DMpT is oxidised to a radical cation of the Wurster-type salt. The formation of this radical cation (Figure 4.5), produces a colouration of its solutions, and is also stable in acid solutions in very low concentrations, so stability is provided by saccharin due to its acidic nature.

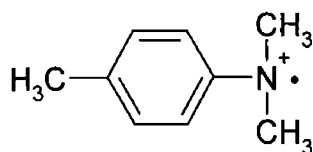


Figure 4.5 The DMpT radical cation

The studies reported by Raftery *et al* [9] [10] revealed that with respect to copper catalysis saccharin performs a unique role in that it not only liberates the Cu(II) ions from the surface but dramatically increases the efficiency of its reduction to Cu(I) by the amine or hydrazine-based reducing agent. However, the subsequent cleavage of the hydroperoxide by Cu(I) is significantly aided by the presence of the reducing agent (amine or hydrazine), but retarded by the presence of acid except in the case of the hydrazine. These studies cast doubt on Beaunez's postulate that the presence of an organic acid catalyses the decomposition of the hydroperoxide.

Studies carried out by George *et al* focussed on the effect of metallic catalysis on the reaction mechanism [11]. They found that copper(I) salts are necessary in the initiation reaction, these cuprous salts are obtained by the acid oxidation of the metal due to saccharin. George's system utilised the monomer together with the curing system, whereas in this study the monomer will be omitted, as the addition of monomer leads to polymerisation which complicates XPS measurements.

4.2 X-ray Photoelectron Spectroscopy

As mentioned previously, surface analysis by XPS involves irradiating a sample in vacuum with monoenergetic soft X-rays and energy analysing emitted core level electrons that have resulted from photoionisation [12]. The X-rays usually used are that of Mg K α or Al K α and these photons have limited penetrating power in a solid, therefore interacting with the atoms in the surface region causing the electrons to be emitted by the photoelectric effect. The emitted electrons have measured kinetic energies which are given by the following equation (Equation 4.2)

$$E_k = h\nu - E_b - \phi_s \quad \text{Equation 4.2}$$

where E_b is the binding energy of the atomic orbital from which the electron originates, and $h\nu$ is the energy of the photon and ϕ_s is the work function of the spectrometer.

The binding energy is regarded as the energy difference between the initial and final states after the photoelectron has left the atom, which is roughly equal to the Hartree-Fock energy of the electron. Therefore peaks can be identified with specific atoms so a surface compositional analysis can be performed. Chemical bonding will have an effect on both the initial state of the atom and the final state energy of the ion created by emission of the photoelectron. The changes brought about in the initial state energy by bond formation can be calculated by quantum chemical methods, and are basically due to the redistribution of electrons as the constituent atoms of a molecule or crystals come together in the solid state and principally depend on the electronegativities of the atoms involved.

A further redistribution of the electrons that surround the target atom will be caused by the creation of the ion by photoemission which will have an impact on the final state energy. This process otherwise known as electronic relaxation, will have an inter-atomic and an extra-atomic component, and is dominated by

the polarizabilities of the atoms involved. For this reason, the presence of chemical bonding will cause binding energy shifts which can be used to extract information of a chemical nature, e.g. such as the atomic oxidation state of the element under investigation, from the surface sample. Multiple splitting and shake-up satellites can also contribute to the final state E_b . The interaction of the core hole with unpaired electrons in the outershell orbitals gives rise to multiple splitting, whereas when the outgoing electron loses part of its kinetic energy to excite a valence electron into the unoccupied orbital, shake-up satellites are produced, e.g. $\pi \rightarrow \pi^*$ transitions.

4.2.2 Quantification

For most XPS investigations it is important to determine the relative concentrations of the various elements, with methods being established for quantifying the XPS measurement using peak area and peak heights, this approach uses atomic sensitivity factor (ASF), (Equation 4.3). These ASFs are available for each element and each core level and account for instrumental factors as well as the cross-section of the photon-electron collision.

$$S_i = I_0 A \sigma_i \theta_i \lambda_i T \quad \text{Equation 4.3}$$

where S_i is the atomic sensitivity factor for element i , I_0 equals the intensity of incident x-ray beam, A is the area of sample from which photoelectrons are detected, σ_i photoionisation cross-section, θ_i is an asymmetry factor for photoemitted electrons that provides the angular dependence of photoemission in terms of the angle between the photon path and the emitted photoelectrons, λ_i is the mean free path of photoexcited electrons and T is the detection efficiency of the analyser. These atomic sensitivity factors can be calculated or can be determined empirically, as several tabulations exist of which the most generally used are those due to Wagner *et al.* who obtained the data [13] from freshly powdered stoichiometric compounds mainly containing fluorine, therefore his empirically derived set of ASF are relative to the $F 1s = 1.00$. These ASFs are utilised throughout the following experiments [12].

Using these ASFs, S , the relative atomic concentration of any element (with the exception of hydrogen) can be calculated as follows, if you consider a strong photoemission line from each of two elements (Equation 4 4)

$$\frac{n_1}{n_2} = \frac{I_1/S_1}{I_2/S_2} \quad \text{Equation 4 4}$$

where n_1 is the density of atoms from element 1 in the analysis volume, this equation can be written in a more general form, so that the atom fraction, C , of any constituent, x , in a sample can be obtained from Equation 4 5, i.e. C_x

$$C_x = \frac{n_x}{\sum_i n_i} = \frac{I_x/S_x}{\sum_i I_i/S_i} \quad \text{Equation 4 5}$$

where \sum_i is summed over all elements observed in the spectrum from the sample, and the peak height is taken as the intensity, I . C_x is usually expressed as atomic %. Atomic ratios can also be calculated

4 2 3 Binding energy scale referencing

Electrons of a low binding energy which are involved in delocalised or bonding orbitals can be found in the valence levels, the spectrum here is made up of many closely spaced levels giving rise to a band structure, whose region is called the valence band. In the case of insulators the occupied 'valence band' is separated from the empty 'conduction band', while for metallic conductors these bands overlap, and the highest occupied state is called the Fermi level, E_F . Usually the $E_F = 0$ eV and is used for energy scale referencing purposes for conductors, but for non-conductors this Fermi level is not very well defined so another type of referencing is required

As binding energy referencing needs to be carried out on an individual basis for each spectrum, it is generally more appropriate to use some form of internal referencing. This is usually done with reference to adventitious carbon at $285.0 \text{ eV} \pm 0.3 \text{ eV}$, as most samples suffer from this adventitious contamination. So in a recorded spectrum, this peak appears at a $E_b \pm \delta \text{ eV}$, then all the other peak energies are corrected for this same charging shift $\pm \delta \text{ eV}$.

4.2.4 Background considerations and curve fitting

As already stated, XPS peaks appear on a background, and after each photoemission event the consequence is an accumulative background signal associated with the photoelectrons that have lost energy due to inelastic collisions in the solid, but these electrons still have enough energy to escape the work function of the surface [14]. There is a range of methods that can be used to define the background, as background removal is complicated as both intrinsic and extrinsic contributions span similar energies and the peak intensity depends on the method used to remove the background. Extrinsic losses from inelastic scattering events during electron transport through the solid can be removed by a Tougaard or a Shirley background, however a Shirley background can also remove some intrinsic losses useful throughout this analysis. Therefore, for quantitative analysis throughout this thesis the linear background was used. The linear background is the most popular method, and it involves drawing a straight line between two suitably chosen points as highlighted in Figure 4.6. However, uncomplicated, the linear background method appears to be the original data is not altered.

The spectra were fitted using a 90% / 10% linear combination of Gaussian and Lorentzian peaks in order to express the influence of instrumental broadening of the energy distribution and the core-hole lifetime respectively. The peaks were fitted using the Winspec [24] program. The FWHM values were varied between $1 \rightarrow 2 \text{ eV}$ for the C 1s and the N 1s emission peaks. While the FWHM values for the O 1s peaks ranged between $1 \rightarrow 2.5 \text{ eV}$. Values for spin-

orbit splitting of 1.18 ± 0.3 eV, 19.3 ± 0.3 eV and 13.1 ± 0.3 eV for S 2p, Cu 2p and Fe 2p respectively were used, with an intensity ratio of 0.5 utilised

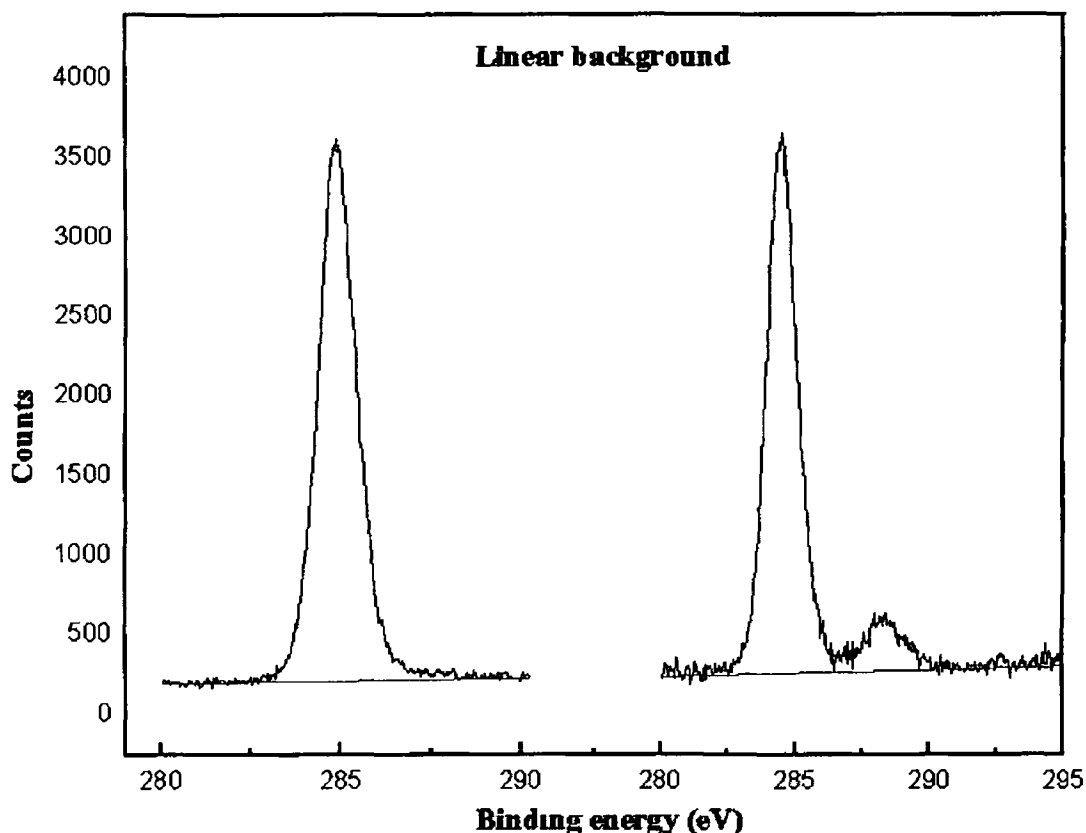


Figure 4.6 Examples of linear background used in the C 1s region of the spectrum

4.2.5 Auger parameters

X-ray induced Auger electron emission peaks are also present in the recorded spectrum, they are readily distinguished from photoemission lines by using an Mg K α source instead of the Al K α source, as the kinetic energy of the Auger line is independent of the irradiation energy used, so the kinetic energy of the Auger lines will remain the same. Auger peaks can be used analytically to distinguish between different chemical species by using the Auger parameter, a concept introduced by Wagner [15, 16] back in 1975, and was defined as follows in Equation 4.6

$$\alpha = E_k(jkl) - E_k(i) \quad \text{Equation 4 6}$$

where $E_k(jkl)$ is the kinetic energy of the Auger transition jkl and $E_k(i)$ is the kinetic energy of the photoelectron emitted from atomic level i . This equation is equivalent to Equation 4 7

$$\alpha = E_k(jkl) + E_B(i) - h\nu \quad \text{Equation 4 7}$$

where $E_B(i)$ is the binding energy of an electron in level i and $h\nu$ is the energy of the exciting radiation. As this equation could produce a negative value a modified Auger parameter, $\alpha + h\nu$, was introduced, i.e. α' as shown in Equation 4 8

$$\alpha' = \alpha + h\nu = E_k(jkl) + E_B(i)$$

or

$$\text{Equation 4 8}$$

$$\alpha' = BE_p + (h\nu - BE_a)$$

where BE_p is the binding energy of the photoelectron line, BE_a is the apparent binding energy of the Auger line and $h\nu$ is the x-ray energy [5]. This modified Auger parameter was used throughout the following study for identification and characterisation of chemical states.

4.3 Experimental

4.3.1 Reagents and apparatus

All of the reagents used were of analytical reagent grade. The methanol was obtained from Sigma-Aldrich (HPLC grade). The organic acids, saccharin (o-benzoic sulphimide) and maleic acid were supplied by Loctite Ltd. The aromatic amines such as 1-acetyl-2-phenylhydrazine (APH), N,N-diethyl-p-toluidine (DEpT), N,N-dimethyl-p-toluidine (DMpT) and N,N-dimethyl-o-toluidine (DMoT) were supplied by Loctite Ltd. The sodium saccharinate and the copper (II) sulphate were supplied by Sigma-Aldrich. The copper and iron-containing substrates were sent to the National Physics Laboratory, Teddington, Middlesex, where they were polished to a mirror finish by initially using various grades of aluminium oxide abrasive (20 and 12 micron grit sizes) in preparation for polishing. They were then polished on a rotary lapping machine tool using an appropriate cloth pad and 3 and 1-micron diamond paste.

All XPS data was acquired using a Vacuum generators, electron spectroscopy for chemical analysis system, ESCA instrument. The photoelectrons were excited using Al K α radiation as the excitation source—photon energy at 1486.6 eV, the source was operated at 15 kV and 20 mA. The photoelectrons were collected along the surface normal and detected with a hemispherical analyser. All spectra were corrected for sample charging by referring the C 1s line for adventitious carbon to 285 ± 0.3 eV. The survey scans were acquired using a pass energy of 50 eV, step increment 0.5 eV, dwell time 0.5 s and number of scans 10. Higher resolution spectra were acquired using a pass energy of 20 eV with step size and dwell times 0.2 eV and 2 s respectively, and number of scans 20. The pressure in the analysis chamber was kept at 10^{-8} mbar during scanning.

4.3.2 Sample preparation

The polished copper specimens were initially wiped with 'lens tissue' that had been soaked in methanol, followed by sonication in methanol for ten minutes before being removed from this solution and dried in a stream of nitrogen before immersion into the reaction mixtures. Figure 4.7 gives the chemical structures of the compounds used in this study.

Solutions

The polished substrates were immersed for a 24-hour period in the following methanol solutions of individual components:

- 1 1 6% Saccharin (BS)
- 2 1 6% Maleic acid
- 3 1 5% Cumene Hydroperoxide (CHP)
- 4 1 5% N,N,-diethyl-p-toluidine (DEpT)
- 5 1 5% N,N,-dimethyl-p-toluidine (DMpT)
- 6 1 5% N,N,-dimethyl-o-toluidine (DMoT)
- 7 1 5% 1-Acetyl-2-phenylhydrazine (APH)

The polished substrates were immersed for a 24-hour period in the following adhesive formulations, all as w/v (weight/volume) solutions in methanol:

- 8 1 6% saccharin and 1 5% N,N,-diethyl-p-toluidine
- 9 1 6% saccharin and 1 5% N,N,-dimethyl-p-toluidine
- 10 1 6% saccharin and 1 5% N,N,-dimethyl-o-toluidine
- 11 1 6% saccharin and 1 5% 1-acetyl-2-phenylhydrazine
- 12 1 6% saccharin and 1 5% cumene hydroperoxide
- 13 1 6% saccharin, 1 5% CHP and 1 5% APH – 43x model
- 14 1 0% BS, 1 0% CHP, 1 5% DMoT and 1 5% DEpT – 90 model
- 15 1 0% BS, 1 0% CHP, 0 3% APH and 0 3% maleic acid – 43 model

The above formulations were also prepared with maleic acid replacing the saccharin.

The samples were removed from these solutions and dried in a stream of nitrogen before being placed in the XPS analysis chamber

Synthesis of Copper (II) Saccharinate BSCu(II)

Cupric saccharinate was synthesised and used as a reference compound, with comparisons being made between its recorded spectra and that of other compounds

This method of synthesis was used by Beaunez *et al* [6] and George *et al* [17] for the synthesis of copper (II) saccharinate and is as follows

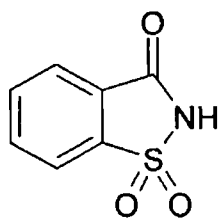
10.35 g of sodium saccharinate was dissolved in 75 ml of water and placed in a 250 ml round-bottomed flask which was fitted with a condenser and a magnetic stirrer and heated to 80° C. An aqueous solution of copper(II) sulphate was made by dissolving 5.02 g of the copper(II) sulphate in water, and slowly adding it to the saccharinate solution. The mixture was kept at 80°C for 1 hour and constantly stirred, it was then cooled to 5°C and kept at this temperature overnight. Blue crystals had formed and were collected by filtration and recrystallised from water. This product was dried in a desiccator over sodium hydroxide and calcium chloride for 24 hours.

Electrochemical reduction of Cu substrates

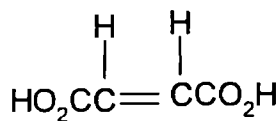
The copper substrates were reduced in order to investigate the effect that the cure components of anaerobic adhesives had on metallic copper Cu(0).

The instrument used for the electrochemical reduction of copper was a CH Instruments electrochemical analyser. The electrochemical cell was a three-electrode cell, with a platinum counter electrode and a Ag/AgCl reference electrode, the copper substrate was the working electrode.

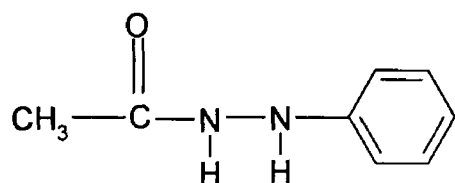
These copper pieces were electrochemically reduced in 0.5 M HClO_4 (analytical grade) for ten minutes. The electrolyte was purged and blanketed with argon to degas the solution before (for 30 minutes) and during the electrochemical reduction. A potential equal to $-0.860 \text{ V} / \text{Ag/AgCl}$ was applied to the copper working electrode for 10 minutes.



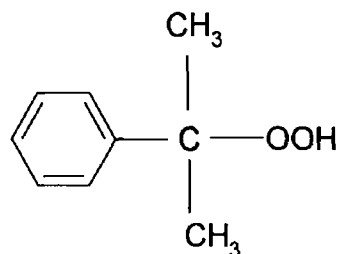
Saccharin



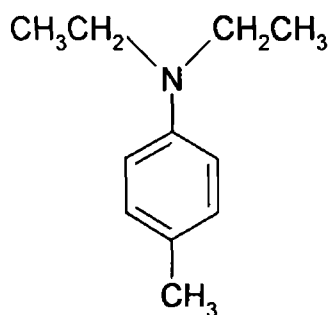
Maleic Acid



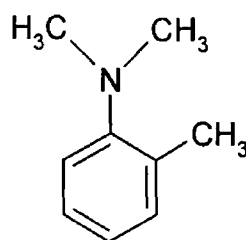
1-Acetyl-2-phenylhydrazine (APH)



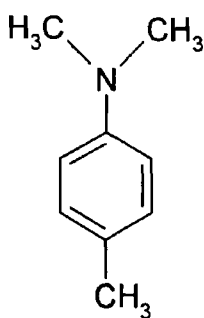
Cumene Hydroperoxide (CHP)



N,N-diethyl-p-toluidine (DEPT)



N,N-dimethyl-o-toluidine (DMOT)



N,N-dimethyl-p-toluidine (DMpT)

Figure 4 7 Structure of individual components of cure system of anaerobic adhesives

4.4 Results and Discussion

4.4.1 Organic acids – saccharin and maleic acid

Initially the polished copper substrate was immersed for a 24-hour period in methanol solutions 1-7 containing the individual components as outlined in section 4.3.2. The atomic percentage calculated from the XPS spectra of the individual cure components in the presence of the polished copper substrate can be seen in Table 4.1. These results are based on three different samples prepared and treated identically.

| Component | Carbon | Oxygen | Copper | Nitrogen | Sulphur |
|-------------|--------|--------|--------|----------|---------|
| Copper | 58 | 19 | 23 | 0 | 0 |
| BS | 56 | 25 | 5 | 7 | 7 |
| BSCu(II) | 58.56 | 26.24 | 3.4 | 7.8 | 6.8 |
| Maleic acid | 45.44 | 42.44 | 13.11 | 0 | 0 |

Table 4.1 Experimental values calculated (atomic %) for the methanol solutions of the individual cure components of anaerobic adhesives in contact with the copper substrate after a 24-hour period. Theoretical values in red.

In order to establish typical levels of uncertainty in these calculated atomic percentages, an error analysis study was carried out on the untreated polished copper substrate, by measuring five separate samples, which were nominally prepared under identical conditions. The % carbon, oxygen and copper were calculated at $58 \pm 3.4\%$, $18.6 \pm 1.3\%$ and $23.2 \pm 2.5\%$ respectively. The large carbon signal has been attributed to a surface contamination layer, or adventitious carbon which is usually unavoidable when surface preparation is performed in an ambient environment. These levels of uncertainty were then taken as representing acceptable error limits on subsequently measured surfaces.

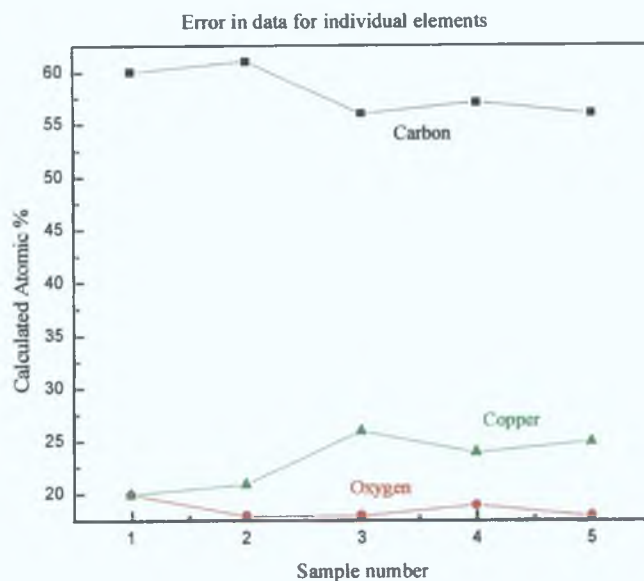


Figure 4.8 Error in calculated data for a) \blacksquare C $58 \pm 3.4\%$ b) \bullet O $18.6 \pm 1.3\%$ and
c) \blacktriangle Cu $23.2 \pm 2.5\%$

Figure 4.9 shows the survey scans recorded for the reference copper substrate, the saccharin and maleic acid treated copper surface and the synthesised BSCu(II) reference compound highlighting the peaks of interest.

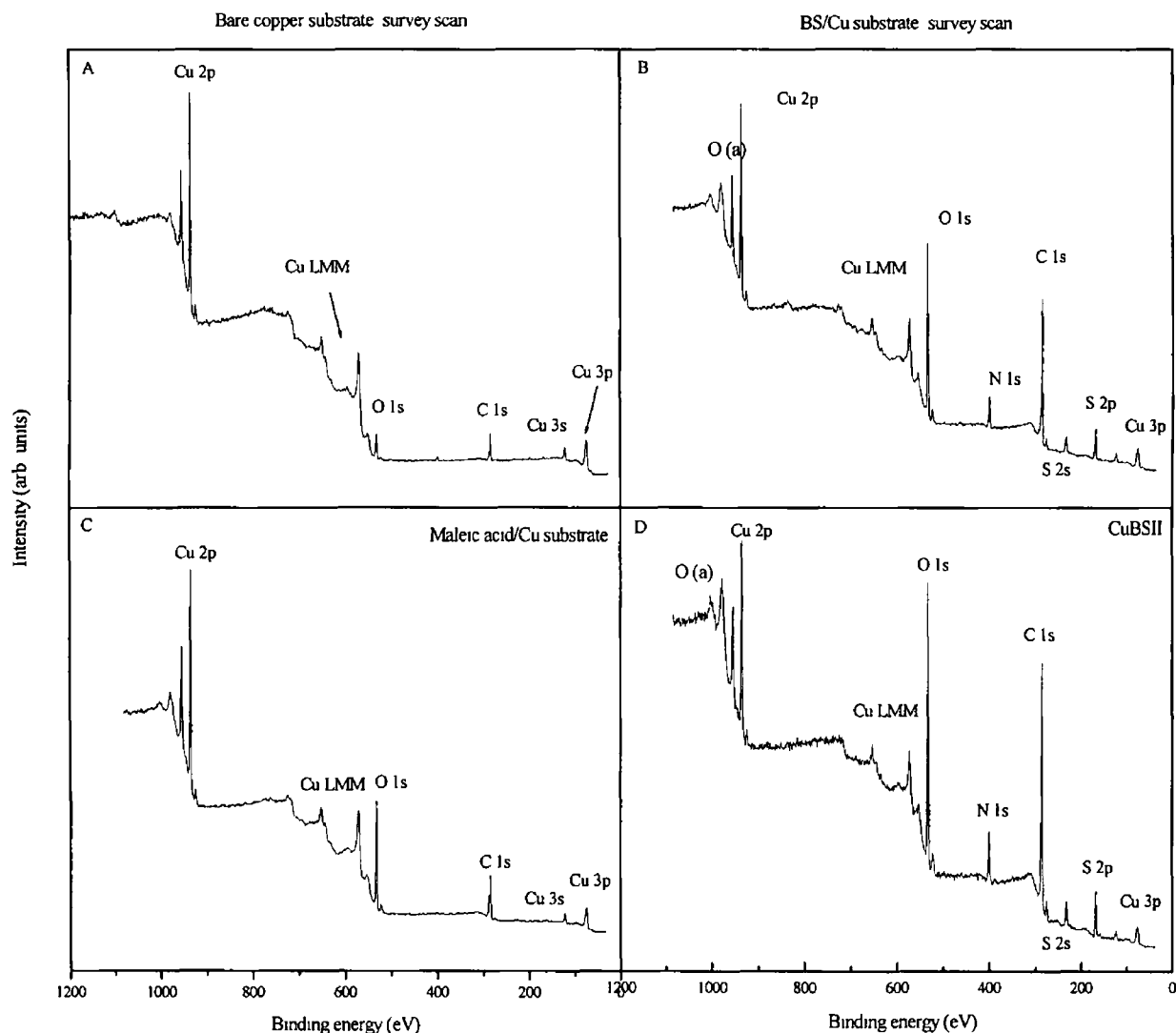


Figure 4.9 Survey scans recorded for A) Cu reference B) BS/Cu C) Maleic acid/Cu and D) synthesised BSCu(II) complex, indicating the peaks of interest

Analysis of the above XPS spectra illustrates the consistent presence of oxygen, carbon and copper in all spectra with the addition of nitrogen and sulfur in some spectra depending on the composition in which the copper was immersed

Organic acids such as saccharin and maleic acid, are used in anaerobic adhesives as a co-accelerator, and play a key role in releasing the transition metal ions from the surface substrate. After interaction of the copper substrate

with a 1.6% BS-MeOH solution a blue film was formed on the surface of the substrate that was an indication of an ion-molecular complex film [18]. These blue crystals are indicative of the copper(II) salts so it was assumed that at this metal/saccharin interface copper(II) saccharinate was formed after a 24-hour immersion time. To verify this, BSCu(II) was synthesised as previously described, and analysed under the same conditions. The atomic percent calculations in Table 4.1 for the BS treated copper and the BSCu(II) reference compound are almost identical and are within the $\pm 1\%$ of the expected composition of the $\text{Cu}(\text{sacc})_2$ complex illustrated in Figure 4.10.

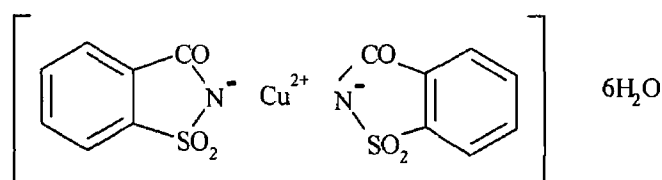


Figure 4.10 Schematic of copper (II) saccharinate complex [11]

The formation of the BSCu(II) complex in the presence of air is disputed by George *et al* [17] who imply that this cupric saccharinate can only be formed in anaerobic conditions, and that the cuprous saccharinate is formed after 5 hrs in aerobic conditions. The Cu(II) complex was found after polished copper was placed in contact with a 1.0% BS-MeOH solution for 110 hrs by Hudak *et al* [5]. They also analysed a ppt from a copper foil which had been placed in a BS-MeOH solution. This was found to contain only the Cu(II) complex.

In order to establish the oxidation state of the copper substrate after contact with the 1.6% BS-MeOH solution, both the Cu LMM Auger peaks, the Cu 2p for the Cu reference, the Cu/BS, Maleic/Cu and the synthesised BSCu(II) were compared in Figure 4.11. Copper surfaces have been extensively studied by XPS, which would suggest that the correlation between peak binding energy and oxidation state would be well understood. Cu^{2+} (paramagnetic) compounds are

usually accompanied by shake-up satellite peaks which are usually a few electron volts lower in kinetic energy than the main photoelectron peak and, depending on the system, these shake-up lines can vary in size [12]. In contrast, Cu^+ and Cu^0 spectra do not have these shake-up lines associated with them and their photoelectron spectra are almost identical. This means that the X-ray induced Auger line observed in the XPS spectra of copper systems (Cu LMM) are significantly different, and can be used to distinguish between the oxidation states of the copper in combination with the modified Auger parameters, α' , as this value can vary between these two species by as much as 3 eV [12] (Equation 4.8)

$$\alpha' = \text{BE}_p + (h\nu - \text{BE}_a) \quad \text{Equation 4.8}$$

The observed binding energies of the Cu $2p_{3/2}$ peak and the kinetic energies of the observed X-ray induced Auger line are summarised in Table 4.2, as well as the calculated Auger parameters, from Equation 4.8

The Cu $2p$ spectrum for the polished copper sample can be seen in Figure 4.11 (A). The copper $2p$ core level was characterised by $2p_{3/2}/p_{1/2}$ spin-orbit split doublets. The peak at 932.8 eV observed in the Cu $2p_{3/2}$ spectrum accompanied by the $2p_{1/2}$ at 952.7 eV are in agreement with reported values for metallic copper [12]. This peak being characteristic of either Cu(0) or Cu(I), the absence of any high energy satellite structures also indicate that only Cu(0) and Cu(I) are present in any substantial quantity. The Auger lines, near 921.5 eV and 918.2 eV give $\alpha' = 1854.3$ eV and 1851.0 eV respectively, are both characteristic of the Cu(0) state. The shoulder peak near 915.9 eV with $\alpha' = 1848.7$ eV is characteristic of Cu_2O or the Cu(I) state. From these x-ray induced Auger features a strong response was noted for the feature associated with the Cu(0), with a weaker response for the higher energy (E_b) Cu(I) indicating that the surface region is predominately Cu(0) [5].

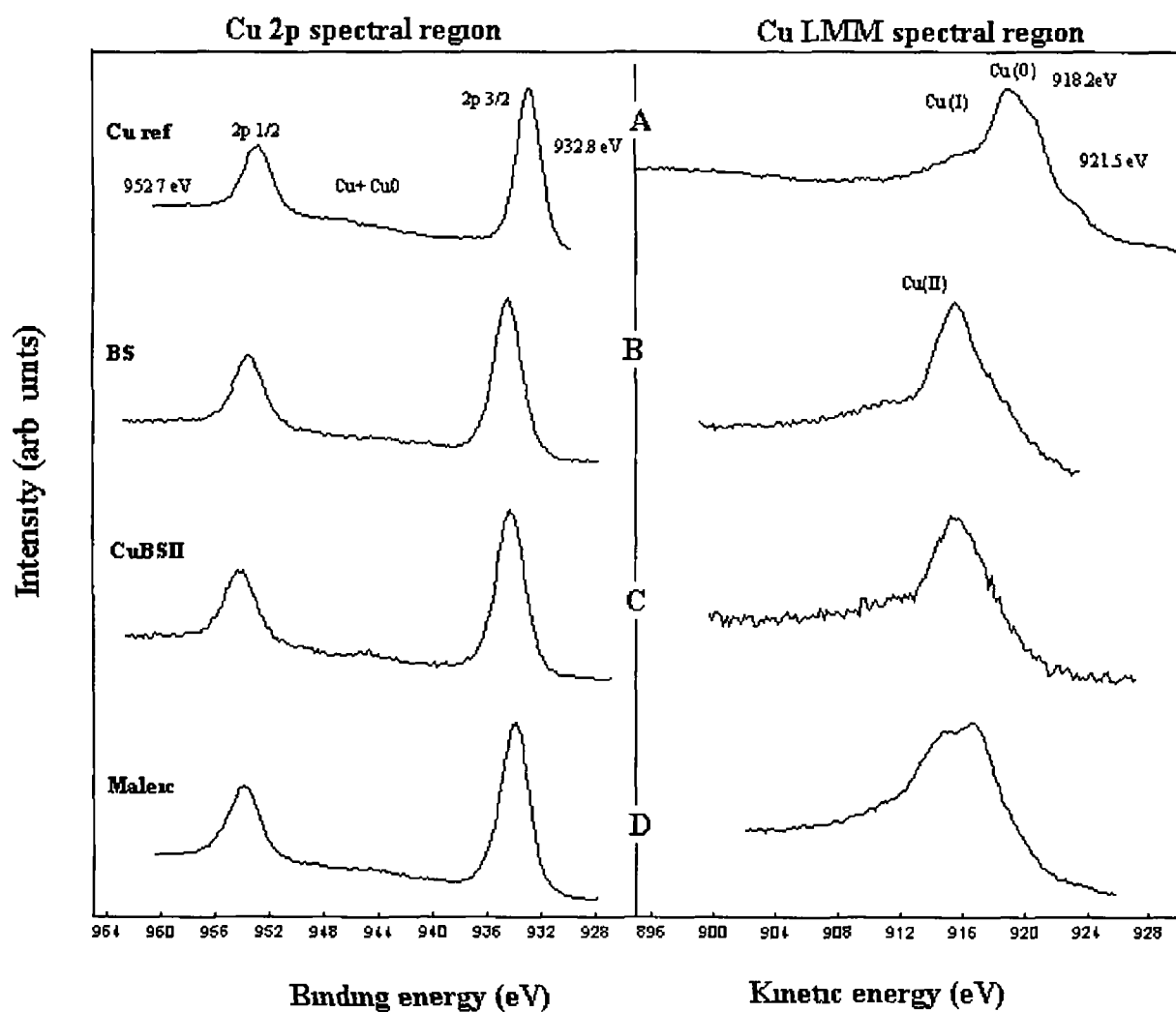


Figure 4.11 Cu 2p and Cu L₃M_{4,5} M_{4,5} spectra obtained from A) polished copper B) Cu in 1.6% BS-MeOH for 24 hr, C) synthesised BSCu(II) complex and D) Cu in 1.6% maleic acid-MeOH solution for 24 hrs

| Sample | Cu 2p _{3/2} Binding energy(eV) | Auger Kinetic energy(eV) | α' (eV) |
|-------------------------------|--|-----------------------------|-------------------|
| Polished Copper | 932 8 | 921 5 | 1854 3 Cu(0) |
| | | 918 2 | 1851 0 Cu(0) |
| | | 915 9 | 1848 7 Cu(I) |
| Cu in 1 6% BS- MeOH,24 hr | 934 7 | 915 7 | 1850 4 Cu(II) |
| Synthesised BSCu(II) | 934 4 | 916 2 | 1850 3 Cu(II) |
| Cu in 1 6% Mal- MeOH, 24hr | 933 8 | 914 9 | 1848 7 Cu(I) |
| | | 916 5 | 1850 3Cu(II) |

Table 4 2 Energy values observed for the Cu 2p_{3/2} peak, the Auger LMM peak and the calculated modified Auger parameter (α') for the spectra in Figure 4 11

The Cu substrate after contact with 1 6% BS-MeOH, as already stated produced a blue film, which after XPS analysis, produced one broad peak in the Auger region. The modified Auger parameter calculated by referring this peak near 915 7 eV to the Cu 2p_{3/2} emission line at 934 7 eV, which corresponds to the Cu(II) line, was 1850 4 eV. This value was consistent with that calculated by Hudak *et al* for Cu(II) complex. They also concluded that after the Cu(II) sample was exposed to X-rays the Cu 2p_{3/2} emission line, in this case 932 8 eV, increased in intensity at the expense of the 934 7 eV peak, indicating that the Cu was being reduced from Cu(II) to Cu(I), and after 150 minutes of exposure only the peak at 932 8 eV remained, but the Auger region did not alter at all. This was also observed by Sesselmann *et al* [19] in dealing with CuCl₂ complexes, they found that the Cu(II) was reduced to Cu(I) after X-ray exposure. The above samples were only exposed to the X-rays for a period of 2 hr maximum. The peaks associated with the synthesised BSCu(II) spectra are almost identical to those observed for the 1 6% BS-MeOH spectra, with the modified Auger parameters being within 0 1eV of each other. Verifying that the blue substance

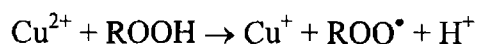
found on the copper substrate after immersion for 24 hr in 1 6% BS-MeOH was indeed BSCu(II)

When the copper substrate was in contact with 1 6% maleic-MeOH for 24 hr, it emerged from the solution with a thin film coating it. From the modified Auger parameters it would appear that the copper was present in this copper-maleate complex in two forms that of the Cu(I) and Cu(II) states, with calculated $\alpha' = 1848.7$ eV and 1850.3 eV respectively. From the survey scan and the calculated atomic %s the composition of this system was calculated as C 45%, O 43% and Cu 12% which was within a 1% error difference for the ratios of each of these components if the Cu(II) complex is the dominant species in this reaction.

The above results highlight the role that the acid plays in the curing system of anaerobic adhesives, namely, releasing metal ions from the metal surface substrate. This can be deduced from the XPS spectra which initially indicated that the polished copper surface was predominately Cu(0), whereas when the copper surface exposed to these organic acids predominately displayed Cu(I) and Cu(II) states. In the curing system of anaerobic adhesives, initiation is started by the decomposition of the hydroperoxide. These two oxidation states of Cu can induce the decomposition of the hydroperoxide, as shown in the following reaction scheme (Scheme 4.1)



Scheme 4.1



The RO^\bullet radical is more reactive than the ROO^\bullet radical, therefore the Cu(II) formed after reaction with an organic acid needs to be reduced to Cu(I) valent state for formation of this more reactive radical. Also the Cu(I) ions, which are present on the polished copper substrate, can have a catalytic effect on the cure speed also [11].

In Figure 4.12 the C 1s and O 1s high-resolution spectra are compared for the Cu substrate, BS/Cu, BSCu(II) and maleic acid/Cu systems. Decomposition of the C1s response indicated that carbon was present in two forms, for the untreated polished copper substrate at 285 ± 0.3 eV and 286.5 ± 0.3 eV of peak areas ratios 88%/12%, respectively, these being attributed to hydrocarbon contamination as previously described, and possibly the C-O-H of the solvent used (methanol-during sonication).

All spectra record two carbon environments, the 1.6% BS-MeOH and the synthesised BSCu(II) C1s spectra, show adventitious carbon / saturated hydrocarbons at 285 ± 0.3 eV which accounts for most of the carbon present on all substrate surface, and a higher binding energy of 287.9 ± 0.3 eV taken to represent strongly overlapping C=O (carbonyl peak) and N-C=O peaks (85%/15%-BS and 80%/20% synte). For the 1.6% mal-MeOH, the peak recorded at 289 ± 0.3 eV was attributed to the acid functionality O-C=O (65/35%) [14].

The O1s response for identifying oxygen functionalities is more disappointing than the C 1s level, as the inherent peak width is greater and the dynamic range more restricted. The polished copper substrate at 531 ± 0.3 eV indicate metal oxides. Generally there are two stable oxides of copper, Cu_2O and CuO , but additionally a cupric hydroxide has also been established. Characterisation of the CuO and the Cu(OH)_2 is normally done by using the Cu $2p_{3/2}$, where for CuO is shifted 1.3 ± 0.3 eV above that for Cu_2O but is always not defined properly with respect to the Cu_2O peak, mainly due to broadening associated with multiple splitting ($1 \text{ e } 934.4 \text{ eV} / 933 \text{ eV}$). These metal oxides been already identified using the modified Auger parameter as explained above. The higher energy peak at 533.1 ± 0.3 eV was attributed to H_2O [12]. For the 1.6% BS-MeOH, and BSCu(II), the peak at 532 ± 0.3 eV was attributed the SO_2 moiety or the C=O carbonyl oxygen present in the acid.

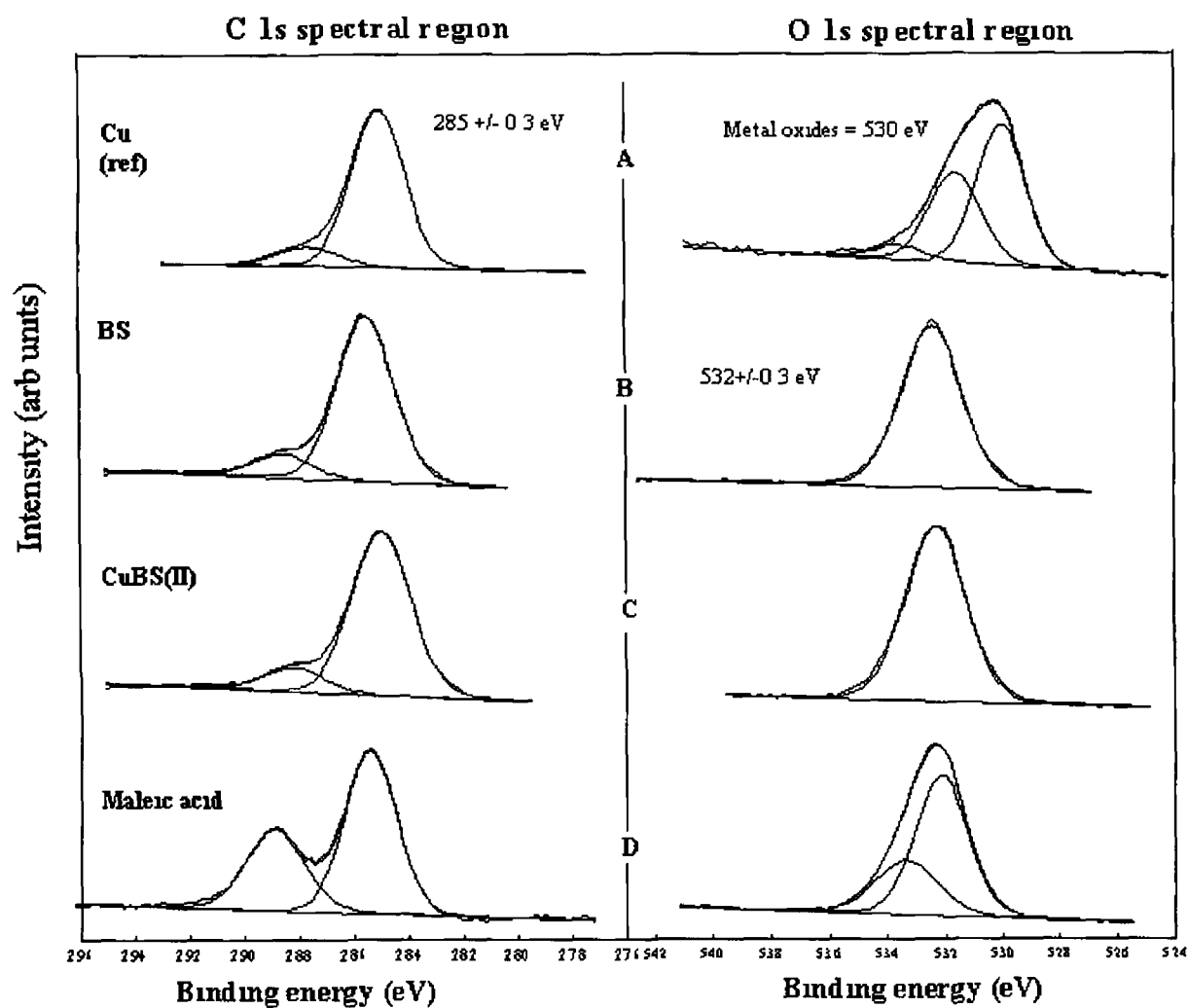


Figure 4 12 Decomposition of the XPS C 1s and O 1s feature, for A) the polished copper reference B) 1.6% BS-MeOH, C) synthesised BSCu(II) and D) 1.6% maleic acid-MeOH

4.4.2 Substituted aromatic amines

The cure system typically incorporates an organic peroxide, an organic acid, such as saccharin or maleic acid and an organic reducing agent. These reducing agents take in a wide variety of compounds but substituted aromatic amines or hydrazines are most frequently used. The amines include DMpT (N,N-dimethyl-p-toluidine), DMoT (N,N-dimethyl-o-toluidine) and DEpT (N,N-diethyl-p-toluidine) whilst typical hydrazines are APH (1-acetyl-2-phenylhydrazine) and TSH (p-toluenesulphonylhydrazine). These are typical examples of hydrazines used in the engineering adhesives area, and have been shown to have similar activity in these redox formulations, however, for the purpose of this study, APH was used.

The elemental composition of the Cu substrate after immersion in 1.5% amine-MeOH solutions (section 4.3.2, solutions 4-7) is outlined in Table 4.3.

| Component | Carbon | Oxygen | Copper | Nitrogen | Sulphur |
|-----------|--------|--------|--------|----------|---------|
| DMoT | 53 | 28 | 19 | 0 | 0 |
| DMpT | 62 | 25 | 13 | 0 | 0 |
| DEpT | 51 | 28 | 21 | 0 | 0 |
| APH | 57 | 18 | 17 | 8 | 0 |

Table 4.3 Experimental values calculated (atomic %) for the methanol solutions of the individual substituted aromatic amines in contact with the copper substrate after a 24-hour period.

These results calculated for the aromatic tertiary amines, of DMpT, DMoT and DEpT, show no evidence of organic molecules binding to the copper surface, indicating that these components produce no immediate effect (within the 24 hr limit) on the polished copper unless coupled with other compounds. The XPS scans of the treated surfaces shown in Figure 4.13 are very similar and show no evidence of chemical interaction with the substrate. These scans almost superimposed onto one another and also onto the Cu reference. A 10% rise in the oxygen content at the expense of the Cu can be seen, so more oxygen was present on this surface, possibly due to 24 hr incubation period in which the

copper substrate was in the solvent solution, (methanol) (Figure 4 13) The decomposition of the O 1s response for the substituted toluidines indicates that oxygen was present in two forms, the peaks at 531.4 ± 0.3 eV and 533.1 ± 0.3 eV correspond to the metal oxide/ H₂O respectively, similar to the oxygen peaks associated with the Cu reference. This increase in the oxygen signal leads to a decrease in other elements signals, so the difference in the % carbon found on the surface deviates from that of the reference copper substrate by $\pm 4\%$, and from recorded spectra the toluidines do not appear to interact with the Cu surface independently.

From Table 4 3 above it can be seen that after the copper substrate was immersed for the 24 hr in 1.5% toluidines-MeOH solution, no segregation of the toluidines occurred at the surface, this was highlighted by the absence of any nitrogen on the surface following XPS analysis. From Table 4 4 the oxidation state of the Cu substrate was evaluated using the Auger parameter. The oxidation state of the Cu substrate prior to any surface pre-treatment indicates that the Cu species present are that of Cu (0) and Cu(I), after surface treatment (immersion for 24 hrs in the toluidines solutions) the copper was still only present in these forms.

Treatment of copper with APH produces a different response compared to that of the substituted tertiary amines, the APH segregated to the surface of the copper substrate. A nitrogen response was recorded in the spectra indicating that the APH did segregate to the surface of the copper, this was seen from the results displayed in Table 4 3, where N was found present on the surface (8%). APH appears to be a more active accelerator segregating at the substrate surface without the aid of organic acids.

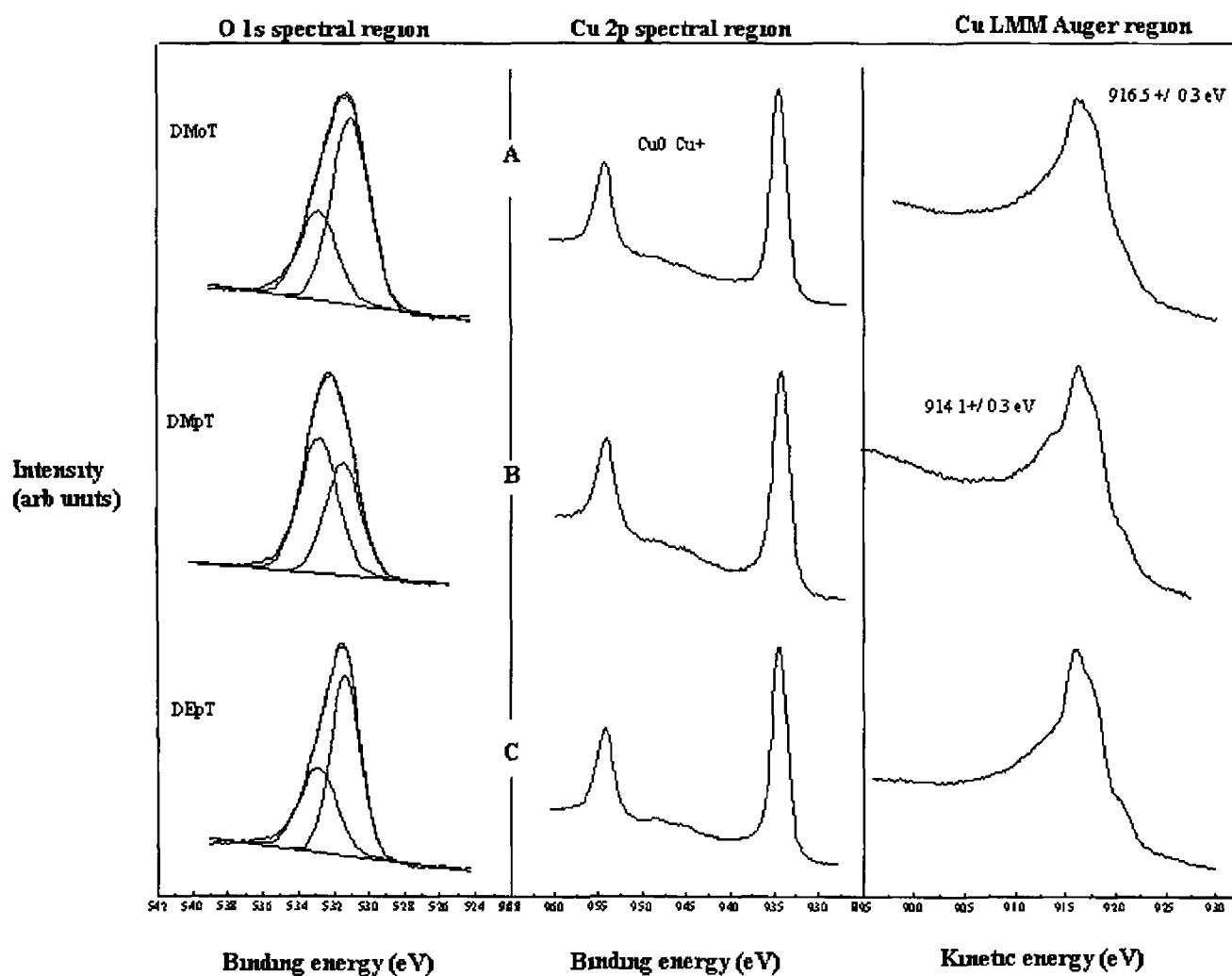


Figure 4.13 Decomposition of the XPS O 1s feature, the Cu 2p emission line and the x-ray induced Auger spectra for substituted aromatic tertiary amines in contact with the Cu substrate A) 1.5% DMoT-MeOH, B) 1.5% DMpT-MeOH and C) 1.5% DEpT-MeOH

| Sample | Cu 2p _{3/2} Binding energy(eV) | Auger Kinetic energy(eV) | α' (eV) |
|-------------------------|--|-----------------------------|-------------------|
| Polished Copper | 932.8 | 921.5 | 1854.3 Cu(0) |
| | | 918.2 | 1851.0 Cu(0) |
| | | 915.9 | 1848.7 Cu(I) |
| Cu in 1.5% DMoT-MeOH | 934.5 | 916.5 | 1851.0 Cu(0) |
| Cu in 1.5% DMpT-MeOH | 933.6 | 914.1 | 1847.7 Cu(I) |
| | | 917.5 | 1851.1 Cu (0) |
| Cu in 1.5% DEpT-MeOH | 933.4 | 915.1 | 1848.5 Cu(I) |
| | | 920.9 | 1854.3 Cu (0) |

Table 4.4 Energy values observed for the Cu 2p_{3/2} peak, the Auger LMM peak and the calculated modified Auger parameter (α') for the spectra in Figure 4.12

4 4 3 Saccharin and substituted aromatic amines

An organic acid acts as the principal character in the formulations of the anaerobic adhesives, this acid interacts with the underlying copper making metallic cations available. For this curing system reducing agents are necessary, as the metal ions in the higher oxidation state only produce inactive free radicals from the decomposition of the CHP. The reducing agents investigated are those of tertiary amines. Previously it was shown that these amines produce no effect on the copper substrate individually (within the time limit of 24 hrs) but when coupled with an organic acid the outcome is different. Saccharin is a weak acid, with the amines being described as weak bases so the formation of a salt between the saccharin and the amine is possible, with the resulting salt shown below (Figure 4 14)

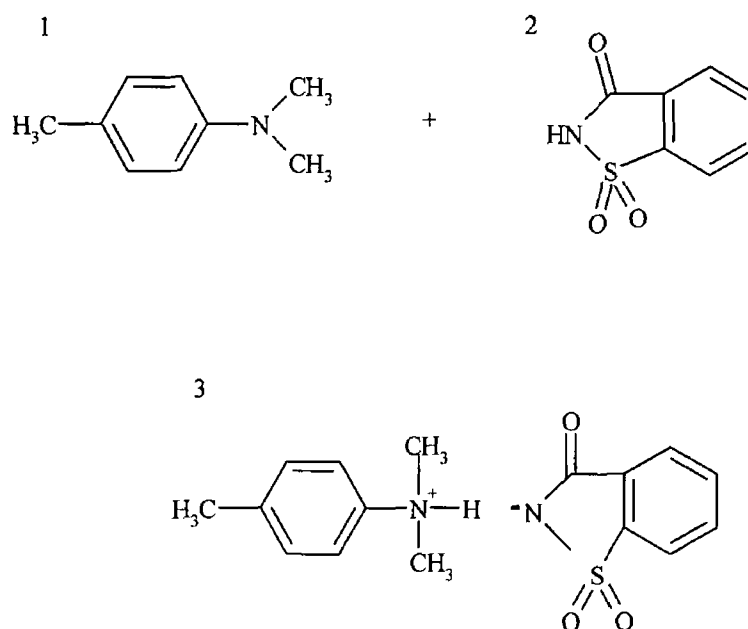


Figure 4 14 Schematic of interaction of DMpT (1) and saccharin (2), acid (2) and a base (1) resulting in a salt (3)

Combinations of the organic acids with the amines were studied using XPS to see what the combined effect was on the metal substrate (Section 4 3 2,

solutions 8-11, saccharin being substituted with maleic acid also) The atomic percentage calculated from the spectra of saccharin combined with the amines as cure components in the presence of the polished copper substrate can be seen in Table 4 5 Again these results are based on the reproducibility between three different samples prepared and treated identically The error analysis carried out on the data, can also be seen in Table 4 4

| Ingredient | Carbon | Oxygen | Copper | Nitrogen | Sulphur |
|-------------------|----------------|----------------|---------------|-----------------|----------------|
| Saccharin | 56.6 ± 2.4 | 24.1 ± 2.4 | 4.5 ± 0.7 | 7.3 ± 0.9 | 7.5 ± 0.9 |
| BS+DMoT | 64.1 ± 3.5 | 23.4 ± 3.0 | 3.7 ± 0.6 | 4.3 ± 0.6 | 4.5 ± 0.6 |
| BS+DMpT | 67.2 ± 1.9 | 18.2 ± 1.6 | 3.1 ± 0.6 | 7.3 ± 0.6 | 4.2 ± 0.7 |
| BS+DEpT | 64.2 ± 3.0 | 20.6 ± 1.5 | 3.6 ± 0.6 | 7.3 ± 0.9 | 4.3 ± 0.6 |
| BS+APH | 61.7 ± 0.6 | 22.5 ± 1.0 | 3.6 ± 0.6 | 7.6 ± 0.6 | 4.6 ± 0.6 |

Table 4 5 Experimental values calculated (atomic %) for the methanol solutions of 1 6% saccharin (BS)/ 1 5% amine, in contact with the copper substrate after a 24-hour period

From the atomic %s calculated in this table, it was apparent that the saccharin has accumulated at the copper surface in all cases, as saccharin was the only compound which contained sulfur and, sulfur was present on all surfaces ($\approx 4\%$) The SO_2 in the molecule results in a S $2p_{3/2}$ peak at 167.7 ± 0.3 eV, which can be seen in Figure 4 16

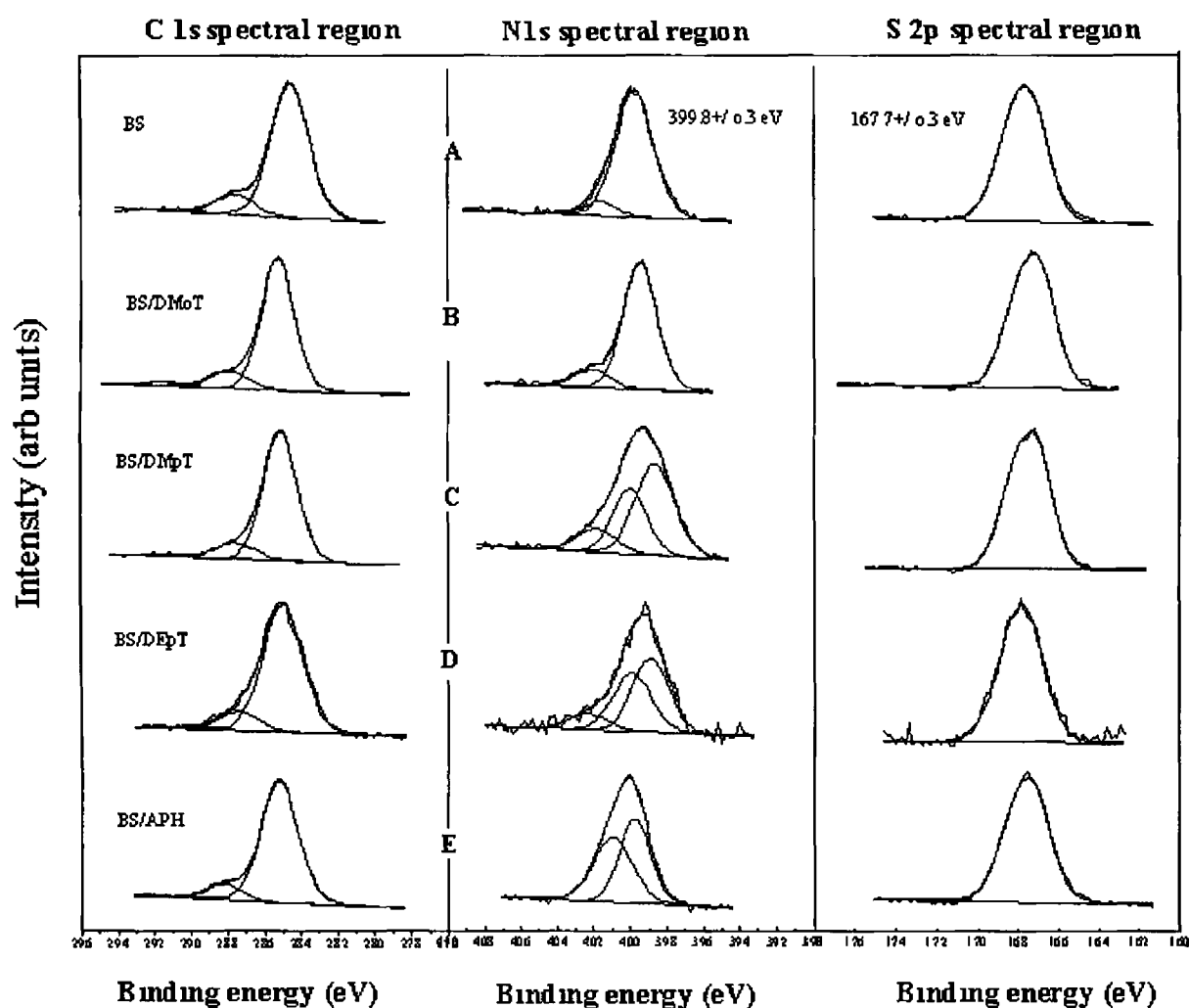


Figure 4 16 Decomposition of the XPS C 1s feature, the N 1s emission line and S 2p emission line for A) 1.6% BS-MeOH B) 1.6% BS/1.5% DMoT-MeOH, C) 1.6%BS/1.5% DMpT-MeOH D) 1.6% BS/1.5% DEpT-MeOH and E) 1.6% BS/1.5%APH-MeOH, in contact with the Cu substrate

Nitrogen was also present on all surfaces. The atomic per cent calculations would suggest that when saccharin was combined with the para-substituted amine (i.e. DMpT and DEpT), both of these molecules accumulate at the surface. This can be deduced from the fact that saccharin contains sulfur and nitrogen in a 1:1 ratio while these surface treatments result in there being approximately a 1:2 ratio of sulfur to nitrogen. The additional nitrogen was attributed to the presence of the para-substituted amine at the surface. Decomposition of the C 1s and N 1s spectra region for saccharin combined with these aromatic amines can be seen in Figure 4.16. The C 1s signature for saccharin has been mentioned, whereas the N 1s region for saccharin (Figure 4.16 A) contains a peak near 399.8 ± 0.3 eV, this peak was due to the acid form of the molecule. For the spectra recorded for the BS/DMoT (Figure 4.16 B) the N 1s region contains two peaks, one located near 399.6 ± 0.3 eV due to the acid form of BS and the other near 401.9 ± 0.3 eV, which may be due to some type of adsorbed species as this photoemission line is observed in all the other spectra, possibly from small amounts of the amine which are left on the surface. The C 1s response for all of these compounds show adventitious carbon / saturated hydrocarbons at 285 ± 0.3 eV and a binding energy at 287.9 ± 0.3 eV which is taken to represent strongly overlapping $\text{C}=\text{O}$ (carbonyl peak) and $\text{N}-\text{C}=\text{O}$ peaks of the saccharin or in the case of APH the $\text{O}=\text{C}-\text{N}$.

For saccharin in combination with the para-substituted aromatic amines new peaks are evident in the N 1s region at binding energies of 398.6 ± 0.3 eV and 402.2 ± 0.3 eV. If the N 1s peak at energy of 399.8 ± 0.3 eV was allocated to the acid form of BS, when this N becomes unprotonated it can shift to a lower binding energy of 398.6 ± 0.3 eV (chemical shift of ≈ 1.2 eV) [20] and the peak 400.1 ± 0.3 eV could be attributed to a protonated nitrogen and the formation of the salt outlined in Figure 4.14 becomes more credible. With Lewis bonded /unprotonated nitrogen being associated with lower binding energies and protonated / Brønsted nitrogen at higher binding energies [13, 18]. The third nitrogen peak at the higher binding energy of 402.1 ± 0.3 eV possible due to some form of unreacted amine as previously stated.

Wellmann *et al* [8] suggested that a new compound was formed by the interaction of the saccharin with the DMpT, this compound was called aminal and its structure can be seen in Figure 4 4 This fact was disputed above by the decomposition of the N 1s spectral region The DMpT /BS system decomposition was similar to that for the DEpT/BS system decomposition indicating that these para-substituted amines undergo the same reaction with saccharin, and if aminal was formed the N 1s regions would appear different, as aminal is a compound formed by the interaction of DMpT and BS and not that of DEpT and BS

Figure 4 17 represents the Cu 2p and the X-ray Auger induced Cu LMM Auger line of the spectra for these amines in combination with saccharin Table 4 6 shows the Cu 2p_{3/2} binding energy and the corresponding Auger kinetic energy, and the calculated modified Auger parameter As already explained when BS comes into contact with the Cu substrate, it releases metal ions from the substrate surface Most of these ions are in the Cu(II) form (i e BSCu(II)), so from the modified Auger parameters the Cu⁺ species found present on the surface after immersion in this acid-base solution, would indicate that a reduction of the copper from the +2 oxidation state to the +1 oxidation has occurred According to Beaunez *et al* [6] DMpT could not reduce Cu(II) ions, and DMpT was unlikely to complex copper (II) saccharinate, suggesting that the cupric ions are reduced by the CHP But if a salt was formed between the saccharin (weak acid) and DMpT (base), then this salt appears to facilitate the reduction of the Cu(II) to Cu(I) This is supported by Raftery *et al* who revealed that saccharin in combination with DMpT is a powerful reductant for Cu(II) [21]

APH was found to accumulate at the surface of the copper in the absence of BS as previously explained Both the APH and the BS are found at the copper surface in this APH-BS system, and this was seen by the calculated atomic percent shown in Table 4 5 where sulfur was found on the surface ($\approx 4.5\%$) due to the saccharin and the % nitrogen found on the surface was attributed to the nitrogen from both species This APH can act as a reducing agent and reduce the

Cu(II) ions produced by the action of the saccharin on the polished copper substrate as shown below in Figure 4 15 This was in agreement with results of Okamoto *et al* [4]

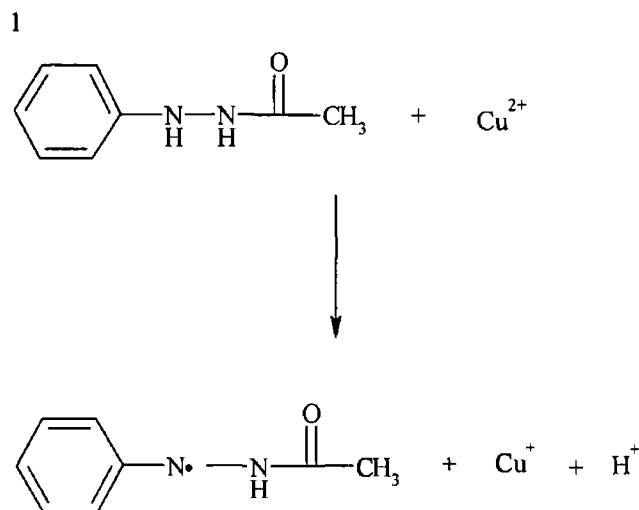


Figure 4 15 Schematic of reduction of the Cu(II) ions by 1-acetyl-2-phenylhydrazine

From the modified Auger parameters, it would seem that Cu was present in the cuprous form after being in contact with BS-APH system for 24 hrs, with the modified parameter of 1848.3 ± 0.3 eV, indicating only Cu(I). For the N 1s spectral region of the APH-BS-Cu system, at least two distinct chemical states are observed at 399.7 ± 0.3 eV and at a higher binding energy of 401.2 ± 0.3 eV. These two chemically shifted components have been ascribed to the nitrogen in the BS and in the APH components.

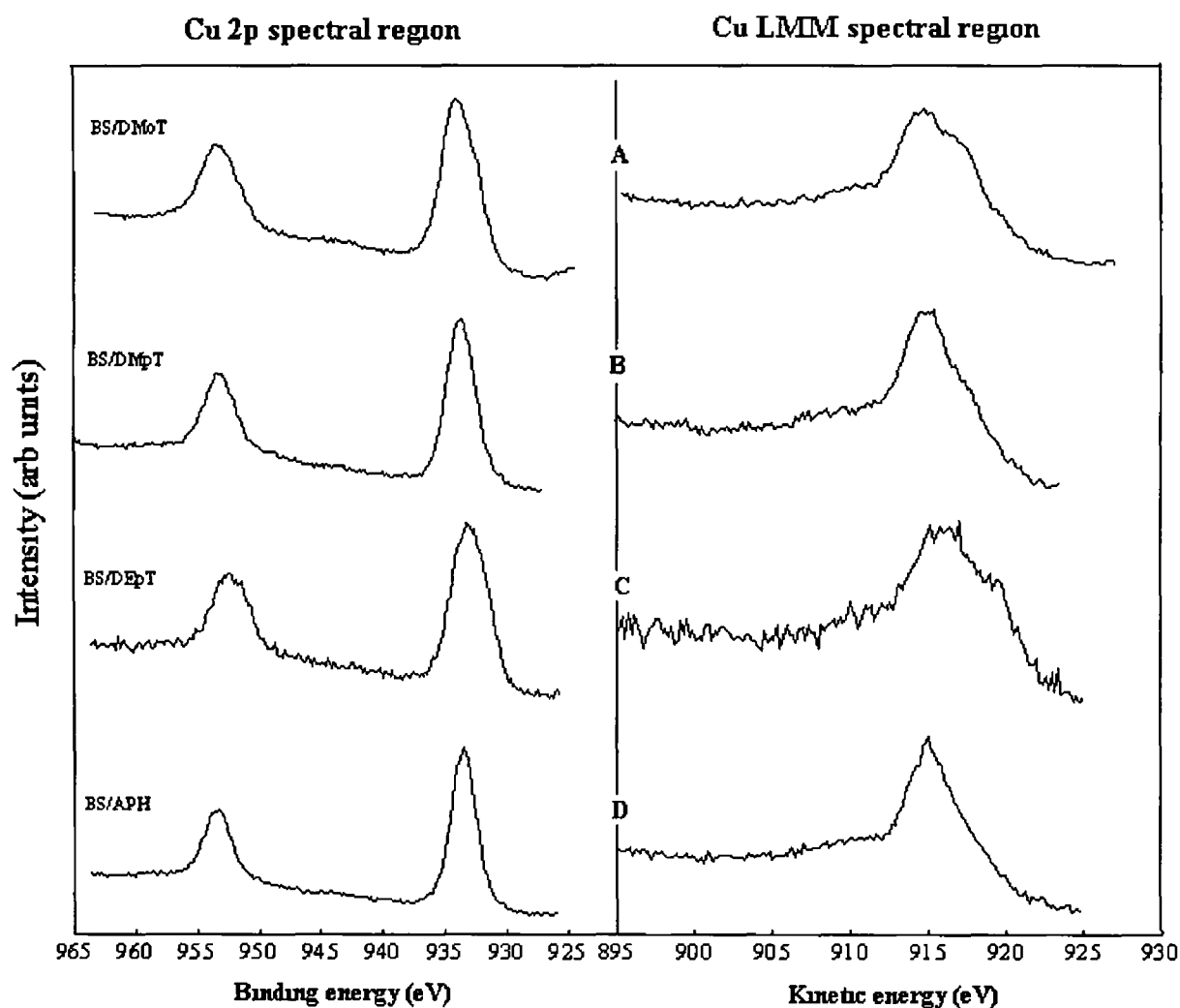


Figure 4 17 Cu 2p and Cu L₃M_{4,5} M_{4,5} spectra obtained from polished copper in contact with A) 1.6% BS-1 5% DMoT/MeOH B) 1.6% BS-1 5% DMpT/MeOH, C) 1.6% BS-1 5% DEpT/MeOH and D) 1.6% BS-1 5% APH/MeOH solutions for 24 hrs

| Sample | Cu 2p _{3/2} Binding energy(eV) | Auger Kinetic energy(eV) | α' (eV) |
|-----------------------------|---|--------------------------|----------------|
| Cu in 1 6%BS-MeOH, 24 hr | 934 7 | 915 7 | 1850 4 Cu(II) |
| Cu in 1 6% BS-1 5%DMoT/MeOH | 933 4 | 914 7 | 1848 1 Cu(I) |
| | | 917 2 | 1850 6 Cu(II) |
| Cu in 1 6%BS-1 5%DMpT/MeOH | 933 1 | 914 8 | 1847 9 Cu(I) |
| Cu in 1 6%BS-1 5% DEpT/MeOH | 932 4 | 915 8 | 1848 2 Cu(I) |
| | | 919 1 | 1851 5 Cu(I) |
| Cu in 1 6%BS-1 5% APH/MeOH | 933 4 | 914 9 | 1848 3 Cu(I) |

Table 4 6 Energy values observed for the Cu 2p_{3/2} peak, the Auger LMM peak and the calculated modified Auger parameter (α') for the spectra in Figure 4 17

Conclusions on BS/DMpT, BS/DEpT, BS/DMoT and BS/APH curing systems

From the above experimental and data analysis, the following mechanism for the curing system of anaerobic adhesives using saccharin as the organic acid was proposed

Saccharin interacts with the polished copper substrate to form a Cu(II) complex (BSCu(II)). This acid oxidation of the metal surface is essential for the initiation reaction of the anaerobic adhesives reaction sequence. In combination with the para-substituted amines such as DMpT or DEpT, a salt appears to be formed at the surface of the substrate, as shown by the N 1s response in this spectral region. As saccharin is a weak acid and DMpT acts as a base, then the salt formed by reaction of this acid / base appears to facilitate the reduction of these metal ions from the higher to the lower oxidation states, i.e. Cu(II) \rightarrow Cu⁺

The formation of a charge-transfer complex as suggested by Okamoto *et al* [3] cannot be ruled out, as this theory was based on the development of colouration when saccharin was in contact with DMpT. This colouration was found in the above studies also, where the purplish colour was noted after 4 days when saccharin and DMpT were in the methanol solution but after approximately 12 hr when the copper was also present in the system, indicating that the copper surface acts as a catalyst for the above reaction. The difference between these studies was that Okamoto's studies were carried out in the absence of a metal substrate.

If, as proposed, above a salt was formed between the BS and the para-substituted amines, this does not appear to be evident with the ortho-substituted amine, with which only saccharin appears to have segregated at the substrate interface. This could be due to steric effects of the electron donating methyl group in the ortho-position as opposed to the para-position.

For the APH-BS system, the saccharin interacts with the copper substrate oxidising the surface releasing metal ions Cu(II) (after a 24 hr time period), the APH then reduces this Cu(II) species to the Cu⁺ species, leaving this Cu⁺ species ready to decompose the hydroperoxide, as outlined in Scheme 4.1

4 4 4 Maleic acid and substituted aromatic amines

The effect of maleic acid on the cure chemistry of anaerobic adhesives has also been investigated. Maleic acid replaced saccharin in the same solutions as in Table 4 5 above. Maleic acid is thought of as a strong acid, and is often used in anaerobic adhesives cure formulations by itself or in combination with saccharin. As described in the previous section, maleic acid interacts with the polished copper substrate, liberating metal ions from the substrate surface. The salt formed at the interface was predominately of the Cu(II) type with some Cu(I) species also present on the surface.

After treating the copper surface with the maleic acid solutions, the experimental values calculated for elements found present on the copper surface (atomic %) are shown in Table 4 7. The presence of nitrogen on all surfaces would indicate that the aromatic amines have been bound to the surface region, with the assistance of the maleic acid. This was deduced from the fact that without maleic acid, there was no evidence of these amines residing at the surface. For the Mal + DMoT combination, the percentage carbon and oxygen remained equal, with nitrogen calculated at approximately 2 % at the expense of the copper peak, i.e. $\approx 12\% \rightarrow 8\%$.

For maleic acid in combination with the para-substituted amines, the carbon content of the surface appears to have increased by approximately 10% at the expense of the oxygen peak which has decreased by about 15%, this would seem to merit the explanation that a combination of maleic acid with either DMpT, DEpT or APH brings about a reduction in the amount of oxygen present on the substrate surface, as the amines and hydrazine are large carbon containing compounds increasing the carbon content of the surface substrate leading to a reduction in the oxygen content.

| Ingredient | Carbon | Oxygen | Copper | Nitrogen |
|-------------|------------|------------|------------|-----------|
| Maleic acid | 44.7 ± 0.9 | 43.3 ± 1.9 | 12.0 ± 0.9 | 0 |
| mal +DMoT | 46.3 ± 0.9 | 43.7 ± 0.9 | 7.6 ± 0.9 | 2.4 ± 0.9 |
| mal +DMpT | 54.3 ± 2.4 | 27.6 ± 0.9 | 15.7 ± 2.4 | 2.4 ± 0.9 |
| mal +DEpT | 54.2 ± 1.6 | 29.3 ± 1.6 | 12.3 ± 2.3 | 4.2 ± 1.6 |
| mal +APH | 61.3 ± 2.4 | 26.1 ± 1.6 | 5 ± 1.0 | 7.6 ± 0.9 |

Table 4 7 Experimental values calculated (atomic %) for the methanol solutions of 1.6% maleic acid (mal)- 1.5% amine (methanoic solutions), in contact with the copper substrate after a 24-hour period

Figure 4 19 shows the decomposition of the C 1s, O 1s and N 1s spectral regions for maleic acid, as well as a combination of 1.6% maleic acid combined with 1.5% DMoT, DMpT, DEpT and APH in methanol solution, after contact with the polished copper substrate for a 24-hour period. Starting with the C 1s spectra region, all spectra recorded show a peak at 285 ± 0.3 eV which was attributed to adventitious carbon / saturated hydrocarbons. The second major peak which was present in all spectra was shifted by 4 ± 0.3 eV to a higher energy of 289 ± 0.3 eV and was attributed to the acid functionality $\text{HO}-\text{C}=\text{O}$ (65/35%) [13, 14]

The decomposition of the O1s peak for 1.6% mal-MeOH (Figure 4 19 A) produces two chemically distinct oxygen environments, the peak at the lower binding energy of 532.1 ± 0.3 eV attributed to O^1 and the higher binding energy of 533.5 ± 0.3 eV attributed to O^2 in the schematic Figure 4 18 below

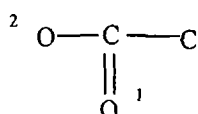


Figure 4 18 Schematic of oxygen that has different binding energies depending on the surrounding atoms

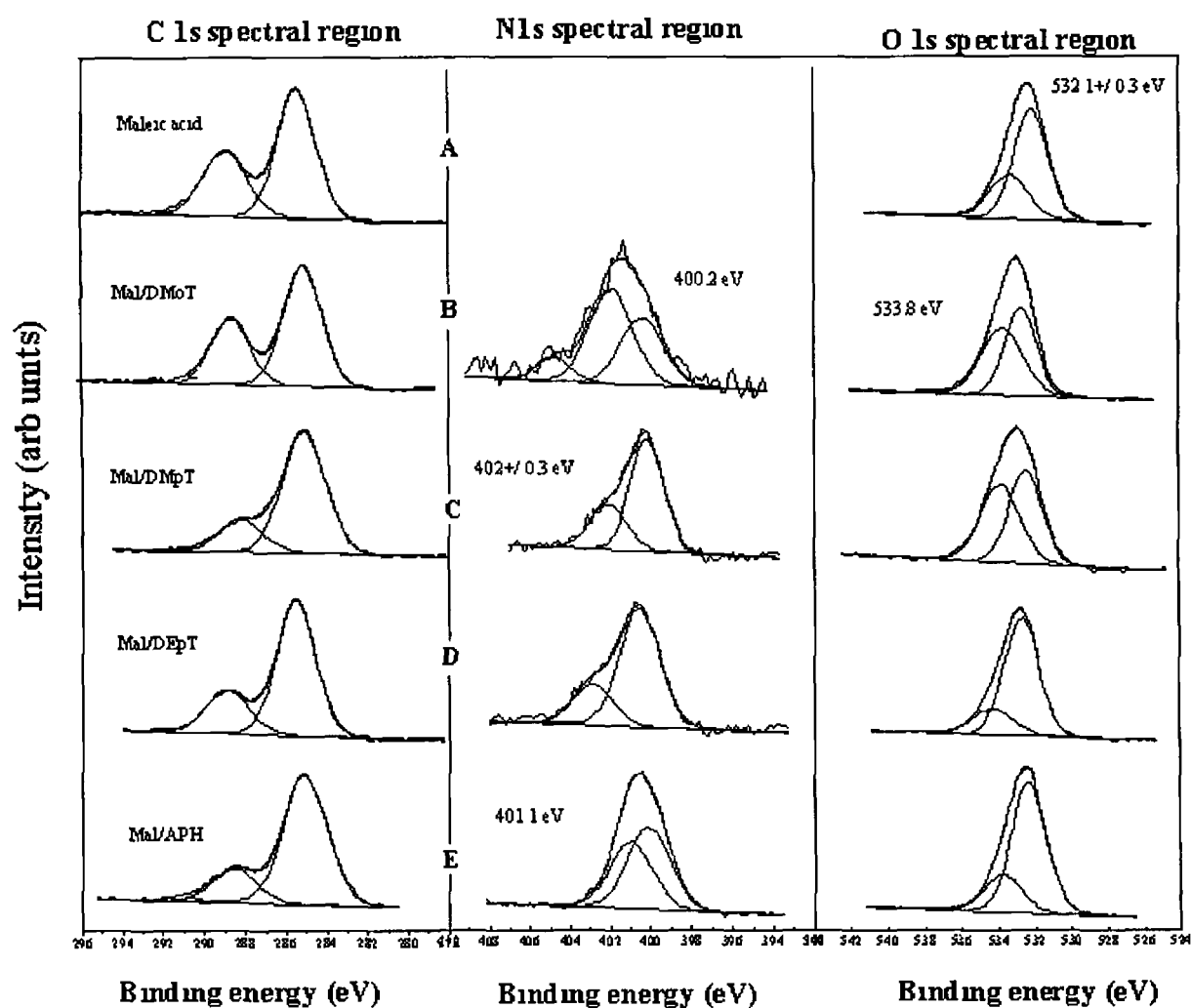


Figure 4 19 Decomposition of the XPS C 1s feature, the N 1s emission line and O 1s emission line for A) 1.6% Maleic acid-MeOH B) 1.6% mal/1.5% DMoT-MeOH, C) 1.6%mal/1.5% DMpT-MeOH D) 1.6% mal/1.5% DEpT-MeOH and E) 1.6% mal/1.5%APH-MeOH, in contact with the Cu substrate

The composition and structure of copper(II)maleate, the compound formed on the surface of the copper substrate after 24-hr incubation period in 1.6% mal-MeOH, is seen in Fig 4.20

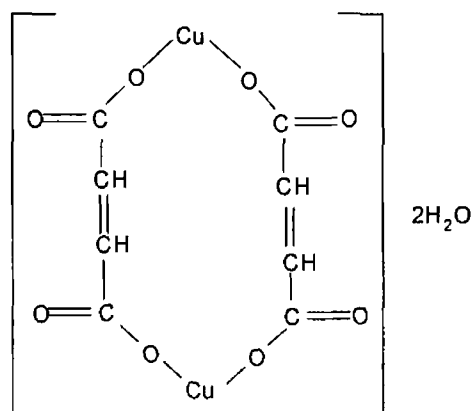


Figure 4.20 Structure of copper (II) maleate

Copper oxides have a O 1s photoemission peak at approximately 529.6 and 530.4 ± 0.3 eV. This peak, unresolved in the above spectra, could be encompassed in the peak resolved at 532.1 ± 0.3 eV. The ratio of the area of these peaks is 2:1 (68%/32%), which would be in good agreement with the 1:1:1 ratio of O in different environments on the above surface.

For maleic acid and the toluidine systems, the two oxygen environments of 532.4 ± 0.3 eV and 533.7 ± 0.3 eV coincide with those of the acid functionality of the maleic acid (Figure 4.18). The percentage ratio of the oxygen peaks was 50%/50% for the mal-DMoT and the mal-DMpT systems, indicating that oxygen on the surface was due to the maleic acid. A substantial reduction in the higher binding energy oxygen (i.e. O-C) 80%/20% ratio determined for the mal-DEpT system can be seen. Again this oxygen was attributed to the acid functionality of the maleic acid, indicating that the proportion of the carbonyl function has increased upon treatment with this mal-toluidine system. The percentage ratio for the mal-APH system was 80%/20%, which indicates that

the proportion of the carbonyl function has increased, and was the expected result as $\text{C}=\text{O}$ was present on the APH molecule as well as the maleic acid molecule, therefore both of these molecules segregate to the copper substrate surface. The decomposition of the N 1s spectral region (Figure 4.19) reveals two nitrogen peaks at 400.2 ± 0.3 eV and 402 ± 0.3 eV, present in the maleic-toluidine systems. These peaks are assigned to the nitrogen environment of the toluidines and possibly some unreacted adsorbed nitrogen respectively.

The formation of a salt between the amines and the maleic acid is possible (as of the saccharin), but maleic acid is a stronger acid than saccharin. This salt would take on the predominantly acidic character, therefore with the ability to provide acid oxidation of the copper substrate. Table 4.8 shows the experimental calculations of the modified Auger parameter for these mixed systems maleic acid. When maleic acid was placed in contact with the polished copper substrate in a methanol solution, the copper Cu(I) and Cu(II) oxidation states were present on the resulting substrate at binding energies for the modified Auger parameter of 1848.7 ± 0.3 eV and 1850.3 ± 0.3 eV respectively. For the system that involved the aromatic substituted amines of mal-DMoT, mal-DMpT and mal-DEpT, the modified Auger parameter indicated that the copper species oxidation states present were also Cu(II) and Cu(I). As maleic acid alone produced the same oxidation state for the underlying copper, it would appear that these particular amines produce no measurable effect on the oxidation state of the copper surface in conjunction with maleic acid. So the formation of a salt between these amines and maleic acid is highly likely, but as it is acidic in character, it could counteract the reducing power of the amines. This would suggest that maleic acid is too strong an acid to use with these substituted amines when the metal to be bonded is copper. The Cu $2p_{3/2}$ emission peak for these toluidines was at a binding energy of 934.4 ± 0.3 eV, which is also indicative of the Cu(II) species.

For the APH-mal system, copper reduction occurs as only the cuprous species of copper was detected from the modified Auger parameter at a binding energy of 1848.4 ± 0.3 eV, with the elimination of the Auger parameter that

accounted for the Cu(II) species. Maleic acid appears not to inhibit the reducing ability of the APH, making these two components compatible in anaerobic adhesive formulations. A possible explanation for this is that APH, a hydrazine has a less basic character than that of an amine, therefore disallowing the maleic acid to curb its reducing ability.

| Sample | Cu 2p _{3/2} Binding energy(eV) | Auger Kinetic energy(eV) | α' (eV) |
|------------------------------------|--|-----------------------------|-------------------|
| Cu in 1.6% maleic acid-MeOH, 24 hr | 933.8 | 914.9 | 1848.7 Cu(I) |
| | | 916.5 | 1850.3 Cu(II) |
| Cu in 1.6% mal-1.5%DMoT/MeOH | 934.4 | 915.9 | 1850.1 Cu(II) |
| Cu in 1.6% mal-1.5%DMpT/MeOH | 934.3 | 915.9 | 1850.2 Cu(II) |
| | | 913.1 | 1847.4 Cu(I) |
| Cu in 1.6% mal-1.5%DEpT/MeOH | 934.5 | 915.9 | 1850.4 Cu(II) |
| | | 913.9 | 1848.4 Cu(I) |
| Cu in 1.6% mal-1.5% APH/MeOH | 932.7 | 915.7 | 1848.4 Cu(I) |

Table 4.8 Energy values observed for the Cu 2p_{3/2} peak, the Auger LMM peak and the calculated modified Auger parameter (α') for the maleic acid and the aromatic amine systems

Conclusions on maleic acid with amines

From the results above, using maleic acid as a substitute for saccharin as a co-accelerator in anaerobic adhesives cure system, it would seem that the maleic acid forms a salt with these toluidines, independent of the position of the electron donating group on the aromatic ring, ortho- or para-positions. But in forming these salts the acidic character of the maleic acid dominates therefore eliminating the reducing ability of these amines. Thus the combination of maleic acid with DMoT, DMpT and DEpT would not produce the desired effect on the substrate as that of saccharin (a weaker acid). The APH-maleic acid system does

not have this problem and after interaction of the APH with maleic acid, this accelerator was still able to reduce the metal ions released from the surface by the maleic acid, implying that maleic acid and APH work well together as co-accelerator and accelerator in anaerobic adhesives formulations. These observations reinforce those of Raftery *et al* [21], in which they concluded that APH was the only accelerator which did not show any reduction inhibition in the presence of the organic acids, whereas all the toluidines suffered a loss in reducing ability towards the Cu(II) in the presence of acids with the sole exception of saccharin.

4.4.5 Formulations

The redox decomposition of hydroperoxides by metal ions at room temperature produces free radicals which, in the absence of oxygen, initiate polymerisation, the principal mode of curing for anaerobic adhesives. There are many types of free radical initiators, but hydroperoxides are the most important due to ease of handling and stability. Cumene hydroperoxide (CHP) is the most frequently used. The formulations presented in this following section contain organic acids (saccharin or maleic) combined with substituted aromatic amines (DMpT, DEpT, DMoT and APH) and the cumene hydroperoxide initiator. The methanol solutions used are as outlined in Section 4.3.2, (formulations 13-15), which were also made up with maleic acid.

The first commercial formulation (model 43) investigated contained saccharin (1%), maleic acid (0.3%), CHP (1%) and APH (0.3%). The copper piece was immersed in a methanol-based solution of the above components for a 24-hour period. The copper substrate emerged from the solution with a yellowish polycrystalline film on the surface, while the solution itself was also yellow. These yellow crystal type structures are indicative of the Cu(I) oxidation state [23]. The atomic % of each compound found on the surface after these immersions are seen in Table 4.9 below. Figure 4.21 represents the decomposition of the spectral regions C 1s, O 1s, N 1s, S 2p, Cu 2p and Cu LMM for the model 43 formulation.

| Model | Carbon | Oxygen | Copper | Nitrogen | Sulphur |
|-------|--------|--------|--------|----------|---------|
| 43 | 61.6 | 24.8 | 3.3 | 6.4 | 3.9 |

Table 4.9 Experimental values calculated (atomic %) for the methanol solutions of the model 43-cure formulation for anaerobic adhesives in contact with the copper substrate after a 24-hour period

The % carbon found on the surface was high at $\approx 62\%$. From the decomposition of the C 1s moiety, two carbon environments were present, that of the saturated hydrocarbons/contamination layer at a binding energy of 284.8 ± 0.3 eV, and a higher binding energy of 288.3 ± 0.3 eV. This second component was attributed to the $\text{N}-\text{C}=\text{O}$ [13] species, found present in both saccharin and APH compounds. From the above-calculated atomic %'s it can be seen from the nitrogen and sulfur percentages that both saccharin and the APH accumulate at the surface of the copper substrate. The sulfur peak at 168 ± 0.3 eV was attributed to the SO_2 entity, this correlated with the O 1s emission peak at 532.5 ± 0.3 eV. The higher binding O 1s emission peak at 533.5 eV was attributed to the C-OOH of the CHP compound. The N 1s peaks at 399.8 ± 0.3 and 401.6 ± 0.3 eV allocated to the nitrogen associated with the saccharin and the APH nitrogen environments respectively.

The Cu 2p peak at 932.5 ± 0.3 eV was indicative of the Cu(I) region. The yellowish coloured substance found on the substrate indicates the Cu(I) state. The Auger parameters at 1848.7 ± 0.3 eV indicates Cu(I) while the higher binding kinetic energy shoulder which produces a modified Auger parameter at 1852.2 ± 0.3 eV is more representative of the Cu (0) state.

Taking all these results together it would appear that saccharin and APH dictate the nature of the interaction between the copper surfaces and this model 43 formulation. The concentration of the saccharin was higher than that of the maleic acid (ratio 3:1), which is possibly why it appears to be the dominant acid in this case. As the CHP can act as an oxidising agent and as a reducing agent, speeding up the generation of Cu(I) metallic cations, but from previous literature

it has been suggested that the curing performance of anaerobic adhesives can occur with formulations that contain only a methacrylate monomer and a organic peroxide. However, these are limited by the stability of the product, sensitivity of the cure process to the substrate and its slow rate of polymerisation. Therefore, the addition of the organic acids and aromatic amines produces a product that is balanced between all of these requirements. The disadvantage of using a 24-hr period for studying these reactions is due to the fact that most anaerobic adhesives cure rapidly, therefore any reaction to take place would have definitely occurred within this time period, and maybe further.

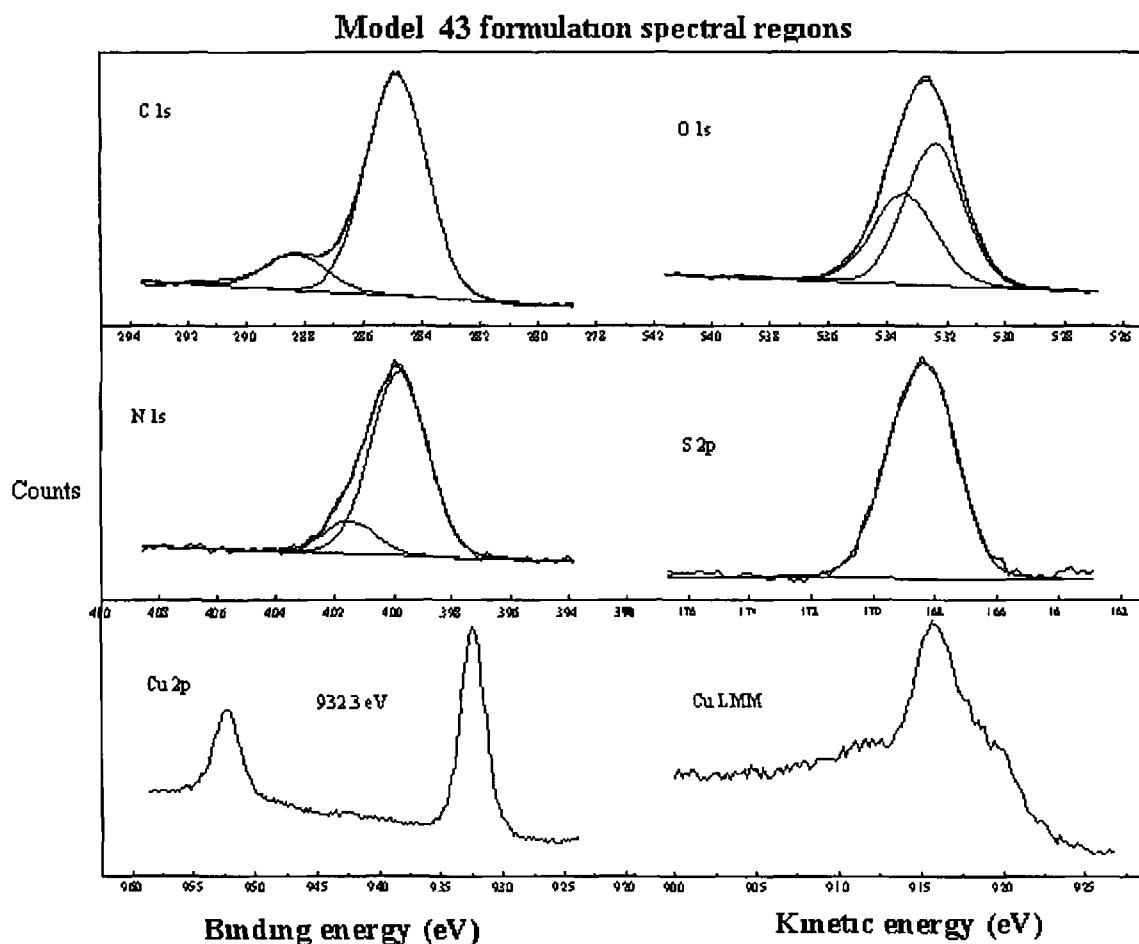


Figure 4 21 Decomposition of the XPS C 1s, O 1s, N 1s, S 2p, Cu 2p and Cu LMM emission lines for formulation model 43 in contact with a polished Cu substrate for 24 hr

For formulation model 90 which contained 1.6% saccharin, 3% CHP, 0.3% DMOt and 0.6% DEpT, after 24-hours immersed in this formulation the copper piece emerged from the solution with a black film covering the surface. This film was too thick for XPS to provide information into the underlying copper so the immersion time was reduced to 15 minutes to coincide with the onset of this film formation. This formulation was also made up with maleic acid replacing the saccharin and the atomic % calculated for the elements found on the surface can be seen in Table 4 10.

| Model | Carbon | Oxygen | Copper | Nitrogen | Sulphur |
|---------|--------|--------|--------|----------|---------|
| 90(BS) | 67.9 | 20.2 | 2.1 | 6.4 | 3.4 |
| 90(mal) | 60.2 | 34.5 | 2.8 | 2.5 | 0 |

Table 4.10 Experimental values calculated (atomic %) for the methanol solutions of the model 90 formulations for anaerobic adhesives in contact with the copper substrate after a 24-hour period

The most noticeable difference in the composition of the surfaces after immersion was that of an increase in the oxygen content when maleic acid was used in the above formulation 19.2% and 34.5% for the saccharin and maleic-based formulations respectively. This indicates the role that maleic acid plays in the acid oxidation of the underlying copper releasing the metal ions from the substrate. The % of copper found is also very low $\approx 2\text{--}3\%$ possibly due to the onset of this film formation therefore masking the copper signal.

Figure 4.22 shows the decomposition of the high-resolution spectral regions recorded for these formulations. For the saccharin-based formulation the Cu LMM peak at 914.6 ± 0.3 eV and the Cu $2p_{3/2}$ emission line at 932.9 ± 0.3 eV indicate that the oxidation state of the copper is predominately +1, which is what is needed to produce the active RO^\bullet radical for polymerisation. The CHP speeds up this process enormously, whereas in the absence of the CHP, the underlying copper was still evident after 24 hours. The O 1s peak was associated with the SO_2 saccharin component. Other chemically shifted oxygen species are so close in binding energies that it is not possible to resolve them. The C 1s environments are identical to those associated with the saccharin and the substituted aromatic amines.

For the model 90 formulation where the organic acid used was maleic acid, the results are different. The Cu LMM region produced a peak at 915.5 ± 0.3 eV with a shoulder at the lower kinetic energy of 913.2 ± 0.3 eV, these values of kinetic energy when combined with the Cu $2p_{3/2}$ peak at 934.9 ± 0.3 eV lead to modified Auger parameters of 1850.4 ± 0.3 eV and 1848.1 ± 0.3 eV.

which correspond to the Cu(II) and Cu(I) states of the copper species present. The Cu $2p_{3/2}$ peak at 934.7 ± 0.3 eV was indicative of the Cu(II) species also, and the onset of shake up satellite peaks are evident in this region. This suggests that saccharin is a more suitable organic acid to use in anaerobic adhesives formulations that bond to copper, as Cu(II) copper species produces the inactive ROO^\bullet radical. When maleic acid was used in model 90 formulation, the Cu(II) ions appear to be the predominant species on this analysed surface. This increased atomic % of oxygen found on the surface could be due to the increased oxygen moiety of maleic and CHP.

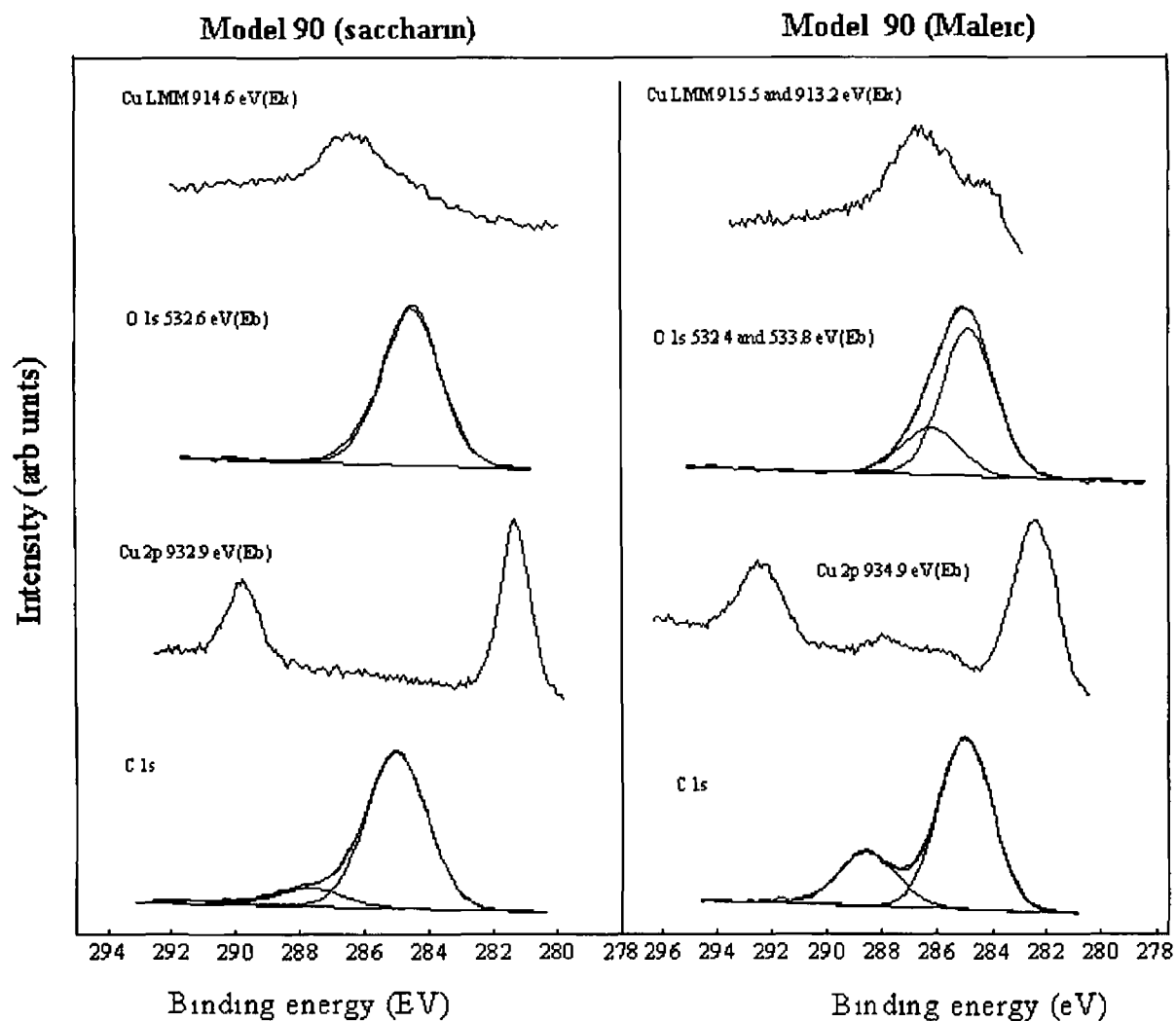


Figure 4 22 Decomposition of the XPS Cu LMM, O1s, Cu 2p and C 1s emission lines for formulation model 90 (saccharin and maleic acid) in contact with a polished Cu substrate for 15 minutes

Formulation model 43x contained the methanolic solution of 1% saccharin, 1% CHP and 0.3% APH (saccharin was substituted with maleic acid also). The atomic % concentration of each element found on the copper surface can be seen in Table 4.11.

| Ingredient | Carbon | Oxygen | Copper | Nitrogen | Sulphur |
|-------------------|---------------|---------------|---------------|-----------------|----------------|
| 43x (BS) | 57.3 | 23.9 | 3.2 | 9.1 | 6.5 |
| 43x (mal) | 61.9 | 28.3 | 0.5 | 9.3 | 0 |

Table 4.11 Experimental values calculated (atomic %) for the methanol solutions of the model 43x formulations for anaerobic adhesives in contact with the copper substrate after a 24-hour period.

The differences in atomic % for the model 43x (BS) formulation and for a combination of 1.6%BS-1.5%APH without the CHP appear to be in the nitrogen content, with nitrogen being present on the surface of the 43x (BS) treated sample at 9.1%. Figure 4.23 shows the decomposition of the spectral regions for the 43x formulations. Starting with the N 1s peak, two peaks are resolved for the 43x (BS) that at 399.8 ± 0.3 eV which was attributed to the BS and at a higher energy of 401.3 ± 0.3 eV due to the nitrogens associated with the APH, (33% 66%).

The Cu 2p_{3/2} peak at 933 ± 0.3 eV is related to the Cu(I) species. These spectra are almost identical to that achieved for the BS-APH system only. The C 1s peaks are indicative of saturated hydrocarbons (285 ± 0.3 eV), with the higher energy of 287.5 ± 0.3 eV associated with the N-C=O present in both compounds.

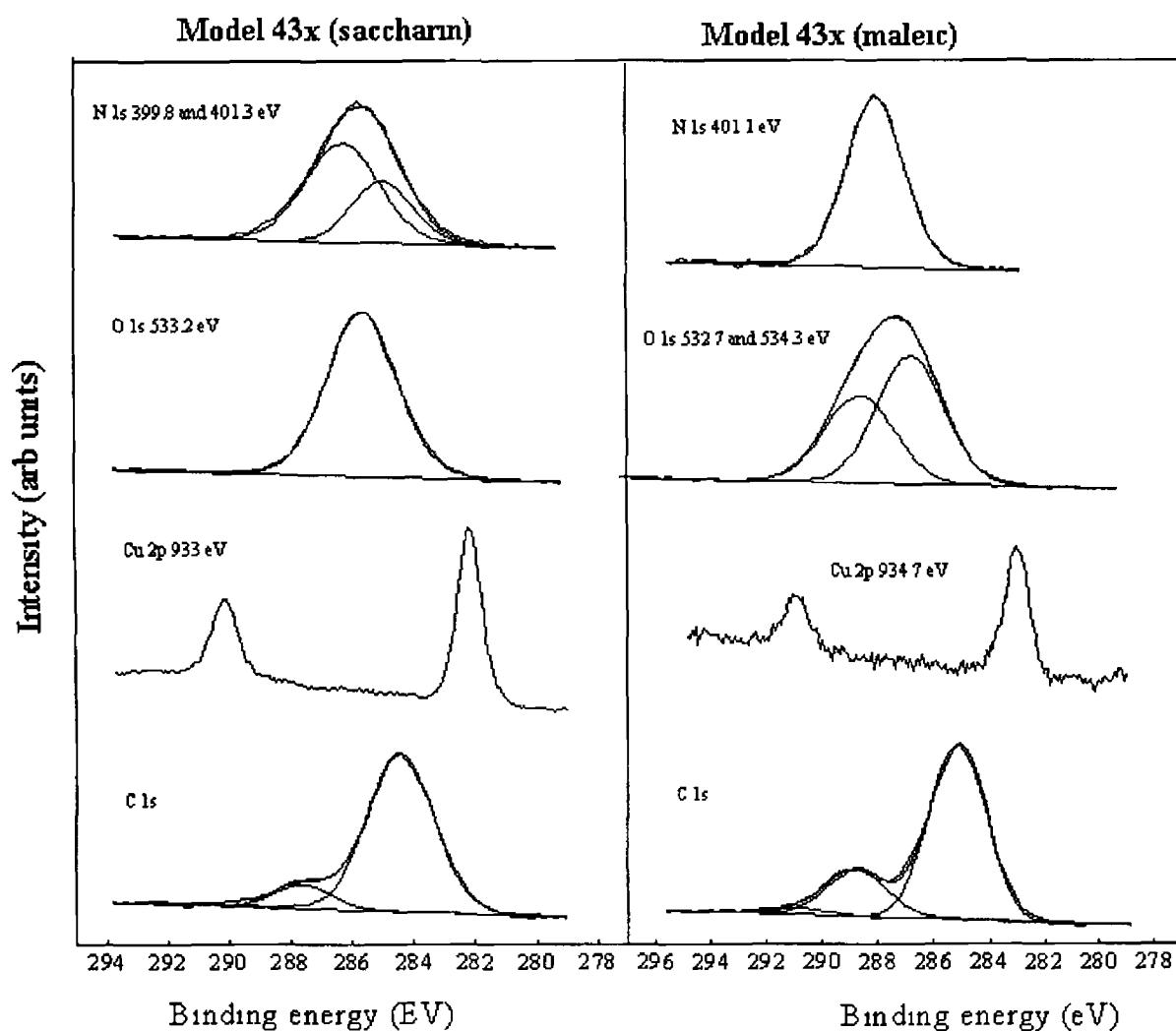


Figure 4 23 Decomposition of the XPS N 1s, O 1s, Cu 2p and C 1s emission lines for formulation 43x (saccharin and maleic acid) in contact with a polished Cu substrate for 24 hr

The percentage copper found on the surface after immersion for 24 hrs in the 43x (maleic acid) formulation was very low $\approx 0.5\%$, therefore the Cu LMM line was too small to be confidently recorded. The binding energy of the Cu $2p_{3/2}$ at 934.7 ± 0.3 eV, indicated that Cu(II) species is present. Nitrogen was found at 9%, which was attributed to APH, as this was the only nitrogen-containing compound in this formulation. When mal-APH solution was used the Cu was found in the Cu(I) state. The addition of CHP to the formulations leads to a more efficient redox reaction in the presence of a peroxide.

4.4.6 Reduced copper substrate

The copper substrate was electrochemically reduced as described in section 4.3.2, the reason for this was to ensure that the copper surface which interacted with the components of the anaerobic adhesive system was in the Cu (0) oxidation state. This reduced copper substrate was placed in solutions containing, 1.6%BS, 1.6% maleic acid, 1.6%BS-1.5% DMoT, 1.6%BS-DMpT, 1.6%BS-DEpT and formulation 43x containing 1%BS-1%CHP-0.3%APH with the saccharin being replaced by the maleic acid in the 43x formulation.

The results obtained for the electrochemically reduced copper, in the 1.6%BS-MeOH were almost identical to those received for the polished copper sample. The C 1s region identified two carbon environments at binding energies of 285 ± 0.3 eV and 288 ± 0.3 eV, corresponding to the saturated hydrocarbons/contamination and the C=O / N-C=O moiety present on the substrate. The O 1s region identified a peak at 532.6 ± 0.3 eV corresponding to the SO_2 moiety, and this peak encompassing the carbonyl oxygen present in the acid. The Cu 2p emission line at 934.4 ± 0.3 eV, combined with the Cu LMM peak at 915.7 ± 0.3 eV indicate that the Cu(II) species is dominant, with the S 2p at a binding energy of 167.9 ± 0.3 eV indicative of the SO_2 environment.

For BS combined with the substituted aromatic amines, the results are as before, with no noticeable differences in the spectra recorded, the Cu 2p and the Cu LMM emission peaks indicating that the Cu(I) oxidation state of copper is

found on the surface. This agrees with the previous results where after polishing, the surface of the copper was found to be predominately in the Cu (0) oxidation state, without the need for further surface pre-treatment to reduce it to this state.

The survey scan of the 1.6%BS, 1.6% maleic acid, 43x (BS) and 43x (maleic acid) using a reduced copper substrate can be seen in Figure 4.24. For the BS and the 43x (BS) formulation the results are within experimental error of the results recorded when the substrate is not electrochemically reduced. For the 43x (BS) formulation it can be seen that both the APH and the BS segregate at the copper surface, with 10% nitrogen and 5% sulfur found on the copper surface, coming from both of these compounds.

For the 1.6% mal-MeOH in contact with the reduced copper the % oxygen found on the surface decreased by about 10%, compared with the previous results, with an increase in the copper signal. This was the desired result of the electrochemical reduction in the way that it decreased the surface oxygen found present on the copper. The main difference between the 43x (mal) formulations was again an increase in the copper signal, where copper was found at $\approx 3\%$ on the electrochemically reduced surface, whereas on the polished copper surface the % copper was that of 0.5%.

Generally the electrochemical reduction of the surface had no significant effect on the chemical composition of the treated surfaces. Therefore the chemical interactions, which occur at these surfaces, are mostly independent of the initial chemical state of the surface. Indicating that no special surface treatment procedures are required to result in satisfactory cure chemistry within the adhesive.

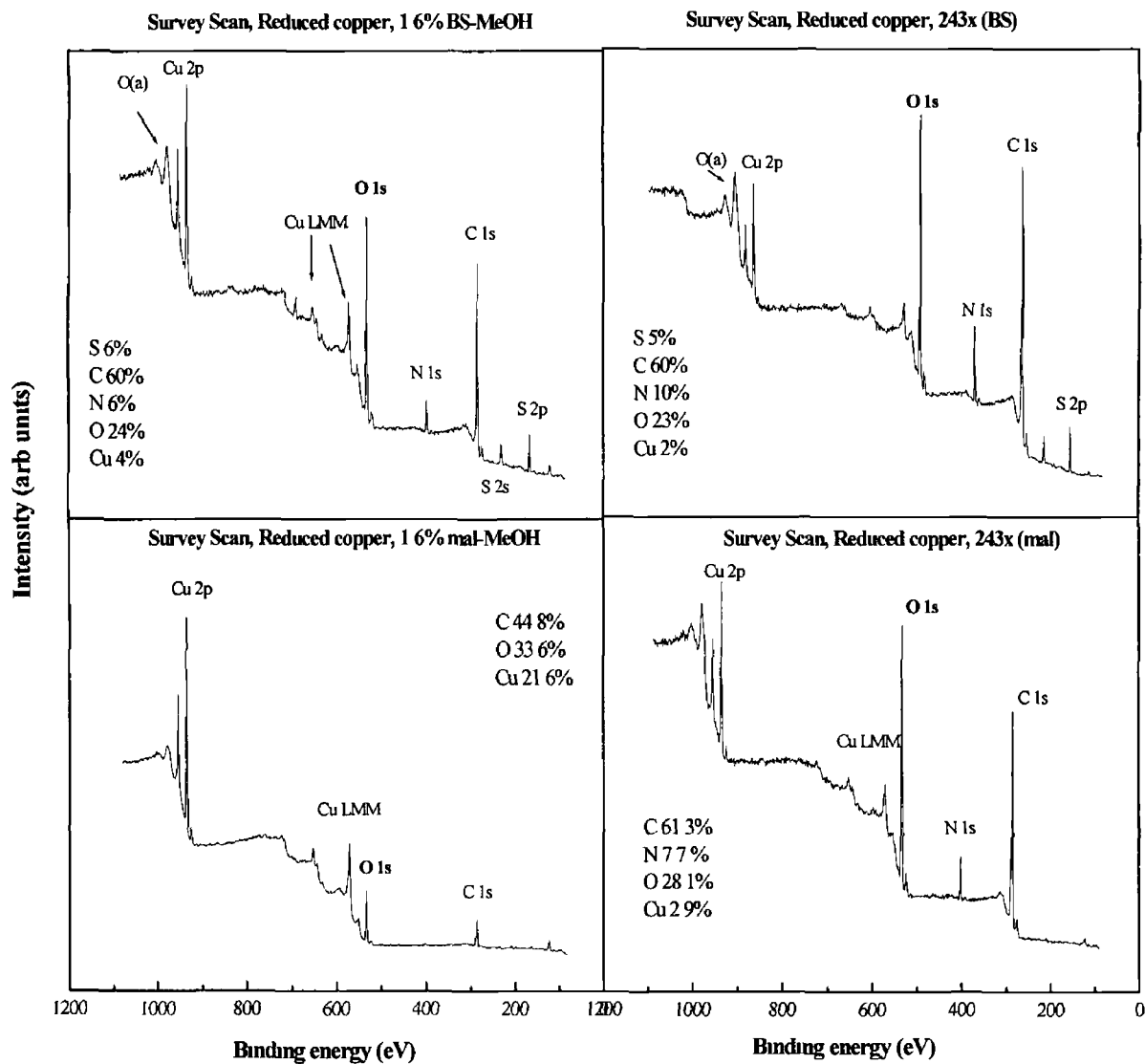


Figure 4 24 Survey scans recorded for reduced copper substrate in contact with A) 1 6% BS B) 43x (BS) C) 1 6% Maleic acid and D) 43x (maleic acid), indicating the peaks of interest

4.5 Conclusions

Throughout this chapter XPS was used to investigate the effect that the individual cure components of anaerobic adhesives had on the substrate surface. An organic acid, a reducing amine and a hydroperoxide were the main ingredients of this anaerobic cure system, and based on the above results the following reaction sequence was suggested:

Saccharin interacted with the polished copper substrate to form a Cu(II) complex (BSCu(II)), this acid oxidation of the metal surface is essential for the initiation reaction of anaerobic adhesives as it releases the metal ions from the substrate. The saccharin combines with the para-substituted amines such as DMpT and DEpT resulting in the formation of a salt, which facilitates basic reduction capable of reducing metal ions from the higher to the lower oxidation states, i.e. $\text{Cu(II)} \rightarrow \text{Cu(I)}$. For the APH-BS system, the saccharin interacts with the copper substrate oxidising the surface releasing metal ions Cu(II) (after a 24 hr time period), the APH then reduces this Cu(II) species to the Cu(I) species, leaving this Cu(I) species ready to decompose the hydroperoxide, and initiate polymerisation.

The results obtained when using maleic acid as a substitute for saccharin as a co-accelerator in anaerobic adhesives cure system would indicate that the maleic acid forms a salt with these toluidines, independent of the position of the electron donating group on the aromatic ring, ortho- or para-positions. But in forming these salts the acidic character of the maleic acid dominates therefore eliminating the reducing ability of these amine. This suggests that combinations of maleic acid with DMoT, DMpT and DEpT would not produce the same reaction sequence on the substrate as that of saccharin (a weaker acid). However, maleic acid is in theory a stronger acid than saccharin and hence would be expected to release proportionately more metal ions from the surface. The benefits of this however only arise when APH is the reducing agent as APH is able to tolerate the presence of maleic acid without its reducing abilities being significantly curbed. This result implies that maleic acid and APH work well together as co-accelerator and accelerator in anaerobic adhesives formulations.

From the formulations tested it would appear that saccharin has advantages over maleic acid in promoting the cure chemistry. Saccharin releases metal ions from the underlying surface, which in turn are reduced by the aromatic amines, or salt that has been formed. When CHP is added to this combination, this reaction sequence happens extremely quickly, thereby speeding up the polymerisation process, which is essential in the curing process. The most rapid reactions occurred when using the 90 formulations, where after 15 minutes a film had formed on the copper surface.

Reducing the copper electrochemically was to no advantage using the above components of the cure system, this eliminates another surface pre-treatment step, which is essential in the adhesive industry, where minimal surface preparation is a must.

4.6 References

- [1] Boeder, C W in "Structural Adhesives", Hartshorn, S R (Ed), Plenum Press, New York, (1986) 217
- [2] Melody, D P in "Handbook of Adhesion", Packham, D E (Ed), Longman Scientific & Technical, New York, (1992) 46
- [3] Okamoto, Y , J Adhesion, 32 (1990) 227
- [4] Okamoto, Y , J Adhesion, 32 (1990) 237
- [5] Hudak, S J , Boerio, F J , Clark, P J and Okamoto, Y , Surf Interface Anal , 15 (1990) 167
- [6] Beaunez, P , Helary G and Sauvet G , J of Polymer Science, 32 (1994) 1459
- [7] Beaunez, P , Helary, G and Sauvet G , J of Polymer Science, 32 (1994) 1471
- [8] Wellmann, St and Brockmann, H , Int J Adhesion and Adhesives, 14 (1994) 47
- [9] Raftery, D , Smyth M R and Leonard, R , J Polymer Sci , 35 (1997) 3327
- [10] Raftery, D , Smyth M R and Leonard, R , Int J of Adhesion, 17 (1997) 9
- [11] George, B , Grohens, Y , Touyeras, F and Verbrel, J , Int J Adhesion Adhesives, 20 (2000) 245
- [12] Briggs, D , Seah, M P , "Practical Surface Analysis by Auger and X-ray Photoelectron Spectroscopy", Wiley, New York, (1994)

- [13] Briggs, D , “Surface Analysis of Polymers by XPS and Static SIMS”, Clarke, D R , Suresh, S and Ward, I M (Eds), Cambridge University Press, (1998)
- [14] Vickerman, J C , “Surface Analysis the Principal Techniques”, Wiley, Chichester, (1997) 68
- [15] Wagner, C D , Farad Discuss Chem Soc , 60 (1975) 291
- [16] Wagner, C D , Anal Chem , 47 (1975) 1201
- [17] George, B , Grohens, Y , Touyeras, F and Verbrel, J , J Adhesion Sci Technol , 12 (1998) 1281
- [18] Marsh, J , Minel, L , Barthes-Labrousse M G and Gorse, D , Appl Surf Sci , 99 (1996) 335
- [19] Sesselmann, W and Chuang, T J , Surf Sci , 176 (1986) 32
- [20] Whelan, C M , Ph D Thesis, Dublin City University, (1997)
- [21] Raftery, D , Ph D Thesis, Dublin City University, (1996)
- [22] Raftery, D , Smyth M R , Leonard, R and Heatley, D , Int J of Adhesion, 17 (1997) 151
- [23] Sharp, D W A , “Dictionary of Chemistry”, 2nd Edition, Penguin (1990)
- [24] Ghijssen, J and Marshall, F , University Notre-Dame de la Prix, Namur, Belgium, *Private communication*

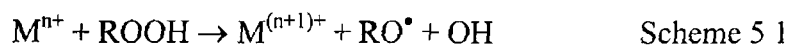
Chapter 5

An X-ray photoelectron spectroscopy study into the effect individual cure components and combinations of same, of anaerobic adhesives have on an iron containing substrate surface

5.1 Introduction

The redox decomposition of a hydroperoxide by metal ions at room temperature produces free radicals which in the absence of oxygen initiate the polymerisation of methacrylic monomers. The high efficiency of these systems, combined with the high inhibiting power of oxygen in this radical polymerisation of methacrylates allowed for the development of anaerobic adhesives and sealants. These anaerobic adhesive formulations are single-component liquids that can be stored at room temperature, and polymerise rapidly when confined between two metallic surfaces such as copper, brass, iron or steel, in the absence of air.

The metal substrate on which the anaerobic adhesive is applied plays an important role in the initiation of polymerisation. The catalytic decomposition of the hydroperoxide generates free radicals. Equation 5.1 represents the fundamental step for the formation of primary radicals, while Equation 5.2 showing metal ions in their higher oxidation state generating free radicals which are incapable of initiating polymerisation, although this reaction does regenerate the metal ion to its lower valent state. A stationary concentration of each ion would be established if the rates in reaction schemes 5.1 and 5.2 were equal, however this is rarely true and the contribution of scheme 5.2 depends on the nature of the metal [1].



The following chapter concentrates on an iron-containing substrate, as iron and copper make up the vast majority of metals encountered in anaerobic adhesive applications and these are also the most active metals in terms of the catalytic decomposition of the hydroperoxide. Some other metals demonstrate activity, such as cobalt, but primers are usually used to increase the cure speeds of these substrates. Primers generally consist of dilute solutions of organic soluble salts of either iron or copper.

5.1.1 The cure chemistry

Anaerobic adhesives are predominately used for bonding metallic substrates. The transition metal ions on the substrate surface play a key role in the cure chemistry reacting with the hydroperoxide to generate free radicals. Anaerobic adhesives are sensitive to the nature of the substrate requiring confinement on an active metal surface, e.g. they cure rapidly on copper and iron rich surfaces, but slowly or not at all on cobalt, cadmium and zinc plated metals [2].

The cure chemistry has been discussed in detail in chapter 4. Briefly, a study performed by Beaunez *et al* [1] focused on the redox polymerisation initiated by cumene hydroperoxide (CHP) and iron saccharinate. Based on their results it was proposed that the DMpT reduces iron(III) to iron(II), and that the iron(II) ions complexed by two DMpT molecules are more reactive than the uncomplexed Fe(II) regarding the CHP, and that the saccharin activates the decomposition of the CHP by protonation of the peroxide bond and facilitating cleavage at room temperature. They also suggested that the uncomplexed iron(II) is unable to decompose the cumene hydroperoxide, regardless of the concentration of the saccharin.

The studies carried out by Raftery *et al* [3] investigated the reactions undergone by APH in the presence of Fe(III) ions. When Fe(III) was substituted for Cu(II) in reaction mixtures containing APH-BS(mal)-CHP and Fe(III) nitrate, the only reactions observed were that of the decomposition of the CHP induced by the Fe(III) ions, with the typical decomposition products of CHP (i.e. cumyl alcohol and cumyl ether) been identified using GC-MS (gas chromatography – mass spectroscopy). This revealed the greater sensitivity that a Cu(II) system shows to this hydrazine-based cure system, as opposed to the iron-based system. Also by using APD (1-acetyl-2-phenyldiazene), which is the oxidation product of APH, the different reaction routes and products catalysed by iron and by copper can be seen in Figure 5.1. For the reaction with copper the major reaction product is 1-acetyl-2,2-diphenylhydrazine, whilst with Fe(III) azobenzene and biphenyl were the main reaction products.

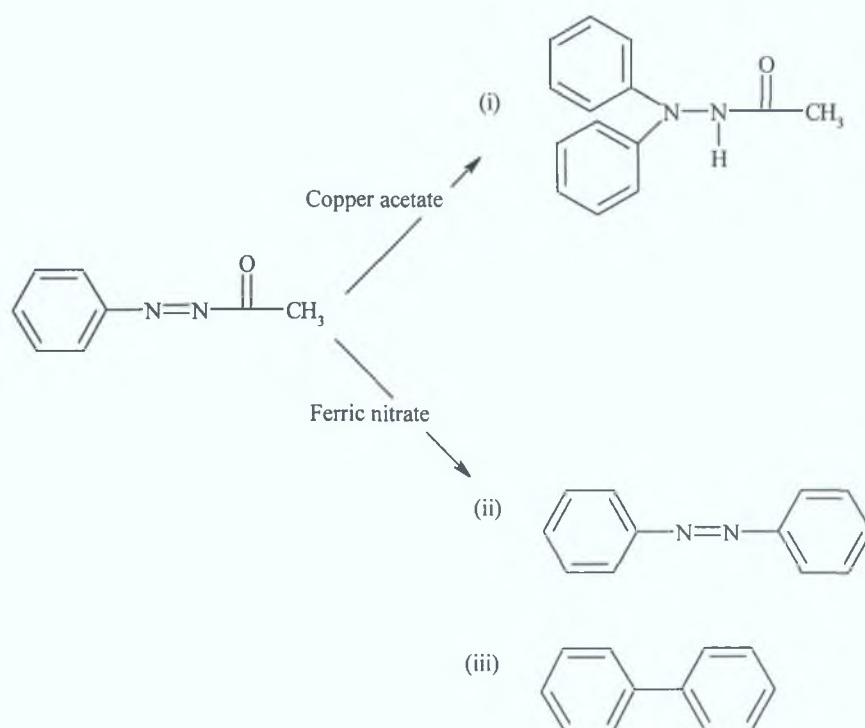


Figure 5.1 Schematic of reactions undergone by APD in the presence of Cu(II) and Fe(III). Major reaction product in the presence of Cu (II) ions is (i) 1-acetyl-2,2-diphenylhydrazine. While in the presence of Fe(III) ions azobenzene (ii) and diphenyl (iii) is formed [3].

Raftery *et al.* continued this line of investigation [4], investigating the organic acids used in anaerobic adhesive, and from their results they found that maleic acid would be the better acid for iron systems that contain CHP as the peroxide. These results suggested that formulations should take into account the type of metal expected to catalyse the redox radical polymerisation as one formulation that has good stability and reactivity properties when catalysed by a particular metal such as copper, may not be appropriate when it is catalysed by another metal such as iron.

More recently, George *et al.* [5] investigated the role played by the substrates and the atmosphere on the overall reaction of adhesive systems. In aerobic media, they found an increased efficiency of the metal catalyst observed in the order aluminium < iron < copper, and in the absence of air the efficiencies

of iron and copper were found to be very similar. In the case of iron and in the presence of air, George obtained yellowish-brown crystals when he placed carbon steel in contact with BS solutions. He assumed these to be ferrous saccharinate, as the infrared spectrum could be superimposed on the spectrum of some ferrous saccharinate synthesised independently. Comparing this to the copper derived saccharinate these Fe(II)sacc crystals were collected after three weeks, while the BSCu(I) the crystals were collected after five hours. George also implied that BSCu(II) was unlikely to form in the absence of air.

The studies mentioned above are to date the main published works carried out on anaerobic adhesives. Throughout this chapter the effects that the individual cure component of anaerobic adhesives have on a polished iron-containing substrate will be investigated. The introduction of another metal would make results more universal as opposed to just a copper substrate which has been shown to be the most active metal surface for these anaerobic cure systems.

5.2 Experimental

5.2.1 Instrumentation

XPS measurements were acquired under the same conditions as outlined in chapter 4

5.2.2 Reagents and sample preparation

All the reagents used were as that for chapter 4. The polished mild steel substrates were initially wiped with 'lens tissue' that had been soaked in methanol, followed by sonication in methanol for ten minutes before being removed from this solution and dried in a stream of nitrogen before immersion into the reaction mixtures. Figure 4.7 (chapter 4) gives the chemical structures of the compounds used in this study. The solutions used have previously been described (chapter 4 solutions) also.

5.3 Results and Discussion

5.3.1 Organic acids: saccharin and maleic acid

The polished iron-containing substrates were immersed for a 24-hour period in a 1.6% (w/v) BS-MeOH, and 1.6%(w/v) maleic acid-MeOH solution. The spectra recorded allowed the calculation in atomic % of the individual elements present on the iron substrate due to the immersion in the above solutions. The results are seen in Table 5.1. Typical levels of uncertainty in the atomic % calculated can also be seen in Table 5.1, these uncertainty levels are calculated by measuring four different iron samples which were treated and analysed under identical conditions.

| Component | Carbon | Oxygen | Iron | Nitrogen | Sulphur |
|----------------------|-----------------|-----------------|--------------|--------------|--------------|
| Mild Steel reference | 55.5 | 33.8 | 10.7 | 0 | 0 |
| BS | 53 (56) (48) | 33 (24) (31) | 4 (4) (7) | 5 (8) (7) | 5 (8) (7) |
| Maleic acid | 47 | 48 | 5 | 0 | 0 |
| Error analysis | ±2.4% | ± 1.7% | ±1% | ± 1% | ± 1% |

Table 5.1 Experimental values calculated in atomic % for the iron substrate (as a reference) and immersed in a 1.6% BS-MeOH and 1.6% maleic acid-MeOH solutions for a twenty-four hour period. **BSFe(II)**, **BSFe(III)**.

The iron reference surface gives an indication of what is present on the substrate surface prior to immersion in a cure solution. From the results above, carbon makes up more than half of the substrates surface, as before this carbon signal is attributed to a surface contamination layer found present on most surfaces, due to polishing and the exposure of the substrate to the ambient atmosphere before transfer to the analysis chamber of the XPS spectrometer. This carbon peak is used for referencing, at a binding energy of 285 eV as most samples have adventitious carbon contamination. The percentage iron found on the substrate is only $\approx 11\%$, this is because the substrate, is that of mild steel,

with iron the most predominant metal found on this surface. For the substrate that was subjected to modification by saccharin, the atomic % of the elements carbon and oxygen found on the substrate surface are within those of the experimental errors calculated, but the decomposition of this C 1s spectral region produces two distinct carbon environments, that associated with the adventitious carbon / saturated hydrocarbons at a binding energy of 285 ± 0.3 eV and a higher binding energy of 288 ± 0.3 eV which represents either the $\text{C}=\text{O}$ / $\text{N}-\text{C}=\text{O}$ associated with saccharin. Also for the iron substrate modified with saccharin the percentage iron found on the substrate surface is nearly halved, indicating that the saccharin forms a overlayer on this substrate surface leading to a decrease in the detection of the underlying iron because of this layer. Taking the iron substrate modified with maleic acid, again two distinct carbon environments are revealed from decomposition of C 1s core level, these peaks come in at 285 ± 0.3 eV, for saturated hydrocarbons and at the higher energy of 288.7 ± 0.3 eV representative of the highly oxidised acid functionality associated with maleic acid $\text{O}-\text{C}=\text{O}$. Again the presence of this acid on the surface of the substrate leads to a decrease in the signal of the iron during XPS analysis.

Figure 5.2 shows the XPS survey spectra of the iron reference (Fe_{ref}), iron immersed in 1.6% BS-MeOH solution (Fe_{BS}) and iron substrate immersed in 1.6% maleic acid-MeOH solution (Fe_{mal}). These spectra reveal the presence of essentially iron, oxygen and carbon, and as a result of the BS treatment, sulfur and nitrogen are present on the surface of this iron substrate. For the Fe_{ref} and the Fe_{BS} the amount of carbon and oxygen on the substrate surface is comparable, but for the Fe_{mal} substrate the amount of carbon has decreased with an increase in the oxygen content. Maleic acid has a higher oxygen content so the change in the O/C ratio is expected as the ratio of O/C is higher in the maleic acid compared to that of saccharin i.e. 4.4 for maleic acid and 3.7 for saccharin.

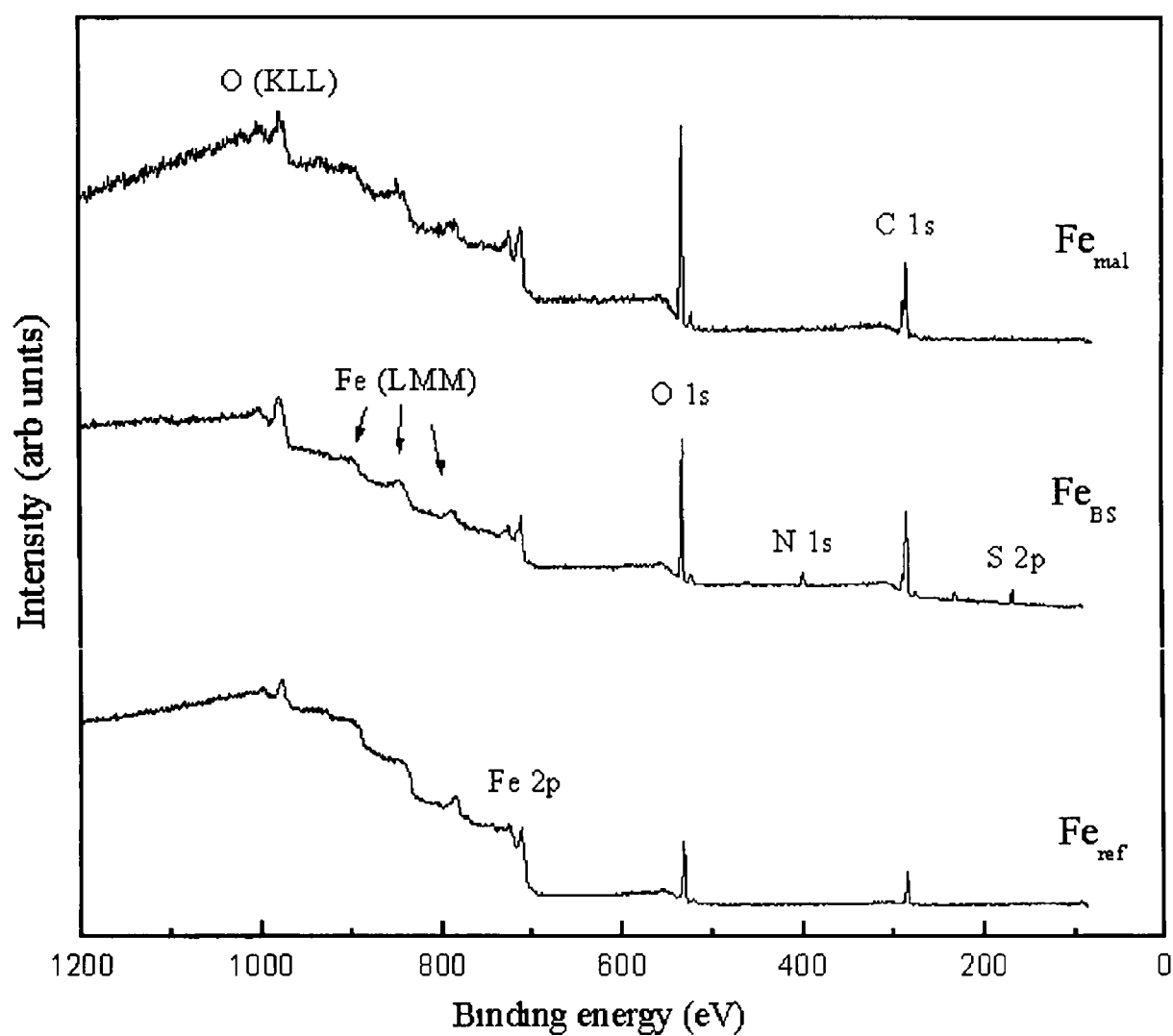


Figure 5 2 XPS survey spectra of iron reference (lower), iron-BS (middle) and iron-maleic (upper), highlighting the peaks of interest

Oxidation state of the Iron

The oxidation state of the iron substrate is crucial in initiation of polymerisation as metal ions in their lower oxidation (i.e Fe(II)) state generate free radicals by the decomposition of a hydroperoxide, which initiate the polymerisation process. Several studies on iron oxides have been made over the past decade [7-10], and the Fe 2p photoelectron spectra of Fe(III) and Fe(II) oxides are particularly complex, due to the large amount of coupling between the core hole created by the photoemission and the high spin states of iron [6]. Spin-orbit splitting, multiple oxidation states and satellite structure complicate the quantitative analysis of Fe (2p) spectra. The spectral line shape is quite sensitive to chemical changes. The multiple oxidation states of iron are those of the metallic iron which has the (0) oxidation state, FeO or ferrous oxide contains iron in oxidation state (II), FeOOH (goethite) and α -Fe₂O₃ (hematite) represent iron in the oxidative state (III) with Fe₃O₄ (magnetite) which is a mixed compound containing iron at (II) and (III) oxidation states.

Figure 5.3 shows the XPS spectra of the Fe 2p core level for Fe_{ref}, Fe_{BS} and Fe_{mal}. For iron in the (0) oxidation state, the binding energy values reported in the literature are generally from 706.3 eV to 707.7 eV [10]. The peaks at approximately 710 eV (for the Fe 2p_{3/2}) and 724 eV (Fe 2p_{1/2}) correspond to the Fe 2p components of oxidised iron. As the chemical shifts for both Fe(II) and Fe(III) are in this range, the presence of the different oxidation states is determined by the presence of satellite peaks. The satellite peaks at an energy shift of 9 eV from the main peak are indicative of the Fe(III) oxidation state of the iron [9, 13], whereas the satellite peak at an energy shift of approximately 5 eV from the Fe 2p_{3/2} emission line is characteristic of the Fe(II) species [11]. From the shape of the spectra and line positions in Figure 5.3 it would appear that the substrates are composed of a mixture of metallic and oxidised iron. In Figure 5.3 a shoulder appears in all the spectra at an energy of 706.5 → 707.1 eV, indicating the presence of the metallic iron, however this shoulder is relatively small in comparison to the other peaks. The binding energy value of the Fe 2p_{3/2} emission line for the Fe_{BS} and Fe_{mal} is that of 710.3 ± 0.3 eV, this

value agrees with that found in literature for the FeO species, indicating that Fe(II) is the prominent state of the iron species after immersion in an organic acid solution of methanol. There is also an indication that Fe(III) satellite structures are present on the substrate surface after modification with the organic acids. These spectra highlight the role played by the acid in releasing metal ions from the substrate surface, with the lower oxidation state of the metal present on the substrate surface after modification in organic acid solutions.

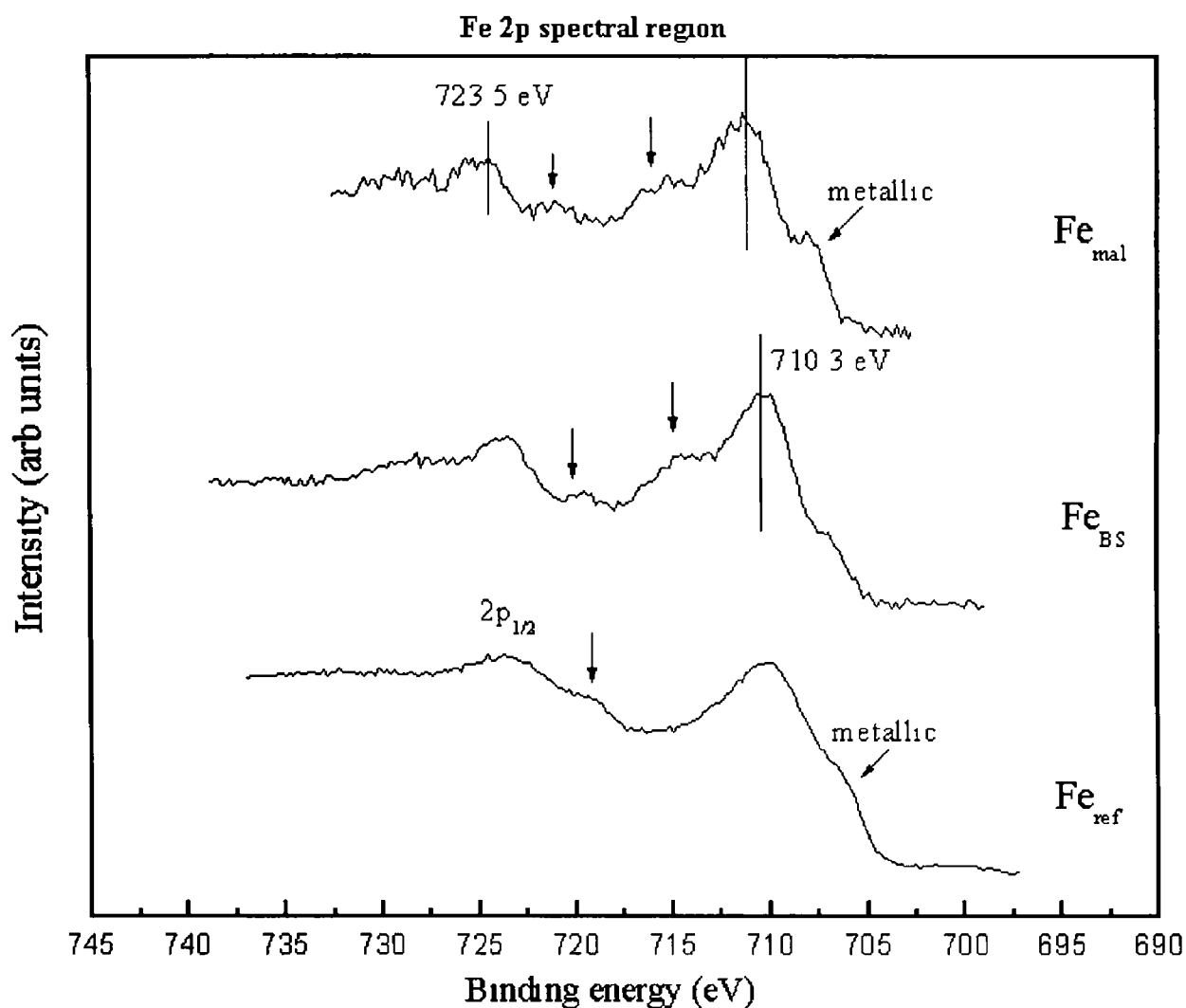


Figure 5.3 XPS spectra of the Fe 2p core levels of a iron reference substrate, iron substrate in 1.6% BS-MeOH solution and iron substrate in 1.6% maleic-MeOH solution, bottom, middle and upper respectively. Arrows indicate satellite peaks.

The O 1s core level emission line, can produce more information on the oxidised iron, the decomposition of the O 1s spectral region for the Fe_{ref}, Fe_{BS} and Fe_{mal} can be seen in Figure 5.4. The Fe_{ref} substrate can be resolved into four components, that located at a binding energy of 530.2 ± 0.3 eV is symbolic of the Fe₂O₃ [11] and Fe₃O₄ [6], a slightly higher binding energy of 531.7 ± 0.3 eV possibly attributed to the Fe(OH)_x hydroxide iron. This hydroxide iron is generally of the form Fe(OH)₃ as Fe(OH)₂ may be formed from Fe(II) and OH in the absence of O₂ but is very readily oxidised. With the peak at 533.1 ± 0.3 eV due to H₂O showing a small amount of H₂O on this sample surface and that of 534.4 ± 0.3 eV due to carbon contamination with a binding energy which is characteristic of the highly oxidised carbon species C_Q-O.

For the iron substrate, immersed in the saccharin solution, two oxygen environments are clearly distinguishable. The peak at 532.6 ± 0.3 eV is the accompanying peak in this O 1s region for the SO₂ moiety, where a peak at 532.2 ± 0.3 eV possibly encompassed in this peak is due to the carbonyl oxygen with the smaller peak at the higher binding energy of 533.2 ± 0.3 eV typical of the H₂O molecule. The two environments for oxygen associated with Fe_{mal} indicate that maleic acid has accumulated at the interface as these peaks at binding energies of 532.4 ± 0.3 eV and 533.8 ± 0.3 eV are representative of the oxygen environments present in maleic acid [16]. The increase in the percentage oxygen found on the iron substrate surface after immersion in this maleic acid solution is indicative of the presence of an iron malaete salt present on the surface. So from the above results it would appear that both of the acids accumulate at the substrate surface with maleic acid producing a greater degree of attack on the substrate surface compared to that of saccharin.

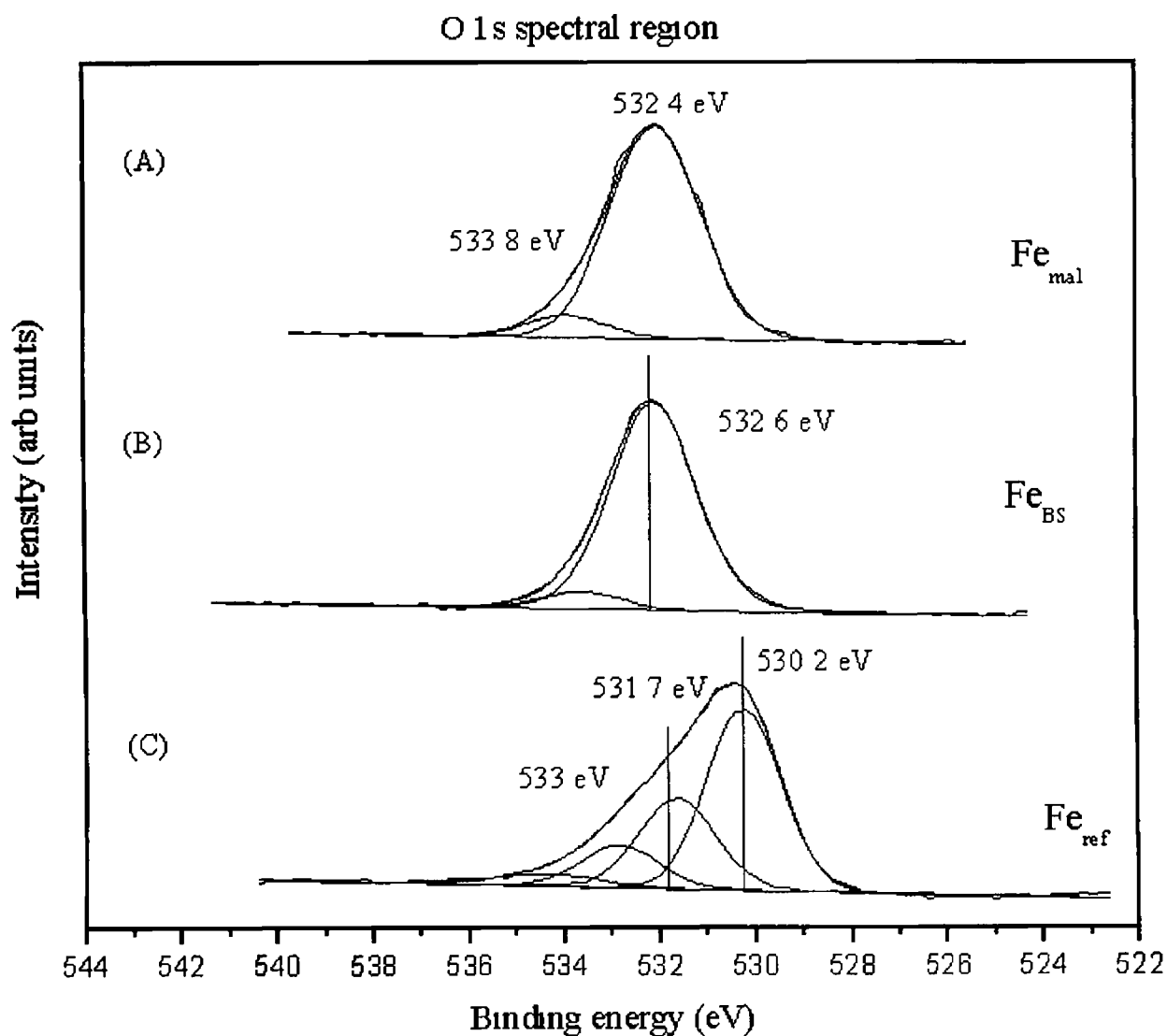


Figure 5.4 Decomposition of the O 1s core levels of (A) Fe_{mal} , (B) Fe_{BS} and (C) Fe_{ref} , after the iron substrate was left for 24 hour in contact with these solutions

5.3.2 Substituted aromatic amines

The iron-containing substrate was placed in the following toluidines – methanol solution, DMoT, DMpT and DEpT, these solutions contained 1.5% (w/v) of the toluidines. After XPS analysis of the substrate, there appeared to be no evidence of any interaction between the iron and these compounds, indicating that these amines have little or no effect on the iron-containing substrate for a 24 hr immersion period. Also APH was placed in contact with the iron-containing substrate and within the 24 hr time limits provided, it appeared to have no effect on the substrate surface. This is most noticeable for all of the above triarylalkylamines as the calculated atomic % of the elements of the surface of the substrate are within a 5 % error limit, and can be seen below in Table 5.2 where the experimental values calculated in atomic % are highlighted. The presence of carbon, oxygen and iron are the only elements evident from the survey spectrum recorded for these substrate modifications, but the absence of any nitrogen also indicated that no interactions occur between the iron and these amines.

| Component | Carbon (%) | Oxygen (%) | Iron (%) |
|-----------|------------|------------|----------|
| DMoT | 50.5 | 38 | 11.5 |
| DMpT | 54.6 | 36.1 | 9.3 |
| DEpT | 51.7 | 37.6 | 10.7 |
| APH | 53.2 | 34.6 | 12.2 |

Table 5.2 Calculated atomic percentages of iron substrate in following amine solutions.

Also the Fe 2p region of the spectra recorded for the above substrate are almost superimposable on one another, and indicate that these reducing amines have no reducing effect on this iron containing substrate surface. This is contradictory to the results of Raftery *et al.* [15] who found that APH, DEpT and DMpT can reduce iron(III) to Fe(II), although Raftery *et al.* were dealing with ionic iron salts in solution which could account for the discrepancy between results. Figure 5.5 shows the Fe 2p spectral region of the above amines in contact with

mild steel, these spectra show similar evolution of the Fe 2p peaks, where the main peak at 711.3 ± 0.3 is suggestive of the Fe(III) species, i.e. Fe_2O_3 , this is reinforced by the satellite structures present at a higher binding energy of 9 eV from the main Fe 2p emission line [10]. The shoulder at a lower binding energy ≈ 707 eV indicates metallic iron, these spectra are almost identical to the spectra region for the Fe_{ref} compound and with the absence of any satellite structure to indicate the presence of the Fe(II) species it can be assumed that these substituted aromatic amines do not have the ability to reduce this iron containing substrate independently. The difference between the mild steel substrate and the copper substrate when dealing with these aromatic amines lies with the APH, as there appears to be a unique association between the APH and Cu substrate (as APH segregated on the copper surface by itself) which was not so when the substrate under investigation was that of mild steel.

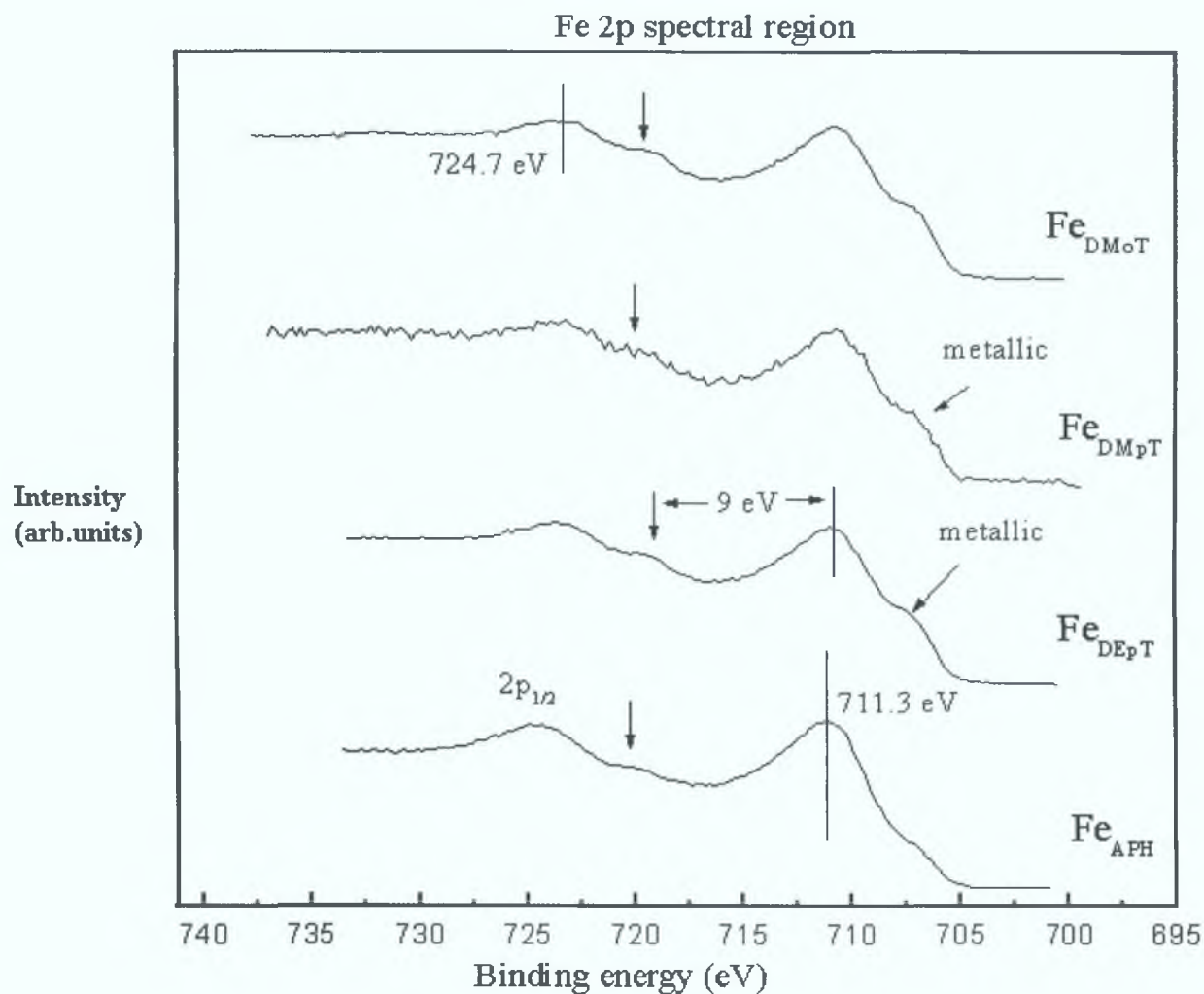


Figure 5.5 XPS spectra of the Fe 2p core levels iron substrate in contact with DMoT-MeOH, DMpT-MeOH, and DEpT-MeOH and APH-MeOH solutions for a 24-hour period. Arrows indicate satellite peaks.

5.3.3 Saccharin and substituted aromatic amines

Combinations of saccharin (BS) and reducing aromatic amines such as DMpT, DMoT, DEpT and APH are often incorporated into the cure system to accelerate the redox initiation. The reduction of the higher oxidation state transition metal to the lower state occurs due to the presence of the amine [12]. In the presence of an iron substrate, it has been shown that these aromatic amines cannot reduce the iron ions independently, so organic acids are added and this effect is investigated.

Survey scans were recorded of the iron substrate after immersion in a BS(1.6%) - aromatic amine (1.5%) methanol solutions for a 24 hr period. The resulting atomic % calculated for the elements present on the surface is shown in Table 5.3.

| Component | Carbon | Oxygen | Iron | Nitrogen | Sulphur |
|-----------|--------|--------|------|----------|---------|
| BS+ DMoT | 58.9 | 26.9 | 6 | 4.2 | 4 |
| BS+ DMpT | 62.8 | 23.1 | 7.2 | 4.4 | 2.5 |
| BS+ DEpT | 57.8 | 25.9 | 9.5 | 3.8 | 3 |
| BS+ APH | 63.6 | 20.9 | 1.2 | 10.8 | 3.5 |

Table 5.3 Calculated atomic percent for BS combined with aromatic amines in the presence of an iron substrate after a 24-hour incubation period.

From the above Table 5.3, it is evident that saccharin segregates to the substrate surface for all mixtures, as is evident by the presence of sulfur in the spectra. For the BS-DMoT and DEpT systems the amount of nitrogen and sulfur found on the surface is approximately equal. This suggests that these mixtures do not result in the segregation of these amines to the surface as the 1:1 ratio of N:S is indicative of saccharin alone. For the BS-DMpT system the ratio of N:S is approximately 2:1 which would suggest that the excess nitrogen originates from the toluidine. The ratio of N:S for the BS-APH system is 3:1, where here 1 nitrogen and 1 sulfur coming from the saccharin with the remaining nitrogen coming from the APH.

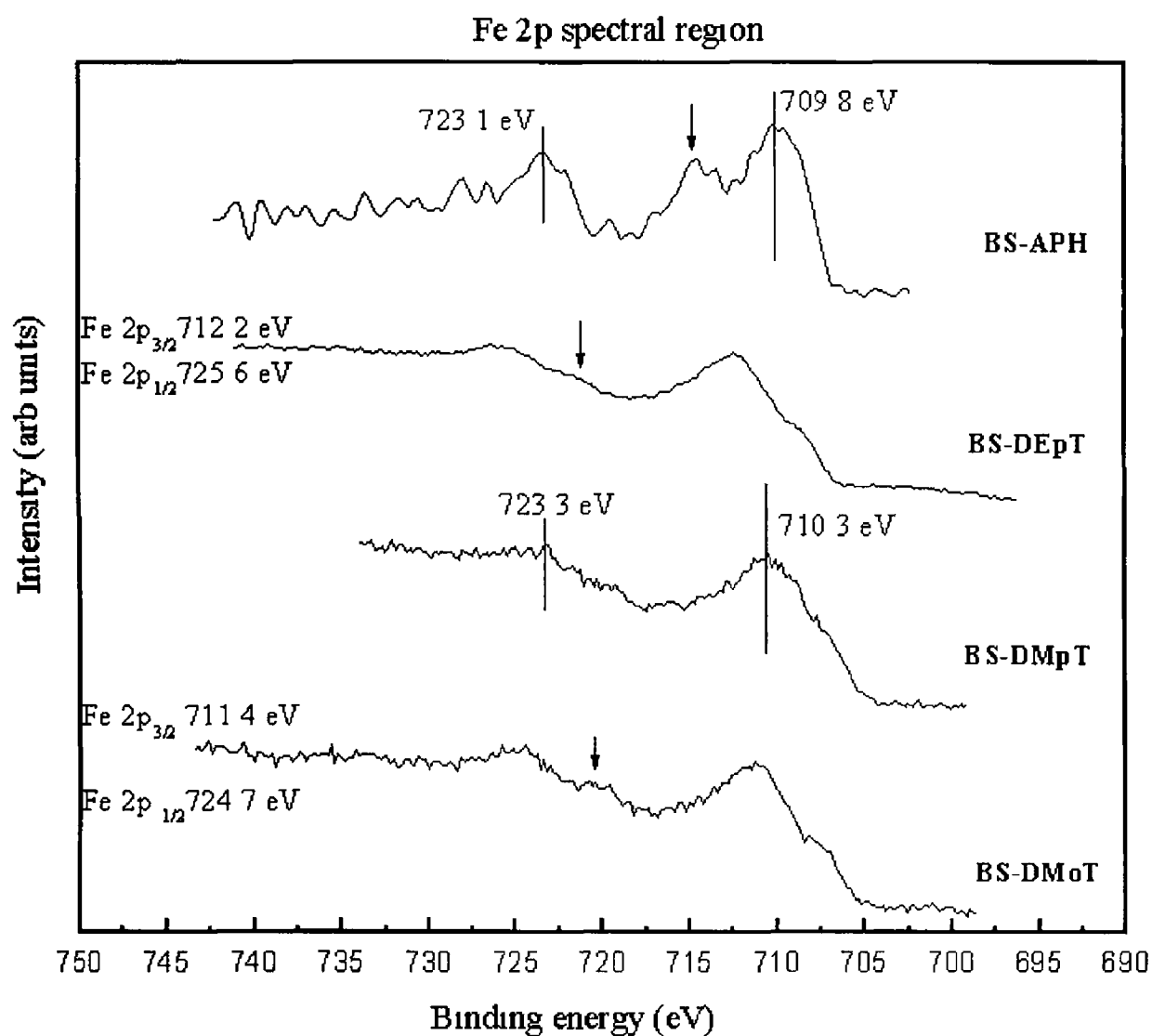


Figure 5 6 XPS spectra of the Fe 2p core levels of an iron rich substrate after immersion in BS-Aromatic amine solutions, arrows indicate satellite structures

Figure 5.6 represents the Fe2p spectral region recorded for the iron substrate after 24 hr immersion in a BS-DMoT, BS-DMpT, BS-DEpT and BS-APH, methanolic solutions. For the BS-DMoT system, the Fe 2p emission lines at 711.4 ± 0.3 eV and 724.7 ± 0.3 eV (e.g. the splitting energy difference between Fe $2p_{3/2}$ and Fe $2p_{1/2}$ is equal to 13.1 ± 0.3 eV), indicate that iron is present in the Fe(III) state, this is confirmed by the presence of the satellite structure which appears at approximately 9 eV higher in energy from the main Fe 2p peak. The lower binding energy shoulder is representative of metallic iron. This result appears to be the same for the BS-DEpT system, where there is a slight hint of a Fe(III) satellite peak recorded in this region.

For the BS-DMpT system, the iron present on the surface is found to be in the Fe(II) state, and this is indicated by the binding energy at which the peaks are located, i.e. 710.3 ± 0.3 eV and 723.3 ± 0.3 eV. For the BS-APH system peaks located at 709.8 ± 0.3 eV and 723.1 ± 0.3 eV are indicative of the Fe(II) system, again this is corroborated by the distinct satellite structure shifted by 5 eV from the main Fe 2p emission peak. From this spectral region there appears to be no indication that metallic iron is present on this surface (i.e. 706.5 ± 0.3 eV) and no sign that Fe(III) is present on this substrate surface either. Taking all these results into account it would appear that when mild steel is used as a substrate and the organic acid is saccharin the optimal results in terms of cure chemistry would only be achieved if the reducing amine was APH.

Figure 5.7 represents the decomposition of O1s and N 1s spectral regions for these saccharin-aromatic amine systems. Dealing with the O1s region, for the BS-DMoT (A) and BS-DEpT (C) systems three distinct oxygen environments can be resolved, the lower binding energy peak at 530.4 ± 0.3 eV is indicative of the Fe₂O₃ state of the iron [14], a binding energy of 532.1 ± 0.3 eV, could correspond to the SO₂ of the saccharin which is known to segregate at the surface. The higher energy peak at 534.6 ± 0.3 eV was attributed to some highly oxidised carbon species found on the surface possibly CO-O. As this peak was evident on the Fe_{ref} O1s region it was attributed to surface contamination. For the BS-DMpT system, the peak at 529.8 ± 0.3 eV was

indicative of O^{2-} species, with the peak at 531.7 ± 0.3 eV indicative of the OH^- hydroxide iron [18]. This substrate appears to be rich in the iron(II) state, with the presence of H_2O obvious from the peak resolved at 533.1 ± 0.3 eV. Dealing with the APH-BS system, the best peak fitted indicates only one oxygen environment. This peak is quite broad so it probably encompass other peaks, but again as the saccharin segregates to the surface this peak is allocated to the SO_2 oxygen environment, which correlates with the S 2p peak at 167.8 ± 0.3 eV, with the carbonyl group falling at a slightly higher binding energy and possible included in this peak.

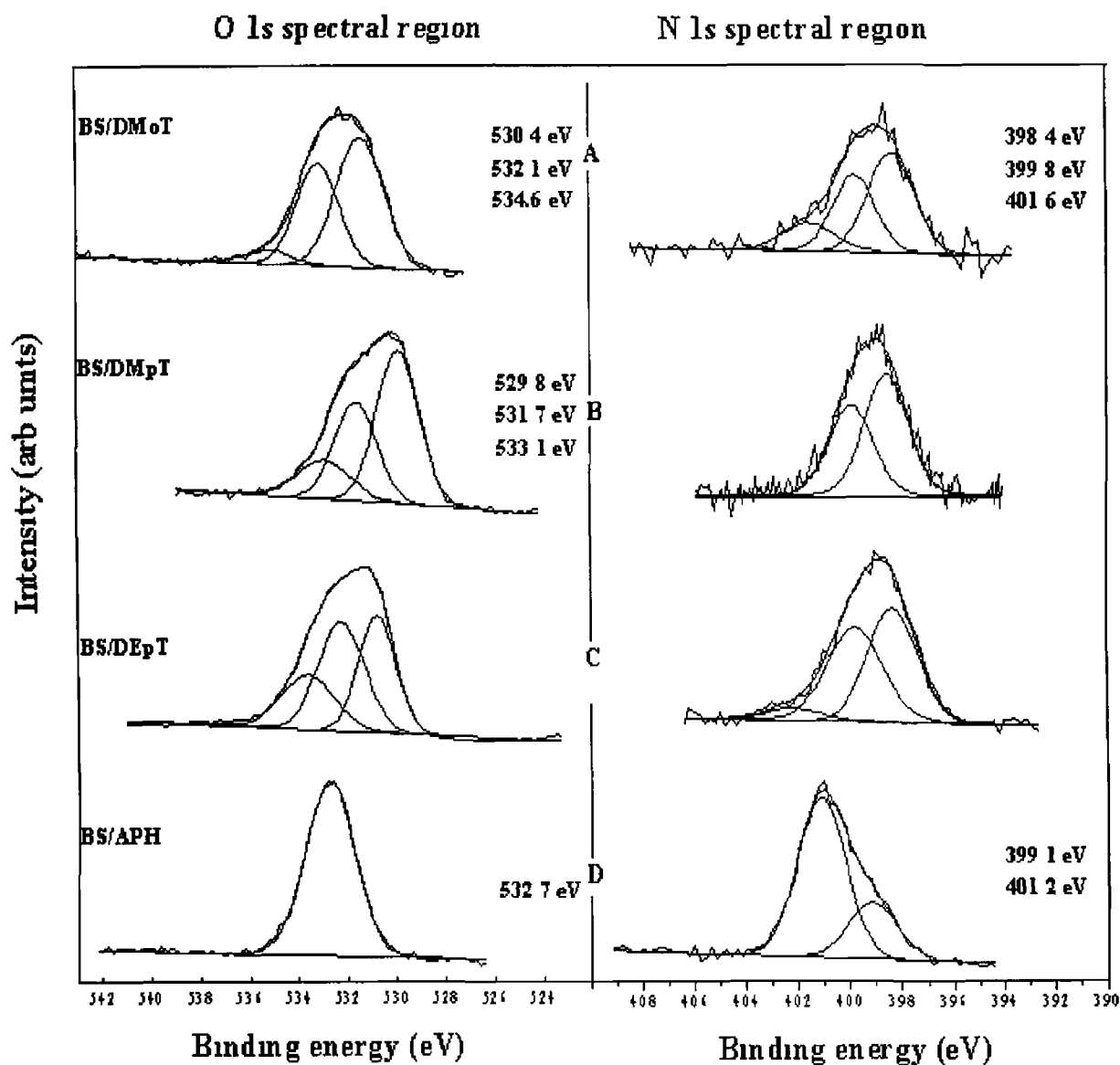


Figure 5.7 XPS spectra of the O 1s and N 1s core levels of the modified iron substrate after immersion in A) BS-DMoT, B) BS-DMpT, C) BS-DEpT and D) BS-APH solutions for 24 hours

As previously stated, many common nitrogen functionalities give N 1s binding energies in the narrow region of 399-401 eV, with oxidised nitrogen functionalities having a much higher binding energy between the values of 405 → 406 eV. From Figure 5.7, in the N 1s area the binding energies of 398.4 ± 0.3 eV and of 399.8 ± 0.3 eV are present in the BS-toluidines system. As with the copper system (chapter 4), the shift of ≈ 1.4 eV is probably due to the unprotonated and protonated nitrogen, in which the binding energy is increased by about this amount above that of the free amine [6]. For the copper-based system this was not the case for the BS-DMoT modified copper substrate, as no indication of protonation was observed in the N 1s spectra region, suggesting that the metal used plays an important role in reactions that occur within the curing system of anaerobic adhesives. A peak at 401.6 eV present on the BS-DMoT and BS-DEpT modified surfaces, was possibly due to unreacted amine left on the substrate surface. The two nitrogen environments linked with the APH-BS system at binding energies of 399.1 ± 0.3 eV and 401.2 ± 0.3 eV are allocated to the nitrogen of the acid and the nitrogen environment associated with the APH respectively (peak areas 32%/68%), or ratio of approximately 1:2, which would be in good agreement with the nitrogens present in saccharin and APH.

5.3.4 Maleic-acid and substituted aromatic amines

Organic acids function in anaerobic adhesives by releasing metal ions from the surface substrate. Maleic acid is a significantly stronger acid than saccharin and is used in anaerobic formulations either in combination with saccharin or at concentrations considerably lower than that of saccharin. Throughout this section the effect that 1.6% (w/v) maleic acid – MeOH solution produces on a polished iron containing substrate is investigated. Maleic acid in combination with 1.5% DMoT, DMpT, DEpT and APH was also studied and Table 5.4 highlights the atomic % of the elements found present on the substrate surface after a 24-hour immersion period in each of the respective solutions. Figure 5.8 depicts the Fe 2p spectral region recorded for the iron-containing substrate modified with maleic acid and maleic acid combined with substituted aromatic amines.

| Solution | Carbon (%) | Oxygen (%) | Iron (%) | Nitrogen (%) |
|----------------|------------|------------|----------|--------------|
| Maleic acid | 47 | 48 | 5 | 0 |
| Mal + DMoT | 52 | 42 | 3 | 9 |
| Mal + DMpT | 62 | 33 | 3 | 2 |
| Mal + DEpT | 62 | 32 | 3 | 3 |
| Mal + APH | 55 | 34 | 2 | 9 |
| Error analysis | ±2.4% | ± 1.7% | ±1% | ± 1% |

Table 5.4 Calculated atomic percent for maleic acid, combined with aromatic amines in the presence of an iron substrate after a 24-hour incubation period.

From Figure 5.8 regarding the Fe 2p spectral region it would appear that only the Fe(II) oxidation state of iron was present, regardless of whether DMoT, DMpT, DEpT and APH was the reducing amine utilised. When the iron containing substrate was immersed in just the 1.6% maleic acid, the Fe(III) and Fe(II) and Fe(0) oxidation states of iron were detected. Therefore, when maleic acid is combined with these amines only the Fe(II) state is apparent from this spectral region, and no metallic shoulder is observed. This Fe(II) oxidation state is required by the CHP to initiate polymerisation.

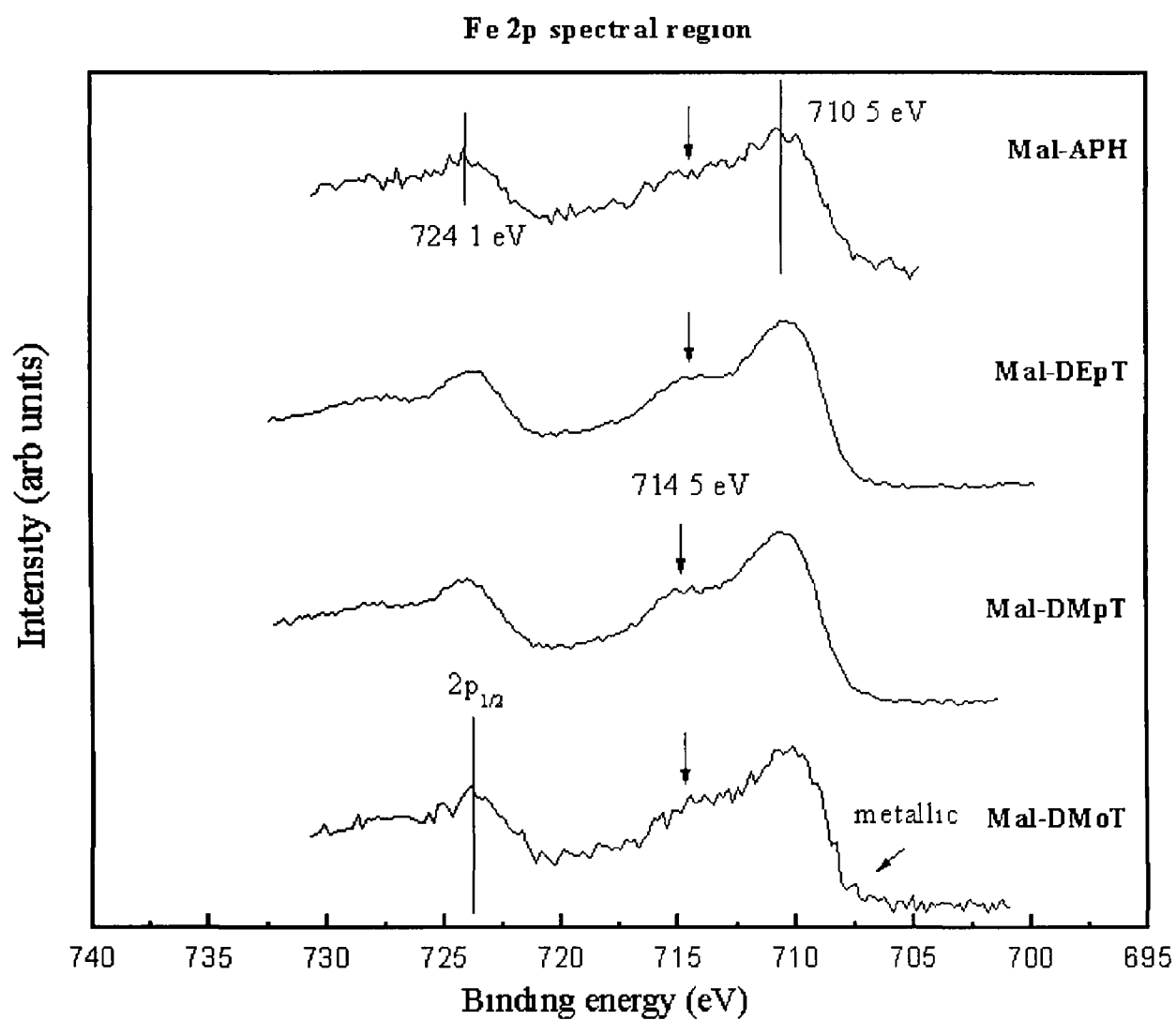


Figure 58 XPS spectra of the Fe 2p core levels of a iron substrate after immersion in maleic acid -aromatic amine solutions, with arrows indicating satellite structures

Figure 5.9 shows the decomposition of the O 1s and the N 1s spectral regions for these maleic acid solutions. For the iron substrate modified with the maleic acid and DMoT, DMpT and DEpT solutions, the O1s peaks are decomposed into the same two components obtained for the maleic acid modified iron. These peaks at binding energies of 531.9 ± 0.3 eV and 533.4 ± 0.3 eV, show that the oxygen found present on the substrate surface coincides with the oxygen environments of the maleic acid. For the APH-maleic acid system, the O 1s components are found at a binding energy of 530.6 ± 0.3 eV and 531.9 ± 0.3 eV. The peak at binding energy of 530.6 ± 0.3 eV is symbolic of the Fe_2O_3 state of iron, which contains Fe(II) [14] which can cause the decomposition of CHP. CHP decomposition can be induced by both oxidation states of the iron as outlined in reaction scheme 5.3.



Scheme. 5.3



Although the RO^\bullet radical is more reactive than the ROO^\bullet radical, this second reaction regenerates the metal ion in its lower valence state, however it has been suggested that ROOH is unable to reduce Fe(III) [17]. This will be investigated further on in this chapter (Section 5.3.5).

For this APH-maleic acid system, the peak at a higher binding energy of 531.9 ± 0.3 eV, is assigned to the $\text{C}=\text{O}$ moiety, this carbonyl group is present in both the maleic acid and APH compounds.

Looking at the N 1s environment found on the substrate surface, for the maleic acid and toluidines system two distinct nitrogen environments are observed at binding energies of 399.8 ± 0.3 eV and 402.6 ± 0.3 eV, protonation of the nitrogen is not evident here as the chemical shift is too large, that of ≈ 2.8 eV. As nitrogen is an element present in these toluidines; the lower binding energy nitrogen is ascribed to these DMpT, DEpT and DMoT, with possibly the higher binding energy nitrogen due to some form of unreacted amine. These observed N 1s peaks could possibly be assigned to species such as NO_2 or NO_3 as these

species have a higher binding energy than 402 eV [18]. For the mal-APH system the N1s peak at 401.4 eV is associated with the nitrogen present in the APH compound.

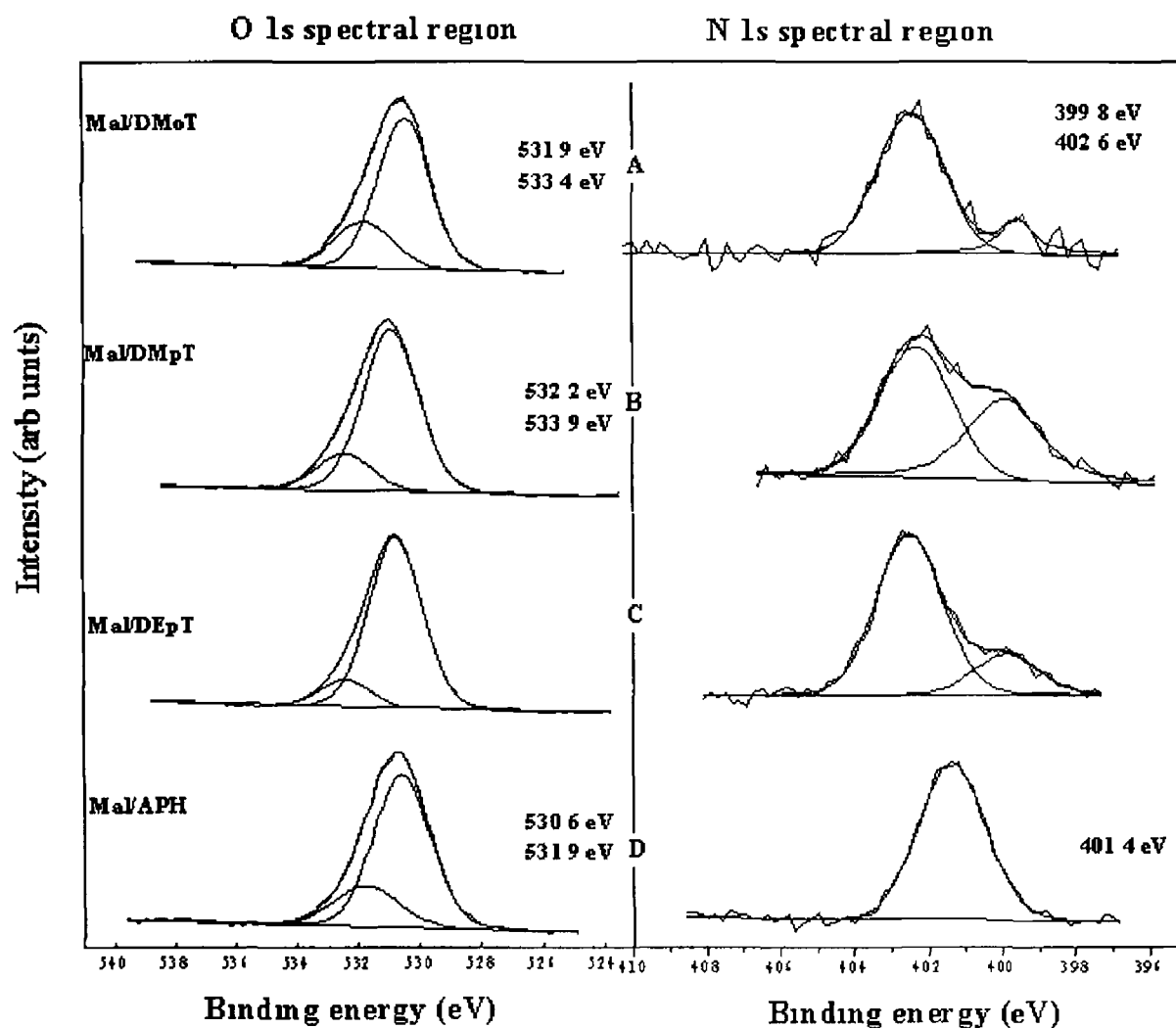


Figure 5.9 Decomposition of the O 1s and N 1s core levels for an iron substrate in contact with the following solution for a 24-hour period: A) 1.6% maleic acid with 1.5% DMOt in methanol, B) 1.6% maleic acid with 1.5% DMpT in methanol, C) 1.6% maleic acid with 1.5% DEpT in methanol and D) 1.6% maleic acid with 1.5% APH in methanol.

5.3.5 Organic acids and CHP

Oxygen forms hydroperoxides by reacting with certain active hydrogen in the monomer. However, cumene hydroperoxide are most frequently used in anaerobic adhesive formulations to act as initiators. Reaction schemes 5.1 and 5.2 depict the role of the hydroperoxide as an initiator. Table 5.5 shows the experimental results calculated for the atomic percentage of the elements found on the iron substrate after immersion in methanol solutions CHP, BS-CHP and maleic acid-CHP.

| Solution | Carbon (%) | Oxygen (%) | Iron (%) |
|----------------|------------|------------|----------|
| CHP | 53 | 35 | 12 |
| BS + CHP | 33 | 48 | 19 |
| Mal + CHP | 46 | 51 | 3 |
| Error analysis | ±2.4% | ±1.7% | ±1% |

Table 5.5 Calculated atomic percent for CHP, combined with organic acids saccharin (BS) and maleic acid (mal) in the presence of an iron substrate after a 24-hour incubation period.

From Table 5.5, after interaction of the iron-containing substrate and 1.5% CHP-methanol solution, the effect this hydroperoxide produces on the substrate surface appears to be minimal, as the atomic %'s of elements present on the surface are within experimental errors of the calculated values found on the untreated substrate surface. The Fe 2p spectral regions for these CHP solutions are illustrated in Figure 5.10. From the Fe_{CHP} 2p spectra the presence of the Fe(III) and Fe(0) oxidation states of the iron is displayed. This leads to the conclusion that by itself CHP is unable to reduce the ferric ions to the ferrous state needed for initiation of polymerisation, as there is no evidence from these results that iron is present in the Fe(II) state. Therefore, CHP has a synergistic effect, and in combination with other compounds produces this desired lower valence state of the iron substrate.

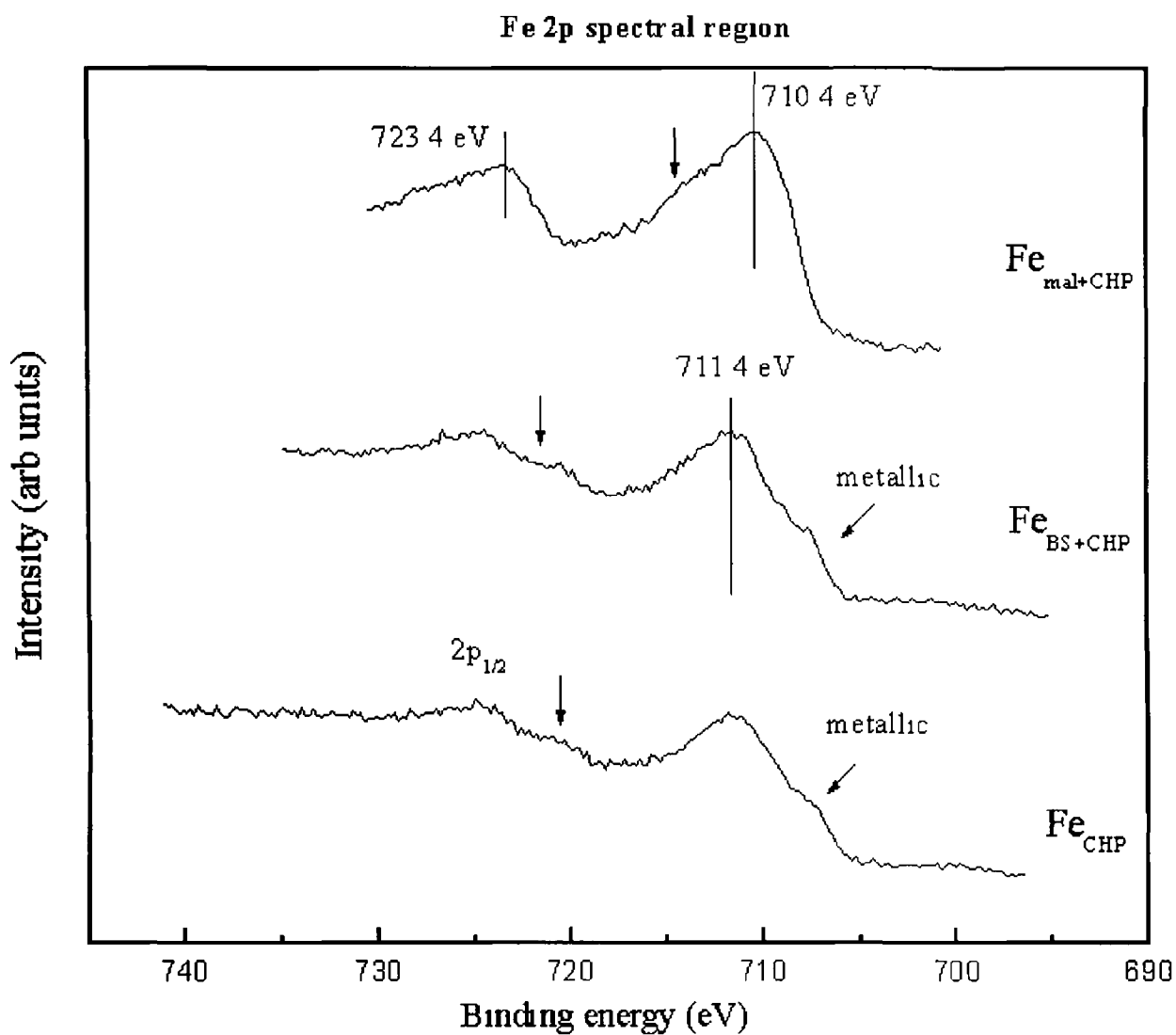


Figure 5 10 XPS spectra of the Fe 2p core levels of a iron substrate after immersion in CHP, CHP-BS and CHP-maleic acid solution, arrows indicate satellite structures

Taking CHP in combination with the organic acids (i.e. maleic acid and saccharin) from Figure 5.10 only the combination of maleic acid with CHP produces this effect, and the Fe(II) oxidation state was observed. From Table 5.5 the increase in the oxygen present on the surface was at the expense of the iron, suggesting a thick oxygen overlayer on the iron surface.

Figure 5.11 reveals the decomposition of the C 1s and O 1s spectral regions for these CHP based systems. From the C 1s region of the Fe_{CHP}, Fe_{mal/CHP} and Fe_{BS/CHP} systems the binding energy of 285 ± 0.3 eV is allocated to saturated hydrocarbons / adventitious carbon found on all surfaces, the higher binding energy of 288.3 ± 0.3 eV was attributed to a highly oxidised carbon environment, possibly associated with the peroxide and correlated within the O 1s region where the peak at 534.2 ± 0.3 eV can be associated with the $(O_2)^{2-}$ peroxide ion [18]. This peak was seen in the O 1s region for Fe_{CHP}, Fe_{BS/CHP} and Fe_{mal/CHP} leading to the conclusion that the CHP does accumulate at the substrate surface. In the Fe_{mal/CHP} system a peak at 286.5 ± 0.3 eV was resolved possibly due to the C=C species within the maleic acid. The decomposition of the O 1s spectral region for the Fe_{CHP} and Fe_{BS/CHP} are almost identical, the peak at 533.1 ± 0.3 eV is attributed to adsorbed H₂O, where the lower binding energy peak at 531.7 ± 0.3 eV is indicative of the Fe(OH)_x state, or in this case the Fe(III) state. For Fe_{mal/CHP} the binding energy at 532.5 ± 0.3 eV is due to the maleic acid with the CHP component of this combination seen at the higher binding energy.

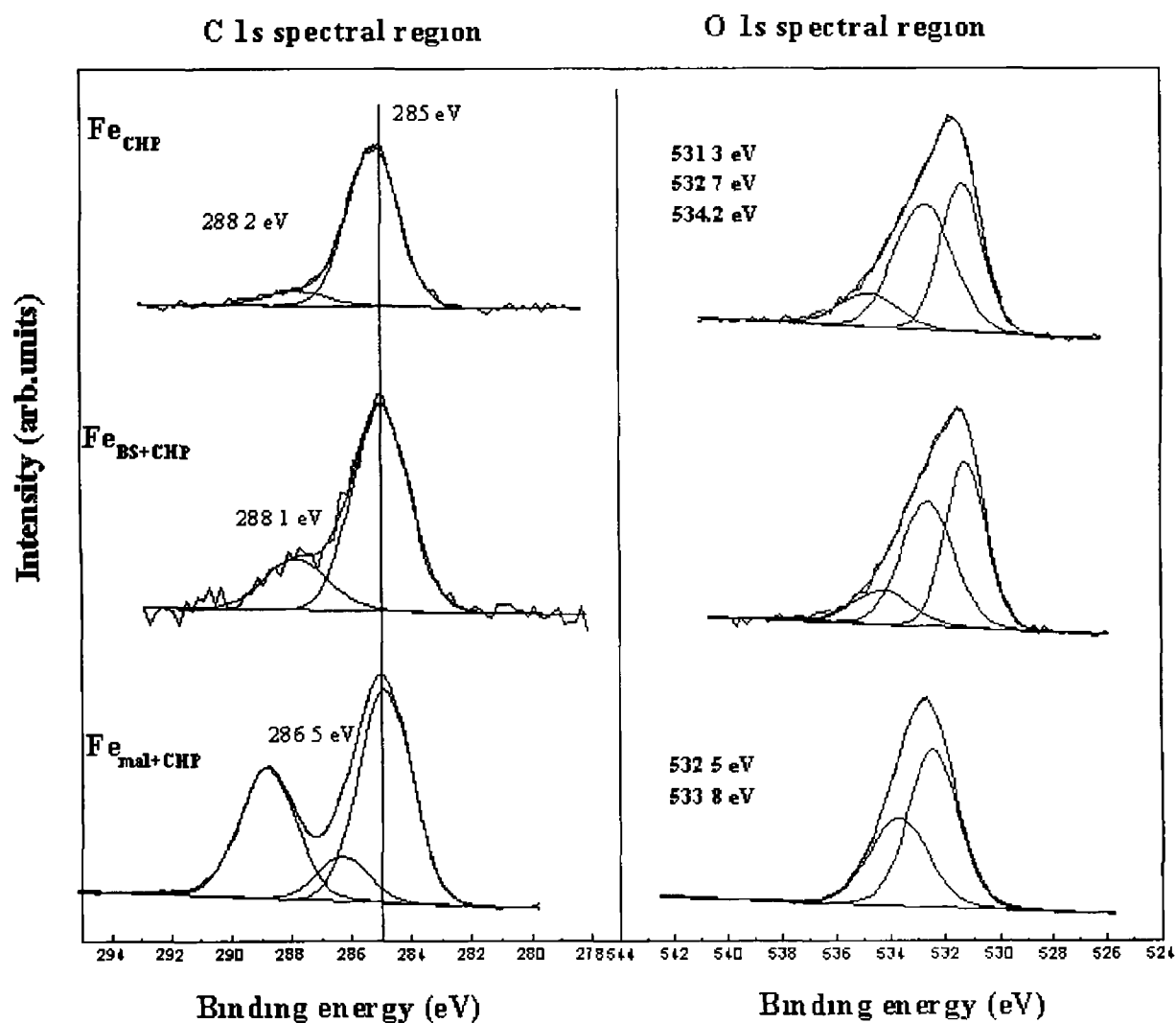


Figure 5.11 XPS spectra of the C 1s and O 1s core levels of an iron substrate after immersion in CHP, CHP-BS and CHP-maleic acid solution

5.3.6 Formulations

The formulations based on the cure systems of anaerobic adhesives were investigated where the substrate of interest was an iron-containing mild steel substrate. The formulations investigated contained the following ingredients:

- 1) Model 43 – 1% saccharin, 0.3% maleic acid, 1% CHP and 0.3% APH.
- 2) Model 43X (maleic acid) – 1% maleic acid, 1% CHP and 0.3% APH
- 3) Model 43X (BS) – 1% saccharin, 1% CHP and 0.3% APH
- 4) Model 90 (maleic acid) – 1.6% maleic acid, 3% CHP, 0.3% DMoT and 0.6% DEpT
- 5) Model 90 (BS) – 1.6% saccharin, 3% CHP, 0.3% DMoT and 0.6% DEpT.

Table 5.6 shows the experimental atomic % calculated for elements found on the substrate surface after a 24-hour immersion period in the above formulations.

| Formulation | Carbon (%) | Oxygen (%) | Iron (%) | Nitrogen (%) | Sulphur (%) |
|-------------|------------|------------|----------|--------------|-------------|
| 43 | 56.7 | 33.3 | 2.6 | 5.7 | 1.7 |
| 43X (mal) | 55.9 | 34.2 | 3.1 | 6.8 | 0 |
| 43X (BS) | 61.8 | 22.9 | 2.1 | 9.8 | 3.4 |
| 90 (mal) | 52.3 | 37.9 | 9.8 | 0 | 0 |
| 90 (BS) | 70.3 | 20.2 | 1.6 | 4.5 | 3.4 |

Table 5.6 Experimental calculated atomic % for elements found on the iron substrate after a 24 hours in the above methanol formulations.

From the above results it can be seen that when saccharin is utilised in any formulation it accumulates at the substrate surface, as indicated by the presence of the sulfur on the surface. The ratio of N: S in model 43 is $\approx 3:1$; with 2 of these nitrogens being assigned to the APH and the remaining coming from the BS. For 43x (BS), this result in the ratio of N: S is similar to that of model 43 in which the ratio of these elements appears to be 3:1 also. In both of these

formulations the APH appears to exert a strong influence on the surface, with the rise in the nitrogen content (due to the APH clearly evident at the surface) at the expense of the iron. For model 90(BS) formulation the nitrogen content was much lower at $\approx 4.5\%$, suggesting that these toluidines have not the same capability as that of the APH in segregating to the substrate surface. However the carbon content for this 90(BS) formulation is extremely high at 70% and when dealing with percentages this sharp increase seen has to induce a decrease in the % composition of the other elements present.

Model 90 (mal) formulation appears to exert very little influence on the substrate surface, and there is no evidence of the toluidines used in this formula being present at the substrate surface (no indication that any nitrogen is present on the surface). Again when APH is used in model 43X(mal) the amount of nitrogen found on the surface is due to APH accumulation at the surface, and there having an influence on the interfacial cure chemistry.

Figure 5.12 shows the Fe 2p spectral region recorded for the iron substrate after immersion in the above formulations. For the formulation 90 irrespective of the organic acid used, the Fe 2p emission line indicates that metallic iron is present after modification with this formulation, at a binding energy of 706.3 eV. There is no indication that the Fe(II) oxidation state is present on these sample surfaces, indicating that this formulation is not suitable when the metal of interest is iron in mild steel. For the remaining three formulations, the main Fe 2p peak comes in at a binding energy of $\approx 710.3 \pm 0.3$ eV, with satellite structures visible shifted by approximately 4.4 eV to a higher binding energy, indicative of the Fe(II) oxidation state of iron. This feature is more prominent in model 43 formulation where a combination of maleic and saccharin is used, with the reducing amine being APH.

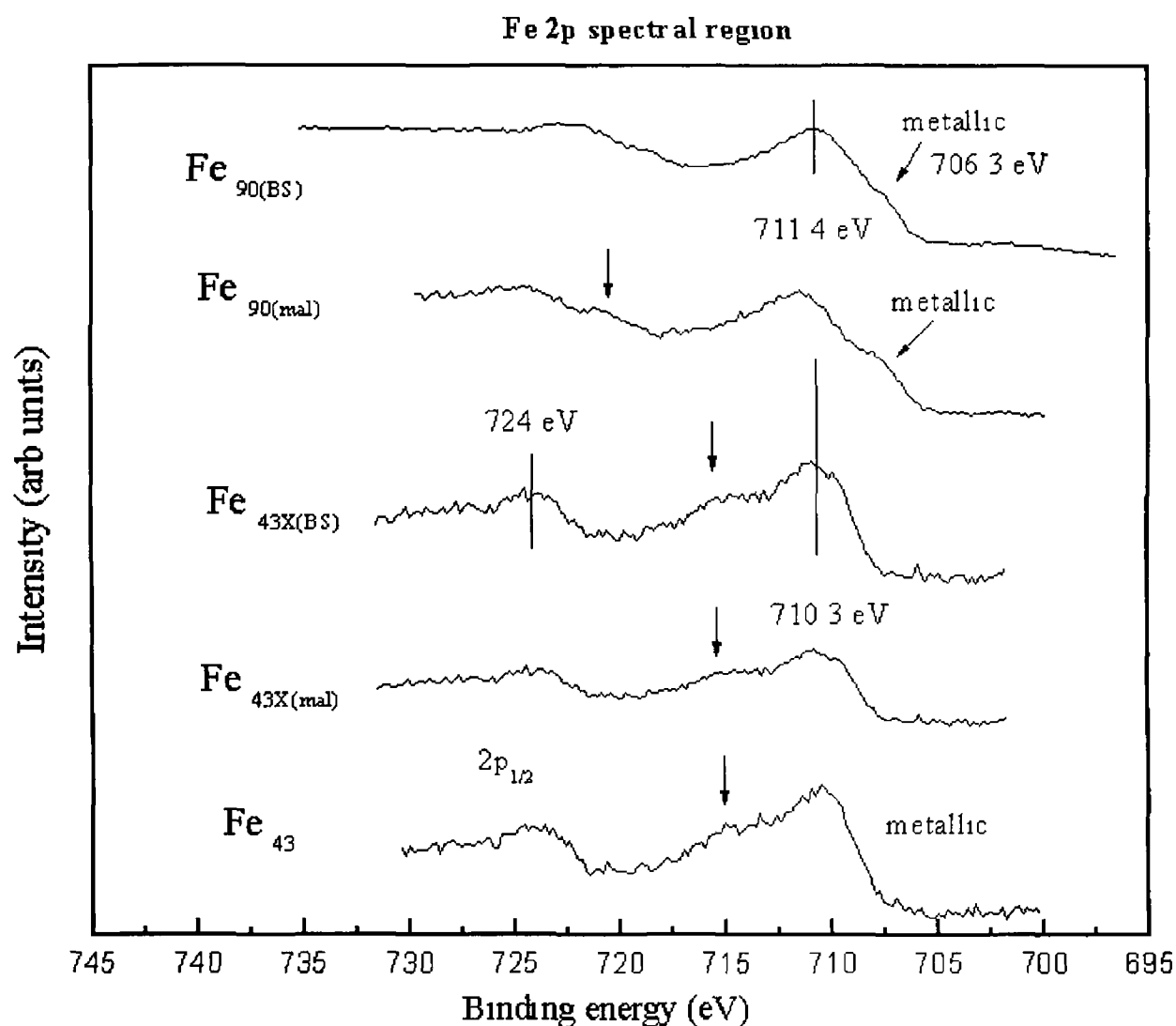


Figure 5.12 XPS spectra of the Fe 2p core levels of a iron substrate after immersion in formulations, 290 (BS), 290 (mal), 243X (BS), 243X (mal) and 243, the arrows indicate satellite structures observed

5.4 Conclusions

Throughout this chapter the role that organic acids, saccharin and maleic acid, play in the anaerobic adhesives cure chemistry with mild steel was investigated. The incorporation of acids into cure formulations is necessary as they play a key role in the release of transition metal ions from the substrate surfaces, with the type of acid used being responsible for the oxidation state of the transition metal ions released. It has been shown that both of these acids can release the Fe(III) and Fe(II) from the iron containing substrate. However, the Fe(II) state is more efficient with respect to promoting homolytic decomposition of the peroxide.

Substituted aromatic amines in combination with organic acids are incorporated into adhesive formulations as they reduce the higher oxidation state of the metal to that of its lower valent form. When using saccharin as the organic acid, only in combination with 1-acetyl-2-phenylhydrazine is this desired Fe(II) oxidation state obtainable. Saccharin in the presence of, DEpT and DMoT did not produce the Fe(II) oxidation state. This contrasts with the results for the copper substrate where saccharin proved to be the ideal organic acid in terms of its chemical reactivity. BS and DMpT was found to reduce the iron but discrete satellites peaks were not observed, this could possibly be due to the overlap of satellites corresponding to the Fe(III) and Fe(II) states.

Maleic acid is a stronger acid than saccharin, and in combination with any of the substituted aromatic amines mentioned above, produces this desired Fe(II) oxidation state. Again it would appear that the substrate under investigation plays an important role in determining which organic acid performs best. Maleic acid was not deemed suitable for the copper substrate, where the cure system involved using toluidines.

These results suggest that for adhesive anaerobic formulations the type of metal required to catalyse the redox polymerisation should be taken into account. For the copper system, saccharin appeared to be the best acid to use and

it can be used in combination with APH, DMpT and DEpT. Whereas using maleic acid in a copper based system only produced the desired effect on the oxidation state of the copper when combined with APH.

For the iron-based system, the preferable organic acid to utilise is that of maleic acid, as this acid can be used with any of the above-mentioned aromatic amines to produce the desired effect on the substrate surface. This is not fully achieved with saccharin and any of the substituted aromatic amines, but again this is achievable if saccharin is used with the stronger reducing agent APH. From the formulations used it would appear that the best combination is one which used both saccharin and maleic acid, combined with APH and CHP. One possible explanation for the differences in the effectiveness of the two acids with respect to the substrates relates to the composition of the materials. While copper is the only element present in the copper substrate, iron is only one constituent of mild steel. Therefore, in order to release iron from the mild steel substrate, a stronger acid is required and this role is fulfilled by maleic acid which is a stronger acid than that of saccharin.

5.5 References

- [1] Beaunez, P., Helary, G. and Sauvet G., *J. of Polymer Science*, 32 (1994) 1471.
- [2] Rooney, J.M. and Malofsky, B.M., in "Handbook of Adhesives", Skeist (Ed), Reinhold, New York, (1977) 451.
- [3] Raftery, D., Smyth M.R., Leonard, R. and Heatley. D., *Int. J. Adhesion and Adhesives*, 17 (1997) 151.
- [4] Raftery, D., Smyth, M.R. and Leonard, R. *Int. J Adhesion and Adhesives*, 17 (1997) 9.
- [5] George. B., Grohens, Y., Touyeras, F. and Verbrel, J., *J. Adhesion Sci. Technol.*, 12 (1998) 1281.
- [6] Briggs, D., Seah, M. P. "Practical Surface Analysis by Auger and X-ray Photoelectron Spectroscopy", Wiley, New York, (1994).
- [7] Maschhoff, B.L. and Armstrong, N.R., *Langmuir*, 7 (1991) 693.
- [8] Jansson, C., Zurawski, D. and Wieckowski, A., *Langmuir*, 6 (1990) 1683.
- [9] Graat, P.C.J. and Somers, M.A.J., *Applied Surf.Sci.*, 100 (1996) 36.
- [10] Descostes, M., Mercier, F., Thromat, N., Beaucaire, C. and Gautier-Soyer M., *Applied Surf.Sci.*, 165 (2000) 288.
- [11] Moulder, J.F., Stickle, W.F., Sobol, P.E. and Bomben, K.D., "Handbook of X-Ray Photoelectron Spectroscopy", Perkin-Elmer Corp., Eden Prairie. (1992).
- [12] Moane, S., Raftery, D., Smyth, M.R. and Leonard, R.G., *Int. J. Adhesion and Adhesives*, 19 (1999) 49.

- [13] Lin, T C , Seshadri, G and Kelber, J A , *Applied Surf Sci* , 119 (1997) 83
- [14] Pirlot, C , Delhalle, J , Pireaux, J J and Mekhalif, Z *Surf And Coatings Tech* , 138 (2001) 166
- [15] Raftery, D , Ph D, Thesis, Dublin City University, (1996)
- [16] Briggs D , “Surface analysis of Polymers by XPS and static SIMS”, Clarke, D R , Suresh, S and Ward, I M (Eds), Cambridge University Press (1998)
- [17] Hiatt, R , Irwin, K C and Gould, W , *J Org Chem* , 16 (1967) 1430
- [18] Badrinarayanan, S , Ganguly, P , Mandale, A B and Sainkar, S R , *J Electron Spec and Related Phen* , 59 (1992) 307

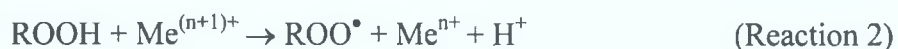
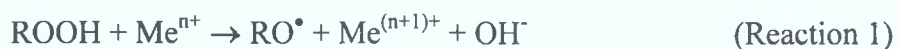
Chapter 6

A FT-IR, ICP-AES and XPS study of the individual cure components of anaerobic adhesives on a copper substrate

6.1 Introduction.

Throughout the past twenty years, engineering adhesives have been used and developed in industry due to the many advantages associated with them, such as lightness of structure, lowering of production costs, ease of application and limited corrosion potential compared to the usual means of joining pieces together such as welding or bolting. Anaerobic adhesives have been used in the automotive industry due to their interesting properties: they can cure via a redox radical mechanism at room temperature as soon as oxygen is removed. Therefore, these one-part systems based on acrylic monomers cure extremely rapidly when confined between the materials to be bonded which are generally common metals [1,2].

Metallic cations, arising from the substrate lead to the catalytic decomposition of initiator molecules, which in turn produces free radicals able to induce the reaction. Initiation generally proceeds through the decomposition of a hydroperoxide leading to the following reactions:



Reaction 2 produces ROO^{\bullet} radicals, which are less efficient at the initiation stage than the RO^{\bullet} radical, but this reaction is important to regenerate metal cations at their lower oxidation state. This regeneration is needed to maintain the initiation rate at a high level in formulations where an inhibiting system is present. Therefore, in order to ensure this continuous reduction of cations to their lower oxidation state a synergistic accelerating system must be used [3]. Okamoto *et al.* [4] and Beaunez *et al.* [5] proposed a charge-transfer system between constituents of the accelerating system, while Wellmann *et al.* [6] isolated a new compound called aminoral resulting from the reaction of saccharin and N,N-dimethyl-p-toluidine. Furthermore Yang *et al.* have shown using FT-IR, that the nature of the substrate as well as surface treatment greatly influences the cure rate and also the final cure degree of an anaerobic adhesive

[7,8], and copper was found to be the most active surface for initiating the polymerisation

Throughout this chapter FT-IR (Fourier Transform Infra Red spectroscopy) and ICP-AES (Inductively Coupled Plasma- Atomic Emission Spectroscopy) are used to assess the effect that these cure components produce on the substrate surface, with copper being the substrate under investigation XPS is used to establish if only the para-substituted toluidines in combination with saccharin form a salt at the substrate surface, as outlined in chapter 4, by analysing meta-substituted toluidines in combination with saccharin and in contact with the copper substrate

6.2 Experimental

6.2.1 Fourier Transform Infrared Spectroscopy.

Infrared Spectroscopy is the study of the interaction of infrared light with matter. Light is composed of electro - magnetic waves and these two components act in planes perpendicular to each other, and the light wave moves through space in a plane perpendicular to the planes containing the electric and magnetic waves. It is the electric part of the light that interacts with molecules, this is represented by the "electric vector" [9]. Infrared radiation is another name for radiant heat, and all objects in the universe at a temperature above absolute zero give off infrared radiation. When infrared radiation interacts with matter it can be absorbed causing the chemical bonds in the material to vibrate. As the positions of atoms in a molecule are not fixed, their motions can be described in terms of a number of different vibrations with the main two categories being stretching and bending. Stretching is a change in inter-atomic distance along a bond axis and bending been a change in the angle between two bonds.

The presence of some of these chemical bonds in a material is essential for the absorption of infrared radiation. Functional groups within the chemical structure of molecules tends to absorb infrared radiation in the same wavenumber range, regardless of the structure of the rest of the molecule, i.e. the C=O stretch of a carbonyl group occurs at around 1700 cm^{-1} in aldehydes, ketones and carboxylic acids. This in turn means that a correlation exists between the wavenumbers at which a molecule adsorbs infrared radiation and its structure which in turn allows the structure of unknown molecules to be identified from the molecules' infrared spectra, making infrared spectroscopy a useful tool for chemical analysis. A plot of the measured infrared radiation versus wavenumber is known as an infrared spectrum.

One of the major disadvantages of the conventional method of producing a spectrum is its slowness, but with the development of Fourier Transform (FT) spectroscopy, simultaneous and almost instantaneous recordings of the whole spectrum in the infrared region can be produced. Fourier transform spectroscopy

in the infrared region operates by observing an interference pattern set up when the radiation beam is reflected between a pair of parallel mirrors which are steadily moving towards or away from each other, it is this pattern which is collected, recorded as a function of distance between mirrors, and later Fourier-transformed into the corresponding frequency signal [10]. The majority of commercially available FT-IR instruments are based on the Michelson interferometer which is depicted in Figure 6.1.

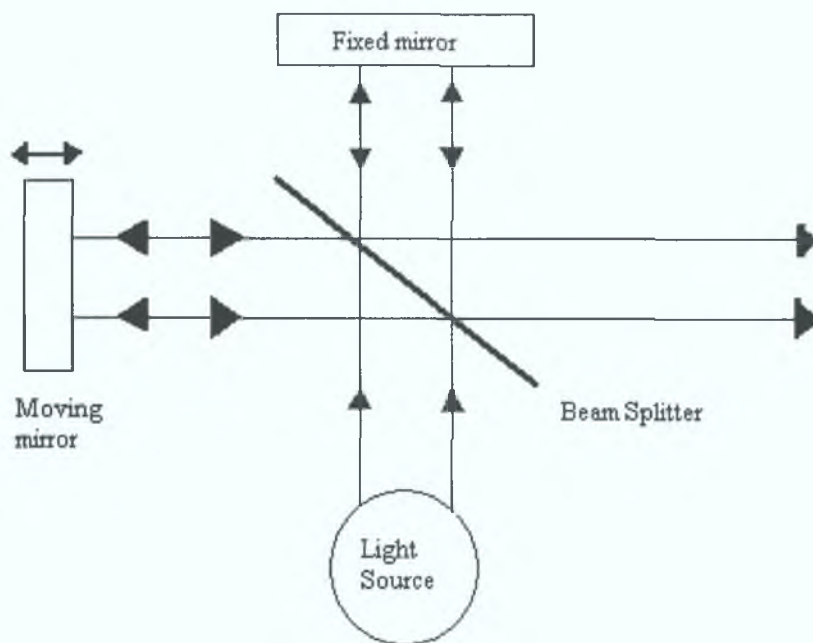


Figure 6.1 Schematic of a Michelson interferometer

The components of a spectrometer as it is assembled for infra-red work are the source; which is usually some form of filament which is maintained at red or white-heat by an electric current, with the most common being the Nernst filament the optical path and monochromator (for dispersive instruments), the detector and the sample [10].

6.2.2 Inductively-coupled plasma – atomic emission spectroscopy.

Inductively-Coupled Plasma Atomic Emission Spectroscopy (ICP-AES) is a major technique for elemental analysis. It will dissociate a sample into its constituent atoms and ions and cause them to emit light at a characteristic wavelength by first exciting them to a higher energy. The sample to be analysed, if solid, is normally first dissolved then diluted with a solvent before being fed into the plasma. Atoms/ions in the plasma emit light (photons) with characteristic wavelengths for each element. This light is recorded by one or more optical spectrometers and when calibrated against standards this technique provides a quantitative analysis of the original sample.

A typical inductively-coupled plasma source is called a torch, which can be seen in Figure 6.2. The green arrow represents the argon flow, and the blue arrow represents the sample flow. Initially argon gas will pass through the quartz tube and exit from the tip. The tip of the quartz tube is surrounded by induction coils that create a magnetic field. The ac current that flows through the coils is at a frequency of about 30 MHz and a power level around 2 KW. The stream of argon gas that passes the coil has been previously seeded with free electrons from a Tesla discharge coil. The magnetic field excites these electrons, and then they have sufficient energy to ionise the argon atoms by colliding with them. The cations and anions present from the initial Tesla spark accelerate due to the magnetic field in a circular pattern that is perpendicular to the stream exiting from the top of the quartz tube. By reversing the direction of the current in the induction coils, the magnetic field is also reversed. This changes the direction of the excited cations and anions, causing more collisions with argon atoms. This results in further ionisation of the argon atoms and intense thermal energy, as a result a flame-shaped plasma forms on top of the torch. A second stream of gas is needed to cool down the inside of the quartz tube, this is provided by a stream of argon that provides a vortex flow which also provides a way of centring and stabilizing the plasma.

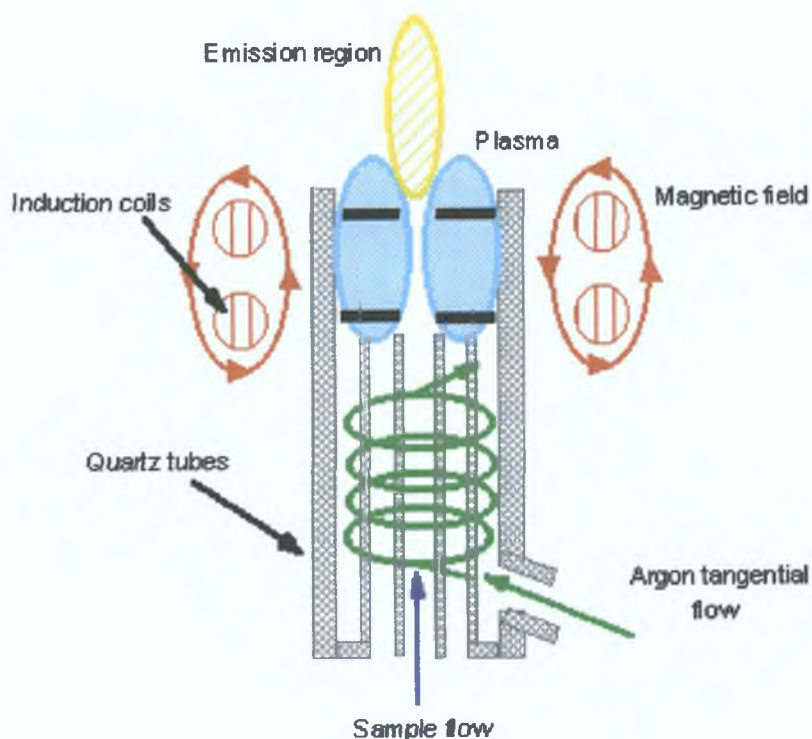


Figure 6.2 Schematic of a typical plasma source.

Samples are carried into the torch, and the device generally used for sample injection is a nebulizer. The sample is nebulized in a cross-flow nebulizer by a stream of argon, and the resulting finely divided droplets are carried into the plasma [11]. When the sample flows into the plasma, the extreme temperatures excite the atoms present. These excited atoms will emit energy at a characteristic wavelength. In ICP analysis, the plasma can reach temperatures in the following range $6,000\text{ }^{\circ}\text{C} \rightarrow 10,000^{\circ}\text{C}$, at this temperature most elements will be atomised. This results in very low detection limits usually of the range $1 \rightarrow 10\text{ppb}$. The most common type of detector used with ICP are photomultiplier tubes (PMTs), these PMTs convert photons to an electrical signal. The incident photons coming from the exit slit liberate electrons from the photocathode and the electron flow is then amplified by a set of dynodes, the final anode current is proportional to the incident photon signal received by the photocathode.

6.2.3 Reagents and instruments

All of the reagents used were of analytical reagent grade. The methanol used was HPLC grade (99.9% assay), and glacial acetic acid was supplied by Sigma-Aldrich. The organic acids (maleic acid and saccharin) and the substituted aromatic amines (APH, DMoT, DMpT and DEpT), were supplied by Loctite. The meta-substituted aromatic amines (DMmT: N,N-dimethyl-m-toluidine and DEmT: N,N-diethyl-m-toluidine) were supplied by Sigma-Aldrich, while the standard copper and iron solutions were supplied by Merck.

The instrument used for the ICP-AES measurements was a Varian ICP-AES Liberty II system. The instrument used to record the FT-IR spectra was a BIO-RAD FTS-40 system. Spectra were scanned with a resolution of 4 cm^{-1} . A total of sixty-four scans were accumulated for the middle infrared measurements and the spectrum of a metallic copper sample, without modification was used as a reference/background. The infrared spectra were recorded in reflectance mode, using a MCT detector (mercury-cadmium-telluride). The XPS system used has been described in detail in chapter 4.

6.2.4 Sample preparation

For the FT-IR analysis, the polished copper substrate was immersed in the following solutions for a 24-hr period, before being removed and dried in a stream of nitrogen, prior to IR analysis.

1. 1.6% saccharin-methanol solution.
2. 1.6% saccharin, 1.5% APH - methanol solution.
3. 1.6% saccharin, 1.5% CHP - methanol solution.
4. 1.6% maleic acid, 1.5% CHP - methanol solution

For ICP-AES analysis the samples were prepared by two methods so the results could be compared. The first method used was that of the evaporation method, whilst the second method used was that of the dilution method. The copper substrate was immersed in the solutions outlined in Chapter 4.

- 1 Evaporation method After the copper substrate was removed from these solutions, the methanol was evaporated using a Pierce model 18780 “Reacti-Vap Evaporating system” The solutions were then dissolved in a known quantity of glacial acetic acid prior to analysis
- 2 Dilution method After the copper substrate was removed from the solutions outlined in chapter 4 1 ml of this original solution was placed in 11 mls glacial acetic acid

Standard copper samples measuring 5 ppm, 10 ppm and 100 ppm were made up with glacial acetic acid in order to establish a calibration curve

For XPS analysis, a polished copper substrate was immersed in the following solutions for a 24-hour period After removal from these solutions the copper substrate was dried in a stream of nitrogen prior to analysis

- 1 1 6% saccharin, 1 5% DEmT – methanol solution
- 2 1 6% saccharin, 1 5% DMmT – methanol solution
- 3 1 5% DEmT- methanol solution
- 4 1 5% DMmT- methanol solution

6.3 Results and discussion

6.3.1 Fourier transform infrared spectroscopy (FT-IR)

FT-IR analysis was performed on the copper substrate following immersion for a 24-hour period in specific solutions. Copper modified with the solutions outlined in Chapter 4 were analysed using FT-IR. Results could only be generated for the following four samples, copper modified with a) saccharin, b) saccharin/APH, c) saccharin/CHP and d) maleic acid/CHP. All of the other substrates analysed produced spectra containing atmospheric water vapour and carbon dioxide, indicating that the compound present on these copper surface was below the limit of detection of the spectrometer used.

When an interferogram is Fourier transformed, a single beam spectrum is obtained as seen in Figure 6.3. This spectrum is a plot of the raw detector response versus the wavenumber. This spectrum was obtained on a copper surface and was used as a *background spectrum*.

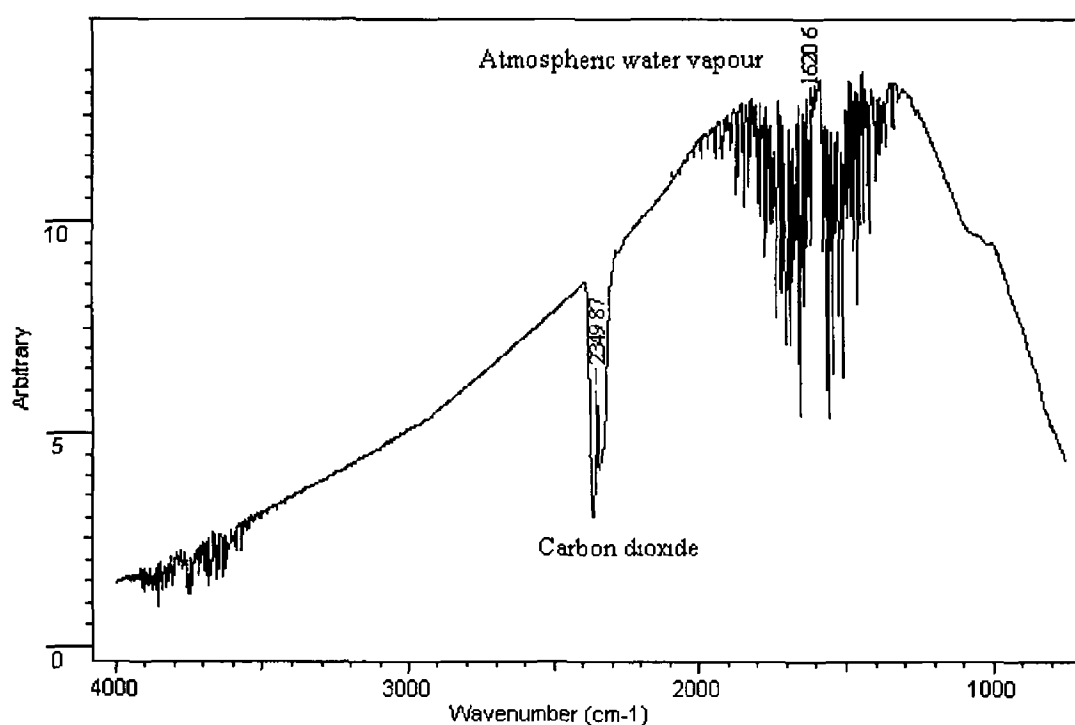


Figure 6.3 A single beam background spectrum for copper

This background spectrum contains the ambient environment's and the instrument contributions to the infrared spectrum [9]. The overall shape of the spectrum is due to many things, such as the sensitivity of the detector, the transmission and reflection properties of the beam splitter, emissive properties of the source and reflective properties of the mirror. Common features around 3500 cm^{-1} and 1630 cm^{-1} are due to atmospheric water vapour, and the bands at 2350 cm^{-1} and 667 cm^{-1} are due to carbon dioxide.

Figure 6.4 shows the FT-IR spectrum recorded for saccharin, this was used as a reference spectrum and compared to Figure 6.5, which was the FT-IR spectrum recorded for the copper substrate immersed in the BS/MeOH solution for a 24-hour period. Figure 6.6 shows the spectrum recorded for the synthesised BSCu(II).

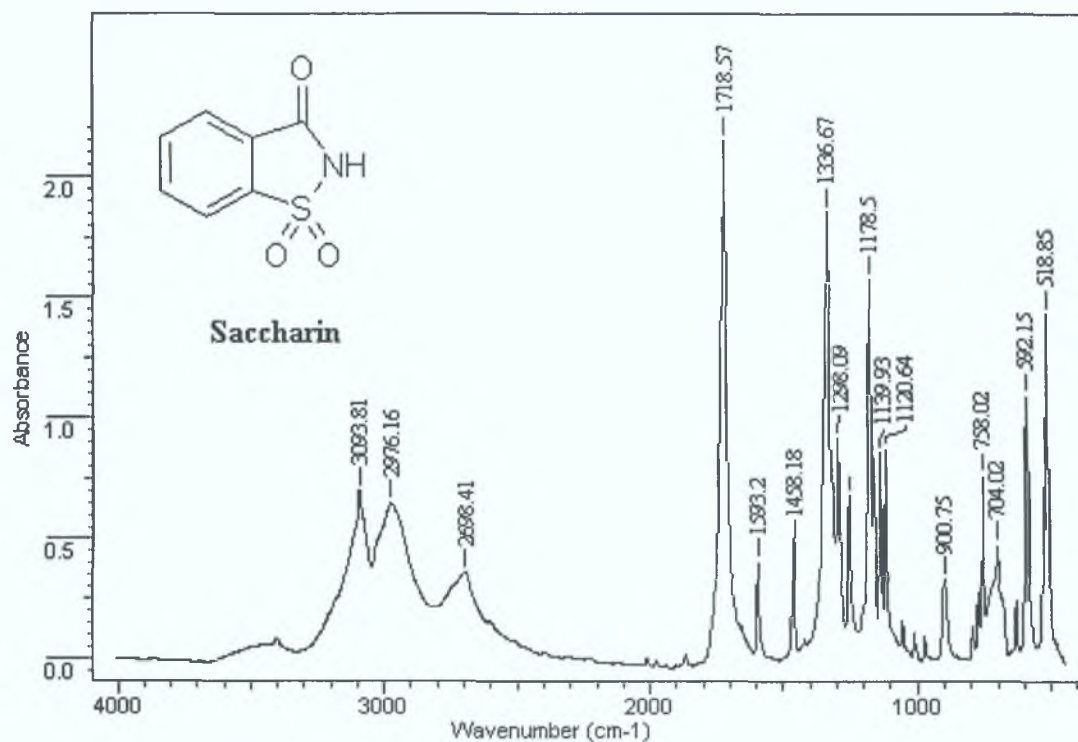


Figure 6.4 A reference spectrum for saccharin.

Generally the IR spectrum is split into two sections, the *fingerprint region* from $1200 \rightarrow 600\text{ cm}^{-1}$ and the *group frequency region* from 3600 to 1200 cm^{-1} . In the fingerprint region small differences in the structure and constitution of a molecule results in significant changes in the appearance and distribution of

absorption peaks in this region, and as a consequence of this a close match between two spectra in this region represents strong evidence for the identity of the compounds yielding the spectrum [11]. The determination of functional groups most likely present is found by examination of the group frequency region.

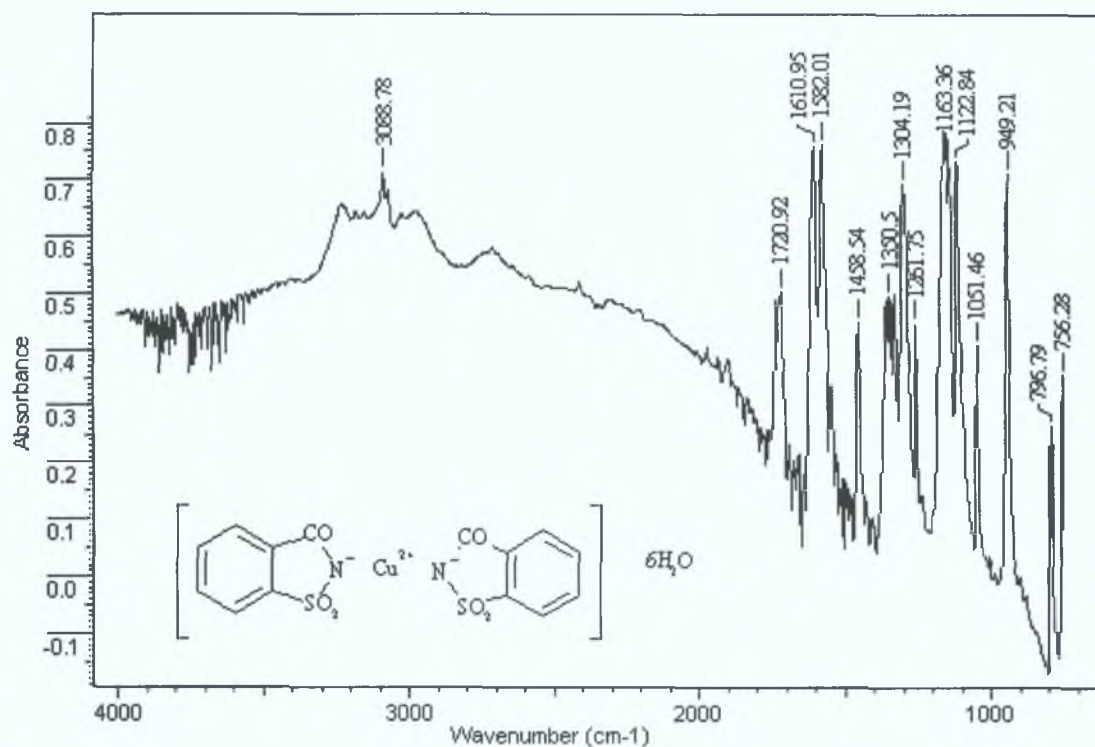


Figure 6.5 Spectrum recorded for copper substrate placed in saccharin-MeOH solution for 24-hour period.

In Figure 6.5 the baseline is not flat, there are many reasons for this including the quantity of material on the substrate surface and the spectra were recorded in reflectance mode. As this spectrum is measured in reflectance, the above peak shapes may be different to that in Figure 6.4; the peak locations are the same in the two spectra but the relative peak heights might differ considerably, with minor peaks generally appearing larger in the reflection spectra. The bands due to saccharin change only slightly in the spectra of the Cu(II)saccharinate. In Figure 6.5 the band at $\approx 1720 \text{ cm}^{-1}$ could be possibly due to an impurity, or form of unreacted saccharin. With a metal salt being formed

between the saccharin and the copper could shift this band to a lower wavenumber of 1610 cm^{-1} (as seen in Figure 6.6) accounting for the main difference seen in the above spectra recorded. Table 6.1 lists the infra-red frequencies for the reference BS, BS/MeOH/Cu (i.e. BSCu(II)) and the synthesised BSCu(II) compounds in the 4000 to 700 cm^{-1} region.

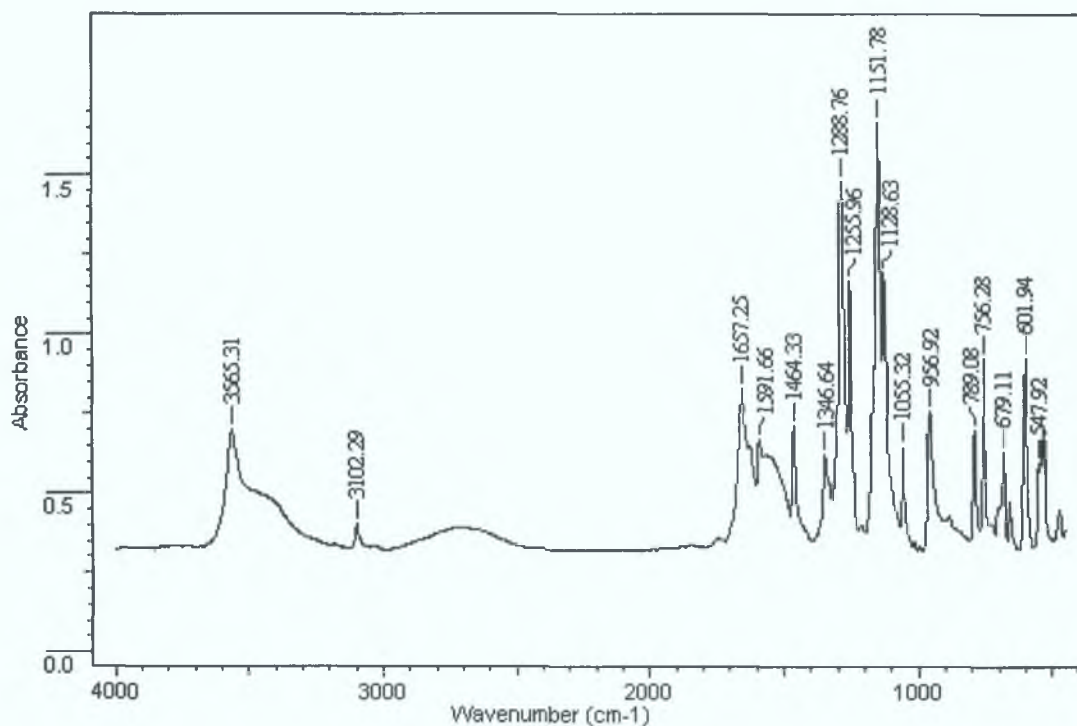


Figure 6.6 Spectrum recorded for synthesised BSCu(II).

The infrared frequencies seen in Table 6.1 for BSCu(II) (on copper substrate), and BSCu(II) synthesised are almost identical, reinforcing that surmised in chapter 4 in which the copper substrate after contact with a saccharin solution produces BSCu(II) at the substrate surface. As previously stated the band at a lower wavenumber of 1650 cm^{-1} is indicative of the BSCu(II) (synthesised) salt. The major difference observed between the BSCu(II) and the synthesised BSCu(II) is a band at 1720 cm^{-1} present on the BSCu(II) due to unreacted saccharin left present on the surface after the copper substrate was immersed in the methanol-saccharin solution

| Saccharin (reference) cm ⁻¹ | BSCu(II) cm ⁻¹ | BSCu(II) cm ⁻¹ (synthesised) |
|---|---------------------------|--|
| - | 3231.55 | 3565.31 |
| 3093.81 | 3088.78 | 3102.29 |
| 2976.16 | 2978.81 | |
| 2698.41 | - | |
| 1718.50 | 1720.92 | |
| - | 1610.95 | 1657.25 |
| 1593.20 | 1582.01 | 1591.66 |
| 1458.18 | 1458.54 | 1464.33 |
| 1336.67 | 1335.06-1350.50-1362.07 | 1346.64 |
| 1298.09 | 1304.19 | 1288.76 |
| 1257.59 | 1261.75 | 1255.96 |
| 1178.50 | - | |
| 1163.07 | 1159.50 | 1151.78 |
| 1139.93 | - | |
| 1120.64 | 1122.84 | 1128.63 |
| 1014.55 | 1051.46 | 1055.32 |
| 974.05 | 949.21 | 956.92 |
| 900.75 | - | |
| - | 796.79 | 789.05 |
| 758.02 | 756.28 | 756.28 |

Table 6.1 Infra-red frequencies of saccharin, and CuBSII

Figure 6.7 and Figure 6.8 shows the spectrum recorded for the copper substrate immersed in a methanol solution of 1.6% BS/1.5% APH and 1.6% BS/1.5% CHP respectively. Reference spectrum of APH and CHP were obtained and Table 6.2 lists the infra-red frequencies for the following reference compounds, saccharin, APH and CHP and the infra-red frequencies recorded for the copper substrate modified with BS/APH and BS/CHP in the 4000 to 700 cm⁻¹ region.

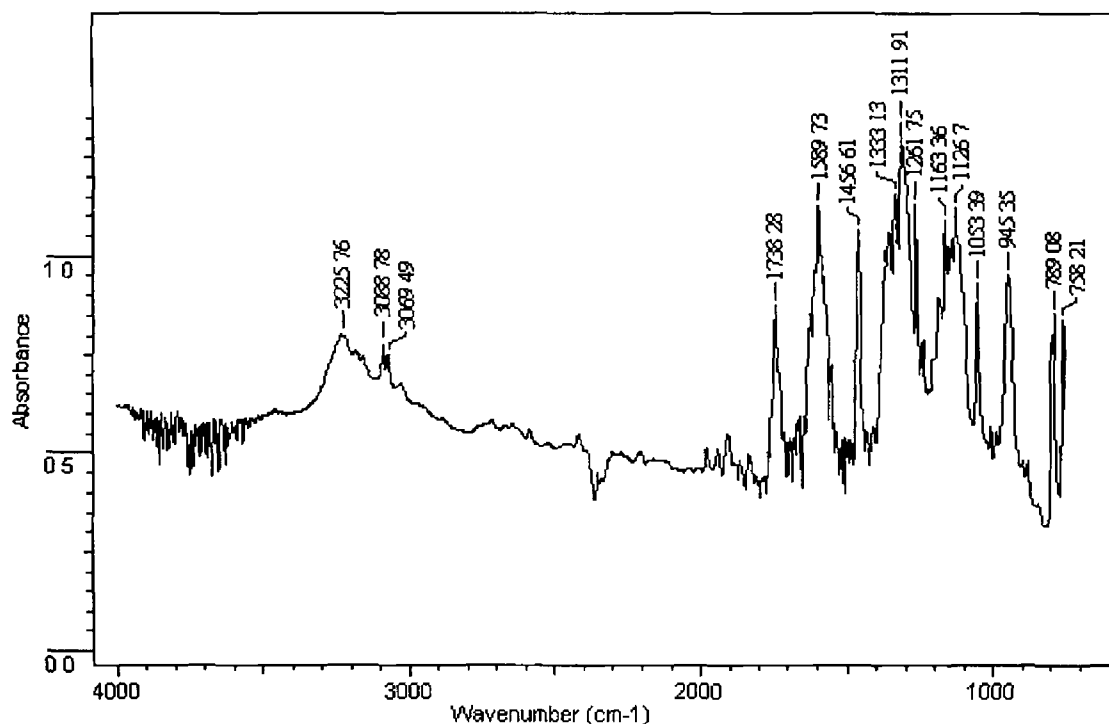


Figure 6 7 Spectrum recorded for copper substrate placed in BS/APH-MeOH solution for 24-hour period

The infrared frequencies recorded in Table 6 2 between the different compounds are compared, the values written in red for the BS/APH and the BS/CHP specimen coincide with those recorded for the BSCu(II) complex above. For BS/APH both of these compounds segregate at the substrate surface; this is confirmed by the FT-IR spectrum recorded where the infrared frequencies in Table 6 2 confirm the bands associated with the saccharin salt, with the remaining bands attributed to the APH. The differences in infrared frequencies noted for the BS/CHP are highlighted in Table 6 2. Saccharin has segregated at the substrate surface, with a contribution from the CHP noted in the $3000 \rightarrow 1600 \text{ cm}^{-1}$ range.

| BS(ref)cm ⁻¹ | APH(ref)cm ⁻¹ | BS/APHcm ⁻¹ | CHP(ref)cm ⁻¹ | BS/CHPcm ⁻¹ |
|-------------------------|--------------------------|------------------------|--------------------------|------------------------|
| - | - | 3227.69 | 3414.83 | 3540.23 |
| 3093.81 | - | 3088.78 | - | 3098.43 |
| - | 3041.74 | 3069.49 | 3061.77 | 3019.33 |
| 2976.16 | - | - | 2982-2936 | 2947-2980 |
| - | - | - | - | 2851.48 |
| 2698.41 | - | - | - | - |
| - | - | - | - | 2002.59 |
| - | - | 1902.27 | - | - |
| 1718.50 | - | - | - | - |
| - | 1666.49 | - | - | 1659.18 |
| - | 1602.84 | - | 1603.23 | - |
| 1593.20 | - | 1589.73 | - | 1587.80 |
| - | 1496.76 | 1549.21 | 1497.12 | - |
| 1458.18 | - | 1460.47 | 1448.89 | 1456.61 |
| - | 1433.11 | - | - | - |
| - | 1371.39 | 1365.93 | 1371-1379 | 1381.37 |
| 1336.67 | - | 1333.13 | - | 1336.99 |
| 1298.09 | 1301.95 | 1311.91 | - | 1292.62 |
| 1257.59 | 1246.01 | 1261.75 | 1269.47 | 1269.47 |
| - | - | - | 1203.87 | - |
| 1178.50 | 1174.65 | 1184.58 | - | 1169-1188 |
| 1163.07 | 1153.43 | 1163.36 | 1153.71 | 1153.71 |
| 1139.93 | - | - | - | - |
| 1120.64 | - | 1126.70 | 1105.48 | 1124.77 |
| 1014.55 | - | 1053.39 | 1030-1076 | 1010-1059 |
| - | 997.2 | - | - | - |
| 974.05 | - | 945.35 | 954.99 | 953.07 |
| 900.75 | - | - | 910.62 | - |
| - | - | 789.08 | 853.38 | 796.79 |
| 758.02 | - | 758.21 | 764.00 | 758.21 |

Table 6.2 Infra-red frequencies of saccharin, APH, BS/APH, CHP and BS/CHP

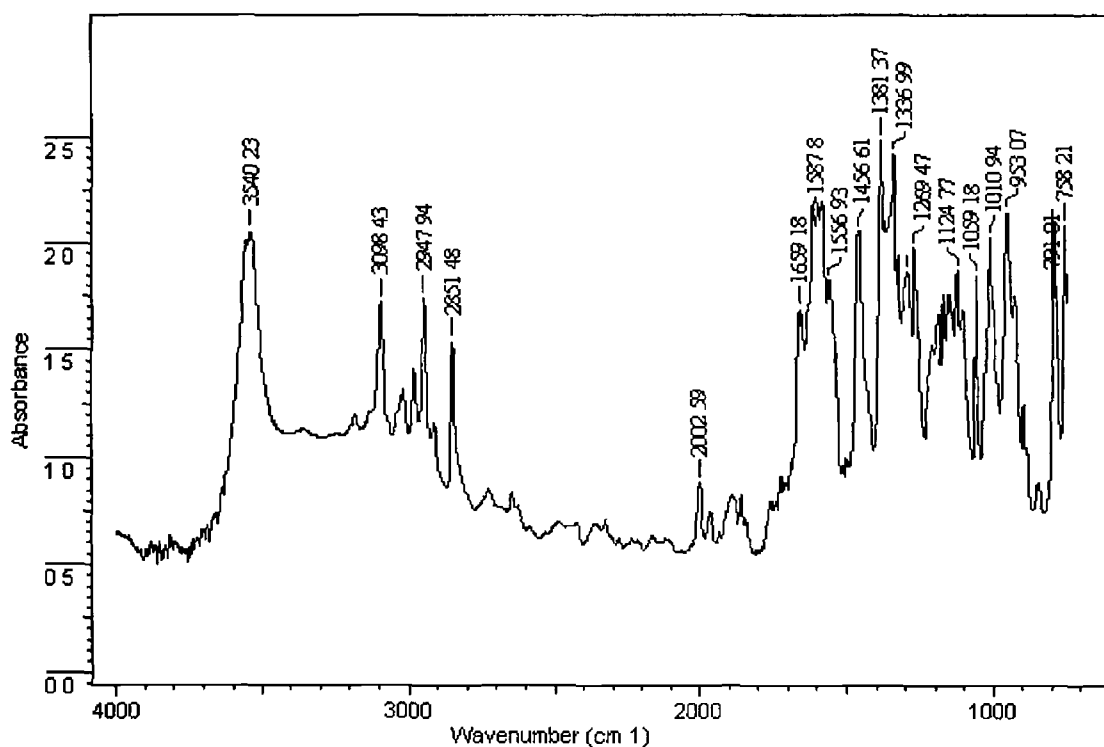


Figure 6 8 Spectrum recorded for copper substrate placed in BS/CHP-MeOH solution for 24-hour period

Similarities the peaks at wavenumber $1325 \pm 25 \text{ cm}^{-1}$ and $1140 \pm 20 \text{ cm}^{-1}$ are indicative of the sulphone or $=\text{SO}_2$ sulfur function, present from the saccharin, this characteristic adsorption is present on all spectra which contain saccharin, i.e. BS_{ref}, BS/APH and BS/CHP. The aromatic ring presents itself at wavenumber $1600 - 1450 \text{ cm}^{-1}$ in the form of two or three sharp bands, and in the $900 - 700 \text{ cm}^{-1}$ region of the spectrum, these bands are present on all

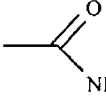
surfaces. The band at $1590 \pm 10 \text{ cm}^{-1}$ is indicative of the  function, which is another part of the saccharin and is present on the spectra recorded and can be seen in Figures 6 3-6 8. Aromatic C-N stretching presents itself as a strong band in the $1180-1360 \text{ cm}^{-1}$ region of the spectra, which is also found in all recorded spectra.

Figure 6.9 shows the FT-IR spectrum recorded for copper substrate immersed in 1.6% maleic acid - 1.5% CHP methanol solution. With Table 6.3 indicating the peaks recorded from each spectrum.

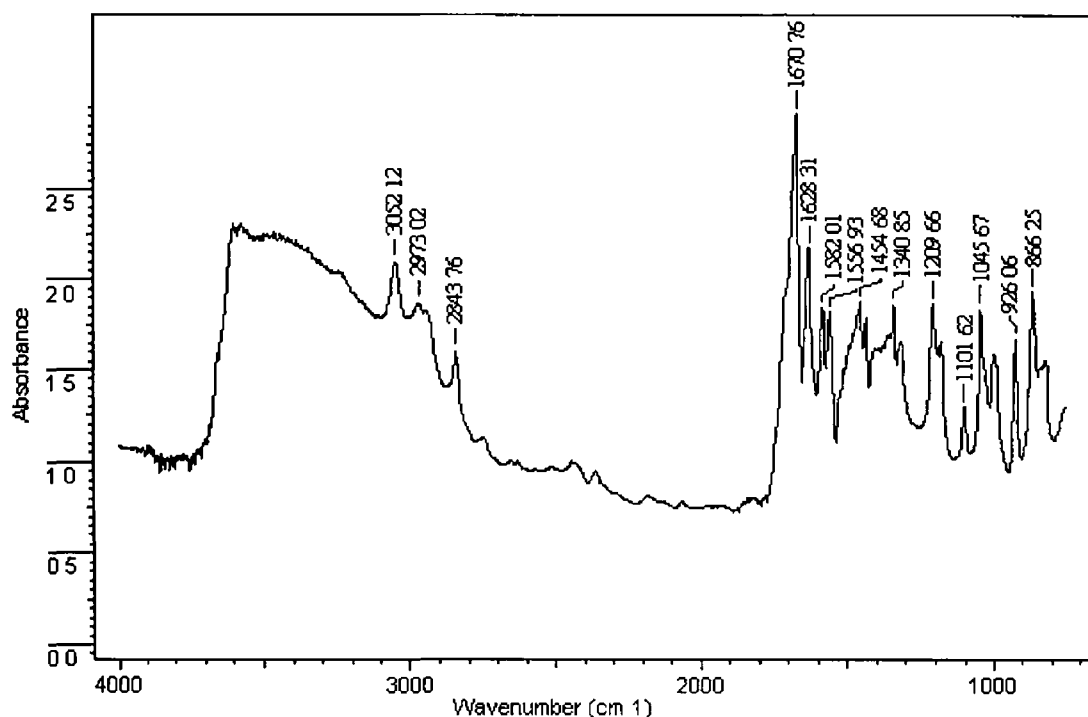


Figure 6.9 Spectrum recorded for copper substrate placed in maleic acid/CHP-MeOH solution for 24-hour period

The major similarities between the FT-IR spectrum for mal_{ref} , CHP_{ref} and mal/CHP can be seen especially in the fingerprint region. Most of the spectral lines recorded can be attributed to the maleic acid, indicating that the maleic acid forms a metal salt with the underlying copper. The shift to a lower wavenumber from 1707 cm^{-1} (maleic reference) to 1670 cm^{-1} (mal/CHP-MeOH) is an indication that a maleic acid segregates to the copper surface forming Cu(II)maleate . The sloping background makes it hard to assign frequencies in the *group frequency* region. The reason for this sloping background is possibly due to the reflectivity of the specimen, and amount of material present on the surface.

| Maleic acid (ref) cm^{-1} | Mal/CHP cm^{-1} | CHP (ref) cm^{-1} |
|------------------------------------|--------------------------|----------------------------|
| - | - | 3414.83 |
| 3059.84 | 3052.12 | 3061.77 |
| - | 2973.02 | 2982-2936 |
| 2897.78 | 2843.76 | - |
| 2687.49 | - | - |
| 2608.39 | - | - |
| 2508.07 | - | - |
| 2170.44 | - | - |
| 1707.41 | - | - |
| 1637.96 | 1628-1670 | 1603.23 |
| 1591.66 | 1582.01 | - |
| 1568.51 | 1556.93 | - |
| - | - | 1497.12 |
| 1460.47 | 1458.54 | 1448.89 |
| 1433.46 | 1435.39 | - |
| - | 1340.85 | 1371-1379 |
| - | 1317.70 | - |
| 1265.61 | - | 1269.47 |
| 1221.24 | 1209.66 | 1203.87 |
| - | 1178.79 | 1153.71 |
| - | 1101.62 | 1105.48 |
| - | 1045.67 | 1030-1076 |
| - | 999.37 | - |
| 949.21 | 926.06 | 954.99 |
| - | - | 910.62 |
| 864.32 | 866.25 | 853.38 |
| - | - | 764.00 |

Table 6.3 Infra-red frequencies of Mal_{ref}, CHP_{ref} and Mal/CHP (recorded).

6.3.2 Inductively coupled plasma – atomic emission spectroscopy (ICP-AES)

ICP-AES was performed on the solutions in which the copper substrate was immersed, after the substrate was removed. The solutions were either evaporated or diluted as outlined in Section 6.2.4, and the results indicated how much of the copper substrate was leached into the solution. Table 6.4 and 6.5 give the amount of copper leached in ppm/cm², for the evaporation and the dilution methods respectively. The wavelength of copper used throughout this experimental section was 327 nm.

| Copper Solution | gms CH ₃ COOH* (1.06) | Reading ppm | Evaporated 2 /15 ml | Surface area (cm ²) | ppm/cm ² |
|-----------------|----------------------------------|-------------|---------------------|---------------------------------|---------------------|
| Saccharin | 9.41 | 8.4394 | 7.5 | 2.695 | 221 |
| BS+DMoT | 9.13 | 8.5546 | 7.5 | 2.5816 | 227 |
| BS+DEpT | 9.21 | 7.3935 | 7.5 | 2.491 | 205 |
| BS+DMpT | 9.16 | 3.8162 | 7.5 | 2.5462 | 103 |
| BS+APH | 9.64 | 6.5274 | 7.5 | 2.8726 | 164 |
| BS+CHP | 8.13 | 27.906 | 8 | 2.4806 | 686 |
| Maleic acid | 9.78 | 28.832 | 7.5 | 2.8054 | 754 |
| Mal+DMoT | 9.93 | 14.854 | 8 | 2.2206 | 531 |
| Mal+DEpT | 9.36 | 17.375 | 8 | 2.5894 | 502 |
| Mal+DMpT | 9.32 | 12.218 | 7.5 | 2.3038 | 371 |
| Mal+APH | 10.60 | 8.4832 | 7.5 | 2.401 | 281 |
| Mal+CHP | 9.64 | 74.063 | 8 | 2.5294 | 2258 |
| DMoT | 9.62 | 0.1859 | 7.5 | 2.6018 | 5 |
| DEpT | 9.75 | 0.1141 | 7.5 | 2.4454 | 3 |
| DMpT | 10.02 | 0.1902 | 7.5 | 2.7558 | 5 |
| APH | 9.37 | 0.9689 | 7.5 | 2.7156 | 25 |
| CHP | 9.32 | 0.6773 | 7.5 | 2.6356 | 18 |
| MeOH | 9.50 | 0.0662 | 7.5 | 2.6422 | 2 |

Table 6.4 Experimental results calculated from evaporation method.

| Copper Solution | Dil/gms CH ₃ COOH* (1.06) | Reading ppm | Original solution | Surface area (cm ²) | ppm/cm ² |
|-----------------|--------------------------------------|-------------|-------------------|---------------------------------|---------------------|
| Saccharin | 11.66 | 3.3795 | 15 | 2.695 | 220 |
| BS+DMoT | 11.66 | 2.9990 | 15 | 2.5816 | 203 |
| BS+DEpT | 11.66 | 2.6014 | 15 | 2.491 | 183 |
| BS+DMpT | 11.66 | 1.3194 | 15 | 2.5462 | 90 |
| BS+APH | 11.66 | 2.4421 | 15 | 2.8726 | 149 |
| BS+CHP | 11.66 | 10.574 | 16 | 2.4806 | 795 |
| Maleic acid | 11.66 | 12.040 | 15 | 2.8054 | 751 |
| Mal+DMoT | 11.66 | 5.4162 | 16 | 2.2206 | 455 |
| Mal+DEpT | 11.66 | 6.2893 | 16 | 2.5894 | 453 |
| Mal+DMpT | 11.66 | 5.2864 | 15 | 2.3038 | 401 |
| Mal+APH | 11.66 | 3.5291 | 15 | 2.401 | 257 |
| Mal+CHP | 11.66 | 28.470 | 16 | 2.5294 | 2100 |
| DMoT | 7.77 | 0.1145 | 15 | 2.6018 | 5 |
| DEpT | 7.77 | 0.1714 | 15 | 2.4454 | 8 |
| DMpT | 7.77 | 0.1589 | 15 | 2.7558 | 7 |
| APH | 7.77 | 0.3849 | 15 | 2.7156 | 16 |
| CHP | 7.77 | 0.2224 | 15 | 2.6356 | 10 |
| MeOH | 7.77 | 0.0647 | 15 | 2.6422 | 3 |

Table 6.5 Experimental results calculated from dilution method.

The results calculated above indicate the amount of copper that has leached from the substrate after 24 hours immersed in methanolic solutions of the above compound. The maximum % error in the results calculated between the two methods, evaporation and dilution, is approximately 5%. The copper substrate was immersed in a methanol only solution, to see if the solvent used contributes to the overall result. This was found not to be the case as only 3 ppm/cm² was leached from the substrate and deemed negligible. The influence that a 1.5% compound-methanol solution of the following compounds, DMoT, DEpT, DMpT, APH and CHP has on the copper substrate was also minimal and falls within the range of 5 → 16 ppm/cm².

Saccharin interacts with the substrate at 220 ppm/cm² and when saccharin was combined with DMoT and DEpT the result fell within the experimental error of the recorded results at 200 → 230 ppm/cm². It would appear that these two tertiary amines do not affect the acidic properties of the saccharin. But when saccharin was combined with DMpT, the amount of copper found in the solution after 24 hr had more than halved at 97 ppm/cm², indicating the this amine neutralizes the acidic solution. For the BS/APH solution the amount of metal released from the solution has decreased to 156 ppm/cm². The results for the combination of BS/APH and BS/DMpT coincide with those found in chapter 4 indicating that both of these reducing amines produce an effect on the metal substrate and segregate to the surface neutralising the acid by the formation of a salt. When BS was combined with CHP the amount of copper found in the resultant solution was high at a value of 740 ppm/cm². A possible explanation for this is that by reacting BS with CHP the products formed include cumyl alcohol and water. If the content of water is increased within the substrate solution, then by introducing water into the solution the leaching efficiency of the solution improves and the reaction proceeds faster making it more powerful in dissolving the metal, hence the high metal content observed for this reaction at 740 ppm/cm².

For maleic acid in contact with the copper substrate 752 ppm/cm² of copper was found in the resultant solution. This value was much higher than that calculated for saccharin and is the expected result as maleic acid is a stronger acid than saccharin. The amount of copper dissolved by maleic acid in combination with DMoT, DEpT, DMpT and APH was reduced, with the best results recorded for maleic acid in combination with DMpT and APH at 386 ppm/cm² and 269 ppm/cm² respectively. This reinforces the conclusions outlined in chapter 4 in which maleic acid forms a salt with the substituted aromatic amines regardless of the position of the methyl substitute on the aromatic ring. This serves to reduce the acidity of the maleic acid by neutralising the acid and reducing its power to dissolve the copper substrate. As with the saccharin the combination of maleic acid with CHP releases 2179 ppm/cm² from the copper substrate. This is explained by the increase in the water content of the

solution and in turn increasing the leaching ability and speeding up the reaction of the solution making it more powerful in dissolving the metal under investigation, hence the high value. This results parallels the result found when using saccharin and CHP.

6.3.3 X-ray photoelectron spectroscopy (XPS)

XPS analysis was carried out on a copper substrate immersed in DMmT (N,N-dimethyl-m-toluidine) and DEmT (N,N-diethyl-m-toluidine). This study was extended combining saccharin with DEmT and DMmT in methanolic solutions, to see if these meta-substituted toluidines are as efficient at forming a salt with saccharin as their para-substituted counterparts DEpT and DMpT (chapter 4). The results of quantitative analysis of the elements found present on the copper substrate are shown in Table 6.6.

| Substrate | Carbon | Oxygen | Copper | Nitrogen | sulfur |
|-------------------|--------|--------|--------|----------|--------|
| Cu _{ref} | 58 | 19 | 23 | 0 | 0 |
| Saccharin | 56 | 25 | 5 | 7 | 7 |
| DEmT | 52 | 22 | 26 | 0 | 0 |
| DMmT | 49 | 26 | 25 | 0 | 0 |
| BS+DEmT | 64 | 22 | 3 | 6 | 5 |
| BS+DMmT | 70 | 17 | 2 | 6 | 5 |

Table 6.6 Experimental values calculated in atomic percent for the Cu_{ref} substrate, 1.6% BS/MeOH, 1.5% DEmT/MeOH, 1.5% DMmT/MeOH, 1.6%BS-1.5% DEmT/MeOH and 1.6% BS-1.5% DMmT/MeOH solutions.

The ratio of nitrogen to sulfur in the saccharin complex is 1:1, therefore the same amount of each of these atoms segregating to the surface agrees with this ratio when saccharin alone was in contact with the copper substrate. When the copper substrate is placed in contact with the individual meta-substituted toluidines, no indication is present of segregation of this compound at the interface of the substrate, as no nitrogen was found on the substrate. The atomic %'s calculated for elements present on these substrate surfaces are relatively similar and fall within a 5-7% error range. As the copper found on these

substrate surfaces (Cu_{ref} , Cu_{DMmT} and Cu_{DEmT}) is in the range of (atomic %) 23 → 26 %, this is an indication that no overlayer is produced at the interface, as a decrease in the copper content would be observed if this was the case. The oxygen content had increased on the copper substrate modified with the meta-substituted toluidines which could be due to the solvent (methanol). The substrate was immersed in this solution for a 24 hr period therefore some unreacted methanol could be left on the substrate prior to analysis accounting for the increase observed in the oxygen.

While saccharin is added to these meta-substituted toluidines an increase in the carbon content was observed at the expense of the Cu. This was to be expected as both of the compounds used (BS and toluidines) contain a high proportion of carbon. The most dramatic rise in the carbon content was observed for the BS/DMmT combination, at 70%. The nitrogen and sulfur content of the substrate is approximately 1:1, leading to the conclusion that these two elements are probably present on the substrate surface due to the interaction of the copper substrate with the saccharin. The ratio of N:S with respect to BS combined with the para-substituted toluidines was 2:1, indicating that the nitrogen found on these substrate surfaces was due to both the saccharin and the amine. The survey scans of the above substrates can be seen in Figure 6.9. From these results it would appear that the position of the electron-withdrawing group on the substituted aromatic amine plays an important role in the formation of a salt with the organic acid. Hence for a salt to be formed the optimal position of the methyl group appears to be in the para-position as opposed to the meta- or ortho-positions. Figure 6.10 shows the decomposition of the C 1s, O 1s and N 1s spectral regions for the copper substrate modified with A) DMmT, B) DEmT, C) BS/DMmT and D) BS/DEmT.

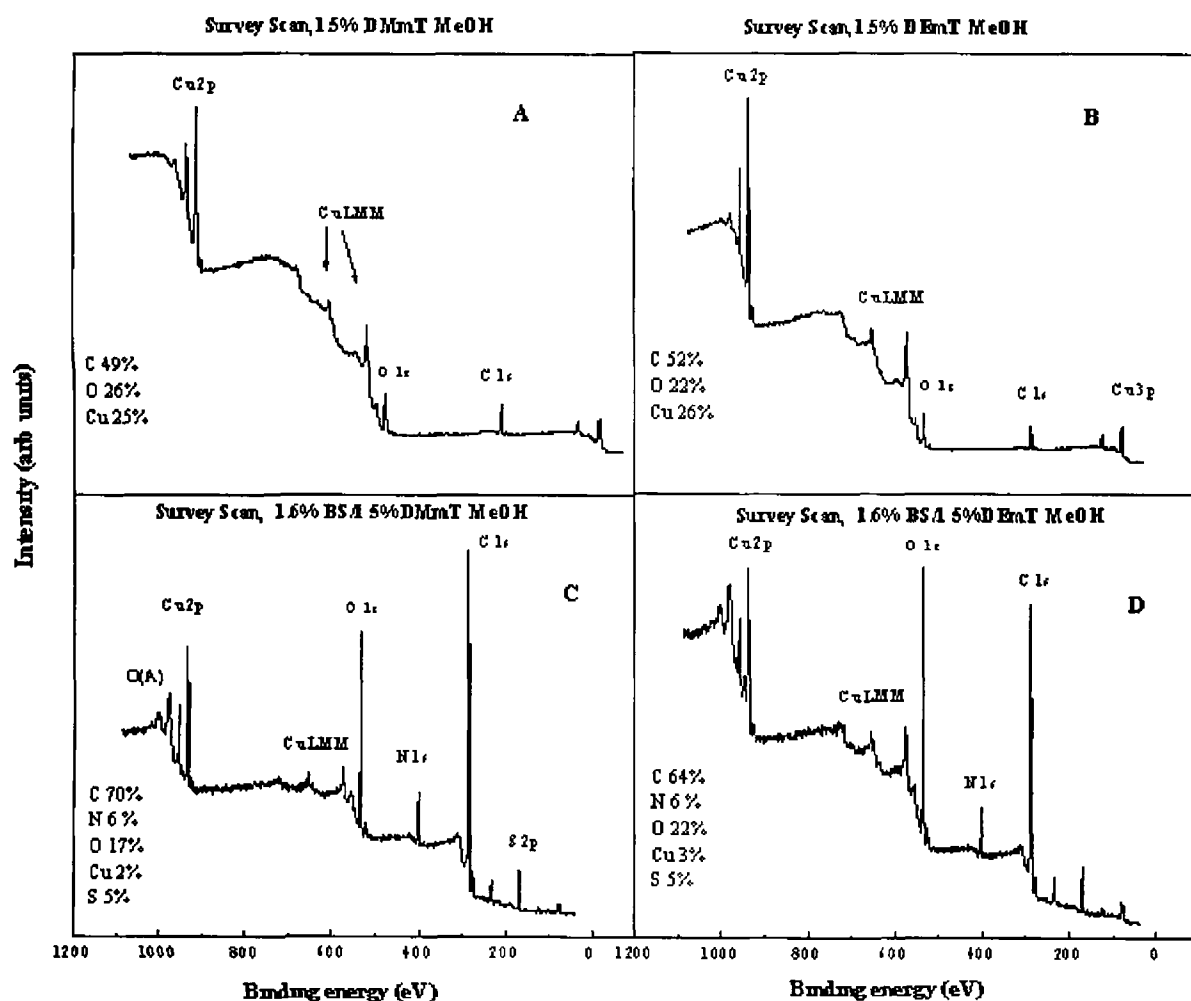


Figure 69 Survey scans recorded for copper substrate after a 24 hour immersion period in the following methanol solutions A) 1.5% DMmT, B) 1.5% DEmT, C) 1.6%BS/1.5% DMmT and D) 1.6%BS/1.5% DMmT, indicating peaks interest

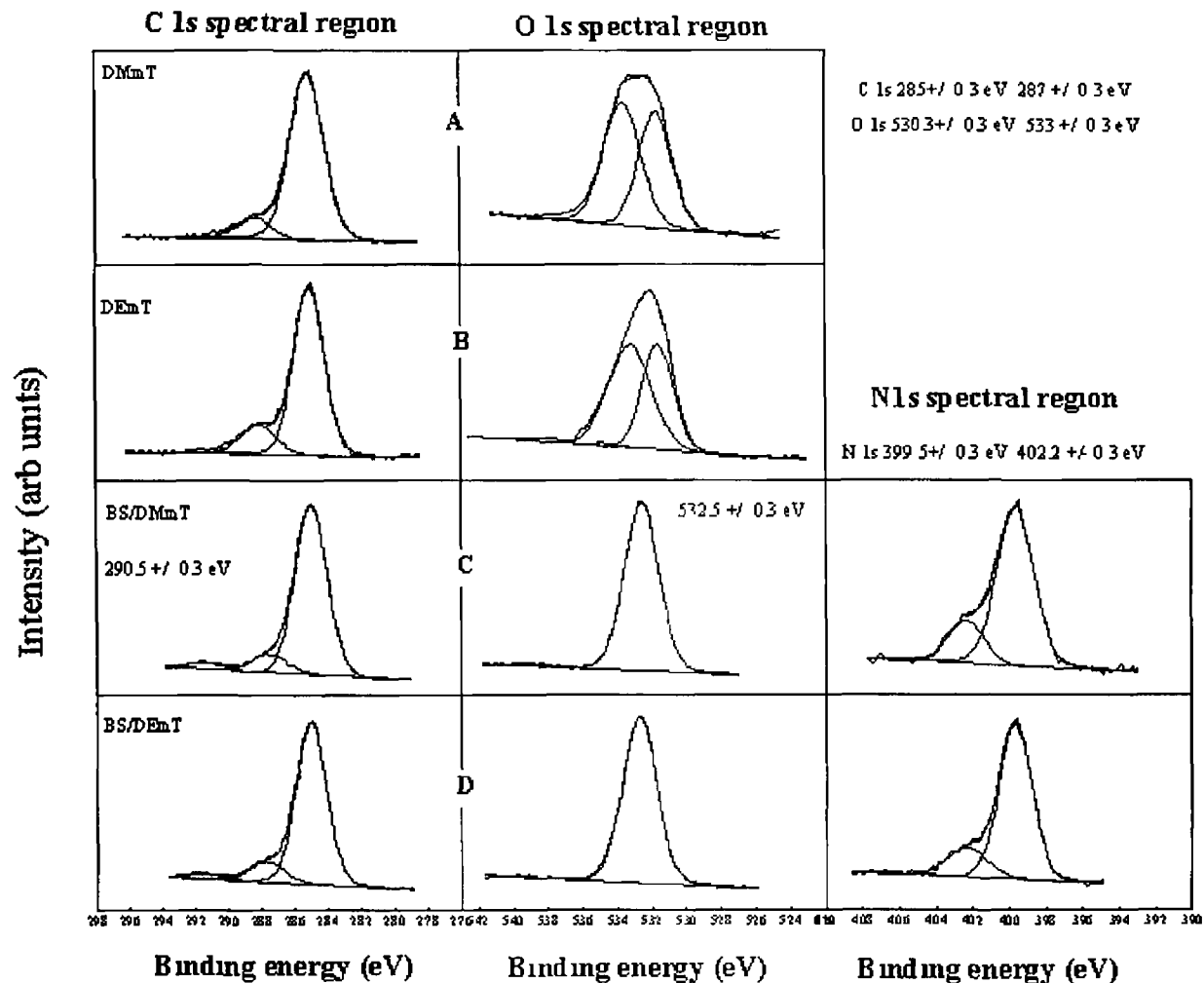


Figure 6.10 Decomposition of the C 1s, O 1s and N 1s spectral regions recorded for copper substrate after a 24 hour immersion period in the following methanol solutions A) 1.5% DMmT, B) 1.5% DEmT, C) 1.6%BS/1.5% DMmT and D) 1.6%BS/1.5% DMmT, indicating peaks interest

From Figure 6.10 the decomposition of the C 1s emission lines indicates two carbon environments for the copper substrate immersed in 1.5% DMmT and 1.5% DEmT (A and B respectively). The peak at 285 ± 0.3 eV was attributed to hydrocarbon contamination, with the higher binding energy of 287 ± 0.3 eV possibly due to residue of the methanol solvent on the substrate surface. Decomposition of these carbon peaks was similar to those recorded for the Cu_{ref} substrate, indicating that the meta-substituted toluidines do not alter the carbon moiety of the substrate surface. The O 1s spectral region for these meta-toluidines was also similar to results recorded for the Cu_{ref} with the binding energy at 530.3 ± 0.3 eV indicative of metal oxides and that of 533 ± 0.3 eV indicative of H₂O [12] or C-OH of the methanol [13].

For combinations of saccharin with the meta-substituted tertiary amines in the O 1s region the binding energy at 532.5 ± 0.3 eV accounts for the SO₂ moiety of the saccharin. The decomposition of the N 1s emission peak consists of a peak at 399.5 ± 0.3 eV, with an asymmetric feature on the higher binding energy side at 402.2 ± 0.3 eV. The peak at 399.5 ± 0.3 eV is assigned to the nitrogen associated with the organic acid, where the peak at a higher binding energy was possibly due to some form of nitrogen from the amine, not chemisorbed on the substrate surface. This nitrogen feature is common to the copper substrate modified with saccharin (Chapter 4, Figure 4.16). The absence of nitrogen peaks characteristic of protonated and unprotonated nitrogen (shift in energy of 1.2 eV) is obvious, leading to the conclusion that only the saccharin has concentrated at the substrate surface in these cases.

6.4 Conclusions

The results recorded in this chapter reinforce the conclusions outlined in chapter 4. From the FT-IR spectrum, it was shown that saccharin concentrates at the substrate surface in all cases, i.e. BSCuII, BS/APH and BS/CHP.

The ICP-AES results show that the individual components of anaerobic adhesives and the solvent used (methanol) do not interact with the copper substrate surface. But in combinations with saccharin a salt is formed when the aromatic amine used is APH or DMpT, neutralising the acid and reducing its acidic properties therefore reducing its ability to leach the metal into the solvent solution. The analogous situation applies when maleic acid is the organic acid used, maleic acid has the ability to form a salt with all of the amines reducing its acidic properties. The dramatic effect in the leaching ability of these acids in combination with CHP is explained by the introduction of water into the solvent solution.

The position of the methyl group on the aromatic amine plays an important part in the formation of a salt with the saccharin. When the methyl group is in the meta-position the toluidine appears not to segregate at the substrate surface as the nitrogen response on the substrate being attributed solely to the saccharin.

6.5 References

- [1] George, B , Touyeras, F , Grohens, Y and Vebrel, J , Int J Adhesion and Adhesives, 17 (1997) 121
- [2] Stamper, D J , British Polymer Journal, 15 (1983) 34
- [3] Yang, D B , Applied Spectroscopy, 47 (1993) 1425
- [4] Okamoto, Y , J Adhesion 32 (1990) 227
- [5] Beaunez, P , Helary, G and Sauvet, G , J of Polymer Science, 32 (1994) 1459
- [6] Wellmann, St and Brockmann, H , Int J Adhesion and Adhesives, 14 (1994) 47
- [7] Yang, D B , J Adhesion, 43 (1993) 273
- [8] Yang, D B , Wolf, D , Wakamatsu, T and Holmes, M , J Adhesion Sci Technol , 14 (1995) 1369
- [9] Smith, B C , “Fundamentals of Fourier Transform Infrared Spectroscopy”, CRC press, New York and London, (1996)
- [10] Banwell, C N and McCash, E , “Fundamentals of Molecular Spectroscopy”, McGraw-Hill Int Ltd UK, (1994)
- [11] Skoog, D A, Holler, F J and Nieman, T A , “Principals of Instrumental Analysis” 5th Ed (1998) 230
- [12] Briggs, D , Seah, M P “Practical Surface Analysis by Auger and X-ray Photoelectron Spectroscopy”, Wiley, New York, (1994)
- [13] Briggs D , “Surface analysis of Polymers by XPS and Static SIMS”, Clarke, D R , Suresh, S and Ward, I M (Eds), Cambridge University Press (1998)

Chapter 7

Surface Characterisation of Alkane-Thiol Adsorption on Polycrystalline
Copper Surface and Au Single Crystal Surfaces

7.1 Introduction

The study of SAM (self-assembled monolayers) dates back to the early 1946, when Zisman *et al* published work, on the preparation of a monomolecular layer by adsorption onto a clean metal surface [1] Self-assembly, in a general sense, can be defined as the spontaneous formation of hierarchical structures from pre-designed building blocks, usually involving multiple energy scales and multiple degrees of freedom SAMs are ordered molecular assemblies that are spontaneously formed on solid surfaces by immersing the appropriate substrate into a solution of an active surfactant in an organic solvent SAMs contain a head group, a hydrocarbon chain and an end group, the head group being the functional group which forms a strong chemical bond with the desired substrate resulting in a close-packed structure of high order While adsorption on the surface is directly due to the affinity of the head group for the surface, the hydrophobic van der Waals interactions of the alkyl chains are the driving force behind the organisation of ordered and closely packed assemblies [2] There are numerous types of self-assembly systems that generate organic monolayers dialkyl sulfides/disulfides on gold, carboxylic acids on aluminium oxide, alcohols and amines on platinum, organosilicon on hydroxylated surfaces, and alkanethiols on Au, Ag and Cu

In this chapter, previous studies of alkanethiols on polycrystalline copper and Au(111) single crystal will be reviewed with particular emphasis on alcohol- and carboxylic-terminated thiols These particular SAMs are investigated because of their synthetic accessibility, their polarity and the reactivity of the end group, and if the terminal group can be controlled these monolayers can be used as building blocks for the adsorption of other species [3]

7.2 SAM Formation

7.2.1 The self-assembly process

As mentioned in the introduction SAMs are molecular assemblies which display high organisation, and are spontaneously formed as a result of immersing a solid surface in a solution that consists of amphifunctional molecules. A self-assembling surfactant molecule can be divided into three parts:

1. The head group.
2. The hydrocarbon chain.
3. The end group.

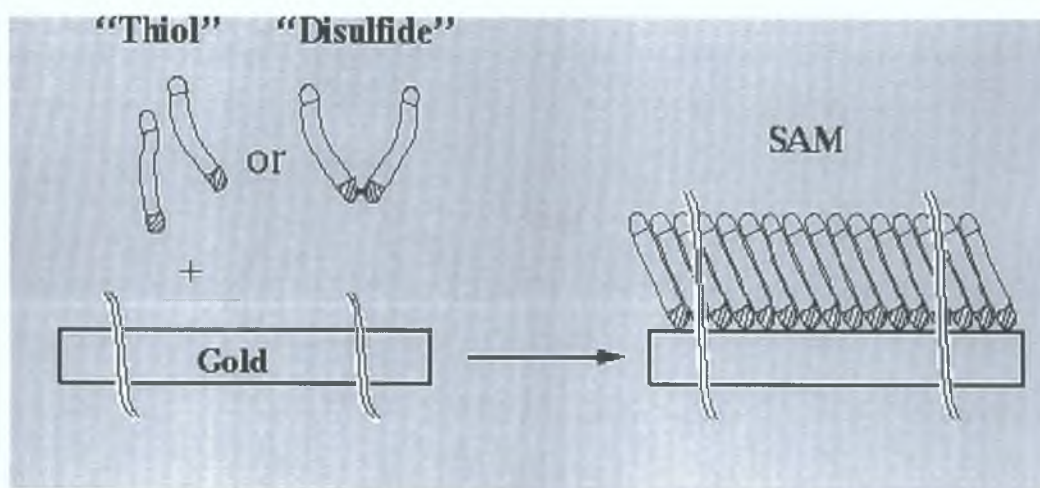


Figure 7.1 Schematic view of a self-assembling monolayer.

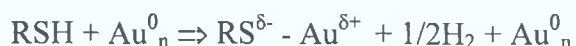
The Head Group

A report by Nuzzo *et al.* showed that alkanethiols adsorb onto a gold surface by a process known as chemisorption [4]. The head group is the most exothermic reaction in this process, involving the chemisorption of the SAM to the surface of the substrate. In the case of alkanethiols on Au, covalent, slightly polar bonds form between the Au-S. This molecular-substrate interaction is very strong, resulting in what appears to be the pinning of the head group to a particular site on the surface via this gold-thiolate bond (Figure 7.1). In other cases these bonds may be covalent or ionic depending on the nature of the SAM

and that of the surface. The energy associated with this thiolate-gold bond is $\approx 40\text{--}45$ kcal/mol, therefore this exothermic head group – substrate interaction results in the molecules trying to occupy all available binding sites on the surface, pushing together molecules that are already adsorbed on the surface. As a result of this spontaneous molecular adsorption, short-range, dispersive, London-type van der Waals inter-chain forces become important.

For this case of thiol adsorption from the liquid phase on Au(111), self-assembly appears to involve two steps, the initial steps consisting of the adsorption process which occurs rapidly, and can be described by simple diffusion controlled Langmuir kinetics, followed by the slower ordering (recrystallisation) step, as the system approaches equilibrium [5-7].

The first step is dominated by the molecule-substrate interactions; these interactions anchor the thiol (R-SH) chemical functionally to specific substrate sites via a strong directional Au-thiolate chemisorption bond [8-9]. If one considers the bond energies for RS-H, H₂ and RS-Au (87, 104 and 40 kcal mol⁻¹, respectively), then the net energy for adsorption is estimated at -5 kcal mol⁻¹ (exothermic). This reaction probably occurs by the following general schematic for the formation of thiolate on Au proposed by Ulman *et al.* [10].



Or



Hydrocarbon Chain

It is only after the molecules are chemisorbed onto the surface that the arrangement of ordered and closely packed assemblies begins. The rates of formation of these packed assemblies depend on many factors, some of which include:

1. The presence of bulky substituents.
2. Influence of gauche bonds
3. The length of the alkyl chain.

The main forces involved for the case of simple alkyl chains (C_nH_{2n+1}) is that of Van der Waals attractions, and the energy associated with these van der Waals interactions is $\approx < 10$ kcal/mol.

If a bulky polar group is substituted into the alkyl chain, long-range electrostatic interactions are energetically more important than that of the van der Waals forces.

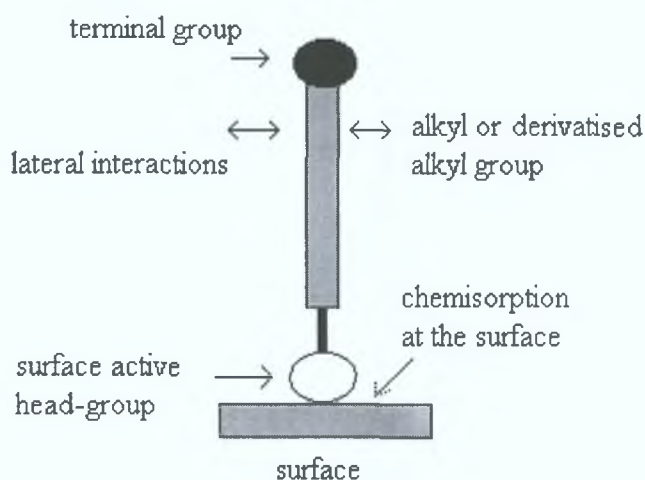


Figure 7.2 A schematic view of the forces in a self-assembled monolayer.

This second self-assembly step, for the n-alkanethiol adsorption on Au(111) maximises lateral intermolecular van der Waals attractions, which are long-range in comparison to the chemisorbed bond, between low polarity alkyl chain segments of the molecule. A strong chemisorption interaction with the substrate is maintained, resulting in a Au-S-C bond angle of $\sim 120^\circ$ [11]. The energy associated with this process depends on the chain length, and studies have shown that the adsorption kinetics increase with an increase in alkyl chain length because of the increase in van der Waals interactions ~ 0.8 kcal mol $^{-1}$ for each CH_2 group. The sulfur-sulfur atom spacing is 4.99 Å, this is greater than

the distance of closest approach of the alkyl chains which is 4.24 Å, so the fully extended chains tilt $\sim 30^\circ$ with respect to the surface normal towards the nearest neighbour in order to maximise their van der Waals interactions [11,12].

Terminal functionality

The third molecular part associated with SAMs is their chain terminal functional groups, which in the case of a simple alkyl chain is the methyl group (CH_3). At room temperature these surface groups are known to be thermally disordered, which was demonstrated by temperature dependant infrared studies performed by Nuzzo *et al.* for the case of methyl-terminated monolayers [13], and by Evans *et al.* from surface reorganization studies carried out on hydroxyl-terminated monolayers [14]. There is a broad range of terminal functional groups and also a wide range of substrates which can be used in the application of SAMs, thus making SAMs a interesting area of study from the point of view of surface science and interfacial reactions.

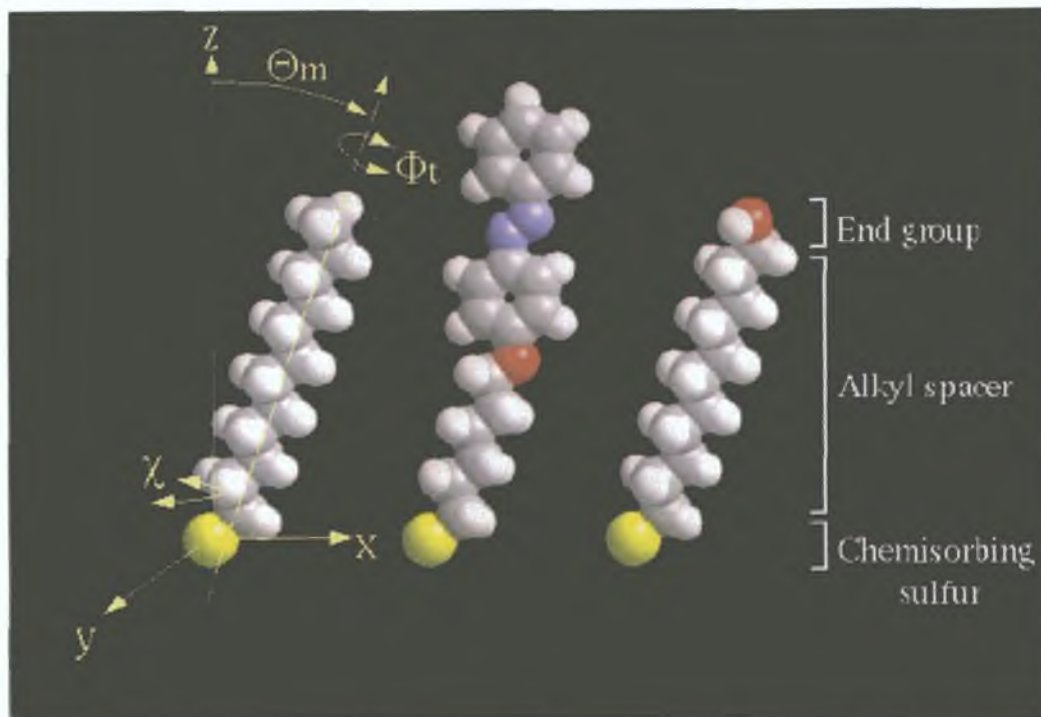


Figure 7.3: Characteristic of an alkane-thiol molecule, Θ_m denotes tilt angle of the alkyl chain, Φ_t denotes the twist angle.

Figure 7.3 highlights the characteristics of an alkane-thiol molecule. Several systems have been used to form SAMs. As the defining feature is the “pair” of the chemisorbing headgroup of the molecule and the substrate, this “chemisorption pair” is used to classify the specific system. The most popular SAM system is that of thiols on Au(111). Some frequently used compounds can be seen below Figure 7.4

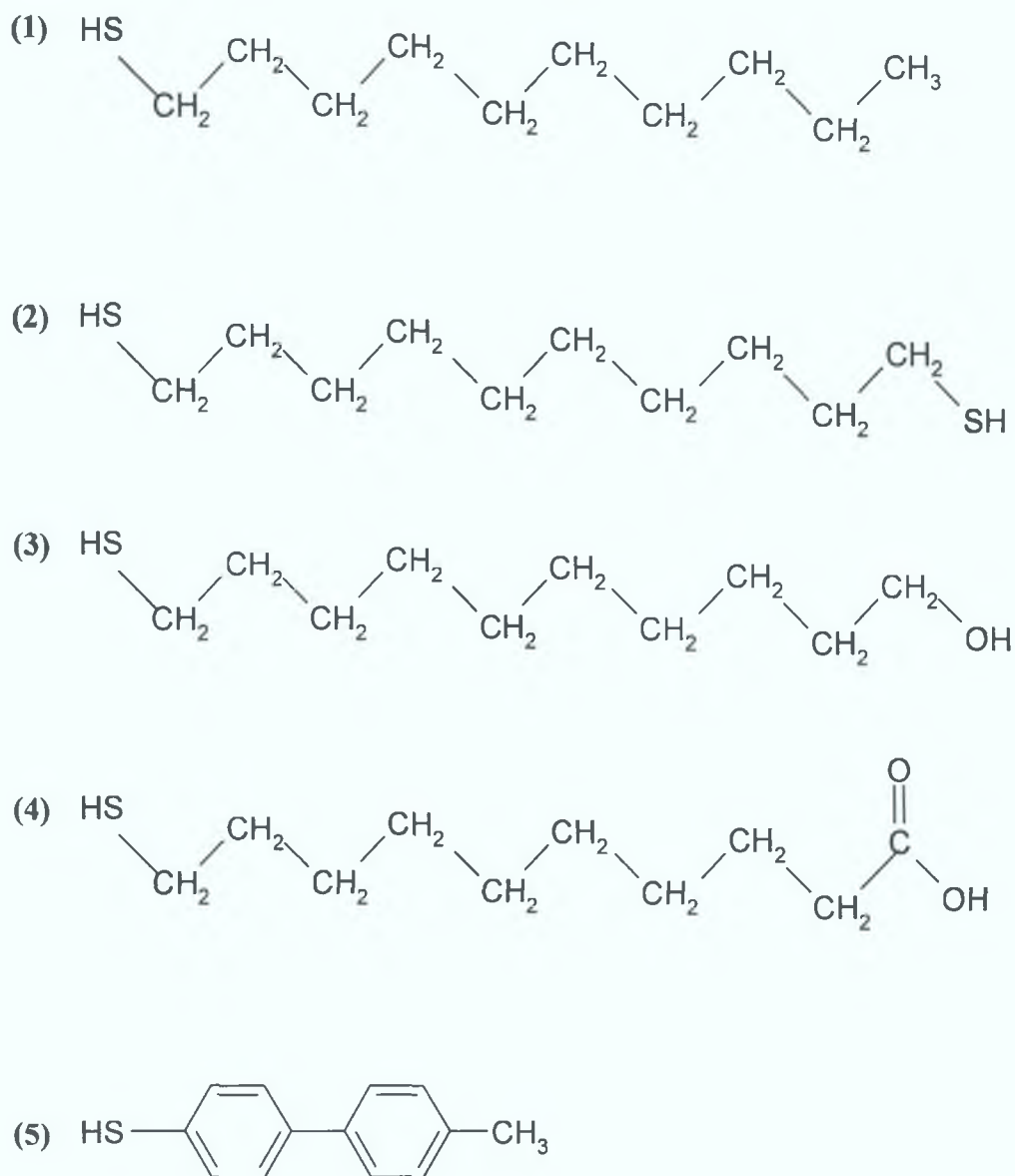


Figure 7.4: (1) *n*-alkanethiol: $\text{HS}-(\text{CH}_2)_{n-1}-\text{CH}_3$; (2) α , ω -alkanedithiol: $\text{HS}-(\text{CH}_2)_n-\text{SH}$; (3) ω -mercaptoalkanol: $\text{HS}-(\text{CH}_2)_n-\text{OH}$; (4) ω -mercaptoalkane carboxylic acid: $\text{HS}-(\text{CH}_2)_{n-1}-\text{COOH}$; (5) 4-methyl-4'-mercaptobiphenyl (MMB): $\text{HS}-(\text{C}_6\text{H}_4)_2-\text{CH}_3$.

7.3 SAMs on Au(111)

Besides the chemical nature of the substrate, the crystalline state and the quality of the surface need to be considered. Therefore, single crystal metal surfaces are most frequently used as they constitute well-defined surfaces, and they offer the possibility to freely choose the crystallographic orientation. As previously stated, one of the most widely investigated, and best-understood systems for SAMs, is that of alkanethiols onto a Au(111) surface and the formation of densely packed monolayer films [15]. Au was taken as being the metal of choice as it is known that sulfur compounds coordinate strongly to gold. Even though no stable oxides of gold are known [16], studies performed by King *et al.* showed that oxidation of gold by UV and ozone at 25°C give a 17 ± 4 Å thick Au₂O₃ layer which was stable to extended exposure to UHV and water and ethanol rinses [17]. Gold can also be handled in ambient conditions, where its surface can be cleaned, removing chemically and physically adsorbed contaminants. Additionally, the Au(111) surface is the lowest energy surface and is thus preferred in the growth of thin Au films.

It is known that alkanethiols adsorb onto Au(111) with the thiol head towards the surface forming a $(\sqrt{3} \times \sqrt{3})R30^\circ$ superlattice/overlayer structure (sulfur atoms in adsorbates forming an epitaxial $(\sqrt{3} \times \sqrt{3})R30^\circ$ overlayer on a predominately Au(111) lattice) [18]. This $(\sqrt{3} \times \sqrt{3})R30^\circ$ structure corresponds to the molecule-molecule spacing of ~ 5 Å and an area per molecule of 21.6 Å², and assuming that the molecules are densely packed, the hydrocarbon chain is tilted away from the normal by about $\theta_t \sim 34^\circ$ [19]. The dependence of the chain length on the structure, was investigated by Fenter *et al.* and they concluded that the longer the alkanethiol chain length the more important the intermolecular interactions become as opposed to the interface interaction which influences the adsorption structure [20].

Changing the end-group can have an impact on the tilt angle and on possible superstructures due to steric constraints and the endgroup-endgroup interactions. One of the smallest changes possible for an alkanethiol is to include

an olefin-terminating group, i.e. C=C, and it was found that the structure of these alkanethiols with an olefin-terminating group show the same unit cell as the corresponding *n*-alkanethiols, and similar tilt angles of the molecular backbone, i.e. a $c(4 \times 2)$ superlattice of the $(\sqrt{3} \times \sqrt{3}) R30^\circ$ structure

In the case of OH-terminating thiols, HS- $(\text{CH}_2)_{16}\text{-OH}$, the tilt structure was determined to be $\theta_t \sim 39^\circ$, with a smaller tilt for HS- $(\text{CH}_2)_{22}\text{-OH}$. For COOH-terminating groups the average tilt is similar as those found for the OH-terminated system, although it was reported by Himmel *et al* [21] that alkylthiols with COOH-termination are largely disordered and exhibit a high density of gauche defects. It was speculated that the reason for this is the stronger interaction of the COOH end groups via hydrogen bonds already in the early stages of growth, which might then prohibit the formation of well-ordered films.

7.4 SAMs on Copper

The study of *n*-alkanethiol as SAMs on copper has only been established as a major area of research in the last 10 years. Copper being chosen because of its low resistivity and high electromigration resistance. Copper has many applications in the advancing fields of corrosion, catalysis and polymers. In the chemical and microelectronics industry copper also plays an important role due to its low cost and high thermal and electrical conductivity. One of the major disadvantages associated with copper is its ability to corrode readily, especially in aqueous environments that contain oxidants.

Although copper surfaces differ in structural detail to that of Au(111), it has been reported that the structure of SAMs on copper are similar qualitatively to those on gold and that alkanethiols adsorb from solution onto copper surfaces to form densely packed SAMs [22].

In 1991 Laibinis *et al.* [23] carried out a study, into the preparation and characterization of alkanethiols ($\text{HS}(\text{CH}_2)_n\text{R}$) on the surfaces of silver and copper. This investigation was done in order to establish whether there was any comparison to be made between the monolayers formed by chemisorption of alkanethiols on Au and those formed on Cu and Ag. The results of this study indicated that the structures of these alkanethiolate monolayers on the three metals were clearly different. *N*-alkanethiols do assemble onto the surface of copper, silver and gold on which they form densely packed oriented monolayer films. For the copper and silver, the films formed were different in structural detail then those formed on gold. With the main structural differences being described as follows:

1. For Cu substrate the hydrocarbon chain is more perpendicularly orientated with respect to the surface than that of the Au substrate, i.e. cant angles relative to the surface normal are 13° for copper and 28° for gold.
2. The monolayers display a lower number of gauche conformations at room temperature.
3. The orientation of the carbon-sulfur bond in relation to the surface plane varies with chain length.
4. Monolayers formed on copper exhibited greater hysteresis then those found on Au or Ag.

Another point of interest taken from this study was that the formations of reproducible films onto copper were extremely sensitive to the experimental techniques used in their preparation and to the history of the copper samples. The solubility of the adsorbate in the solvent and the length of time the substrate is exposed to the alkanethiol solution, as well as the length of exposure of the unfunctionalized surface to the atmosphere, were found to be very important parameters when preparing monolayers on copper. These variables are generally unimportant when it comes to the reproducibility of the assembly of alkanethiols on gold. It was also found that prolonged exposure of the copper substrate to the alkanethiol solutions resulted in a reaction with the copper surface to the

alkanethiol that formed an interphase of metal sulphide on which an organized, oriented monolayer is supported.

So copper proved to be more reactive to alkanethiols and more sensitive to the properties of the alkanethiol than gold. The reaction of the shorter chained alkanethiols ($3 \geq n$) with copper resulted in a surface that appeared discoloured and visibly pitted.

Following on from this, in 1992 Laibinis and Whitesides completed a study of ω -terminated alkanethiolate monolayers on the surfaces of copper, silver and gold. This study was devised in order to discover if these three metals with monolayer films attached to their surfaces have similar wettabilities [24]. The conclusion drawn by Laibinis *et al.* was as follows: the wetting behaviour of the monolayers prepared on Ag and Cu were similar to that on Au, with the hysteresis in the contact angles of water greater on copper surfaces ($\Delta \cos \theta = \cos \theta_r - \cos \theta_a$). This increase was determined to be due to roughening of the copper (oxide) – air (or monolayer) interface which occurred during oxidation and following adsorption of the thiol.

The difference in the wettability of hydroxyl-terminated monolayers on the three metals was negligible. This was in contrast to results reported by Ulman and his team [25] who found that monolayers formed by adsorption of $\text{HS}(\text{CH}_2)_{11}\text{OH}$ on gold and silver had different wettabilities, $\sim 20^\circ$ and $\sim 30^\circ$ respectively. Laibinis *et al.* went on to show that the three metals could accommodate a variety of tail groups: organic surfaces of a wide range of wettabilities $\theta_a^{\text{H}_2\text{O}}$ of $< 15^\circ$ to $\sim 115^\circ$.

Monolayers prepared on each of these metals (Au, Cu and Ag) from mixtures of alkanethiols of similar chain lengths containing different tail groups show similar relations between the composition of the monolayers and the compositions of the solutions from which they are formed and show similar wettabilities. Measurements also taken showed that, the thickness of the alkanethiol monolayer adsorbed onto copper was higher than the theoretical length of the adsorbed molecule.

7.5 SAMs protect Copper against Corrosion/ Oxidation

The purpose of an investigation carried out by Laibinis and Whitesides in 1992, was to establish whether SAMs of *n*-alkanethiolates on copper could protect the metal against oxidation by air [26]. Throughout their study XPS analysis was used to monitor the changes in the SAM, and then in the copper after the SAM was exposed to atmospheric oxygen. XPS was used to provide information into the elemental composition of the surface and, also XPS has the ability to differentiate between the oxidation states of many elements [27].

The results of the study illustrated, that samples which were exposed to the atmosphere for the least amount of time displayed a single peak in the S(2p) spectral region, and this peak was identified as a thiolate ($162.4 \text{ eV} \pm 0.3 \text{ eV}$) [28]. After increased exposure to the atmosphere this peak broadened and could no longer fit within the constraints of a spin-orbit doublet ($\approx 1.2 \text{ eV}$) for S(2p) peaks. The reason for this was that after increased exposure to atmospheric oxygen, the adsorbed thiolates oxidise to a sulfonate. So even though thiolates and sulfonates coexist, the oxidation of these samples does not occur uniformly, but a relationship does exist between the copper and the thiolates. The oxidation process was described as a roughening of the copper surface and a transformation of the adsorbed thiolates to sulfonates. These sulfonates and the Cu(II) species being displaced when the sample is exposed to an alkanethiol.

The overall conclusions based on these results were that SAMs produced from the adsorption of *n*-alkanethiols onto copper protects the metal surface against oxidation [26]. The kinetics of oxidation is compatible with a model in which the SAM provides a barrier to the transport of O₂ to the copper surface. Another significant point presented in this study was that a thin hydrocarbon layer can provide protection against the oxidation of the metal surface, and the rate of oxidation is decreased with an increase in chain-length of the *n*-alkanethiol. This is based on the presumption that the SAM is packed densely enough so that a low-permeability barrier is established which hinders the access of O₂ to the metal.

A thiol covered Cu (100) oriented surface was used which gave new insight into the surface structure and the corrosion behaviour of copper [28]. Scherer *et al.* presented an in-situ STM (scanning tunnelling microscopy) study where octanethiol (OT) and hexadecanethiol (HDT) monolayers were prepared by spontaneous adsorption from ethanolic solutions onto a Cu (100) single crystal. Extended exposure of these surfaces to an HCl electrolyte at potentials in the double layer range caused an increase in surface roughness, which was attributed to an exchange of Cu or Cu thiolates with the electrolyte.

Copper corrosion starts in the $-0.12 \rightarrow -0.10$ V range, with the formation of many wide and deep pits, i.e. 50-100 Å wide and 10-20 Å deep. As the potential increased an increase in surface roughness and a loss of resolution in the STM images were observed which indicated an increasing by disordered SAM. After longer time periods the pits grew to a depth of 100 Å or more. Copper dissolution primarily occurred within this pits, where the surface appeared to be free of adsorbed thiol. This corrosion mechanism involved the nucleation and growth of deep holes was very different to the corrosion behaviour of bare Cu (100), with dissolution occurring in a strict layer-by-layer mode. It appears that the SAM on the surrounding surface significantly inhibited the nucleation of corrosion sites as well as the growth of existing defects.

Yamamoto *et al.* also investigated how self-assembled layers of alkanethiols on copper protected the underlying copper against corrosion [29]. Here it was found that the presence of the oxide layer on the copper surface affected the reproducibility of the monolayer formation. The copper was galvanostatically reduced in 1N HClO₄ under a nitrogen atmosphere, with the cathodic current being 1 mAcm⁻² for a period of 5 minutes, before monolayers were formed on the surfaces. These surfaces were then characterised using XPS (x-ray photoelectron spectroscopy), SERS (surface-enhanced Raman spectroscopy), contact angle measurements and impedance measurements.

From impedance measurements the interfacial capacitance, C , was obtained. The copper surface that was not electrochemically reduced and did not

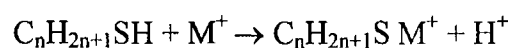
have a monolayer deposited has a capacitance value of $85.5 \mu\text{F cm}^{-2}$. The copper that was not reduced but did have a monolayer of 1-octadecanethiol on its surface saw a decrease in the capacitance value to $7.18 \mu\text{F cm}^{-2}$, indicating that the presence of the oxide layer hinders the adsorption of the alkanethiol onto the copper surface. The copper was therefore galvanostatically reduced prior to monolayer deposition.

The XPS spectra obtained by Yamamoto *et al* [29] showed that the intensity of the O (1s) peak on copper covered with a monolayer remained unchanged, after exposure to the atmosphere. In addition, no copper oxide peak appeared in the Cu (2p) spectra, indicating the absence of an oxide layer on this surface. While a much larger peak was observed in the spectra for the O (1s) of the uncovered copper similarly exposed to the atmosphere, suggesting that the adsorbed monolayer has the ability to protect the copper against oxidation with air.

During this study it was also established that the alkanethiol chemisorbs onto the copper surface by the formation of a surface thiolate. The formation of self-assembled-monolayers by the immersion of copper in the ethanol solutions of the thiols was completed within thirty minutes. The binding energy of the S (2p_{3/2}) peak taken from the spectra recorded by Yamamoto *et al* is 162.3 eV, which is in good agreement with the literature [29]. It was concluded that the alkanethiol chemisorbs on the copper surface by the formation of a surface thiolate, and a schematic is outlined below.



Or



SERS spectra results confirmed that the SAMs of these alkanethiols on the copper substrate have a packing structure similar to that of a crystalline structure.

and that for the densely packed monolayer the trans conformation of the hydrocarbon chain was preferable to the gauche conformation.

Polarisation curves, i.e. Tafel plots, recorded by Yamamoto *et al.* [29] indicated that the alkanethiolate layers on the copper did not demonstrate the ability to protect the copper substrate against corrosion. This was the view taken when it was noted that the cathodic reaction was not sufficiently suppressed, behaviour attributed to rapid permeation of oxygen molecules through the films. Also suppression of the anodic process was deemed to be difficult, as the interfacial capacitances for the monolayer-covered electrodes increased markedly up to the level of the bare electrodes.

Continuing on from this, a monolayer of 11-mercapto-1-undecanol was adsorbed onto a copper surface and treated with a 1-hexadecane solution of 5×10^{-2} M octyltrichlorosilane ($\text{C}_8\text{H}_{17}\text{SiCl}_3$) for 30 minutes. The reason for this was to enhance the protection ability of the film against corrosion. The value of the contact angle measurement obtained for this particular type of monolayer was 90° higher than that of the unmodified monolayer, indicating an effective modification for the water-repellant behaviour. The interfacial capacitance for this siloxane-modified monolayer, and the Faradaic conductance were obtained, and found to be smaller than those of the 1-octadecanethiolate monolayer. This shows the formation of a more protective film against corrosion as opposed to the straight chain thiolate monolayer adsorbed on copper. It is thought that the ability of a monolayer to protect the substrate against corrosion not only depends on the water-repellent property but also on the ability of the monolayer to block the diffusion process of oxygen within the film, and it was thought that the cross-linked structure in the siloxane-modified layer enhanced this ability [29].

In 1994 Itoh *et al.* carried out a study that involved [30] chemically modifying a self-assembled monolayer of 11-mercapto-1-undecanol chemisorbed onto a copper surface, by reacting the monolayer with alkyltrichlorosilane and water to form alkylsiloxane polymer in the film. This study was carried out in order to see if these modified monolayers (or bilayers),

could offer better protection of the underlying copper against corrosion in contrast to just a monolayer. The reaction scheme is outlined below.



The monolayer of the thiol then reacts with octyltrichlorosilane as follows



The product of this reaction was then hydrolysed with water to form siloxane linkages:



From this research it was construed, that this cross-linked monolayer film provides increased protection against the corrosion of copper in aerated 0.5M Na_2SO_4 , as a thicker and more densely packed barrier layer is present to prohibit diffusion of the O_2 . XPS analysis was used to characterise the surface while, polarisation curves and impedance data also used to determine the protective ability of the layer. The increase in protection was attributed to the enhanced stability of the siloxane-linked bilayer under the conditions of measurement [30]. It was established that 93% of the protection efficiency against copper corrosion was obtained from the alkylsiloxane modified monolayer with the optimum carbon number of the alkyl group being in the range of 4 to 8. The protection efficiency, P, is calculated as follows:

$$P (\%) = 100 (1 - i_{\text{corr}}/i_{\text{corr}}^0)$$

where i_{corr}^0 and i_{corr} represent the corrosion current densities for the bare copper electrode and for the copper covered with a monolayer, respectively, which is obtained by extrapolation of the Tafel plot.

XPS analysis performed in 1995 by Itoh *et al.* [31] was used to compare the effectiveness of the tetrachlorosilane (TCS) or 1,2-bis-(trichlorosilane) ethane (BTCSE) modified MUO self-assembled layer, with a SAMs formed from just HS(CH₂)₁₁OH. The outcome of this investigation was as follows, the protection efficiency of the two-dimensional monolayer adsorbed on a copper substrate increased against copper corrosion in aerated 0.5 M Na₂SO₄. This was credited to the fact that the chemical modification of the self-assembled layer by TCS or BTCSE leads to planar polymers, therefore diminishing the hydroxyl groups remaining in the layer. From the polarisation results it was seen that that these planar polymer layers suppressed the anodic process by the formation of a strongly chemisorbed and tightly networked film on the surface, and the cathodic process of copper corrosion was suppressed by blocking the diffusion of oxygen through the layers.

In 1996 a study performed by Jennings *et al.* involved an investigation into self-assembled monolayers of alkanethiols on copper [32], to determine whether these monolayers provide corrosion resistance in aqueous environments. From this study it was concluded that SAMs derived from C₂₂H₄₅SH, were among the thickest and most well-defined monolayers, and that these thicker SAMs on the copper substrate show superior ability to impede corrosion over that of the shorter chained alkanethiols. So it was assumed then that longer chained adsorbates would provide even better protection, but their synthesis and insolubility in many solvents made this difficult to realise. So instead, in order to produce thicker hydrocarbon based films on the copper surface, bilayer films were created on the copper substrate using mercaptoalcohol HS(CH₂)₁₁OH or HS(CH₂)₂₂OH as the first layer, and an alkyltrichlorosilane CH₃(CH₂)_nSiCl₃, n = 17, as the second layer. The thickness of the SAMs was that of 3 nm, with the thickness of the bilayer being that of 5 nm. These samples were exposed to 1 atm of O₂ at 100% relative humidity.

The wetting properties (hexadecane) [32] of the SAM before being exposed to the oxidising conditions proved to be superior to that of the bilayer,

indicating a more well-defined structure for the SAM. Upon exposure, these wetting properties decreased, indicating that there was some level of surface reconstruction during the initial stages of oxidation. In contrast to the above result, the wetting properties of the bilayer remained uniform throughout the experiment under the above conditions. However, the ability of the bilayer to inhibit corrosion of the underlying copper was poorer in performance to that of the SAM derived from $\text{HS}(\text{CH}_2)_{22}\text{OH}$.

Aramaki *et al.* have also studied the effects of SAMs and bilayers on the inhibition of copper corrosion, and, the above results from Jennings *et al.* appear to be compatible with the results recorded by Aramaki *et al.* [29-31].

In 1997 Aramaki *et al.* published a study on the chemical modification of an alkanethiol self-assembled layer to prevent corrosion of copper [33]. In this study a two-dimensional polymer monolayer, which was ultrathin, highly water repellent and closely packed was prepared by modifying a self-assembled monolayer of 11-mercapto-1-undecanol (MUO) that was adsorbed on copper with 1,2-bis(trichlorosilyl)ethane (BTCSE) followed by octadecyltrichlorosilane (C_{18}TCS) or octyltrichlorosilane (C_8TCS). This doubly modified layer proved to be highly protective against the atmospheric corrosion, and significantly water repellent. Analysis methods used in the above study consisted of XPS and AES (Auger electron spectroscopy), contact angle measurements and electrochemical measurements, i.e. polarisation curves and impedance measurements. From the polarisation curves obtained it was recognised that these modified layers contributed to the suppression of both the cathodic and anodic processes of copper corrosion, in comparison to a bare copper electrode.

The modified layer was seen to act as a barrier to oxygen diffusion, as reduction of molecular oxygen is known to occur in the potential region of the cathodic process. Based on the assumption that a closely packed and tightly interconnected monolayer was formed on the surface, one would think that the thicker layer, i.e. (C_{18}TCS), would be more effective in the inhibition of the cathodic process, but this was deemed not to be the case and the BTCSE and

C₁₈TCS-modified MUO monolayer inhibited this cathodic process to a lesser extent than the BTCSE and C₈TCS-modified MUO monolayer.

The protection efficiency of the modified layers were also calculated from extrapolation of the Tafel plots, and the values of 94.8 and 55.6% were obtained for the electrode covered with a BTCSE and C₈TCS-modified MUO monolayer and the electrode covered with a BTCSE and C₁₈TCS-modified MUO monolayer, respectively. The protection efficiency (P) of the BTCSE and C₁₈TCS-modified MUO monolayer, was improved by increasing the immersion time, as suppression of the anodic process seemed to increase with immersion time. Therefore, the P of the monolayer in the dilute C₁₈TCS solution increased from 98.9 to 99.3% for 24 hrs and 100 hrs respectively. The overall conclusion being that these prepared layers were considered to be partly disordered, tightly interconnected, closely packed and water-repellent, and also offer significant protection against atmospheric corrosion of copper.

Aramaki *et al.* [34] then studied the effects that surface roughness has on the water repellence of the surface covered with these doubly modified layers, and on the P value of an unmodified or modified alkanethiol monolayer. The treatment of the copper surfaces prior to modification was that of mechanical abrasion and electropolishing. An AFM (atomic force microscopy) study of these two polished surfaces concluded, that for the mechanically polished surface the maximum height of the hillocks was 11.6 nm and for the electrically polished surface the max height was 2.6 nm. As the wettability of the covered surface is related to the roughness of the surface, and the structure of the outermost part of the adsorbed molecule, contact angle θ measurement were undertaken. For the mechanically abraded copper surface covered with the BTCSE and C₁₈TCS-modified MUO monolayer the a contact angle, θ , value of 131° was reported, and for the electrochemically polished copper coated with the same film the θ value was that of $112 \pm 3^\circ$.

The difference between these results was credited to the surface roughness of the mechanically polished surface determined by AFM. Although contact

angle values of $112 \pm 3^\circ$ is thought to be sufficient to provide protection against atmospheric corrosion of a modified copper surface.

It was also reported by Hockett *et al.* [35] following a STM (scanning tunnelling microscopy) and voltammetry study of a polycrystalline gold surface which, had being modified with an alkanethiol self-assembled monolayer, that the microscopic roughness is very important to the quality of the monolayers whereas the macroscopic roughness appears to be less important.

Staying with this topic, the protection of copper against corrosion, Feng *et al.* [36] modified a copper surface, which had being pre-treated with different surface treatment methods,

1. HNO_3 etching
2. HCl etching
3. Cathodic reduction
4. Polishing.

The objective of this study was to improve the quality of the alkanethiol monolayer. After these different surface treatments were performed, a monolayer of 1-dodecanthiol (DT) was formed on the copper surface after 30 mins immersion in the thiol solution. Impedance measurements were used to analyse the effects of these different surface treatments on monolayer formation.

From this data (derived from the Nyquist plot) it was concluded that HNO_3 etching is the most effective method of surface pre-treatment for the formation of DT-monolayer on copper. The polarisation resistance after 30 min DT-treatment following HNO_3 etching is larger than that of the copper electrode after 24 hour treatment with the inhibitor benzotriazole (BTA).

The effect of exposure to air on the formation of DT-monolayers was investigated in this study [36]. Copper electrodes were first rinsed with ethanol and then exposed to the atmosphere for 1, 5 and 30 min before immersion in 1 mM DT solution. It was revealed, that the exposure of bare copper to air reduces the adsorption of DT molecules onto the copper surface, with longer exposure

time, the adsorption capabilities decrease, therefore it is important to exclude oxygen in order to form a high quality monolayer on copper.

The copper surface oxidises rapidly during sample preparation and as copper oxides are known to be detrimental to monolayer formation, the copper sample is dipped rapidly into the DT solution after the rinsing step, which occurs after etching. An oxide free surface is not the only factor that influences the formation of a high quality monolayer. In these studies it was noted that after HCl etching the surface was oxide free, but the Cl in the HCl solution could adsorb on the copper surface during etching which can then also reduce the adsorption ability of the surface.

But when the copper surface was etched in HNO_3 , this nitric acid solution removed the top layer of copper atoms, providing a fresh and active surface, which strongly favours the chemisorption of alkanethiols.

Effects of immersion time and dodecanethiol concentration on monolayer formation were investigated [36]. These parameters were monitored using polarisation resistance (R_p) and capacitance (C) measurements. After 30 min immersion the R_p increased from 4.5 ± 0.2 to $55 \pm 10 \text{ k}\Omega \text{ cm}^2$ during the first 20 min of immersion and remained constant after that. While the values obtained for the capacitance were significantly reduced after 1 min DT immersion from 40 ± 5 to $1.7 \pm 0.3 \text{ }\mu\text{F/cm}^2$ but stabilised at $1.3 \pm 0.3 \text{ }\mu\text{F/cm}^2$ after 20 min immersion. Therefore, it was concluded that the formation of a monolayer onto fresh copper is quiet rapid and complete within 30 min. These results were in agreement with results reported by Yamamoto *et al.* [29] from polarisation resistance and capacitance measurements. The effect of DT concentration was monitored also, and it was suggested that a minimum concentration of 10^{-4} M DT is needed to form a protective monolayer on the copper surface.

Polarisation curves of dodecanethiol, benzotriazole (BTA) and mercapto-benzothiazole (MBT) monolayer-covered copper were studied by Feng *et al.* [36] and from these results, the electrodes treated with BTA and MBT, for 30

min, inhibited slightly the anodic and cathodic currents. Whereas, for the DT-covered electrode, both currents were reduced more significantly than electrodes treated with BTA and MBT, with the cathodic current more markedly reduced than the anodic current.

Also, the corrosion potential for this DT covered monolayer was more negative than for the other inhibitors. The above result indicating that the alkanethiol monolayer has a significant effect of impeding the reduction of dissolved oxygen and inhibiting the anodic dissolution of copper, which was attributed to the hydrophobicity of the alkane moiety in the densely packed monolayer.

Corrosion current densities were determined from polarisation curves, and protection efficiencies calculated, were 67, 86 and 96% respectively for the BTA, MBT and DT monolayer covered samples, indicating that the DT monolayer offers more protection than the films formed by the other inhibitors. Cyclic voltammograms obtained also showed that the DT covered monolayer inhibits the oxidation of the copper substrate.

A protective dodecanethiol self-assembled monolayer can be formed on a copper surface within 30 min immersion, this result was in line with the results of Aramaki *et al.* [29] and the concentration of the alkanethiol can be as low as 10^{-2} to 10^{-4} M. From this study, it was seen that the corrosion resistance of the monolayer depends on the surface treatment prior to monolayer deposition, and that HNO_3 etching provided the best results. Also alkanethiol monolayers have potential application as corrosion inhibitors in aqueous and air environments.

In 1998 Laibinis *et al.* reported the results of a study in which he and his team of co-workers studied the effects of the chain length on the protection of copper by *n*-alkanethiols [38]. Laibinis *et al.* altered the chain length of the adsorbate, *n*-alkanethiols, $n = 8$ to 29. This in turn brought about Å-level changes of 10 to 40 Å in the film thickness, the effect of these changes on the barrier properties and the structural stability of the SAMs were studied.

XPS was used to measure the attenuation of photoelectrons from the underlying copper substrate, hence the differences in the relative thickness of the *n*-alkanethiols films was examined. The intensity of the underlying copper was found to decrease exponentially with increasing chain length, indicating a consistent and regular increase in the thickness of the SAM. 1.24 Å was the distance calculated per CH₂ group in a trans-extended hydrocarbon chain, therefore the thickness of the hydrocarbon within these films could be varied from 10 to 36 Å, using adsorbates with various chain lengths, i.e. 8 to 29. The thickness of the film placed on a copper substrate could then be controlled at angstrom level depending on the adsorbate selected.

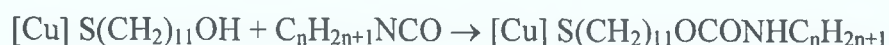
For initially formed SAMs on copper, the barrier properties depend on the chain length of the adsorbate that forms the monolayer. SAMs formed from C_{*n*}SH where *n* ≥ 16, provide coating resistance that is 30 times larger the SAMs where *n* ≤ 12. The densely packed, crystalline hydrocarbon layer, of the thicker films, separates the copper substrate from the external environment, providing superior barrier properties against diffusion of oxygen. A linear increase between coating resistance and film thickness for *n* ≥ 16 indicates that these hydrocarbon chains can act as a series of resistive components. The structural stability of these thicker SAMs was enhanced because of the greater number of intermolecular interactions i.e. van der Waals interactions, which occur within the hydrocarbon chains of these films [38]. When the adsorbates within the SAMs were exposed to 1 atm of O₂ and 100% relative humidity, they become less densely packed but still remain at the metal surface.

The most recent study carried out investigating self-assembled monolayers was that of Aramaki *et al.* when they investigating how a modification of an alkanethiols self-assembled monolayer with alkylisocyanates can act as a protective agent against copper corrosion [39]. This was a continuation of their previous study [29] when Aramakai and his team show that a self-assembled monolayer of 11-mercapto-1-undecanol HS(CH₂)₁₁OH modified with alkyltrichlorosilanes increased the protection of copper against atmospheric corrosion.

In this study [39] a self-assembled monolayer of 11-mercapto-1-undecanol $\text{HS}(\text{CH}_2)_{11}\text{OH}$ was chemisorbed onto an oxide-free copper surface as seen below.



This monolayer was then modified with alkylisocyanate $\text{C}_n\text{H}_{2n+1}\text{NCO}$



This modification was found to be superior to that in which alkylchlorosilane modifiers were used because procedures in the film preparation were simpler and the film was not contaminated with Cl^- . The presence of aggressive Cl^- within the film promoted copper dissolution at the surface. But it was found in the case of the alkylisocyanates that no lateral polymerisation between adjacent molecules adsorbed on the copper occurred within the film, resulting in loosely interconnected structure of the film.

From polarisation curves of the copper electrodes bare and covered with the alkylisocyanates-modified 11-mercapto-1-undecanol monolayer, it was seen that the cathodic process was greatly suppressed by covering the copper with this layer. This indicated that the layer acted as a barrier to diffusion of oxygen and water. Corrosion of copper in a solution mainly comprises anodic dissolution of copper and cathodic oxygen reduction, as



The anodic process was not inhibited in the presence of this layer. When the anodic process dissolved a copper atom at the substrate surface, the adsorbed molecule was desorbed from the surface without difficulty, resulting in the lack of suppression of the anodic process. The protection efficiency, P , of the $\text{C}_{18}\text{H}_{37}\text{NCO}$ -modified 11-mercapto-1-undecanol monolayer for copper corrosion

in aerated 0.5 M Na₂SO₄ was 94.7%, which is a little higher than that of previously studied modified 11-mercapto-1-undecanol monolayer.

The protection efficiency, (P%), is expressed by the following equation:

$$P (\%) = 100(1 - i_{\text{corr}} / i_{\text{corr}}^0)$$

where i_{corr}^0 and i_{corr} refers to the corrosion current densities obtained by Tafel extrapolation in the polarisation curves for the electrodes bare and covered with the film, respectively.

7.6 Effect of Solvents and Concentrations, on the self-assembly process.

The self-assembly of long-chained alkanethiols on copper was studied by Rubinstein *et al.* with their main areas of interest being [40]:

1. The chemical reactivity of the copper to the solvent.
2. Surface pre-treatment – influences concentration of surface oxide and surface morphology

In the self-assembly of alkanethiols on gold these factors are of less importance due to the chemical inertness of the Au.

For a self-assembled monolayer of *n*-octadecanethiol (C₁₈SH), on evaporated Au, to be considered a “high quality” monolayer, it must emerge dry from a 1 mM solution in ethanol [5]. For *freshly evaporated* copper under the same experimental conditions, i.e. identical ethanoic solutions, the adsorbed surfaces emerge wet from the adsorption solution which is in total contrast to that of Au.

The effects that different solvents (ethanol and iso-octane) have on the SA process on freshly evaporated copper have already been thoroughly studied by Laibinis *et al.* [23]. The authors found that the reproducibility in the case of iso-

octane was better than that of the ethanol, due to the fact that the thiols were more soluble in the iso-octane. This solubility solution was questioned in light of studies performed by Bain *et al.* [5] where the effects of different solvents on the wettability and the thickness (ellipsometric measurements) of the monolayer were studied.

Altering the solvents, *n*-hexadecanethiol was self-assembled onto Au and Cu, the results obtained for Cu were not the same as the results obtained for Au. This suggests that there might be a significant interaction between ethanol and the Cu surface in addition to the reaction between the thiol and the Cu. Studies performed in the late 70s and early 80s by Sexton *et al.* [41] showed that the mechanism for the conversion of alcohols to aldehydes involves the formation of stable methoxy and ethoxy intermediates. Cu was used as a catalyst for the conversion of alcohols to aldehydes, and these ethoxy intermediates were chemically bound to Cu and only decomposed above a temperature of 370 K. The differences seen in the monolayers formed on Cu by SA from ethanol as opposed to isooctane are probably due to the interactions of the solvent with the Cu surface and not the solubility of the thiol in the solvent.

Rubinstein *et al.* found that the difference in CA measurements for SA from ethanol onto Au and Cu was due to the increased corrugation of the Cu surface as well as the presence of Cu oxide underneath the adsorbed monolayer [40]. The SA of C₁₈SH in toluene onto freshly evaporated Cu showed low hysteresis in CA measurements, this hysteresis was comparable to that of Au, indicating a well organised and closely packed monolayer. With toluene being used as the solvent, the monolayers obtained were found to be very reproducible, as the contact angle values observed for a 20 mM solution of C₁₈SH in toluene assembled on Cu were well within the precision limits, i.e. $\pm 2^\circ$. The concentration of the amphiphile in the SA solution can play an important role in the quality and on the properties of the monolayer.

Maoz and Sagiv [42] on studying the wetting properties of *n*-alkane monolayers, stated “ adsorption from solutions below a certain critical

concentration, characteristic of each particular system, produces incomplete monolayers with lower density and poor orientation of their molecular constituents". The effect concentration had on the kinetics of C₁₈SH monolayer formation were studied by Bain *et al.* and after 1 week, the monolayers of C₁₈SH in ethanol (low-concentration solutions) formed on Au were imperfect [5].

As the solubility of the thiol in toluene was greater than that of the thiol in ethanol, Rubinstein *et al.* increased the thiol concentration in toluene relative to ethanol, in order to construct organised monomolecular structures [40]. The poor reproducibility of the CAs measured, when C₁₈SH was adsorbed onto Cu from 1 mM solutions in isooctane was recognised as a problem that was due to the thiol concentration, which could have being lower than the critical concentration for that system.

The major conclusions with respect to the self-assembly of alkanethiols on Cu surfaces were that as with Au, Cu surface oxidation induces an increase in surface roughness, which has an influence on the surface assembly process. If the monolayer is adsorbed from toluene this reduces the surface roughness as opposed to alkanethiols adsorbed from ethanol. Ethanol as a solvent may cause the formation of low-quality monolayers because of the chemical interactions of ethanol with copper. Much better results are obtained when toluene is used, but higher thiol concentrations need to be used because of the higher solubility of alkanethiols in toluene. The presence of a thin oxide film on the Cu surface does not prevent the formation of high-quality C₁₈SH monolayers, providing that certain conditions are met, particularly those of solvent and thiol concentration. The effect of chemical interactions with the solvent is more important than the presence of a thin oxide layer, since high-quality monolayers showing superior contact angles are obtained reproducibly for adsorption from concentrated alkanethiols solutions in toluene onto Cu surfaces covered with thin Cu₂O films.

Also, alkanethiols monolayers of unusual quality can be prepared on evaporated Cu pre-treated by sputter annealing in UHV, which exhibits a reduction in both the amount of oxide and the surface corrugation. These

monolayers show a very high degree of crystallinity and orientation even when the self-assembly process is carried out after short exposure to air.

7.7 Multi-component and mixed SAMs

One of the ideas that is creating interest in multi-component SAMs is the ability to tailor the surface energy and the wetting properties by mixing the appropriate compounds such as a hydrophobic CH_3 -terminated and hydrophilic OH-terminating molecules. The essential question asked about these systems is whether the different species show or exhibit phase separation.

Several groups have investigated this problem, using different systems that include different end groups and chain lengths. Whitesides *et al.* have studied various systems of mixed SAMs and found indications that the phase separates to some extent, but not completely [43]. While other studies conclude random molecular mixing occurs rather than phase separation, and IR data taken by Bertilsson *et al.* indicate that there are no traces of intermolecular interactions (H-bonding) between neighbouring OH groups mixed with CH_3 -terminating molecules.

7.8 Adsorption on SAMs

As already stated in the introduction, a very attractive feature of SAMs is the possibility of using them to tailor, by virtue of different end-groups, the surface energies and therefore the adsorption process. 'Simple adsorbates' like alkanes or H_2O are related to wetting. H_2O , which probes the polar characteristics of a surface, has a high contact angle on CH_3 -terminated SAMs with $\theta_a \approx 110^\circ$. Whereas on the other hand H_2O tends to wet OH-terminating SAMs i.e. $\theta_a \approx 10^\circ$ or less. Hexadecane can also be used as a wetting agent also, with the contact angle on CH_3 -terminated SAMs is $\sim 45^\circ$, and this value differs for alkanes with different chain lengths. OH-terminated SAMs are wet by hexadecane and $\theta_a \approx 10^\circ$.

7.9 Discussion

Although the Cu surfaces differ in structural details from the Au(111) surface, it can be concluded that the structures of SAMs on copper are qualitatively similar to those on gold. Studies of the structure of alkanethiols on Au(111) with molecular-level resolution exhibited $(\sqrt{3} \times \sqrt{3}) R30^\circ$ structure relative to the underlying Au(111) substrate, and that the hydrocarbon chain is tilted away from the normal by $\sim 28^\circ$. The orientation of an average single chain, on a Au(111) substrate, with the structure consisting of an all-trans zig-zag chain is canted by $\sim 32^\circ$ from the surface normal.

For alkanethiols on Cu substrate, however, the hydrocarbon chain is more perpendicularly orientated with respect to the surface, than that of the Au substrate and the cant angles relative to the surface normal are 13° . For monolayers on copper the orientation of the carbon-sulfur bond in relation to the surface plane varies with chain length and the monolayers formed on copper exhibited greater hysteresis than those found on Au or Ag.

It has been proven that monolayers protect copper against corrosion and that modifying monolayers with other compounds offers increased protection against copper corrosion.

The effect of the oxidised layer on copper surfaces has been investigated and the monolayers on the oxidised copper surface have a similar structure to those on the clean copper surfaces, except that the former surfaces have more oxygen and Cu(I) present than the latter. This difference may result in a decrease in desorption temperature of the monolayer. It is also possible that the bond strength, RS-Cu, of the oxidised copper surface is weaker than that of the clean surface. The stability of the thiolate groups on copper is related to the electron density of the thiolate sulfur, i.e. the more electron density on the thiolate sulfur, the weaker the bond strength of the RS-Cu. Since the electron density of the thiolate sulfur on the cuprous surface is probably greater than that on the

metallic copper surface, the monolayers on the oxidised copper are less stable than those on metallic copper

7.10 Conclusions

The structure and formation of alkanethiols on copper has been studied using a multiple range of techniques from XPS, SPM, electrochemistry to FT-IR. Alkanethiols are known to chemisorb onto a copper surface, forming a densely packed structure. The formation of the monolayer depends greatly on the methods of surface treatment used.

The manipulation of these alkanethiols, by further modification or by controlling the end group offers a wide range of possibilities from corrosion inhibition in aqueous and air environments to molecular engineering at a molecular level.

c

7.11 References

- [1] Bigelow, W.C., Pickett, D.L., Zisman, W.A., J., *Colloida Interface Sci.*, 1 (1946) 513.
- [2] Ulman, A., in "Introduction to Ultrathin Organic Films from Langmuir Blogdett to Self-Assembly", Academic, New York (1991) Chapter 3.
- [3] Li, J., Liang, K.S., Scoles, G., Ulman, A., *Langmuir*, 11 (1995) 4418.
- [4] Nuzzo, R.G., Fusco, F. and Allara, D.L., *J. Am. Chem. Soc.*, 109 (1987) 773.
- [5] Bain, C.D., Troughton, E.B., Tao Y.-T., Evall, J., Whitesides, G. M. and Nuzzo, R. G., *J. Am. Chem. Soc.* 111 (1989) 321.
- [6] Thomas, R.C., Sun, L. and Crooks, R.M., *Langmuir*, 7 (1991) 620.
- [7] Sun, L. and Crooks, R.M., *J. Electrochem. Soc.*, 138 (1991) 123.
- [8] Porter, M.D., Bright, T.B., Allara, D.L., and Chidsey, C.E.D., *J. Am. Chem. Soc.*, 109 (1987) 3559.
- [9] Nuzzo, R.G., Fusco, F A. and Allara, D L., *J. Am. Chem. Soc.*, 109 (1987) 2358.
- [10] Ulman, A., "Introduction to Ultrathin Organic Films: from Langmuir-Blogdett to Self-Assembly", Academic, New York (1991).
- [11] Dubois, L.H. and Nuzzo, R.G., *Annu. Rev. Phys. Chem.*, 43 (1992) 437.
- [12] Ulman, A., *Chem. Rev.*, 96 (1996) 1533.
- [13] Nuzzo, R.G., Korenic, E.M. and Dubois, L.H., *J. Chem. Phys.* 93 (1990) 767.
- [14] Evans, S.D., Ulman, A. and Sharma, R., *Langmuir* 7 (1991) 7.

- [15] Feng, Y., Teo, W., Siow, K., Gao, Z., Tan, K. and Heieh. A., J Am Chem Soc., 144 (1997) 1.
- [16] Somorjai, G.A., "Chemistry in Two Dimensions – Surfaces", Cornell University. Press: Ithaca, New York, (1982).
- [17] King, D.E., J. Vac. Sci. Tech., 13 (1995) 1281.
- [18] Alves, C.A., Smith, E.L., and Porter, M.D., J. Am. Chem Soc., 114 (1992) 1222.
- [19] Nuzzo R.G., Dubois L.H. and Allara D.L., J. Am. Chem Soc., 112 (1990) 558.
- [20] Fenter, P., Eisenberger, K. S. and Liang, K.S., Phys. Rev. Lett., 70 (1993) 2447.
- [21] Himmel, H., Weiss, K., Dannenberger, O., Grunze, M., and Woll, C., Langmuir, 13 (1997) 4943.
- [22] Laibinis, P.E. Whitesides, G.M., J. Am. Chem Soc., 114 (1992) 9022.
- [23] Laibinis, P.E., Whitesides, G.M., Allara, D L., Tao, Y., Parikh, A. N. and Nuzzo, R.G., J. Am. Chem. Soc., 113 (1991) 7152.
- [24] Laibinis, P.E., Whitesides, G.M., J. Am. Chem. Soc., 114 (1992) 1990.
- [25] Ulman, A. and Penner, T.L., Langmuir, 5 (1989) 101.
- [26] Laibinis, P.E., Whitesides, G.M., J. Am. Chem. Soc., 114 (1992) 9022.
- [27] Ghijsen, J., Tjeng, J., Van Elp, J., Eskes, H., Westerink, J. and Sawatzky, G. A., Physics Reviews B., 38 (1988) 16.
- [28] Briggs, D., Seah, M.P., "Practical Surface Analysis by Auger and X-ray Photoelectron Spectroscopy", Wiley, New York, (1994).
- [28] Scherer, J., Vogt, M.R., Magnussen, O.M. and Behm, R.J., Langmuir. 13 (1997) 7045.

- [29] Yamamoto, Y., Nishihara, H., Aramaki, K., J. Electrochem. Soc., 140 (1993) 436.
- [30] Itoh, M., Nishihara, H., Aramaki, J. Electrochem. Soc., 141 (1994) 2018.
- [31] Itoh, M., Nishihara, H., Aramaki, J. Electrochem. Soc., 11 (1995) 1839.
- [32] Jennings, G., Laibinis, P.E., Colloids and surfaces, 106 (1996) 105.
- [33] Haneda, R., Nishihara, N. and Aramaki, K., J Electrochem Soc., 144 (1997) 4.
- [34] Haneda, R., and Aramaki, K., J Electrochem Soc., 145 (1998) 6.
- [35] Creager, S.E., Hockett, L.A. and Rowe. G.K., Langmuir, 8 (1992) 854.
- [36] Feng, Y., Teo, W., Siow, K., Gao, Z., Tan, K., Heieh. A., J. Am. Chem. Soc., 144 (1997) 1.
- [37] Yamamoto, Y., Nishihara, H., Aramaki, K., J. Electrochem. Soc., 140 (1993) 436.
- [38] Jennings, G., Munro, J.C., Yong, T., Laibinis, P.E., Langmuir, 14 (1998) 6130.
- [39] Taneichi, D., Haneda, R. and Aramaki, K.M., Corrosion Science, 43 (2001) 1589.
- [40] Ron, H., Cohen, H., Matlis, S., Rappaport, M. and Rubinstein, I., J. Phys. Chem. B., 102 (1998) 9861-9869.
- [41] Sexton, B.A., Surf. Sci., 88 (1979) 299.
- [42] Maoz, R. and Sagiv, J., J. Colloid Interface Sci., 100 (1984) 465.
- [43] Folkers, J.P., Laibinis, P.E. and Whitesides, G M., Langmuir, 8 (1992) 1330.

Chapter 8

A combined XPS (X-ray photoelectron spectroscopy) and
electrochemical study into alcohol and carboxylic terminated thiols on
reduced copper

8.1 Introduction

In this study, the interaction of alcohol- and carboxylic acid-terminated thiols, of different chain lengths and different immersion times, on a polycrystalline copper surface are investigated. These particular self-assembled monolayers (SAMs) on polycrystalline copper are studied because of their synthetic accessibility, polarity and reactivity of the end group (-OH, -COOH), and if the end group can be precisely controlled these monolayers can be used as building blocks for the adsorption of other species [1].

Principally, the end group X determines the surface physicochemical properties of alkanethiol monolayers, and the ability to customize these surface properties by simply varying the terminal groups is what makes this system so attractive for surface engineering at a molecular level. These monolayers, having being prepared on the copper surface, are characterised using XPS, electrochemistry and contact angle measurements.

The combination of cyclic voltammetry and XPS as interactive techniques has being proven to be very effective [2] while studying corrosion chemistry, providing information concerning the structural integrity of the film. With electrochemical control the macroscopic distribution and the concentration of the reaction products can be reproduced through many runs and therefore a good association between the conditions of the electrochemical reaction and the resultant XPS spectra is possible, especially if the reacted electrode can be protected from atmospheric oxidation during transfer to the photoelectron spectrometer.

In comparison to other coating methods, there are many advantages associated with SAMs, e.g. the thickness of the film can be controlled (\AA level), the film is formed by the simple chemisorption process which allows strong adhesion to the metal surface, and the chemical composition of the film can be altered by design.

8.2 Purpose and Aims of Research

The development of coatings that provide the required protection of the copper surface is essential for its efficient use in applications, and throughout this study the self-assembly of *n*-alkanethiols onto polycrystalline reduced copper was investigated. The effect of chain length of the *n*-alkanethiols was investigated, as previous studies have indicated that the longer the alkanethiol chain length, the more important the intermolecular interactions become, as opposed to the interface reaction, which influence adsorption structure [3]. The effect immersion time has on the formation of monolayers is also explored.

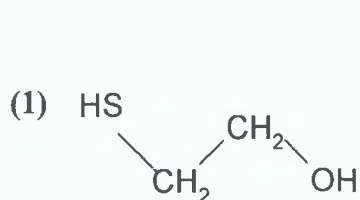
The *n*-alkanethiols under scrutiny are of the following structure, HS-(CH₂)_{*n*}-X, where *n* = 2, 6 and 11 and X = OH. Also HS-(CH₂)_{*n*}-X, where *n* = 1, 5 and 10 and X = COOH.

These particular self-assembled monolayers (SAMs) on polycrystalline copper are studied because of their synthetic accessibility, polarity and reactivity of the end group (-OH, -COOH), and if this particular end group can be precisely controlled they can act as molecular connectors for the adsorption of other compounds.

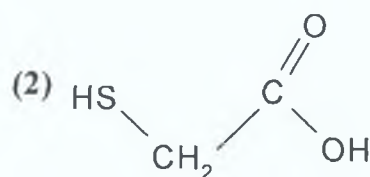
8.3 Experimental

8.3.1 Materials.

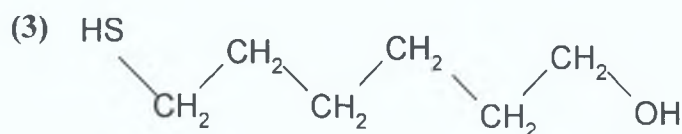
The structure of the self-assembly molecules are shown in Figure 8.1



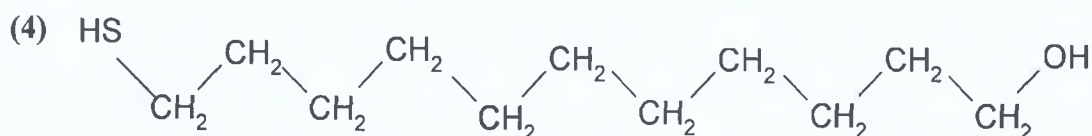
2-mercaptoethanol



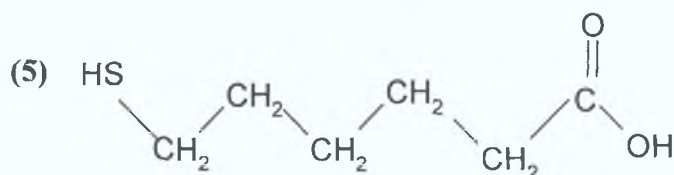
mercaptoacetic acid



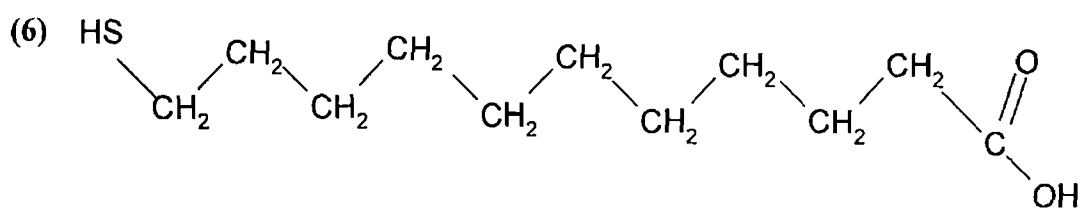
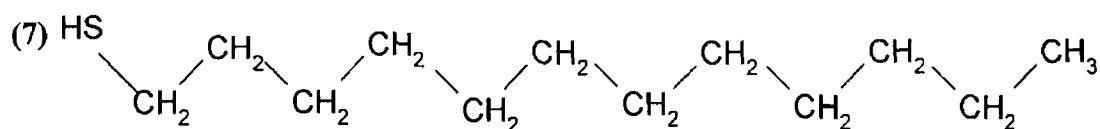
6-mercapto-1-hexanol



11-mercapto-1-undecanol



6-mercapto-1-hexanoic

**11-mercaptoundecanoic****1-dodecanthiol****Figure 8 1** Alkane-thiols molecules that were self-assembled on copper

| Chemical | Supplier | Purity % |
|-----------------------------|---------------|----------|
| 1-dodecanethiol | Sigma-Aldrich | 97 |
| 2-mercaptoethanol | Acros | 99 |
| 6-mercapto-1-hexanol | Acros | 99 |
| 11-mercapto-1-undecanol | Sigma-Aldrich | 97 |
| mercaptoacetic acid | Acros | 98 |
| 6-mercapto-1-hexanoic | Sigma-Aldrich | 97 |
| 11-mercaptoundecanoic | Sigma-Aldrich | 95 |
| Absolute ethanol | Sigma-Aldrich | |
| Copper sheets | Goodfellows | 99 99 |
| 1, 3, 9 μ diamond paste | Beuhler | |

The materials and their suppliers used in the following study are listed above

8.3.2 Sample preparation.

The polycrystalline copper substrate were supplied as sheets approximately 1mm thick, and were cut to 1cm x 2cm. These copper pieces were placed under UV/ O₃ activation for 30 minutes, they were then polished with 1200 grit silicon carbide paper, and subjected to additional polishing with 9 micron, 3 micron and 1 micron diamond paste suspensions. A colloidal silica suspension was used with a felt cloth in the final polishing stage. The samples were washed after each stage of polishing with deionised water (18.2 MΩ cm⁻²). Polishing was performed on a Phoenix 4000 sample preparation system (Figure 8.2). Following on from the above, the copper pieces were then rinsed in absolute ethanol.

Prior to modification the copper pieces were subjected to 15 min of UV/O₃ activation, and sonicated for a further 20 min in absolute ethanol. These copper pieces were then electrochemically reduced in 0.5M HClO₄ (analysis grade) for 10minutes. The HClO₄ solution was purged with argon for ten minutes in order to remove all oxygen containing air from the cell, before the copper pieces were reduced, and the HClO₄ was blanketed with argon throughout the reduction process. The objective of this preparation procedure was to minimise surface oxidation prior to monolayer deposition.

The monolayer assemblies were formed by immersing the reduced copper into dilute carboxylic / alcohol terminated thiol solutions of absolute ethanol (0.01M solutions for 2, 12 and 24hr) as schematically shown in Figure 8.3. As outlined extensively in the previous chapter, the copper surface readily oxidises in air, and that copper oxide reduces the adsorption capability of the thiol onto the copper. The whole procedure was therefore performed [4] as quickly as possible. Immediately after modification, the copper samples were removed, rinsed with absolute ethanol and dried under a stream of argon. The copper pieces were then subjected to a further 10 min sonication in absolute ethanol to remove excess reactants and dried and stored under argon.

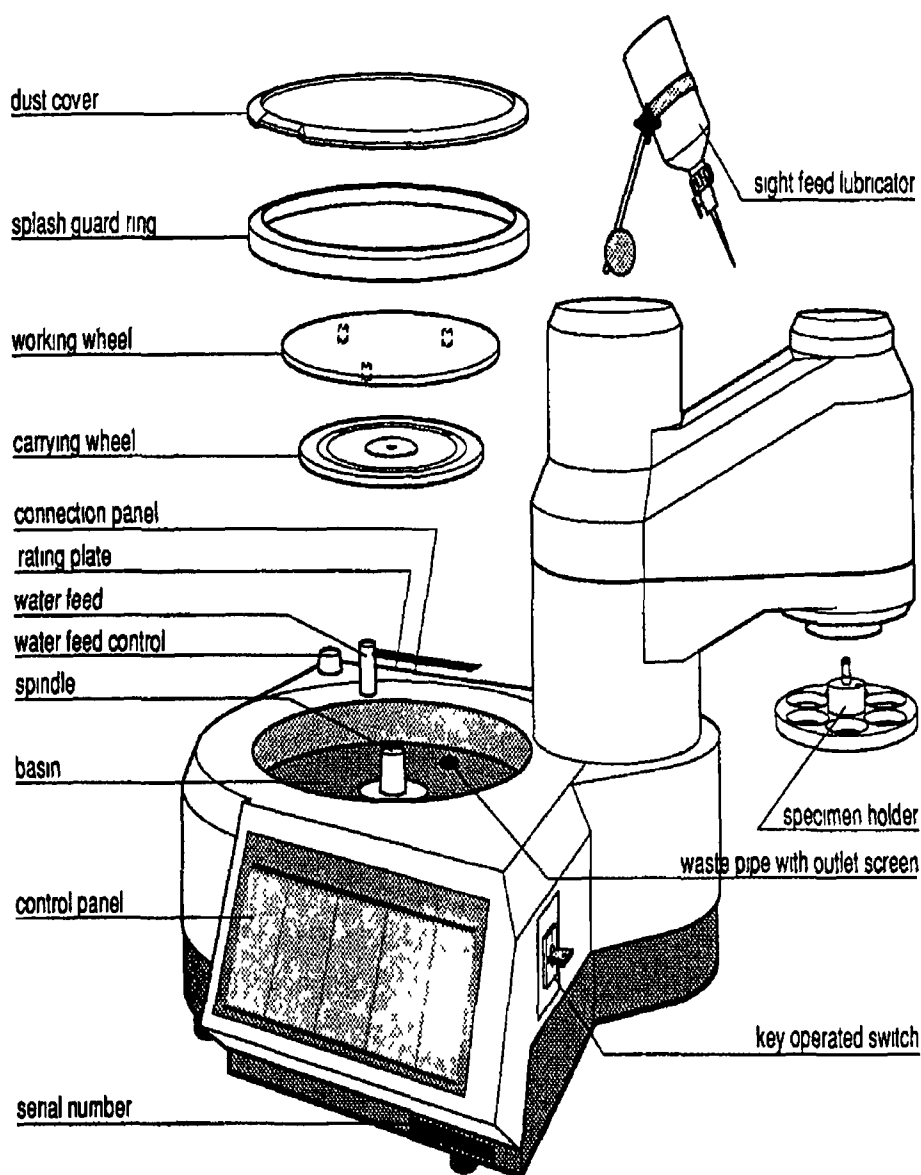


Figure 8 2 Schematic of Phoenix 4000 sample preparation system

Throughout this chapter, for simplicity, $\text{HS}(\text{CH}_2)_n\text{X}$ on polycrystalline copper will be abbreviated as C_nX , e.g. $\text{HS}(\text{CH}_2)_{11}\text{OH}$ self-assembled on polycrystalline copper will be abbreviated to C_{11}OH .

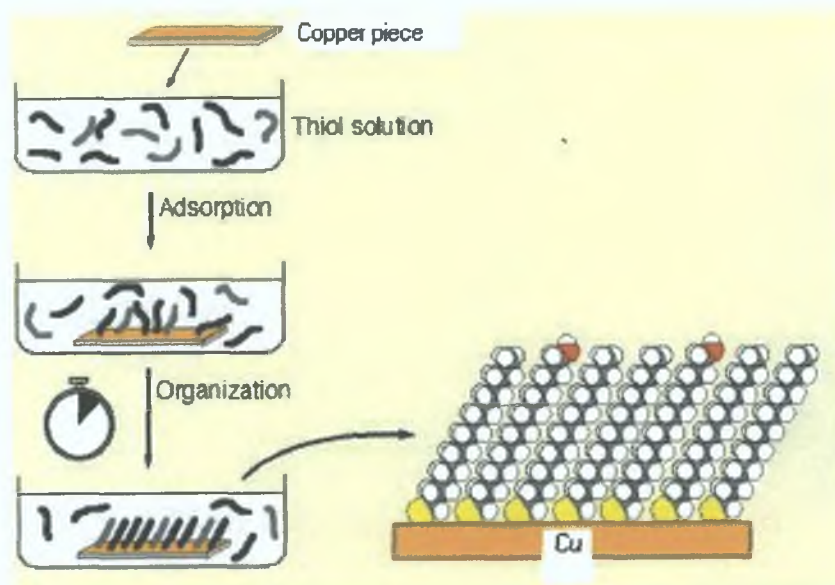


Figure 8.3 Preparation of SAMs. The substrate, Cu is immersed into an ethanol solution of the desired thiol(s). Initial adsorption is fast (seconds); then an organization phase follows, which was allowed to continue for 2 hr, 12hr and 24hr in this study. A schematic of a fully assembled SAM is shown to the right.

8.4 Instrumentation

8.4.1 X-Ray photoelectron spectroscopy

X-ray photoelectron spectra were collected on a surface science SSX-100 spectrometer Figure 8.4. The photoelectrons were excited using Al K α radiation as the excitation source (photoelectron energy 1486.6 eV, monochromated source was operated at 10 KV and 12.5 mA). The photoelectrons were collected at 35° from the surface normal and detected with a hemispherical analyser.

The spectral regions, C(1s) was accumulated over 10 scans with a 20 eV window, O(1s) – 10 scans with 15 eV window, S(2p) – 40 scans with 20 eV window, Cu(2p) – 5 scans with 45 eV window and Cu LMM – 15 scans 20 eV window, were recorded. The x-ray spot size used in acquiring the spectra recorded was 600 μm , with a pass energy of 50 eV. During data acquisition the pressure was kept below 1×10^{-9} Torr, and the binding energies of the peaks obtained were referenced to the binding energy of the C 1s $_{1/2}$ at $284.5 \text{ eV} \pm 0.3 \text{ eV}$.

The spectra was fitted using 80% / 20% linear combination of Gaussian and Lorentzian profiles, using a Winspec program [16]. This Winspec program allows the user to perform different tasks for the evaluation and treatment of spectroscopic data. These tasks namely being:

1. Removing spikes.
2. Smoothing of data in order to reduce noise (the program does not diminish the noise but improves the appearance of the curves).
3. Analysing spectra so that peaks can be located with better accuracy.
4. Adding and subtracting spectra.
5. Shifting spectra to correct for charging effects.
6. Creating synthetic spectra by adding together peaks of Lorentzian or Gaussian shape (or a mixture), as well as some baselines (background).
7. Finding synthetic spectra that best match the experimental data.



Figure 8.4 Surface Science SSX-100 spectrometer.

8.4.2 Contact Angle measurements

One of the most sensitive methods for surface characterisation of solid materials is determined by the contact angle at the phase boundary – solid/liquid/gaseous. By placing a drop of water, or any other liquid, onto the flat surface it will assume the shape that gives the lowest total energy. For example, if you have a hydrophilic surface, i.e. if it has -OH or -COOH groups in its outermost layer it is more favourable for the water to spread out over the surface. Whereas if the outermost group is hydrophobic, i.e. CH_3 or CF_3 , the drop will take a shape that wets a minimal area of the surface as schematically illustrated in Figure 8.5.

The contact angle (CA) was then measured by optical inspection and the result is a measure of the hydrophobicity of the surface i.e. if $\theta = 0$ then the surface is completely wet, where $\theta = \text{finite}$ then surface partially wet.

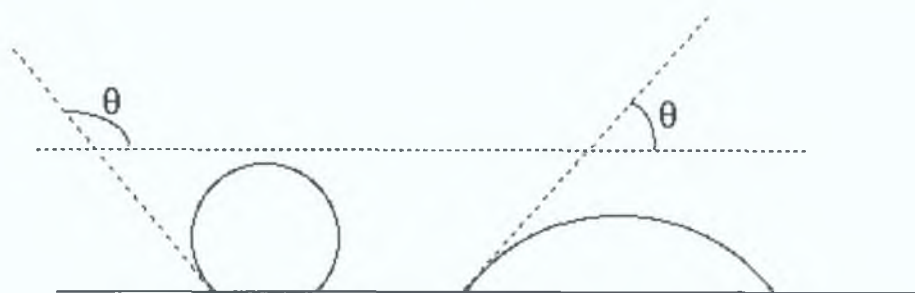


Figure 8.5 Hydrophobic and Hydrophilic contact angles respectively.

The advancing contact angle of $\cong 2\mu\text{L}$ H_2O drops in air at room temperature was measured using a VCA 2500XE (video contact angle) system. Three sets of measurements were taken on each surface and an average value calculated.

8.4.3 Cyclic voltammetry

Cyclic voltammetry (CV) is commonly used for acquiring qualitative information about electrochemical reactions. CV can provide information on the thermodynamics of redox processes, the kinetics of heterogeneous electron transfer on coupled chemical reactions and adsorption processes.

CV consists of applying a continuously time-varying potential to a working electrode. During this potential sweep, a potentiostat measures the current resulting from the applied potential. The resulting plot of current vs. potential is called a cyclic voltammogram.

Basically the system starts at an initial potential at which no redox reaction can take place. Then at a critical potential during a forward scan an electroactive species will be reduced. The direction of the potential scan is subsequently reversed, and with this depletion of the oxidised species i.e. oxidation takes place.

A three-electrode cell is the most commonly used cell in controlled potential experiments. The electrodes are placed in the cell, which contains the

analyte and the supporting electrolyte, as shown in Figure 8.6. The purpose of the auxiliary (counter) electrode is to conduct electricity from the signal source into the solution, maintaining a correct current. At the working electrode oxidation of the analyte occurs and the potential of the reference electrode is known and constant. The potential that is cycled is the difference in potential between the working electrode and the reference.

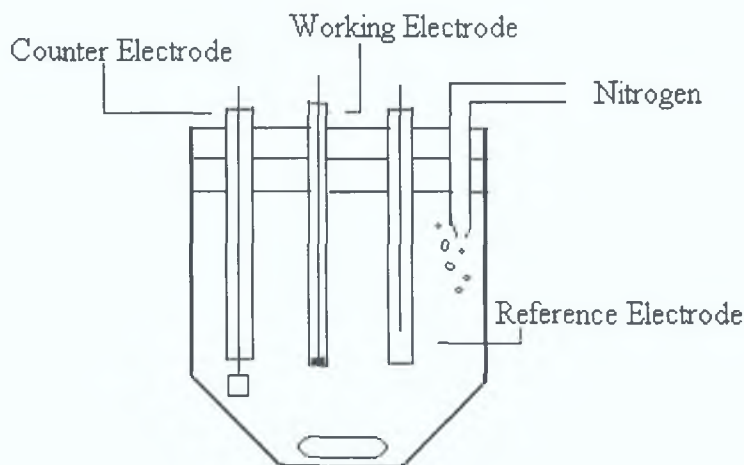


Figure 8.6 Schematic diagram of a cell for voltammetric measurements

All cyclic voltammetry measurements were carried out in 0.1M NaOH solutions. The electrochemical cell used was a spot cell. The electrode was scanned over the potential range of -1.0 to 1.0 V, with a scan rate of 20 mVs^{-1} . All electrochemical measurements were made with reference to a SCE (saturated calomel electrode) and a platinum counter electrode, with the working electrode being the modified Cu samples. The instrument used was an EG+G Princeton applied Research Potentiostat / Galvanostat Model 273A.

8.4.4 Polarisation measurements

Electrodes with potentials that change only slightly when a current passes through them are classified as non-polarisable. Those with strongly current-

dependent potentials are classified as polarisable, and the criterion for low polarisability is high ion-exchange current density.

Corrosion refers to the loss or the conversion into another insoluble compound of the surface layers of a solid in contact with a fluid. In the electrochemistry laboratory corrosion may be studied by voltammetry and the kinetic parameters can be determined from Tafel plots, where the log of the current density is plotted against the overpotential, η .

$$\log I = \log I_o + \frac{\alpha_A nF}{2.3RT} \eta \quad \text{Equation 8.1}$$

$$\log -I = \log I_o - \frac{\alpha_c nF}{2.3RT} \eta \quad \text{Equation 8.2}$$

I_o = Exchange current density

α_A and α_C = transfer coefficients for anodic and cathodic reactions respectively

F, R = Faraday's and gas constant respectively

T = temperature

η = overpotential.

At high positive overpotentials, Equation 8.1 gives the anodic current density and at high negative overpotentials Equation 8.2 represents the cathodic current density. These two Equations are known as the Tafel Equations and are the basis of a simple method for determining the exchange current density, I_o , and the transfer coefficients, α_A and α_C . These two parameters characterise the kinetics of the electrode reaction.

In the subsequent study all polarisation measurements were performed in 0.5 M NaCl. The polarisation curve was recorded from -1.0 to 1.0 V and the sweep rate was 50 mVs⁻¹ using platinum and SCE (saturated calomel electrode).

8.5 Results and Discussion

8.5.1 Contact Angles



Figure 8.7 Picture of H₂O drop on metal surface.

The water contact angle on the monolayers was measured in order to establish the wettability of the modified copper surfaces. As the wettability of the surface is related to the outermost part of the adsorbed molecule, the presence of a hydrophilic group on the surface should give rise to an increase in the wettability of the layer, e.g. –OH [5, 6]. The wettability of the surface is also related to the roughness of the surface, and contact angle measurements do not give you any information about the structure of the monolayer. What they can do is provide a useful guide to the quality of the monolayer; a low contact angle value for alkanethiols on Cu is an indication of low substrate coverage. The results reported in Table 8.1 are those recorded by Laibinis and Whitesides, for *n*-alkanethiols of different chain lengths (*n*) and different endgroups (X) on copper and gold substrates [7]. The molecular length is defined as the number of close atoms in the adsorbed molecule comprising the monolayer/metal (CH₂)_{*n*}X.

| n | X | Molecular length | CA (θ°) |
|---------|-------------------|------------------|----------|
| 7 | CH ₃ | 10 | 115, 112 |
| 11 | CH ₃ | 14 | 120, 115 |
| 21 | CH ₃ | 24 | 117, 117 |
| 10 | OH | 13 | <15, <15 |
| 11 | OH | 14 | <15, <15 |
| <15 -22 | OH | 25 | 44, 25 |
| 10 | CO ₂ H | 14 | 35, <15 |
| 15 | CO ₂ H | 19 | 53, <15 |
| 21 | CO ₂ H | 25 | 50, <15 |

Table 8.1 Values of static advancing Contact Angles (θ_a°)H₂O on films prepared by the adsorption of *n*-alkanethiols onto Copper and Gold surfaces, reported by Laibinis and Whitesides [7].

| Alcohols | 24 hr | Au (24 hr) | 12 hr | 2 hr |
|--------------------|-------|------------|-------|------|
| C ₁₂ | 111° | | 120° | 115° |
| C ₁₁ OH | 44° | 45° | 42° | 48° |
| C ₆ OH | 68° | 48° | 71° | 56° |
| C ₂ OH | 35° | 66° | 58° | 61° |

Table 8.2 Contact angles (θ_a°)H₂O results recorded for copper and gold surfaces modified with *n*-alkanethiols. i.e. C₁₁OH → Cu/S-(CH₂)₁₁OH, C₆OH → Cu/S-(CH₂)₆OH, C₂OH → Cu/S-(CH₂)₂OH and C₁₂→ Cu/S-(CH₂)₁₁CH₃.

| Carboxylic | 24 hr | Au (24 hr) | 12 hr | 2 hr |
|--------------------|-------|------------|-------|------|
| C ₁₂ | 111° | | 120° | 115° |
| C ₁₁ OH | 72° | 71° | 52° | 69° |
| C ₆ OH | 39° | 41° | 83° | 53° |
| C ₂ OH | 54° | 24° | 95° | 39° |

Table 8.3 Contact angles (θ_a°)H₂O results recorded for copper and gold surfaces modified with *n*-alkanethiols. i.e. C₁₁OOH → Cu/S-(CH₂)₁₀COOH, C₆OH → Cu/S-(CH₂)₅COOH, C₂OH → Cu/S-(CH₂)-COOH and C₁₂→ Cu/S-(CH₂)₁₁CH₃.

The contact angle (CA) measurements taken in this study are seen in Tables 8.2 and 8.3. These values indicate disorder (the term order is generally used to describe molecular assemblies with translational symmetry, i.e. a 2-D crystalline-like monolayer) and the increased corrugation (ridges, grooves) of the copper surface which could be associated with the presence of copper oxide underneath the adsorbed monolayer. The CA measurements seen in Table 8.2 and 8.3 are higher than those reported by Laibinis *et al.* in Table 8.1, which is an indication of disorder within the monolayer.

The wetting behaviour of alkanethiols on copper is similar to that of alkanethiols on Au [8] but considerably lowered when $n \leq 8$ and $n \geq 11$. Porter *et al.* showed this previously [9] with monolayers formed on gold, in which the suggested degree of crystallinity of monolayers alters in this region. Surface –OH and –COOH groups should vary the wetting behaviour of the monolayer. With SAMs of alkanethiols, i.e. C₁₂ on Cu, the CA measurements are usually in the region of ≈ 110 – 120° [10] as CH₃ is hydrophobic. The results obtained in this study for 1-dodecanethiol on Cu are well-matched with those obtained by Laibinis *et al.* and as the methyl surface formed by self-assembly of n-alkane amphiphiles is a low free-energy surface, which explains the poor wetting of these surfaces [11].

The –OH and –COOH are hydrophilic end groups, and this feature should increase the wettability of the surface, e.g. if $\theta_a^{H_2O} = 0$ then the surface is completely wet and classified as hydrophilic. When $\theta_a^{H_2O} = \text{finite}$ then surface partially wet which is assigned as hydrophobic. For these hydrophilic endgroups you would expect the contact angles recorded to be quite low ≈ 10 – 15° for alcohol-terminated thiols on Cu and 35 – 50° for carboxylate thiols. This was not the case from the results recorded in Table 8.2 and 8.3, the CA values varied with chain length and immersion time, with no regular pattern emerging. High CA values lead to the suggestion that multilayers were formed on the copper substrate, however from the XPS results obtained for the S2p spectral region does not support this (discussed later).

8.5.2 Cyclic voltammetry

Cyclic voltammetry can be used for evaluating the interfacial behaviour of electroactive compounds, from the voltammograms recorded of the different *n*-alkanethiols on copper substrate, a blocking factor was determined using Equation 8.3

$$\text{Blocking Factor} = \frac{Q_{\text{Ref}} - Q_{\text{SAM}}}{Q_{\text{Ref}}} \times 100 \quad \text{Equation 8.3}$$

The charge (*Q*) from both peaks is referenced to a bare copper electrode Q_{Ref} . *Q* is the quantity of charge transferred by the surface process and is obtained by integrating the peak area at saturation, and can be used to calculate the area occupied by the adsorbed molecule. Table 8.4 and 8.5 are the blocking factors calculated in this study for copper surfaces modified with *n*-alkanethiols for alcohol and acid end groups respectively.

| Alcohol | 2hr immersion | 24hr immersion |
|--------------------|---------------------|----------------------|
| Cu Reference | 386.3 μC | 271.77 μC |
| C ₁₁ OH | 77% | 41% |
| C ₆ OH | 54% | 35% |
| C ₂ OH | (--) | (--) |

Table 8.4 Calculated Blocking Factors, C₁₁OH → Cu/S-(CH₂)₁₁OH, C₆OH → Cu/S-(CH₂)₆OH, C₂OH → Cu/S-(CH₂)₂OH and Cu Reference → bare copper electrode

| Carboxylic Acid | 2hr Immersion | 24hr immersion |
|---------------------|---------------|----------------|
| Cu Reference | 386.3 μ C | 271.77 μ C |
| C ₁₁ OOH | 92% | 51% |
| C ₆ OOH | 48% | (--) |
| C ₂ OOH | (--) | (--) |

Table 8.5 Blocking Factors for chemisorbed *n*-alkanethiols on Cu substrate. C₁₁OOH \rightarrow Cu/S-(CH₂)₁₀COOH, C₆OH \rightarrow Cu/S-(CH₂)₅COOH, C₂OH \rightarrow Cu/S-(CH₂)-COOH and Cu Reference \rightarrow bare copper electrode

The alkanethiols are chemisorbed onto the Cu substrate following its reduction. When the first scan is started the thiols desorb, leaving a bare copper electrode, which is used to obtain Q_{ref} . Figure 8.8 shows the cyclic voltammograms obtained for bare Cu and for Cu electrodes that have being coated with a series of alcohol-terminated thiols, in 0.1 M NaOH with a scan rate of 20 mVs⁻¹. The peaks at -375 mV and -160 mV in the anodic sweep direction are associated with copper dissolution and Cu oxidation respectively. The cathodic peak observed at \cong -490 mV in the cathodic sweep is attributed to the electro-reduction of copper ions in the solution near the electrode.

A blocking factor higher than that recorded was expected from the longer chain thiols, i.e. C₁₁OH and C₁₁OOH, as according to literature [17] the optimum chain length is $20 < n \leq 11$. The copper samples that were immersed in the thiol solution for 2hr presented a blocking factor of 92% and 77% for Cu/S-(CH₂)₁₀COOH and Cu/S-(CH₂)₁₁OH respectively. Blocking factor of 48% and 54% were reached for Cu/S-(CH₂)₅COOH and Cu/S-(CH₂)₁₁OH respectively. A blocking factor for the smallest chain length thiols i.e Cu/S-(CH₂) COOH and Cu/S-(CH₂)₂OH, could not be determined. It can be seen from the voltammograms that the area under the oxidation curve for the thiol is much greater than that of the bare copper reference. After 24 hr immersions the blocking factor has decreased for all thiols, even though there is a slight increase with increasing chain length, no regular pattern seems to emerge. In a study carried out by Laibinis and co-workers [8] on Cu (111) modified surface, they

found that after extended exposure of the copper surface to solutions containing alkanethiols, the resulting films were too thick to be described as monolayers. The major difference between the XPS spectra of these surfaces showed an increased amount of sulfur present with continued exposure to the alkanethiol solution. The amount of sulfur was found to be too large to be explained if sulfur is only present as alkanethiolate. So it was believed by Laibinis *et al* that C-S bond cleavage had occurred to generate a thin film of copper sulphide at the copper/monolayer interface. However, these surfaces did not allow characterisation by wetting due to pitting. The 2hr immersion appears to produce better results of both immersion times, which is in good agreement with results obtained by Feng *et al* [12], where they concluded that the formation of a monolayer was rapid and could be complete within 30 minutes immersion.

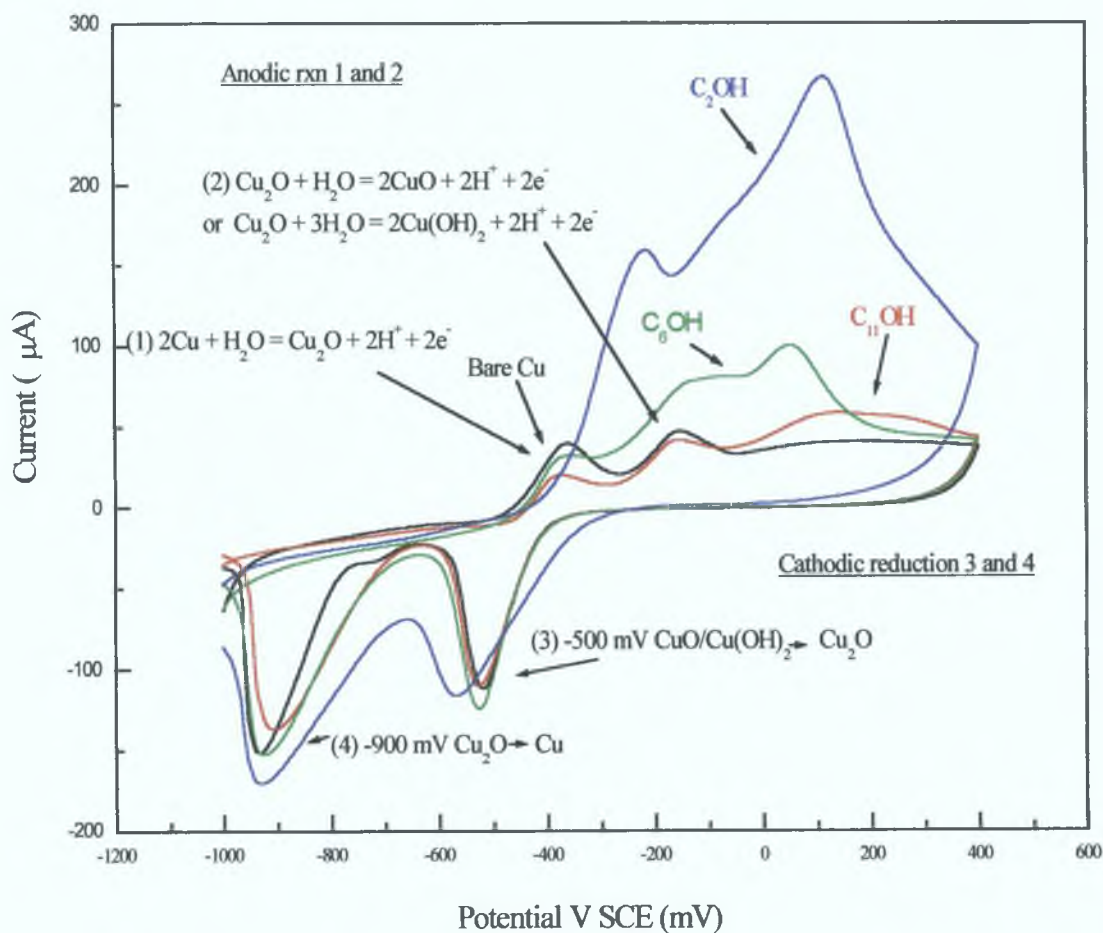
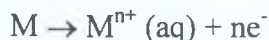


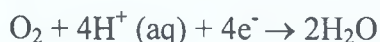
Figure 8.8 Representative Cyclic Voltammetric response of a bare Cu electrode, $\text{Cu}/\text{S}(\text{CH}_2)_{11}\text{OH}$ electrode, $\text{Cu}/\text{S}(\text{CH}_2)_6\text{OH}$ electrode and a $\text{Cu}/\text{S}(\text{CH}_2)_2\text{OH}$ electrode after 24 hr immersion in 0.01 M alcohol-thiol solutions in ethanol. Scan rate 20 mVs^{-1} . Electrolyte 0.1 M NaOH

8.5.3 Polarisation

The corrosion of a metal, which is in contact with an aqueous solution, can be represented as follow:



In acid environment



And / or



In alkaline environment



And / or



The metal ions can react immediately with OH^{-} to form insoluble oxides/hydroxides that cover the metal surface, or the metal ion can be released to bulk solution. The current of metal ions leaving the metal surface in the anodic region measures the rate of corrosion. This flux gives rise to a corrosion current I_{corr} . The coverage of copper with a modified layer (SAMs), has being studied in the hope that it will suppress the anodic / cathodic process of copper corrosion.

Tafel plots were recorded for the copper electrode bare and covered with *n*-alkanethiol.

Figure 8.9 and 8.10 shows the polarisation curves obtained for the copper electrode bare and covered with alcohol and carboxylic acid terminated thiols respectively, at varied immersion times (24 hrs). From these Tafel plots the E_{corr} mV (corrosion potential), and I_{corr} μ A (corrosion current) can be evaluated by extrapolation of the Tafel plot, and used to determine the protection efficiency, P.

Since reduction of molecular oxygen occurs in the potential of the cathodic branch, the modified layer should act as a barrier to oxygen diffusion. This structure also if arranged tightly enough should contribute to the inhibition of the anodic copper dissolution. Assuming that a closely packed and tightly interconnected monolayer was constructed on the copper surface, a thicker layer, i.e. $C_{11}OH$ should have a greater effect on the inhibition of the cathodic process. This appears to be true for the 24 and 12 hr immersions for $C_{11}OH$ on Cu, where this cathodic process is suppressed to a higher extent than with the Cu/ C_6OH and Cu/ C_2OH modified copper electrodes. Although as can be seen from the Tafel plots, all the modified electrodes reduce the cathodic process in comparison to the bare Cu electrode.

The values of P , protection efficiency, for the alcohol-thiol covered electrodes can be seen below in Tables 8.6, 8.7, and 8.8 for 24 hr, 12 hr and 2 hr immersion times, respectively.

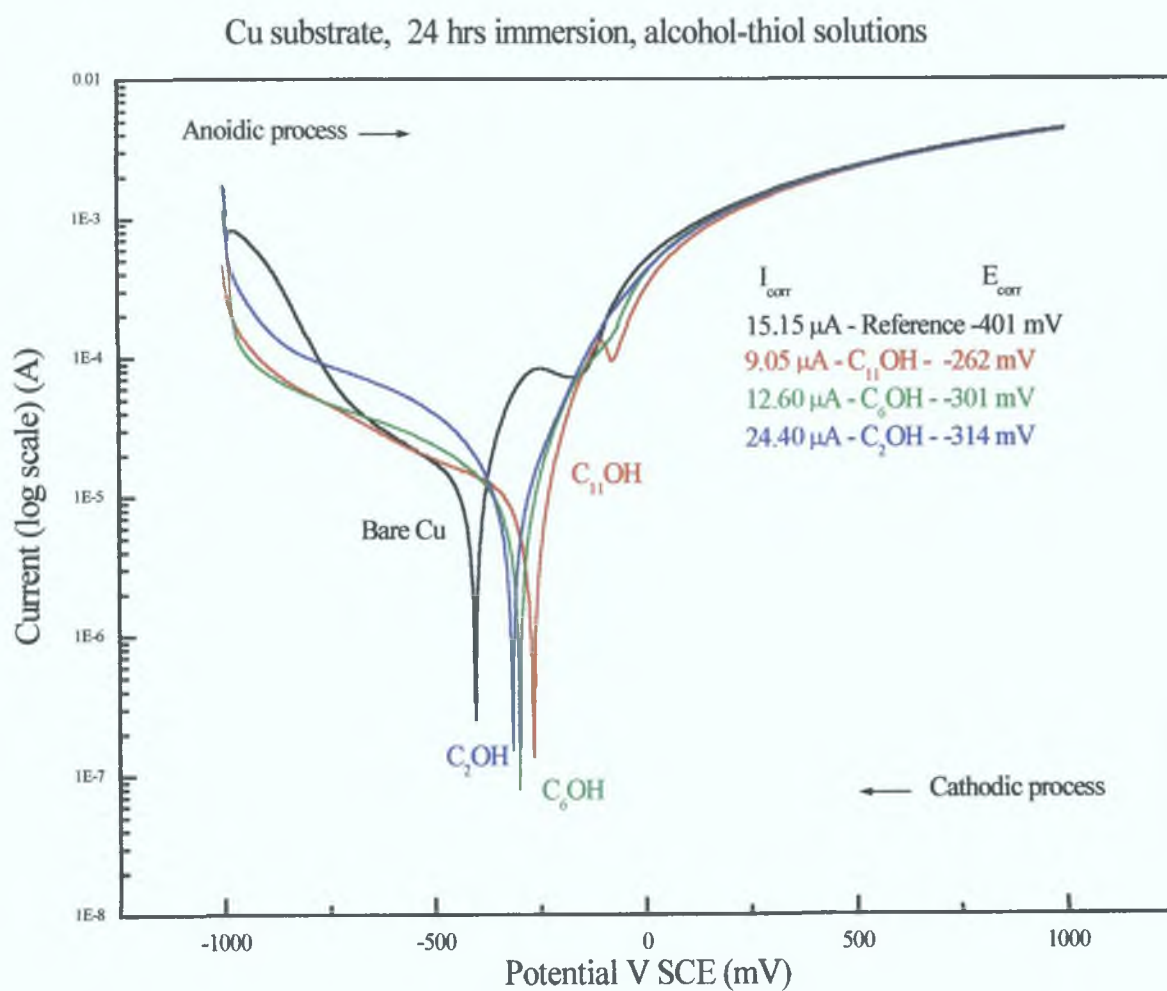


Figure 8.9 Representative Tafel plot for bare Cu electrode, $Cu/S(CH_2)_{11}OH$ electrode, $Cu/S(CH_2)_6OH$ electrode and a $Cu/S(CH_2)_2OH$ electrode after 24hrs immersion in 0.01 M alcohol-thiol solutions in ethanol.

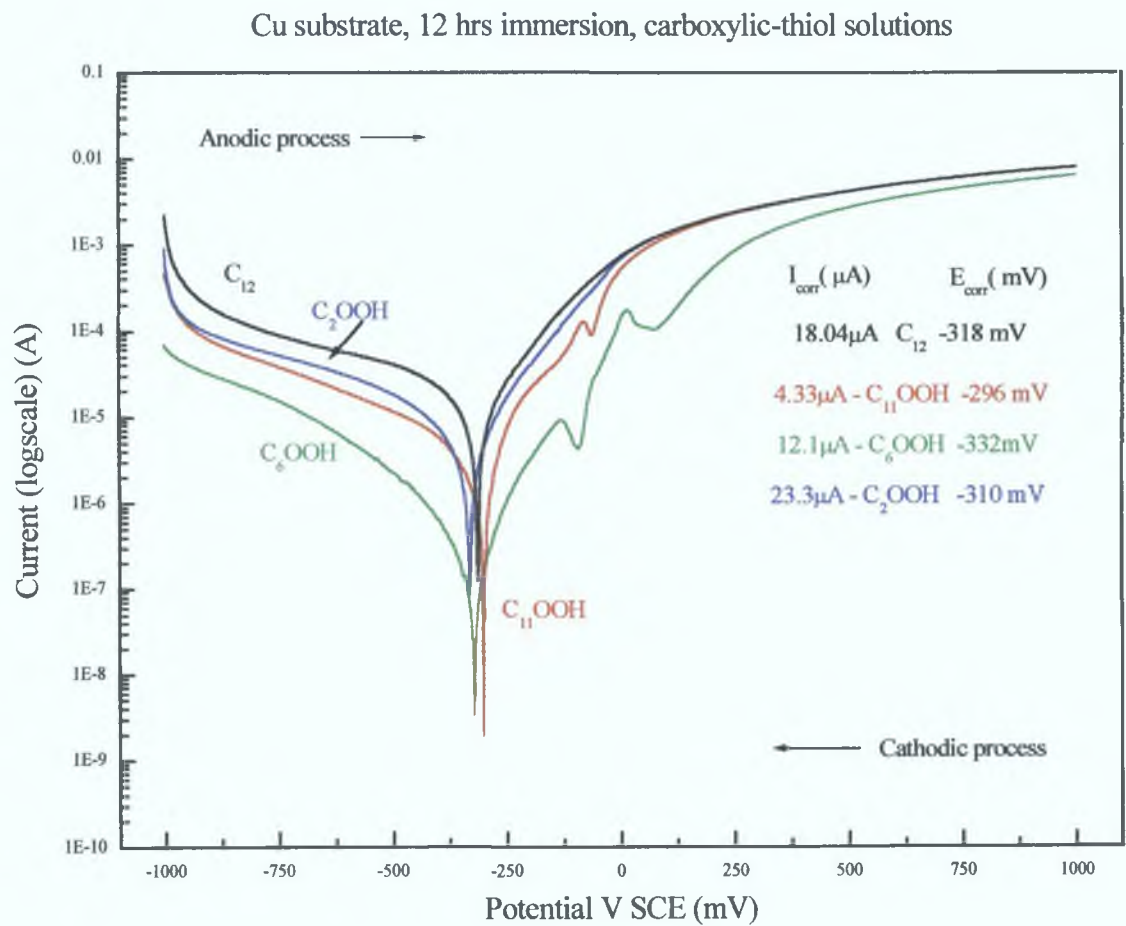


Figure 8.10 Representative Tafel plot for, bare Cu electrode, Cu/S(CH₂)₁₀COOH electrode, Cu/S(CH₂)₅COOH electrode and a Cu/S(CH₂)COOH electrode after 12 hrs immersion in 0.01 M carboxylic-thiol solutions in ethanol.

| Alcohol | E _{corr} mV | I _{corr} μA | P % | Carboxylics | E _{corr} mV | I _{corr} μA | P % |
|--------------------|----------------------|----------------------|------|---------------------|----------------------|----------------------|-----|
| Reference | -401 | 15.15 | | Reference | -401 | 13.42 | |
| C ₁₁ OH | -262 | 9.05 | 40 | C ₁₁ OOH | -272 | 1.39 | 89 |
| C ₆ OH | -301 | 12.60 | 17 | C ₆ OOH | -364 | 9.31 | 31 |
| C ₂ OH | -314 | 24.40 | (--) | C ₂ OOH | -324 | 6.87 | 48 |

Table 8.6 E_{corr} (mV), I_{corr} (μA) and Pro.eff (%), calculated for modified Cu surface after 24 hrs immersion in dilute thiol solns. C₁₁OH → Cu/S-(CH₂)₁₁OH, C₆OH → Cu/S-(CH₂)₆OH, C₂OH → Cu/S-(CH₂)₂OH and Cu Reference → bare copper electrode. C₁₁OOH represents Cu/S-(CH₂)₁₀COOH, C₆OOH → Cu/S-(CH₂)₅COOH, C₂OOH → Cu/S-(CH₂)COOH

| Alcohol | E _{corr} mV | I _{corr} μA | P % | Carboxylics | E _{corr} mV | I _{corr} μA | P % |
|--------------------|----------------------|----------------------|------|---------------------|----------------------|----------------------|------|
| Reference | -313 | 18.04 | | Reference | -313 | 18.04 | |
| C ₁₁ OH | -296 | 3.32 | 82 | C ₁₁ OOH | -296 | 4.33 | 76 |
| C ₆ OH | -332 | 9.21 | 49 | C ₆ OOH | -332 | 12.10 | 33 |
| C ₂ OH | -366 | 20.57 | (--) | C ₂ OOH | -366 | 23.30 | (--) |

Table 8.7 E_{corr} (mV), I_{corr} (μA) and Pro.eff (%), calculated for modified Cu surface after 12 hrs immersion in dilute *n*-alkanethiol solutions.

| Alcohol | E _{corr} mV | I _{corr} μA | P % | Carboxylics | E _{corr} mV | I _{corr} μA | P % |
|--------------------|----------------------|----------------------|-----|---------------------|----------------------|----------------------|-----|
| Reference | -417 | 9.71 | | Reference | -417 | 9.71 | |
| C ₁₁ OH | -292 | 8.25 | 15 | C ₁₁ OOH | -312 | 2.80 | 71 |
| C ₆ OH | -313 | 8.95 | 8 | C ₆ OOH | -325 | 6.60 | 32 |
| C ₂ OH | -302 | 4.87 | 50 | C ₂ OOH | -287 | 6.11 | 6 |

Table 8.8 E_{corr} (mV), I_{corr} (μA) and Pro.eff (%), calculated for modified Cu surface after 2 hrs immersion in dilute *n*-alkanethiol solutions.

The P values, for the 24 and 2 hr immersions are far lower than those recorded after 12 hr immersion. For the 12 hr immersion the P values for the C₁₁OH-modified electrode and the copper modified with C₆OH were calculated as 82 and 49%, respectively. As the P value for the C₆OH is far lower than that of the longer-chained molecule, this could suggest that the closely packed structure is incomplete and not giving maximum protection.

For the C₁₁OOH, C₆OOH and C₂OOH modified copper electrodes, the C₁₁OOH seems to have a greater effect on the delaying of the cathodic process for immersion times of 24 and 12 hr, but for the 2 hr immersion, the C₂OOH seems to have a greater effect on hindering this process (E_{corr} (mV)). The protection efficiency for all the longer chained carboxylate modified electrodes is quite high (89 – 71 %), this figure decreases with decreasing chain lengths, possibly due to disorder of the closely-packed self-assembled monolayer.

Summarising these results, the optimum immersion time appears to be 12hrs, with the longer-chained molecules, i.e. C₁₁OH and C₁₁OOH providing the best protection and most complete monolayer formation. The shorter chains exhibit more disorder within the monolayer or incomplete monolayers formation. These results agree with those published by Aramaki *et al* [14] in which they state that the protection efficiency against copper corrosion increases with the increase in the carbon number in the alkyl chain.

8.5.4 X-ray Photoelectron Spectroscopy

Figure 8.11 represents a survey scan of alcohol-thiols on Cu substrate, after 24 hrs immersions for the following combinations, $C_{11}OH \rightarrow Cu/S-(CH_2)_{11}OH$, $C_6OH \rightarrow Cu/S-(CH_2)_6OH$, $C_2OH \rightarrow Cu/S-(CH_2)_2OH$ and $C_{12} \rightarrow Cu/S(CH_2)_{11}CH_3$. From this survey scan (wide scan), the peaks of interest have been identified as Cu ($3p_{1/2}$) at 77 ± 0.3 eV, Cu ($3s$) at 123 ± 0.3 eV, Cu ($2p_{3/2}$) at 933 ± 0.3 eV, S ($2p_{3/2}$) at 164 ± 0.3 eV, S ($2s$) at 228 ± 0.3 eV, C ($1s_{1/2}$) at 284.5 ± 0.3 eV, O ($1s_{1/2}$) at 532.5 ± 0.3 eV and Cu LMM emission lines at 567.6 eV ± 0.3 eV.

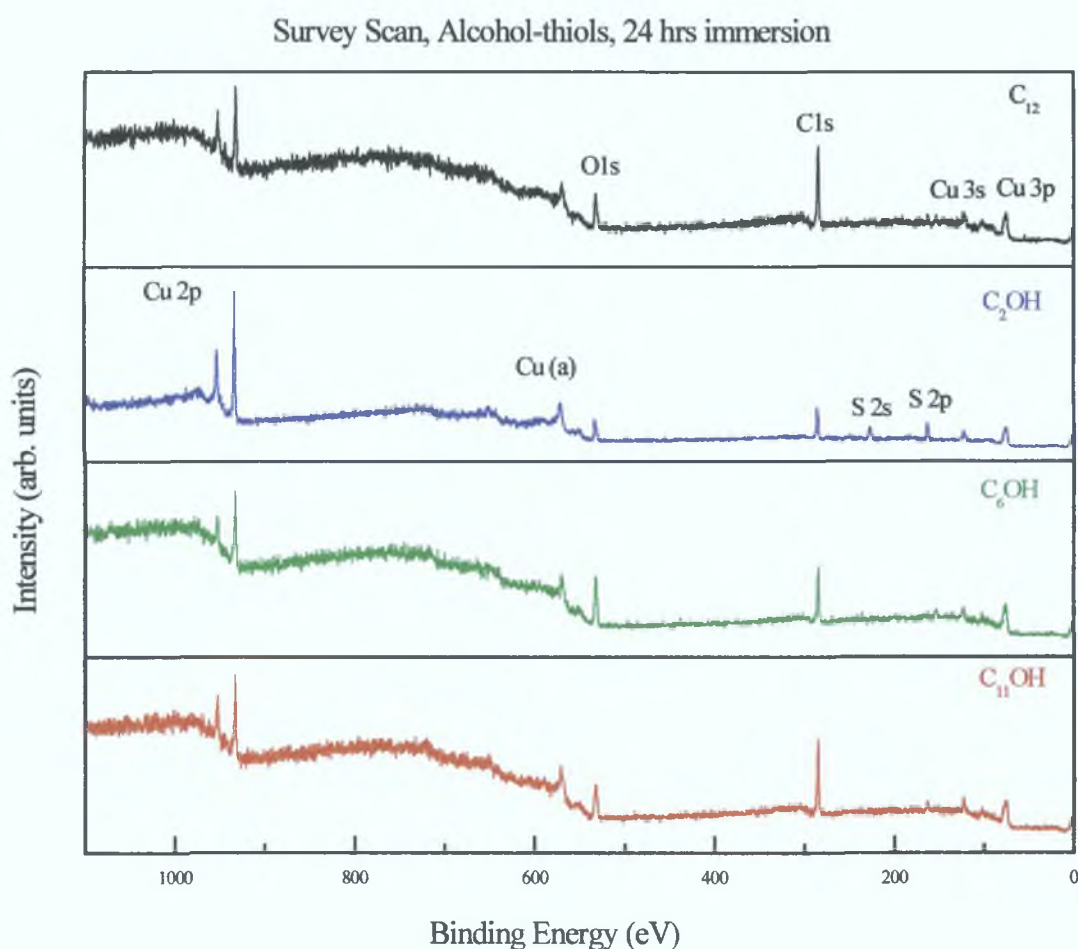


Figure 8.11 Survey Scan of alcohol-thiols on Cu substrate, after 24 hrs immersions. $C_{11}OH \rightarrow Cu/S-(CH_2)_{11}OH$, $C_6OH \rightarrow Cu/S-(CH_2)_6OH$, $C_2OH \rightarrow Cu/S-(CH_2)_2OH$ and $C_{12} \rightarrow Cu/S(CH_2)_{11}CH_3$. From this survey scan (wide scan), peaks of interest can be located i.e. Cu ($3p_{1/2}$), Cu ($3s$), Cu ($2p_{3/2}$), S ($2p_{3/2}$), S ($2s$), C ($1s_{1/2}$), O ($1s_{1/2}$) and Cu LMM peaks

Results for C 1s spectral region

As can be seen from the spectra of the C1s region (12 eV window), at different immersion times (Figure 8 12), the dodecanthiol on Cu (top spectrum), exhibits only one peak in this region at a value of 284.5 eV. This binding energy corresponds to the $-\text{CH}_2-\text{CH}_2$ bond, which is the only C-C bond present in this alkanethiol if monolayer formation is complete.

For all the alcohol terminated thiols at every immersion time (with the exception of C_{11}OH at 2hr immersion), only two peaks are observed in the C1s region of the spectrum, these peaks have a binding energy of 284.5 eV and 286.4 eV (± 0.3 eV). These binding energies correspond to $-\text{C}-\text{OH}$ and $-\text{CH}_2-\text{CH}_2-$ respectively, which correspond to the carbon bonds found in alcohol-terminated thiols. The area under each component carbon peak was calculated and ratios were derived and the results for C_2OH gave a 1:1 ratio, for C_6OH a ratio 5:1 and for C_{11}OH a ratio 10:1. This XPS data is reflecting the chemical composition of the adsorbed molecules – therefore variations from these ratios would indicate that a certain amount of molecular fragmentation had occurred. After 2hr immersion with C_{11}OH , a peak was observed at binding energy 288.9 eV, indicating the presence of another carbon bond, which could be attributed to a highly oxidised carbon species.

For the carboxylic thiols (Figure 8 13) there are three distinct peaks seen in the spectral region for C1s, these peaks have the corresponding binding energies 284.5 eV, 285.5 eV and 288.3 eV (± 0.3 eV), these binding energies in turn correspond to the following carbon to carbon bond links, $-\text{CH}_2-\text{CH}_2-$, $-\text{C}-\text{COOH}$ and $\text{C}-\text{OOH}$. For the longer chain thiol, at all immersion times, the results are satisfactory, 1:1:1. Whereas for the shorter chain thiols $-\text{C}_2\text{OOH}$ this is not the case, indicating molecular disorder within the shorter chained molecules.

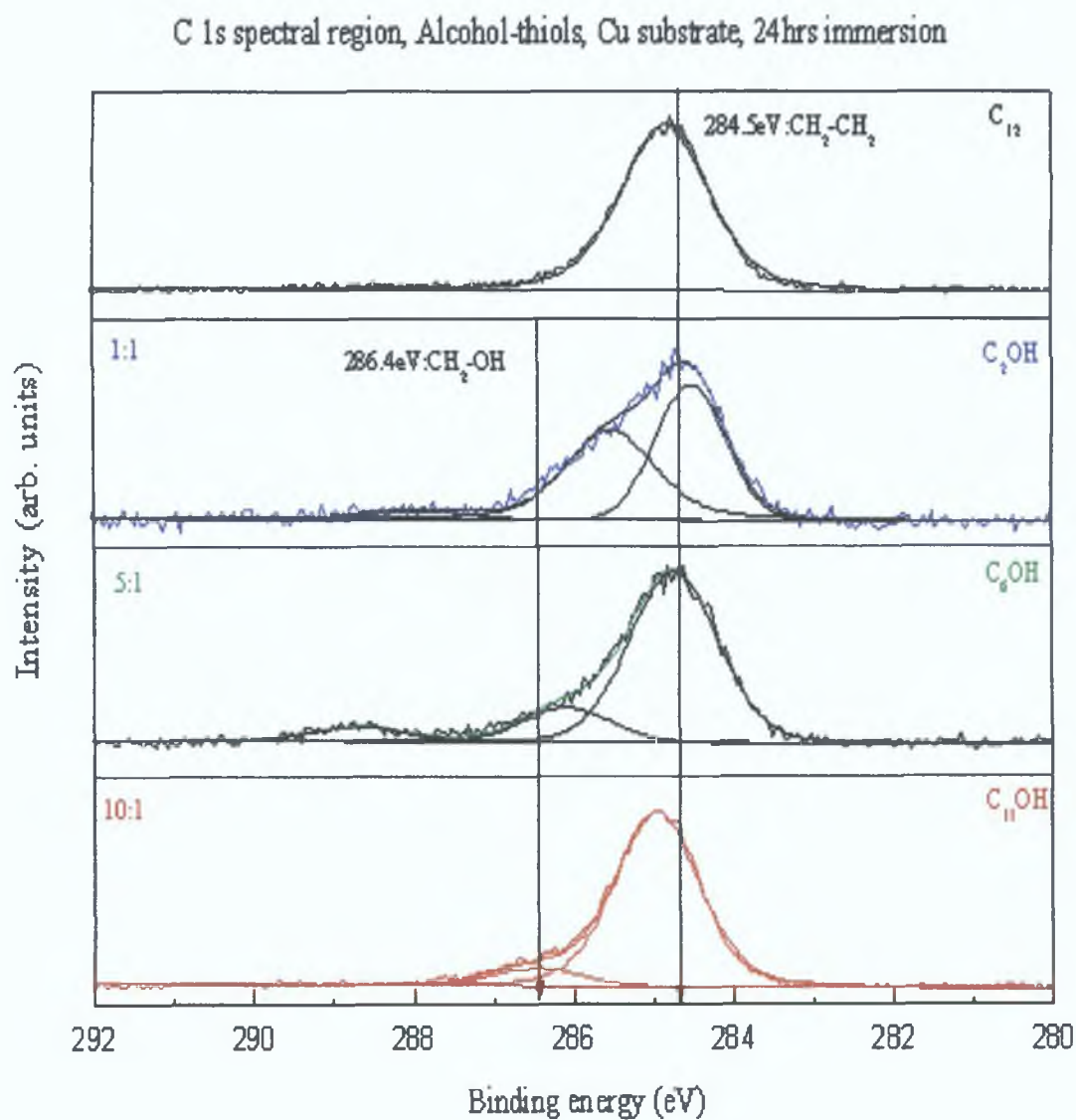


Figure 8.12 C1s spectral data collected for alcohol-thiols on Cu substrate, after 24 hr immersions. $C_{11}OH \rightarrow Cu/S-(CH_2)_{11}OH$, $C_6OH \rightarrow Cu/S-(CH_2)_6OH$, $C_2OH \rightarrow Cu/S-(CH_2)_2OH$ and $C_{12} \rightarrow Cu/S(CH_2)_{11}CH_3$.

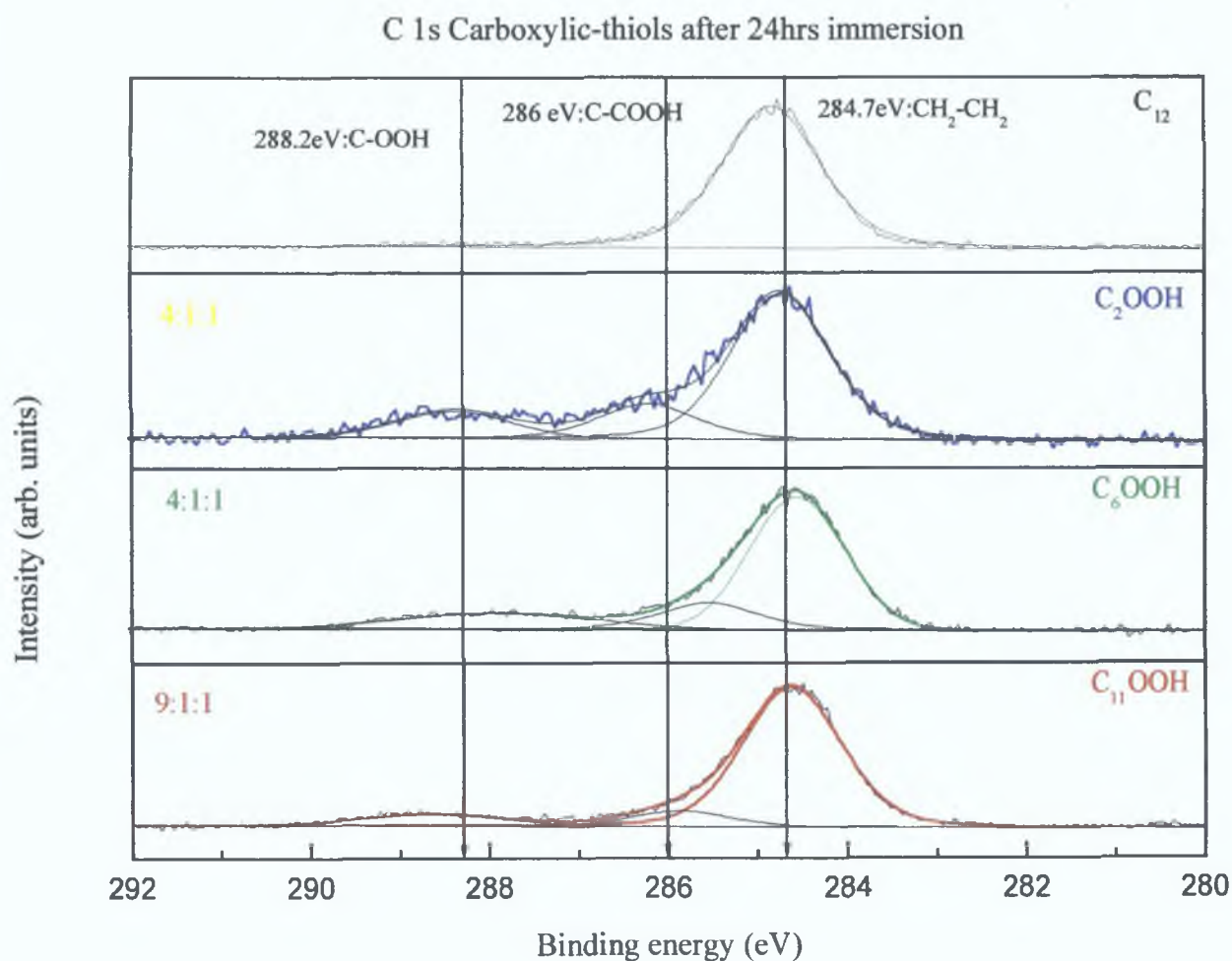


Figure 8.13 C1s spectral data collected for carboxylic-thiols on Cu substrate, after 24 hr immersions. C₁₁OOH → Cu/S-(CH₂)₁₀COOH, C₆OOH → Cu/S-(CH₂)₅COOH, C₂OH → Cu/S-(CH₂)COOH and C₁₂ → Cu/S(CH₂)₁₁CH₃.

Results O1s region

Figure 8.14 shows XPS spectra of the O1s core level spectral region for alcoholic-thiols on reduced copper after 24hr immersion in dilute thiol solution. Oxygen is present in two different environments on the modified Cu. The binding energies that are associated with the spectral peaks 530.7 eV, 532.5 eV (± 0.3 eV), which are present on the C₂OH modified Cu substrate are related to that of the oxygen bonded to Cu (Cu₂O) and –OH respectively. For the longer chained thiols like C₆OH and C₁₁OH, the binding energies are shifted to slightly higher values i.e 533.1 eV and 532.5 eV (± 0.3 eV). As before the 532.5 eV peak is associated with the OH of the alcohol and 533.1 eV is the binding energy related to H₂O. For 1-dodecanthiol, an emission at 529.6 eV is observed which is attributed to CuO.

For the 12 hr immersion the C₂OH-modified Cu shows only the presence of oxygen which is bound to the hydrogen of the alcohol. For the longer chained thiols a second emission line for oxygen is recorded which is representative of CuO (529.9 eV ± 0.3 eV). This is contradictory to the results documented for the Cu 2p spectral region where it was suggested that CuO was not present on the surface, or that the concentration of CuO was minimal. For the 2hr immersion, Cu₂O was on the surface of the C₂OH and C₆OH, with H₂O found present on the C₁₁OH surface. From these results it can be seen that some form of copper oxide exists on all surfaces.

For the carboxylic-thiols at 24 hr immersion [Figure 8.15] and at 2 hr immersion, Cu₂O (530.7 eV), –Q=COH (532.2 eV) and –HQ-C (533.5 eV) were found to be present on the surface. For the 12hr immersion time limit only –Q=COH (532.2 eV) and –HQ-C (533.5 eV) are found on the surface, indicating maybe that 12hr would be the optimum time for immersion, as it appears that no form of copper oxide is present and only the oxygen from the carboxylic group is prominent on these surfaces.

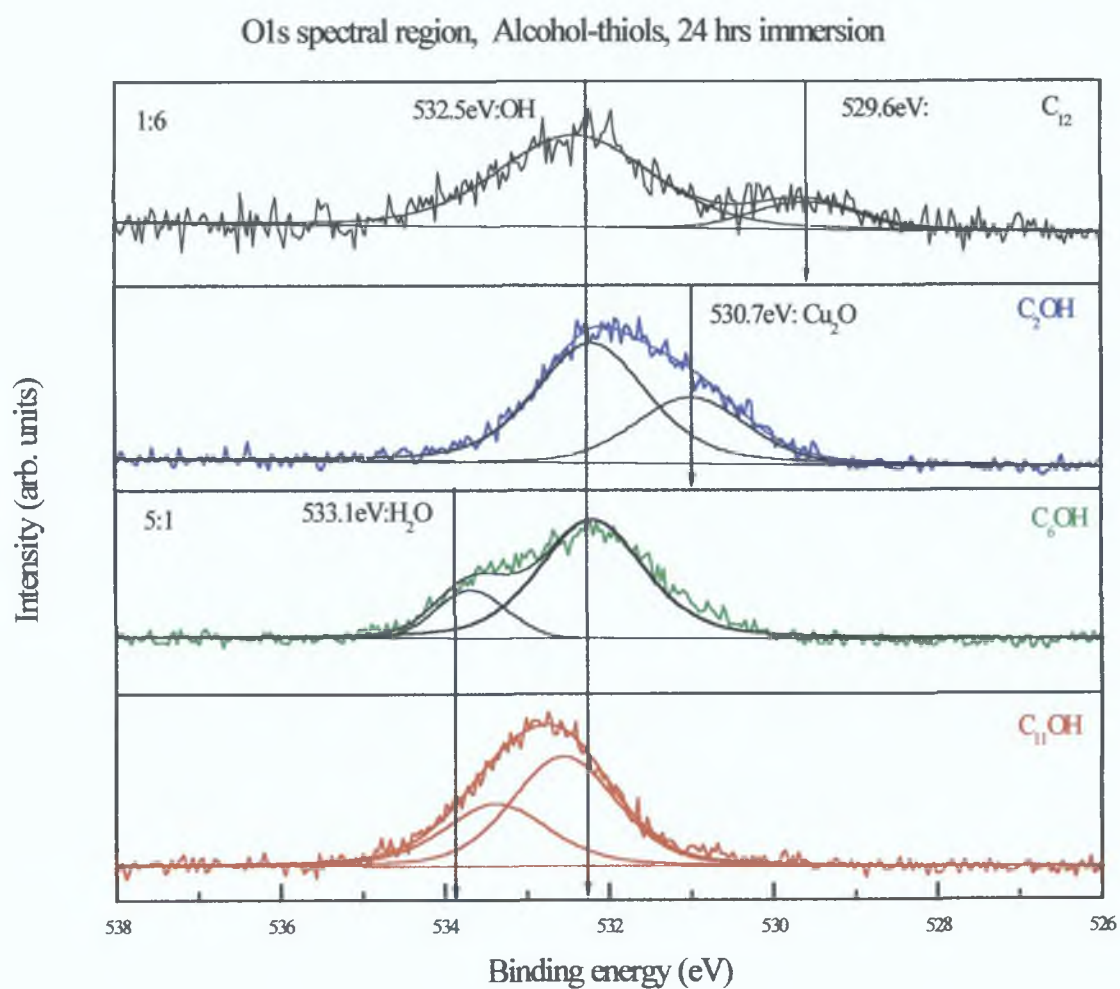


Figure 8.14 O1s spectral data collected for alcohol-thiols on Cu substrate, after 24 hr immersions. $C_{11}OH \rightarrow Cu/S-(CH_2)_{11}OH$, $C_6OH \rightarrow Cu/S-(CH_2)_6OH$, $C_2OH \rightarrow Cu/S-(CH_2)_2OH$ and $C_{12} \rightarrow Cu/S(CH_2)_{11}CH_3$.

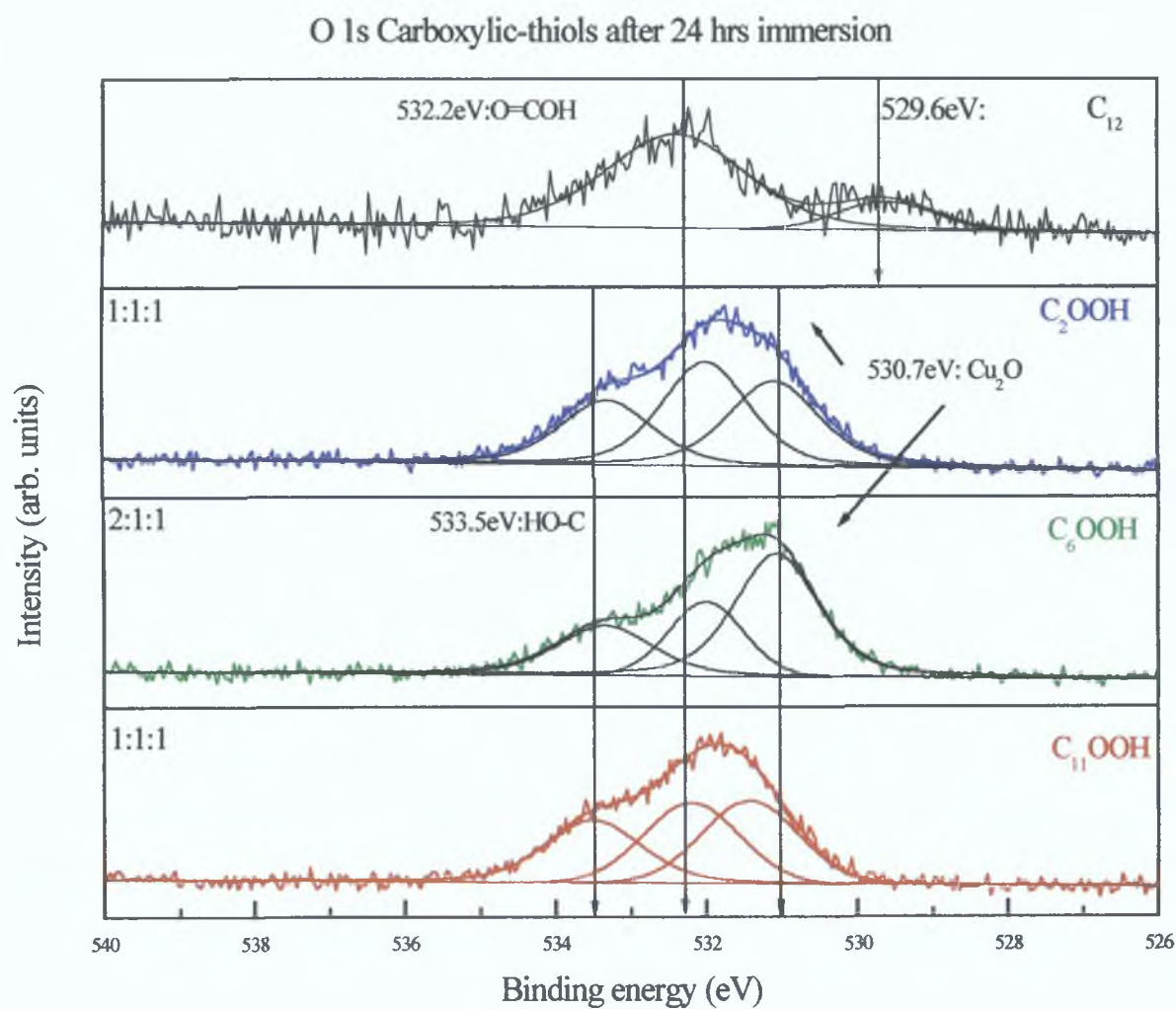


Figure 8.15 O 1s spectral data collected for Carboxylic-thiols on Cu substrate, after 24 hr immersions. C₁₁OOH → Cu/S-(CH₂)₁₀COOH, C₆OOH → Cu/S-(CH₂)₅COOH, C₂OOH → Cu/S-(CH₂)COOH and C₁₂ → Cu/S(CH₂)₁₁CH₃.

Sp2 spectral results

In Figure 8 16, the sulfur (2p) core level is characterised by a $2p_{3/2}/p_{1/2}$ spin-orbit split doublet. The dominant $2p_{3/2}$ emission at 162.2 eV accompanied by the $2p_{1/2}$ component at 163.4 eV is typical of a thiolate sulfur, i.e. S-Cu bond. Deconvolution of the sulfur emission reveals the characteristic splitting ratio of 2:1 and peak separation of 1.18 eV.

Oxidised sulfur would be chemically shifted to a higher binding energy value of ≈ 168 eV which is not present on these spectra, indicating that there is no free sulfur, suggesting formation of ordered monolayers.

Free sulfur is any other form of sulfur whether it be di-sulfur or sulfur bonded to anything that is not copper. As this metal-thiolate bond is the only sulfur bond found present on the Cu surfaces, it is an indication of monolayer formation.

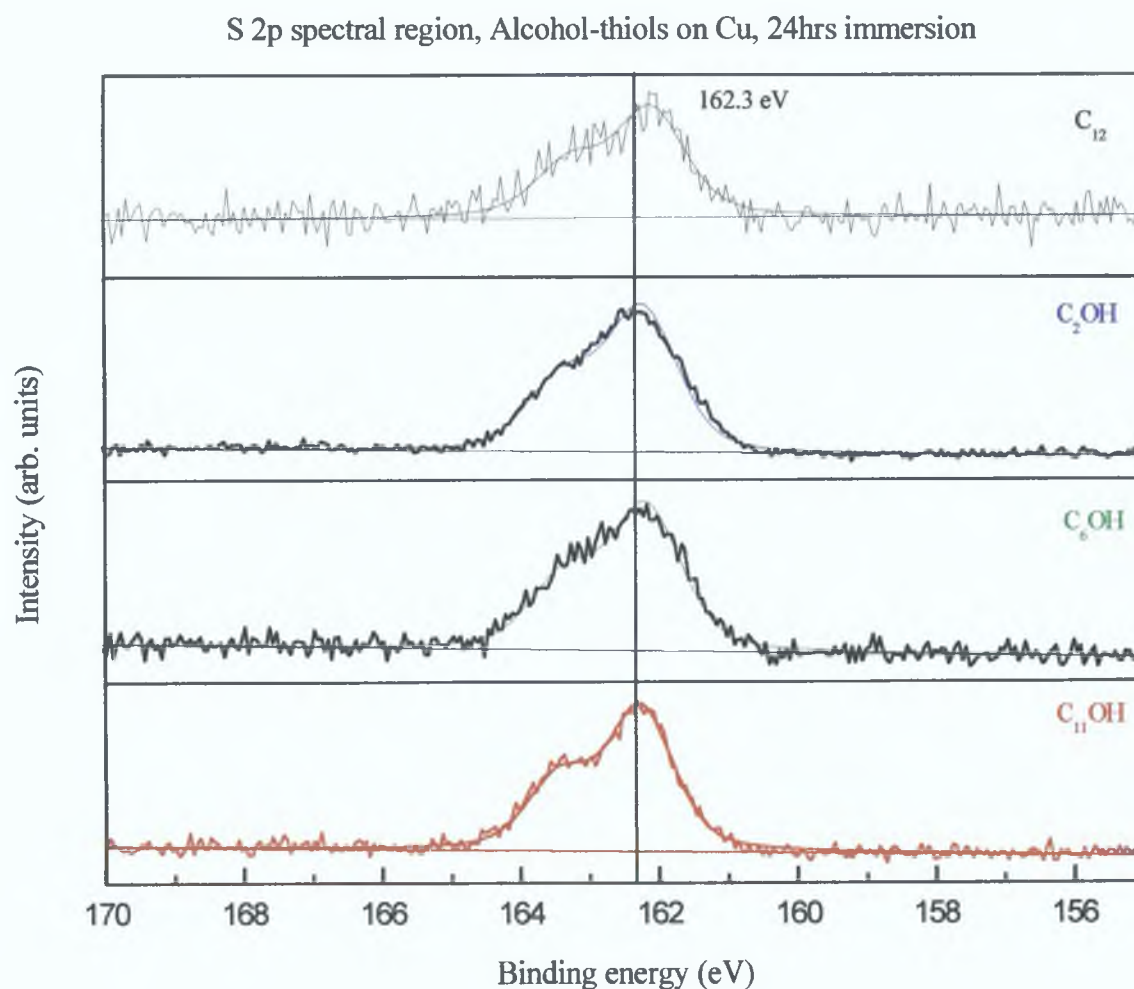


Figure 8.16 S 2p spectral data collected for alcohol-thiols on Cu substrate, after 24 hr immersions. $C_{11}OH$ represents $Cu/S-(CH_2)_{11}OH$, $C_6OH \rightarrow Cu/S-(CH_2)_6OH$, $C_2OH \rightarrow Cu/S-(CH_2)_2OH$ and $C_{12} \rightarrow Cu/S(CH_2)_{11}CH_3$.

Results Cu 2p_{3/2} region

The Cu 2p_{3/2} spectra for the modified Copper with varying immersion times can be seen in Figure 8.17. The copper (2p) core level is characterised by 2p_{3/2}/p_{1/2} spin-orbit split doublet. The dominant 2p_{3/2} emission at 932.4 eV accompanied by the 2p_{1/2} component at 952.2 eV is in agreement with reported values for metallic copper, Cu(0) and Cu(1) [15].

The copper surface oxidises readily in air, and although the samples were electrochemically reduced, ambient oxidation would have occurred during sample preparation. This could have happened when transporting the copper pieces to the dilute *n*-alkanethiol solutions.

The possible components of the oxide layer that can exist are Cu₂O, CuO, Cu(OH)₂ and CuOH. These oxides can be distinguished from one another with the results obtained from XPS analysis of the Cu 2p_{3/2}.

The presence of Cu(II) can be ruled out, as the peak for this oxide is positively shifted to 934.7 eV and is also accompanied by characteristic shake-up satellite peaks at 941.5 eV and 943.8 eV which are readily distinguishable and separated from the Cu 2p_{3/2} primary peak, these were not observed in the spectra collected [15]. Hence CuO was not present on the surface or the concentration of this element decreased below the detection limit of the SSX-100.

The Cu 2p_{3/2} peak for Cu(OH)₂ is reported to be found at the binding energy value of 933.1 eV [5], therefore it can be inferred from the spectra obtained *little or no intensity* was seen in this region for any of the modified surfaces at any immersion time. Therefore, Cu(OH)₂ is a minor or nonexistent component of the samples analysed.

The oxide that seems to be present on these surfaces is Cu₂O and this was confirmed from the emission lines recorded in the O 1s spectral window.

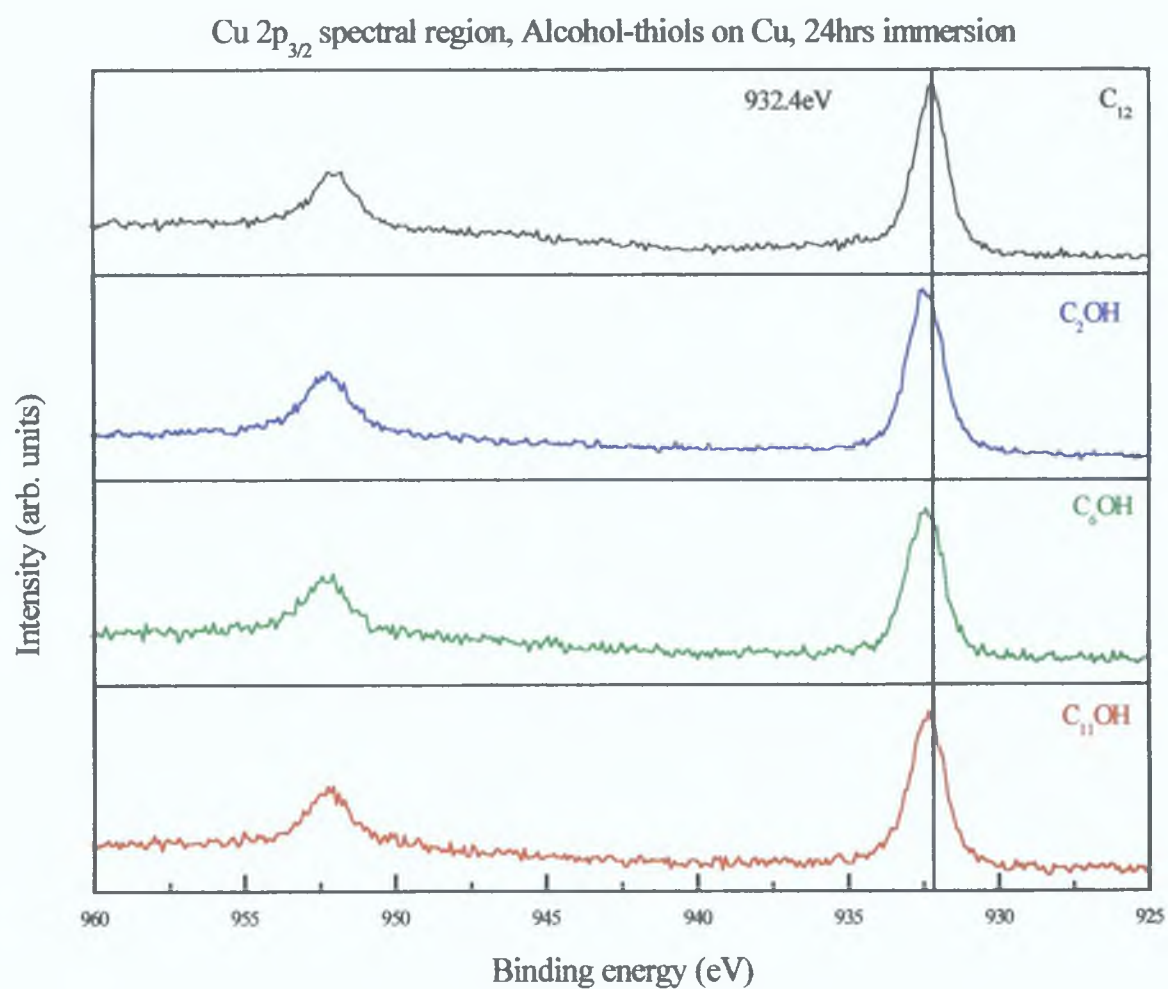


Figure 8.17 Cu 2p_{3/2} spectral region, for data collected for alcohol-thiols on Cu substrate, after 24 hr immersions. C₁₁OH represents Cu/S-(CH₂)₁₁OH, C₆OH → Cu/S-(CH₂)₆OH, C₂OH → Cu/S-(CH₂)₂OH and C₁₂ → Cu/S(CH₂)₁₁CH₃.

Cu LMM Spectral region

Figure 8 18 shows the Cu LMM auger lines for the modified Cu after different *n*-alkanethiols were chemisorbed onto the reduced Cu surface. For the Cu surface modified with 1-dodecanthiol, i.e. C₁₂, it would appear that only metallic Cu is present i.e. 567.6 eV \pm 0.3 eV, but for the other self-assembled alcohol-thiols after 24 hr immersion (i.e. Cu/S-(CH₂)₁₁OH, Cu/S-(CH₂)₆OH and Cu/S-(CH₂)₂OH) Cu(I) is present on the surface with an emission line at 570.1 eV. This emission line gives a kinetic energy value of 916.5 \pm 0.3 eV which would suggest the Cu₂O or Cu(I) oxidation state [15]. These results are comparable with the emission lines recorded for the carboxylic thiols after 24 hr immersions.

After 12 hr immersion for the alcohol terminated longer chained thiols i.e. the Cu/S-(CH₂)₁₁CH₃, Cu/S-(CH₂)₁₁OH and Cu/S-(CH₂)₆OH, metallic Cu is observed in this spectral region i.e. 567.8 eV \pm 0.3 eV, and Cu⁺ is found on the surface of the Cu/S-(CH₂)₂OH modified substrate. The results recorded for the carboxylic-thiol, regardless of chain length, indicated that only metallic Cu was present in this part of the spectral region after 12 hr immersions.

From this it would appear that the 12 hr immersion limit would be the optimum time for immersion, as it suggests that only metallic Cu is present on the surface when analysed using XPS.

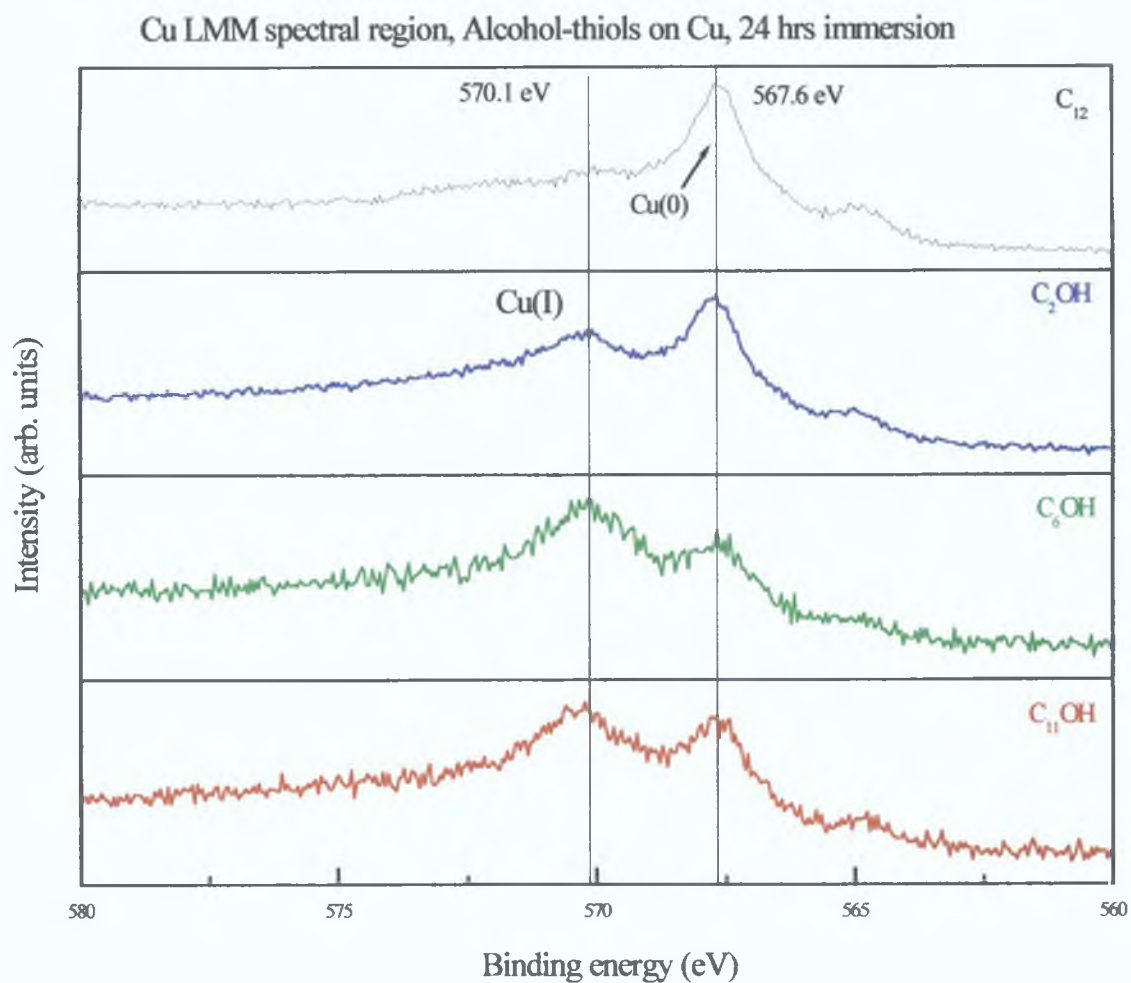


Figure 8.18 Cu Auger spectral region for alcohol-thiols on Cu substrate, after 24 hr immersions. C₁₁OH → Cu/S-(CH₂)₁₁OH, C₆OH → Cu/S-(CH₂)₆OH, C₂OH → Cu/S-(CH₂)₂OH and C₁₂ → Cu/S(CH₂)₁₁CH₃.

Table 8.9 gives the values calculated for the composition in atomic % for the surfaces investigated. These values are used to make a comparison between the elements present on the surface of the modified copper. The value written in red is the theoretical value if ideal monolayer formation consisting of a tightly packed network of molecules occurred. From these results it would appear that 12 hours was the ideal time limit as the results show it gives the calculated results closest to the theoretical values (error \cong 10%). Almost perfect monolayer formation occurs for the longer chained thiols, i.e. Cu/S-(CH₂)₁₁OH and Cu/S-(CH₂)₁₀COOH. For the 1-dodecanethiol on Cu, a small % of oxygen was found on the surfaces, this is to be expected as copper oxidises rapidly in air, and it is impossible to escape some form of ambient oxidation during sample preparation without using a glove box.

From the XPS data the composition in Atomic % could be calculated:

| 12-hr | % Carbon | % Sulfur | % Oxygen | % Copper |
|---------------------|-----------|-----------|-----------|-----------|
| C ₁₂ | 83.5 (86) | 4.0 (7) | 5.9 (0) | 6.6 (7) |
| C ₁₁ OH | 78.6 (78) | 3.9 (7) | 14.2 (8) | 3.3 (7) |
| C ₆ OH | 69.3 (67) | 10.0 (11) | 12.0 (11) | 8.7 (11) |
| C ₂ OH | 68.2 (40) | 9.0 (20) | 17.4 (20) | 5.4 (20) |
| C ₁₁ OOH | 74.3 (72) | 5.1 (7) | 15.3 (14) | 5.3 (7) |
| C ₆ OOH | 68.3 (60) | 4.7 (10) | 22.6 (20) | 4.4 (10) |
| C ₂ OOH | 53.6 (34) | 11.6 (17) | 22.5 (34) | 12.3 (17) |

Table 8.9 The composition in atomic percentage (%) for *n*-alkanethiols self-assembled on a reduced polished Copper surface. C₁₁OH → Cu/S-(CH₂)₁₁OH, C₆OH → Cu/S-(CH₂)₆OH, C₂OH → Cu/S-(CH₂)₂-OH and C₁₂ Reference → Cu/S-(CH₂)CH₃. C₁₁OOH represents Cu/S-(CH₂)₁₀COOH, C₆OH → Cu/S-(CH₂)₅COOH, C₂OH → Cu/S-(CH₂)-COOH.

8.6 Discussion

This study, has investigated the chemical modifications of mechanically polished copper substrates with SAMs. The surfaces were electrochemically reduced prior to their exposure to the functionalised thiols. Results from this study indicate that the optimum time limit for formation of densely packed monolayers on a electrochemically reduced copper substrate is 12 hr, with the longer chained thiols, i.e. Cu/S-(CH₂)₁₁OH and Cu/S-(CH₂)₁₀COOH exhibiting better protection for the underlying copper. The longer chain acid provides significantly better corrosion resistance for the 12 and 24-hour immersion times as determined by the XPS results.

From the cyclic voltammograms recorded and blocking factor calculations, it would seem that 2 hr was enough time for monolayer formation. In terms of the polarisation measurements, the corrosion current was reduced in all case. The best result indicates that the corrosion current has been reduced by a factor of 5 after 12 hr immersion for the 11-mercapto-1-undecanol with the corrosion potential shifted to a higher potential.

From the contact angles measurements taken, the results are less conclusive in terms of indicating significant changes in the surface termination groups for the thiols. It would appear that monolayer formation was not complete within any time limit. Multilayers could possibly have been formed on the Cu substrate, but from the XPS spectral results of the S 2p region, only the metal-thiolate bond was found in this spectral region, indicating the absence of multilayer formation.

8.7 References

- [1] Li, J , Liang, K S , Scoles , G , Ulman, A , *Langmuir*, 11 (1995) 4418
- [2] Mc Intyre, M S , *Journal Vac Science Technology*, 18 (1981) 3
- [3] Fenter, P , Eisenberger, K S , Liang, K S , *Phys Rev Lett* , 70 (1993) 2447
- [4] Lawless, K R , Gwathmey, A T , *Acta Metall* , 4 (1956) 153
- [5] Dubois, L H Zegarski, B R and Nuzzo, R G , *J Am Chem Soc* , 112 (1990) 570
- [6] Evans, S D , Sharma, R and Ulman, A , *Langmuir*, 7 (1991) 156
- [7] Laibinis, P E and Whitesides, G M , *J Am Chem Soc* , 114 (1992) 9022
- [8] Labinis, P E , Whitesides, G M *J Am Chem Soc* , 113 (1991) 7152
- [9] Porter, M D , Bright, T B , Allara, D L , Chidsey, C E D , *J Am Chem Soc* , 109 (1987) 3559
- [10] Labinis, P E , Whitesides, G M , *J Am Chem Soc* , 114 (1992) 1990
- [11] Ron, H , Cohen, H , Matlis, S , Rappaport, M and Rubinstein, I , *J Phys Chem B*, 102 (1998) 9861
- [12] Feng, Y , Teo, W , Slow, K , Gao, Z , Tan, K and Heieh A , *J Am Chem Soc* , 144 (1997) 1

- [13] Brett, C M and Brett, A M , “Electrochemistry Principles, Methods and Applications”, Oxford University Press, (1993)
- [14] Haneda, R , Nishihara, N and Aramaki, K , J Electrochem Soc , 144 (1997) 4
- [15] Briggs, D , Seah, M P , “Practical Surface Analysis by Auger and X-ray Photoelectron Spectroscopy” , Wiley, New York, (1994)
- [16] Ghijssen, J and Marshall, F , University Notre-Dame de la Prie, Namur, Belgium, *Private communication*
- [17] Jennings, G , Munro ,J C , Yong, T and Laibinis, P E , Langmuir, 14 (1998) 6130

Chapter 9

| |
|---|
| Overview, general conclusions and future work |
|---|

Overview

This thesis comprises studies where XPS (x-ray photoelectron spectroscopy) was used to analyse and investigate A) the effect that cleaning procedures produce on the substrate surface, B) the effect individual cure components and combinations of same, of anaerobic adhesives have on a copper substrate and an iron containing substrate and C) functionalised thiols on a reduced copper substrate. Other techniques such as FT-IR, ICP-AES, contact angle measurements and electrochemistry were utilised to elucidate the results obtained from the XPS experiments.

General conclusions/future work

Mild steel surfaces were exposed to an aqueous wash and an organic wash and XPS was used to determine which procedure produces a result most indicative of the underlying substrate. The aqueous wash produced the better result, dealing with environmental pressures associated with organic washes in which trichloroethylene was used as one is unable to obtain trichloroethylene these days without following a strict protocol.

Anaerobic adhesives were developed in the 1950s and research at the time concentrated on obtaining sufficient knowledge to commercialise the technology. Fifty years later research is still being carried out in order to understand the complex cure chemistry of these particular adhesives. The individual cure components of anaerobic adhesives are organic acids, substituted aromatic amines, hydrazines and hydroperoxides. The complexity of the cure chemistry is illustrated by the role of the accelerators used in anaerobic adhesives. Initially an organic acid was used to provide soluble metal ions from the substrate surface, these ions in turn are reduced by the aromatic amines or hydrazine to their lower oxidation state, which decompose the CHP resulting in free radical polymerisation. The metal to be bonded dictates which accelerators should be used in the adhesive formulation. A combination of saccharin with APH produces the desired effect on both transition metals investigated. While DMpT and DEpT, whose reducing ability is less than that of APH, can be used

in combination with saccharin, when the metal of interest is copper to produce the desired cure chemistry. The results indicate that maleic acid in combination with these tertiary aromatic amines produces a more effective cure chemistry for mild steel substrates.

Throughout this research it has been shown that the chemistry of anaerobic adhesives is complex due to the numerous reactions and interactions that occur in adhesive formulations. The chemistry of maleic acid and saccharin, DMpT, DEpT, DMoT and APH as well as the transition metals must be dealt with individually and not in a general fashion. Future research will have to look at in detail the addition of the monomer to these anaerobic adhesive cure systems.

Interest in the study of *n*-alkanethiols as SAMs has grown enormously in recent years. A comprehensive range of data has been accumulated and interpreted for self-assembly of *n*-alkanethiols on various substrates while information regarding the adsorption of functionalised thiols on copper has receiving considerable interest over the last ten years. This thesis has detailed the study of carboxylic acid and alcohol terminated thiols self-assembled on reduced polycrystalline copper using XPS and electrochemical techniques. The formation of such SAMs has been investigated in terms of immersion times and as one of the major disadvantages associated with copper is its tendency to oxidise, the ability of these SAMs to reduce this oxidation was examined.

The influence of these self-assemblies and monolayer coverage suggest that the optimum time limit for the formation of densely packed monolayers on an electrochemically reduced copper substrate is twelve hours, with the longer chain thiols exhibiting better corrosion resistance for the underlying copper. In terms of future work with respect to these SAMs on copper *in situ* STM characterisation of these self-assembled monolayers should be undertaken to confirm and clarify the adsorption behaviour of these functionalised thiols.